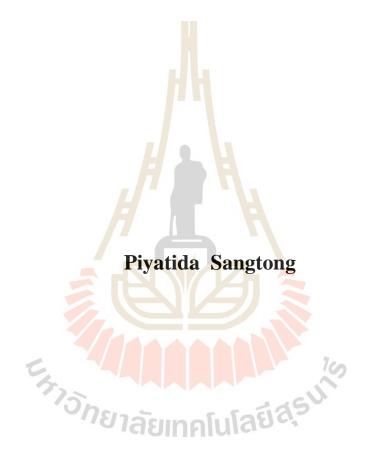
DEPOSITIONAL ENVIRONMENT AND PETROLEUM SOURCE ROCK POTENTIAL IN MAE TEEP BASIN,

LAMPANG PROVINCE



A Thesis Submitted in Partial Fulfillment of the Requirements for

the Degree of Doctor of Engineering in Geotechnology

Suranaree University of Technology

Academic Year 2018

สภาพแวดล้อมการสะสมตัวและศักยภาพของหินต้นกำเนิดปิโตรเลียม ในแอ่งแม่ตีบ จังหวัดลำปาง



วิทยานิพนธ์นี้เป็นส่วนหนึ่งของการศึกษาตามหลักสูตรปริญญาวิศวกรรมศาสตรดุษฎีบัณฑิต สาขาวิชาเทคโนโลยีธรณี มหาวิทยาลัยเทคโนโลยีสุรนารี ปีการศึกษา 2561

DEPOSITIONAL ENVIRONMENT AND PETROLEUM SOURCE ROCK POTENTIAL IN MAE TEEP BASIN, LAMPANG PROVINCE

Suranaree University of Technology has approved this thesis submitted in partial fulfillment of the requirements for the Degree of Doctor of Philosophy.

Thesis Examining Committee

(Dr. Prinya Putthapiban)

Chairperson

(Asst. Prof. Dr. Akkhapun Wannakomol) Member (Thesis Advisor)

(Assoc. Prof. Dr. Benjavun Ratanasthien)

Member (Thesis Co-Advisor)

Yupa thased (Asst. Prof. Dr. Yupa Thasod)

Member Barokita Tera

(Asst. Prof. Dr. Bantita Terakulsatit)

Member hughphun

(Asst. Prof. Dr. Decho^{Phueakphum)}

Member

(Dr. Tawisak Silakul)

Member

Pomstoi Jonskil

(Assoc. Prof. Flt. Lt. Dr. Kontorn Chamniprasart) (Assoc. Prof. Dr. Pornsiri Jongkol) Vice Rector for Academic Affairs and Internationalization

Dean of Institute of Engineering

ปียะธิดา แสงทอง : สภาพแวคล้อมการสะสมตัวและศักยภาพของหินต้นกำเนิดปีโตรเลียม ในแอ่งแม่ตีบ จังหวัคลำปาง (DEPOSITIONAL ENVIRONMENT AND PETROLEUM SOURCE ROCK POTENTIAL IN MAE TEEP BASIN, LAMPANG PROVINCE) อาจารย์ที่ปรึกษา : ผู้ช่วยศาสตราจารย์ คร. อัฆพรรค์ วรรณโกมล, 275 หน้า.

้วัตถุประสงค์หลักสองประการของการศึกษาครั้งนี้ คือ 1) เพื่อระบศักยภาพของหินต้นกำเนิด ป โตรเลียมในแอ่งแม่ตีบ โดยใช้การวิเคราะห์ทางธรณีเคมีและเทคนิคศิลาวรรณาวิทยาในอินทรีย์วัตถุ และ 2) เพื่อประเมินสภาพแวคล้อมการสะสมตัวและลักษณะของหินต้นกำเนิดปีโตรเลียมที่มีศักยภาพ ในแอ่งแม่ตีบ ตัวอย่างจำนวน 44 ตัวอย่าง <mark>จาก</mark>เหมืองถ่านหินแม่ตีบ ถูกรวบรวมจากชั้นหินอินทรีย์ หลัก 3 ชั้น จากหน้าเหมืองปัจจุบันในแนว<mark>ตั้ง ประ</mark>กอบด้วย ตัวอย่างหินน้ำมัน 14 ตัวอย่าง ตัวอย่างถ่าน หิน 26 ตัวอย่าง และตัวอย่างลี โอนาร์ ไค<mark>ต์</mark> 4 ตัวอ<mark>ย่</mark>าง ตัวอย่างเหล่านี้ถูกนำมาวิเคราะห์ด้วยวิธีการทาง ศิลาวรรณาและทางธรณีเคมีเพื่อการต<mark>ีค</mark>วามถึงสภาพแวดล้อมของการสะสมตัวและศักยภาพด้าน ู้ปีโตรเลียม ผลการศึกษาทางด้านศิล<mark>าวร</mark>รณาแสด<mark>งมา</mark>เซอรัลหลักเป็น ลิบติในต์และวิตทริในต์ซึ่งบ่ง ้ชี้ให้เห็นว่าสภาพแวดล้อมของการส<mark>ะ</mark>สมตัวจากค้านล่างขึ้นไปด้านบนของชั้นหินที่ทำการศึกษามีการ เปลี่ยนแปลงจากที่ลุ่มน้ำขังตื้น<mark>ๆไป</mark>เป็นป่าน้ำขังที่มีต้นไ<mark>ม้ให</mark>ญ่และเปลี่ยนไปเป็นทะเลสาบน้ำลึกและ นิ่ง ผลการวิเคราะห์ทางธรณีเคมีแสดงค่าเฉลี่ยของปริมาณเถ้า 57.28 wt.% ปริมาณสารระเหยเฉลี่ย 28.45 wt.% ปริมาณธาตุ<mark>กา</mark>ร์บอนกงที่เฉลี่ย 14.28 wt.% ปริมาณธาตุการ์บอนเฉลี่ย 23.44 wt.% และ ปริมาณธาตุไฮโครเจนเฉลี่ย 3.17 wt.% ผลจากการวิเคราะห์ไพโรไลซิสแสดงค่าปริมาณของธาตุ คาร์บอน โดยรวมทั้งหมด (TOC) มีค่าเฉลี่ยเป็น 23.04 wt.% ค่า SI เฉลี่ย 1.47 mg/g ค่า S2 เฉลี่ย 53 mg/g ค่า S3 เฉลี่ย 5.57 mg/g และมีค่าอุณหภูมิสูงสุด (T_{max}) อยู่ช่วงระหว่าง 422 และ 434 องศา เซลเซียส ค่าศักยภาพการให้สารกำเนิดปีโตรเลียม (S1+S2) ของตัวอย่างที่นำมาศึกษามีค่าค่อนข้างสูง มาก (22.13 ถึง 72.12 mg/g) ซึ่งบ่งชี้ถึงการเป็นหินต้นกำเนิดปีโตรเลียมที่ดีมาก อย่างไรก็ตามระดับขั้น ภาวะการได้ที่อันเนื่องมาจากความร้อนของตัวอย่างที่นำมาศึกษาที่ได้จากการวิเคราะห์การสะท้อน แสงของวิตทริในต์นั้นมีค่าระหว่าง 0.31 และ 0.50 % Ro ซึ่งบ่งชี้ถึงระดับขั้นภาวะการได้ที่อัน เนื่องมาจากความร้อนที่อยู่ในช่วงระดับขั้นภาวะก่อนการได้ที่ถึงระดับขั้นภาวะการได้ที่เริ่มต้น

สาขาวิชา <u>เทคโนโลยีธรณี</u> ปีการศึกษา 2561

ลายมือชื่อนักศึกษาป <i>ิปุร</i> โรกา <u>11/200</u> 2
ลายมือชื่ออาจารย์ที่ปรึกษา
ลายมือชื่ออาจารย์ที่ปรึกษาร่วม <i>/ 🔊 จ</i> – 🧹

PIYATIDA SANGTONG : DEPOSITIONAL ENVIRONMENT AND PETROLEUM SOURCE ROCK POTENTIAL IN MAE TEEP BASIN, LAMPANG PROVINCE. THESIS ADVISOR : ASST. PROF. AKKHAPUN WANNAKOMOL, Ph.D., 275 PP.

PETROLEUM POTENTIAL SOURCE ROCK/PROXIMATE AND ULTIMATE ANALYSIS/ORGANIC PETROLOGY/DEPOSITIONAL ENVIRONMENT/ MAE TEEP BASIN

Two main objectives of this study are: 1) to identify potential petroleum source rocks in Mae Teep basin using geochemical analysis and organic petrography techniques, and 2) to assess depositional environment and characteristics of potential petroleum source rocks in Mae Teep basin. Total of 44 samples from Mae Teep coal mine were collected in vertical succession from the present mining face. They were from 3 main organic units, including 14 oil shale, 26 coal and 4 leonardite samples. Petrological and geochemical analyses of samples were undertaken to interpret their depositional environments and petroleum potentiality. Petrology study shows that macerals in these samples are mainly liptinite and vitrinite which indicate that depositional environments of the studied succession changed from shallow swamp, forested swamp to a deep and stagnant lacustrine, as from the bottom to the top respectively. Geochemical analyses show an average of 57.28 wt.% ash, 28.45 wt.% volatile matter, 14.28 wt.% fixed carbon, 23.44 wt.% carbon and 3.17 wt.% hydrogen. Pyrolysis analyses show an average of 23.04 wt.% TOC, 1.47 mg/g of S1, 53 mg/g of S2, 5.57 mg/g of S3, and T_{max} ranges between 422 °C and 434 °C. The genetic potential (S1+S2) of the studied samples are very high and vary from 22.13 to 72.12 mg/g which indicates their excellent source

rock potentiality. However, thermal maturation determined by vitrinite reflectance of the studied samples ranges between 0.31 and 0.50 %Ro, indicating the immature to early mature stage.



School of <u>Geotechnology</u> Academic Year 2018

Student's Signature	Piyatida Sangtono
Advisor's Signature	
Co-Advisor's Signature_	p. Ratemesstin -

ACKNOWLEDGEMENT

I am grateful to all those, who by their direct or indirect involvement have helped in the completion of this thesis.

First and foremost, I would like to express my sincere thanks to my supervisors Asst. Prof. Dr. Akkhapun Wannakomol (SUT), who gave me the possibility to complete this thesis and for their immense help in planning and executing the works. With a deep sense of gratitude, Assoc. Prof. Dr. Benjavun Ratanasthien for her invaluable help and constant encouragement throughout the course of this research. I am most grateful for her teaching and advice, not only the research methodologies but also many other methodologies in life. I would not have achieved this far and this thesis would not have been completed without all the support that I have always received from her.

I express my indebtedness to Major analyses of this study were conducted at Laboratory Section, Geology Department of Mae Moh Mine Planning and Administration Division and Department of Geological Sciences, Faculty of Sciences, Chiang Mai University. In addition, I am grateful to Suntitranon Co., Ltd. for supporting my samples collection from Mae Teep coal mine and others person for suggestions and all their help. They advised me immensely by giving me encouragement and would also like to gratefully acknowledge the support of some very special individuals.

Special thanks to Asst. Prof. Dr. Bantita Terakulsatit for her supported and granted be a research assistant and encouraged me to learn engineering geology and

provided me the opportunity for work and study on an integrated multidisciplinary topic in geosciences. This includes the support from Institute of Research and Development of Suranaree University of Technology.

Many thanks are conveyed to the officials at the Laboratory of Suranaree University of Technology. And are also conveyed to Mr. Sakchai Glumglomjit who assisted me on field works.

Finally, I most gratefully acknowledge my parents and my friends for all their support throughout the period of this research.



V

TABLE OF CONTENT

ABSTRACT (THAI)	I
ABSTRACT (ENGL	ISH)II
ACKNOWLEDGEM	ENTIV
TABLE OF CONTE	NTSVI
LIST OF TABLES	X
LIST OF FIGURES.	
CHAPTER	
I INT	TRODUCTION1
1.1	Study area
1.2	Research objectives
1.3	Limitations and scope of works5
1.4	Expected result
1.5	Research methodology
1.6	Thesis contents6
II LII	TERATURE REVIEW
2.1	Petroleum and coal in Tertiary basin of Thailand8
2.2	Mae Teep basin
2.3	Source rocks classification and environment
	deposition18

TABLE OF CONTENT (Continued)

	2.4	Petroleum source rock evaluation and maturity	24
III	ME'	TRODOLOGY	
	3.1	Field Work	
	3.2	Organic sediments sampling	35
		3.2.1 Samples collection and preservation	35
		3.2.2 Sample description	
	3.3	Methodology of sample analysis	
		3.3.1 Geochemical analysis	
		3.3.2 Petrographic methods	47
IV	RES	SULT	49
	4.1	Geology of studied sedimentary succession	49
		4.1.1 Leonardite sub-unit	56
	57:	4.1.2 Coal C sub-unit	56
		4.1.3 Coal B sub-unit	56
		4.1.4 Coal A sub-unit	57
		4.1.5 Oil Shale in Coal A sub-unit	59
		4.1.6 Lower Oil Shale sub-unit	61
		4.1.7 Upper Oil Shale sub-unit	61
		4.1.8 Fine-grain sediment unit	63
		4.1.9 Fluvial deposits	64

TABLE OF CONTENT (Continued)

4.2	Organic Petrological Results		
	4.2.1	Leonardite sub-unit78	
	4.2.2	Coal C sub-unit	
	4.2.3	Coal B sub-unit127	
	4.2.4	Coal A sub-unit143	
	4.2.5	Oil Shale in Coal A sub-unit185	
	4.2.6	Lower Oil Shale sub-unit	
	4.2.7	Upper Oil Shale sub-unit220	
	4.2.8	Vitrinite Reflactance	
4.3	Geoch	nemical analysis237	
	4.3.1	Result of proximate, ultimate and heating	
		value analysis237	
57:	4.3.2	HAWK pyrolysis	
4.4	Discu	ssions	
	4.4.1	Depositional environment and maceral	
		characters with petrography and	
		geochemical results related to source rocks	
		quality245	
	4.4.2	The evolution and thermal maturation of	
		petroleum source rocks related to energy	
		potential in Mae Teep deposited250	

TABLE OF CONTENT (Continued)

V	CONCLUSION AND RECOMMENDATION256		256
	5.1	Depositional environment and characteristics of	
		Mae Teep organic sediments	256
	5.2	Potential of petroleum source rocks	258
	5.3	Recommendation	260
REFERENCE.			260
BIOGRAPHY.			275



TABLE OF TABLES

Table

2.1	Source rock data of coal
2.2	Source rock data of oil shale12
2.3	The rocks boundary around Mae Teep basin divided by age16
2.4	The results proximate and ultimate analysis of Mae Teep coal and
	oil shale samples18
2.5	Relationship among kerogen, maceral types, hydrocarbon index
	(HI), S2 to S3 ratio, and petroleum product expelled at maturity22
2.6	The relationship among palynofacies, geochemical and
	Environment factors
2.7	The main type and evolution paths of kerogen occurred in
	difference type of palynology
2.8	Classification of maceral based on International Committee for
	Coal and Organic Petrology (ICCP)
4.1	Tertiary rock units of Mae Teep coal mine deposits
4.2	Environment of deposition, rock units, sub-units and number of
	samples collected from each sub-unit
4.3	Organic rock sample descriptions of the studied organic sedimentary
	succession
4.4	Composition in percentage of leonardite samples

TABLE OF TABLES (Continued)

Table	Page
4.5	Composition in percentage of Coal C sub-unit samples
4.6	Composition in percentage of Coal B sub-unit samples129
4.7	Composition in percentage of Coal A sub-unit samples145
4.8	Composition in percentage of Oil Shale in Coal A
	sub-unit samples
4.9	Composition in percentage of the Lower Oil Shale sub-unit
4.10	Composition in percentage of the Upper Oil Shale
	sub-unit samples
4.11	Vitrinite Reflectance (Ro) of Coal A and Coal B sub-unit235
4.12	Results of proximate, ultimate and heating value analysis of
	the studied leonardite samples (Air dry basis)238
4.13	Results of proximate, ultimate and heating value analysis of
	the studied coal samples (Air dry basis)
4.14	Results of proximate, ultimate and heating value analysis of
	the studied oil shale samples (Air dry basis)
4.15	Results of HAWK pyrolysis analysis of studied organic sediment
	samples from each sub-unit
4.16	The organic source rock maturation estimation based on kerogen
	type, Tmax and Ro244
4.17	Depositional environments of each Mae Teep deposit sub-unit
	based on maceral type and petrography study results

TABLE OF FIGURES

Figure

1.1	Four petroleum provinces in Thailand; the North and Central, the
	Northeastern, the Gulf and the Andaman areas
1.2	The location of the study area on map Ban Pa Dange, Map sheet
	5046 III scale 1:50,000, Map Index L70184
1.3	Flowchart showing research strategies and activities in this study6
2.1	Geological map of Mae Teep basin and surrounding area15
2.2	Relationship among organic-rich rock, known precursors, rock
	types and environment of depositional
2.3	Van Krevelen diagram showing the evolutionary trends of
	dominant coal types27
2.4	Van Krevelen diagram (left) showing thermal maturation trends
	of the different kerogen types on a plot of H/C vs. O/C.
	The modified Van Krevelen diagram (right) showing the same
	kerogen as that on the left, but analyzed using rock-Eval pyrolysis
	and plotted in terms of Hydrogen Index and Oxygen Index29
3.1	Steps of work and methodologies conducted and used in this study
3.2	Fieldwork activities: measuring thickness of each layer by
	measuring tape (A), note taking everything on field note book (B),
	samples collecting (C)

Figure	e Page
3.3	Processes of samples preparation for geochemical and
	Petrographical analysis
3.4	Leco TGA-701 (an automatic instrument for proximate analysis)
3.5	The temperate process during conducting the proximate analyses
	for moisture, volatile matter and ash content determination40
3.6	The process of the ultimate analysis to detect carbon, hydrogen
	and nitrogen content by IR cell and thermal
	conductivity detector cell
3.7	The process of ultimate analysis for sulfur detection
3.8	The bomb calorimeter Leco AC-35044
3.9	The relationship among S1, S2, S3, CO2, CO generating and
	elevated temperature and time during the pyrolysis process of
	the HAWK instrument
4.1	Overview of Mae Teep coal mine (A) (look south-west), the strata
	showing bedding plane strike NE direction (B) and dip
	eastwards (C)
4.2	The western wall of the Mae Teep coal mine showing units
	boundary between the Quaternary, fluvial, and lacustrine
	sequences(A), the feature of coal and leonardite in
	the swampy environment at the western wall of mine (B)52

Figur	e Page
4.3	The contact boundary between oil shale unit (dark color) and
	the Fine-grained sediment unit (light color) can be observed at
	the Mae Teep coal mine front (look south)
4.4	Contact boundaries of the swamp environment deposits
	(Leonardite, Coal C, Coal B, and Coal A sub-unit) and lacustrine
	environment deposits (Oil shale) at the Mae Teep coal mine
4.5	Lithostratigraphic column of Mae Teep deposit at the Mae Teep
	coal mine showing the sedimentary sequences and their related
	depositional environment
4.6	The western wall of Mae Teep coal mine showing the bedding
	plane of leonardite sub-unit: the layer of the lower leonardite
	sub-unit (A), leonardite showing surface character of clays (B)57
4.7	Thin layer of coal interbedded in the leonardite (A), the platy
	Cleavage and crumbly surface of leonardite (B)58
4.8	Thin layer claystone with impure coal interbedded in the
	Coal C (A), glossy luster and conchoidal fracture of the Coal B (B)58
4.9	The Coal A sub-unit showing the oil shale parting in
	the upper part (A), Coal A massive texture (B) and Coal A
	conchoidal fracture with cubicle crack (C)
4.10	The oil shale parting layers in Coal A (look west)

Figure Page		
4.11	The samples show both character of oil shale, dark brown	
	oil shale with thin layer of coal and siltstone (A) and laminated	
	black shale (B)60	
4.12	The character of the oil shale in fresh rock show dark gray to	
	yellowish brown (A), weathered laminated oil shale show	
	yellowish brown and pale gray (B), and fossils remains found in	
	the Lower Oil Shale sub-unit (C)	
4.13	Out crop of the upper sub-unit oil shale interbedded with siltstone	
	(A) and brown oil shale with fossils remains (B)63	
4.14	The Fine-grained sediment unit from mine front. The outcrop	
	shows intercalated siltstone and mud rock sequences (A and B),	
	the weathered sample displaying desiccation cracks (C)and fossil	
	remains of leaves and shells in the mud rocks (D)64	
4.15	Overburden fluvial sedimentary sequences at the Mae Teep mine	
4.16	Overburden sedimentary rocks: gray sandstone (A),	
	conglomerate (B), reddish mottled sandstone calcite cement (C)	
	and conglomeratic sandstone with coal fragments (D)66	
4.17	Conglomerate and sandstone deposited with coal lens (A) and	
	planar cross bedded and laminar of coal (B) at the lower part of	
	the fluvial sequences (look north-earth)67	

Figure Page	
4.18	Reverse faults trending N $10 - 38$ W cut conglomerate and
	sandstone sequences of the fluvial sediment sequences
4.19	Correlation among lithostratigraphic unit, environment of deposition,
	and locations of the collected organic rock samples of the studied
	organic sedimentary succession at the Mae Teep coal mine
4.20	The microscopic picture of leonardite sample No. L7-180
4.21	The microscopic picture of leonardite sample No. L7-3
4.22	The microscopic picture of leonardite sample No. L7-4
4.23	The microscopic picture of leonardite sample No. 14-1
4.24	The microscopic picture of leonardite sample No. L14-2
4.25	The microscopic picture of leonardite sample No. L14-3
4.26	The microscopic picture of leonardite sample No. L19-1
4.27	The microscopic picture of coal sample No. C2-192
4.28	The microscopic picture of coal sample No. C2-293
4.29	The microscopic picture of coal sample No. C2-494
4.30	The microscopic picture of coal sample No. C2-795
4.31	The microscopic picture of coal sample No. C2-896
4.32	The microscopic picture of coal sample No. C2-997
4.33	The microscopic picture of coal sample No. C2-1098
4.34	The microscopic picture of coal sample No. C3-1
4.35	The microscopic picture of coal sample No. C4-1100

Figure

4.36	The microscopic picture of coal sample No. C4-2101
4.37	The microscopic picture of coal sample No. C4-3102
4.38	The microscopic picture of coal sample No. C4-5103
4.39	The microscopic picture of coal sample No. C4-6104
4.40	The microscopic picture of coal sample No. C4-7105
4.41	The microscopic picture of coal sample No. C5-1106
4.42	The microscopic picture of coal sample No. C6-1107
4.43	The microscopic picture of coal sample No. C6-2108
4.44	The microscopic picture of coal sample No. C6-4109
4.45	The microscopic picture of coal sample No. C8-1110
4.46	The microscopic picture of coal sample No. C8-2111
4.47	The microscopic picture of coal sample No. C9-1112
4.48	The microscopic picture of coal sample No. C9-2113
4.49	The microscopic picture of coal sample No. C10-1114
4.50	The microscopic picture of coal sample No. C10-3115
4.51	The microscopic picture of coal sample No. C11-1116
4.52	The microscopic picture of coal sample No. C11-2117
4.53	The microscopic picture of coal sample No. C11-3118
4.54	The microscopic picture of coal sample No. C11-6119
4.55	The microscopic picture of coal sample No. C12-1120
4.56	The microscopic picture of coal sample No. C12-2121

XVIII

TABLE OF FIGURES (Continued)

Figure

4.57	The microscopic picture of coal sample No. C12-5122
4.58	The microscopic picture of coal sample No. C12-7123
4.59	The microscopic picture of coal sample No. C13-2124
4.60	The microscopic picture of coal sample No. C13-3125
4.61	The microscopic picture of coal sample No. C13-5126
4.62	The microscopic picture of coal sample No. B15 – 4130
4.63	The microscopic picture of coal sample No. B15 – 5131
4.64	The microscopic picture of coal sample No. B15 – 8132
4.65	The microscopic picture of coal sample No. B16 – 2133
4.66	The microscopic picture of coal sample No. B16 – 4134
4.67	The microscopic picture of coal sample No. B17 – 2135
4.68	The microscopic picture of coal sample No. B17 – 4136
4.69	The microscopic picture of coal sample No. B17 – 8137
4.70	The microscopic picture of coal sample No. B17 – 11138
4.71	The microscopic picture of coal sample No. B17 – 12139
4.72	The microscopic picture of coal sample No. B17 – 14140
4.73	The microscopic picture of coal sample No. B18 – 2141
4.74	The microscopic picture of coal sample No. B18 – 4142
4.75	The microscopic picture of coal sample No. A1 – 1148
4.76	The microscopic picture of coal sample No. A1 – 5149
4.77	The microscopic picture of coal sample No. A1 – 7150

Figure

4.78	The microscopic picture of coal sample No. A2 – 3151
4.79	The microscopic picture of coal sample No. A2-4152
4.80	The microscopic picture of coal sample No. A2-5153
4.81	The microscopic picture of coal sample No. A2-6154
4.82	The microscopic picture of coal sample No. A2-8155
4.83	The microscopic picture of coal sample No. A3-1156
4.84	The microscopic picture of coal sample No. A5-3157
4.85	The microscopic picture of coal sample No. A5-4
4.86	The microscopic picture of coal sample No. A5-5159
4.87	The microscopic picture of coal sample No. A5-6160
4.88	The microscopic picture of coal sample No. A6-1161
4.89	The microscopic picture of coal sample No. A6-2162
4.90	The microscopic picture of coal sample No. A7-2
4.91	The microscopic picture of coal sample No. A7-4164
4.92	The microscopic picture of coal sample No. A7-5165
4.93	The microscopic picture of coal sample No. A9-1166
4.94	The microscopic picture of coal sample No. A9-3167
4.95	The microscopic picture of coal sample No. A9-6168
4.96	The microscopic picture of coal sample No. A9 – 9169
4.97	The microscopic picture of coal sample No. A9 – 11170
4.98	The microscopic picture of coal sample No. A9 – 13171

Figure

4.99	The microscopic picture of coal sample No. A10 – 1172
4.100	The microscopic picture of coal sample No. A10 – 3173
4.101	The microscopic picture of coal sample No. A10 – 6174
4.102	The microscopic picture of coal sample No. A10 – 8175
4.103	The microscopic picture of coal sample No. A10 – 10
4.104	The microscopic picture of coal sample No. A10 – 11177
4.105	The microscopic picture of coal sample No. A11 – 3178
4.106	The microscopic picture of coal sample No. A11 – 5179
4.107	The microscopic picture of coal sample No. A11 – 7180
4.108	The microscopic picture of coal sample No. A13 – 1181
4.109	The microscopic picture of coal sample No. A13 – 2182
4.110	The microscopic picture of coal sample No. A13 – 3183
4.111	The microscopic picture of coal sample No. A13 – 4
4.112	The microscopic picture of oil shale sample No. AS1 – 1188
4.113	The microscopic picture of oil shale sample No. AS1 – 2189
4.114	The microscopic picture of oil shale sample No. AS1 – 3190
4.115	The microscopic picture of oil shale sample No. $AS2 - 1/1$ 191
4.116	The microscopic picture of oil shale sample No. AS2 – 1/2192
4.117	The microscopic picture of oil shale sample No. AS2 – 2193
4.118	The microscopic picture of oil shale sample No. AS2 – 3194
4.119	The microscopic picture of oil shale sample No. AS3 – 1195

Figure

4.120	The microscopic picture of oil shale sample No. AS3 – 2196
4.121	The microscopic picture of oil shale sample No. AS3 – 3197
4.122	The microscopic picture of oil shale sample No. AS3 – 4
4.123	The microscopic picture of oil shale sample No. AS3/21199
4.124	The microscopic picture of oil shale sample No. AS3 – 2/1200
4.125	The microscopic picture of oil shale sample No. AS3 – 2/2201
4.126	The microscopic picture of oil shale sample No. AS3/21 – 3202
4.127	The microscopic picture of oil shale sample No. AS3/21 – 4203
4.128	The microscopic picture of oil shale sample No. OH1 – 1207
4.129	The microscopic picture of oil shale sample No. OH2 – 1208
4.130	The microscopic picture of oil shale sample No. OH2 – 2209
4.131	The microscopic picture of oil shale sample No. OH3 – 1210
4.132	The microscopic picture of oil shale sample No. OH3 – 2
4.133	The microscopic picture of oil shale sample No. OH4 – 1212
4.134	The microscopic picture of oil shale sample No. OH4 – 2213
4.135	The microscopic picture of oil shale sample No. OH4 – 3214
4.136	The microscopic picture of oil shale sample No. OH5 – 1215
4.137	The microscopic picture of oil shale sample No. OH5 – 2216
4.138	The microscopic picture of oil shale sample No. OH5 – 3217
4.139	The microscopic picture of oil shale sample No. OH6 – 1218
4.140	The microscopic picture of oil shale sample No. OH6 – 2219

Figure

4.141	The microscopic picture of oil shale sample No. OH7 – 1222
4.142	The microscopic picture of oil shale sample No. OH7 – 2223
4.143	The microscopic picture of oil shale sample No. OH8 – 1
4.144	The microscopic picture of oil shale sample No. OH8 – 2
4.145	The microscopic picture of oil shale sample No. OH8 – 3226
4.146	The microscopic picture of oil shale sample No. OH8 – 4227
4.147	The microscopic picture of oil shale sample No. OH9 – 1
4.148	The microscopic picture of oil shale sample No. OH9 – 2
4.149	The microscopic picture of oil shale sample No. OH9 – 3230
4.150	The microscopic picture of oil shale sample No. OH9 – 4231
4.151	The microscopic picture of oil shale sample No. OH10 – 1232
4.152	The microscopic picture of oil shale sample No. OH10 – 2233
4.153	The microscopic picture of oil shale sample No. OH10 – 3234
4.154	Results of the vitrinite reflectance (Ro) measurement of
	coal samples of Coal A and Coal B sub-unit
4.155	Geochemical compositions and dominated maceral type of
	each sub-unit250
4.156	Kerogen type classification of the studied samples by the HI
	and OI cross-plot on the Modified Van Krevelen diagram252

Figure	e	Page
4.157	Cross-plot of remaining hydrocarbon potential (S2) and	
	TOC (wt.%) show good to excellent potential hydrocarbon	
	generation of the studied samples	253
4.158	Evaluation of the thermal maturity stage of the studied organic	
	samples based on HI vs Tmax cross-plot (A) and HI vs measured	
	vitrinite reflectance cross-plot (B)	254
4.159	Cross-plot of Productive Index (PI) versus Tmax of the studied	
	organic samples	255



CHAPTER I

INTRODUCTION

Most of petroleum production in Thailand has been obtained from Tertiary basins. They occur both onshore and offshore (Chaodumrong *et al.*, 1983). The main petroleum producing areas in 4 geological terrains of Thailand are Gulf of Thailand, onshore Northern and Central, onshore Northeastern (Khorat basin) and Mergui basin of Andaman Sea (DMF, 2007) (Figure 1.1) and especially in northern Thailand there are more than 40 basins (Polachan *et al.*, 1991).

Tertiary basin occurred during Oligocene to Early Miocene (approximately 19 to 31 Ma), with unconformities occurred during the Upper Oligocene/Lower Miocene boundary (~24.5 Ma) and the Lower/Middle Miocene boundary (~17 Ma) (Ratanasthien, 2002). The basins developed during this age have been recognized as Cenozoic rift basins. They are very important resources for their deposited oil shales and coals throughout northern Thailand. Many of these northern Thailand basins have already generated petroleum such as Sirikit and Fang oil field. However, there are many of these basins which are uplifted and exposed their content of coals and oil shales association such as Wiang Haeng, Mae Chaem (Na Hong) in Ching Mai province, Ban Pa Kha, Li, Mae Than and Mae Teep in Lampang province, Mae Tun and Mae Lamao in Tak province. A well-known oil shale area is Mae Sot basin in Tak province (Morley and Racey 2011; Ratanasthien 2011).

1.1 Study Area

The Mae Teep basin is one of the uplift basins which exposed Tertiary oil shales and coals. It was interested in this study because of its organic deposits were clearly seen and there was not many information of these organic successions have been studied in details. The information of depositional environments of this basin could be an important key to other burial oil fields in northern Thailand.

Mae Teep basin is located about 80 kilometers northeast of Lampang city, Ngao district, Lampang province (Figure 1.2). The basin trends north-northeast – south-southwest direction and it is situated between the Ngao and Phrae basin. The valley of the basin has flat-rolling topography with the elevation of 220 - 280 m. msl. and the surrounding mountains rise to nearly 1200 m. msl. The northeastward along the basin is Mae Nam Tip stream which flows into the Mae Nam Ngao at the northern end of the basin. The study area is coal mined by the Suntitranon Co., Ltd. The mine area is 300 x 1,600 square meters. It is located on the 1:50,000 topography map, Ban Pa Dange L 7017 sheet 5046 III, bounded by the grid lines 2058000 N to 2055500 N and 606000 E to 609000 E of the UTM coordinate system of zone 48 N (WGS84 datum).

2

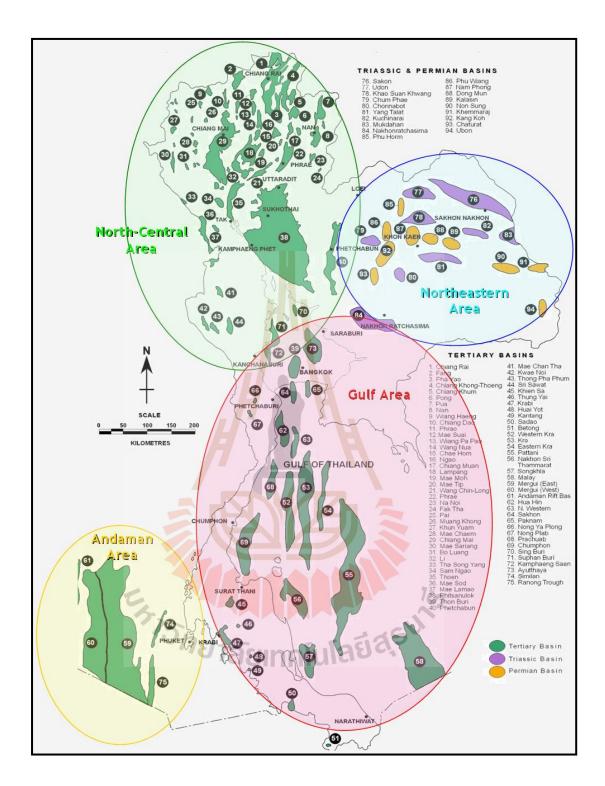


Figure 1.1 Four petroleum provinces in Thailand; the North and Central, the

Northeastern, the Gulf and the Andaman areas (after DMF, 2007).

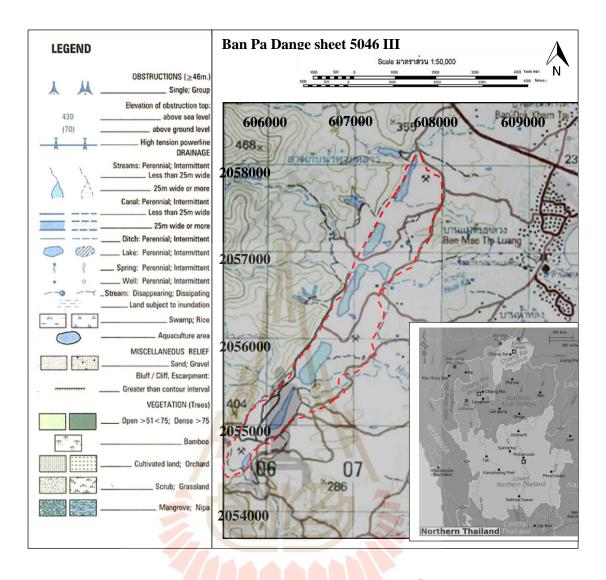


Figure 1.2 The location of the study area on map Ban Pa Dange, Map sheet 5046 III scale 1:50,000, Map Index L7018 (modified after The Royal Thai Survey Department, 1999).

10

1.2 Research Objectives

The two main objectives of this study are to identify the potential of petroleum source rocks by geochemical and organic petrology techniques, and to study the depositional environment and characteristics of potential petroleum source rocks in Mae Teep deposit.

1.3 Limitations and Scope of works

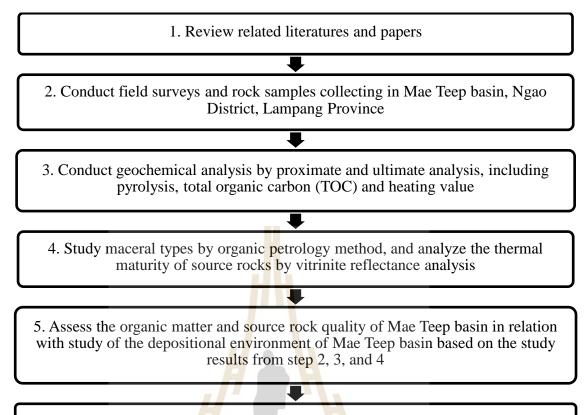
The study had been scoped only in the Mae Teep coal field of Sintitranon Ltd. in Mae Teep basin. Rock samples were prepared at Rock and Fluid Laboratory of Suranaree University of Technology, Nakhon Ratchasima province, Thailand. Geochemical analysis in this study were conducted by proximate and ultimate analysis according to the ASTM standard methods. Heating values of samples were examined at chemical lab testing unit of EGAT' Mae Moh coal mine, Lampang Province. Maceral types of samples were studied by petrography analysis at the Department of Geological Sciences, Chiang Mai University, Thailand. Pyrolysis analysis, including TOC and vitrinite reflectance (Ro), were conducted by Energy Resources Consulting Pty Ltd in Australia.

1.4 Expected Result

A better understanding in geology, stratigraphy, depositional environment of organic sedimentary rocks, and characteristics of potential source rocks in Mae Teep basin are the expected results of this study. In addition, results from this study could be applied to other petroleum potential basins in Thailand where have the similar depositional environments.

1.5 Research Methodology

The research methodology conducted is this study are showed in Figure 1.3, including literature review, field surveys, geochemical analysis, study of maceral types, quality and thermal maturity of the possible source rocks, the organic matter and source rock quality evaluation and study of the depositional environment of Mae Teep basin, respectively.



6. Discussion & Conclusion.

Figure 1.3 Flowchart showing research strategies and activities in this study.

1.6 Thesis contents

This thesis is divided into five chapters: Chapter I contains the research objectives and details of the study area, research methodology and scope of works that will be followed. Chapter II reviews the previous works, techniques and methodology for depositional environment of petroleum source rock evaluation, maceral classification and interpretation of petroleum potential. Chapter III describes methodology used in this study in detail, including fieldwork, sampling method, geochemical and petrographic analysis. Chapter IV presents results of the study and discussions in 2 topics: 1) the depositional environment and maceral character related to geochemical composition and 2) the evolution and thermal maturation of Mae Teep deposits. Chapter V concludes and summarized results of the study and gives same recommendations for the future study.



CHAPTER II

LITERATURE REVIEW

This chapter presents the summary of the reviewed literatures that related to this study, including 1) Petroleum and coals in Tertiary basins of Thailand, 2) Mae Teep basin, 3) source rock classification and 4) petroleum source rocks evaluation respectively.

2.1 Petroleum and coal in Tertiary basins of Thailand

The main petroleum province of Thailand can be classified as follows: (1) Gulf of Thailand, (2) Onshore Northern and Central, (3) Onshore Northeastern (Khorat basin) and (4) Mergui basin, Andaman Sea (DMF, 2007). Gulf of Thailand is the main area for oil, gas and condensate production. The Northern and Central is the main area for oil exploration and development. The current production of gas, oil and condensate has been from 19 producing gas fields (18 offshore and 1 onshore) and 22 oil fields (19 onshore and 3 offshore).

From the economic important, the knowledge of hydrocarbon source rocks is recognized in Tertiary basins occur onshore and offshore, more than any other stratigraphic age (Polachan et al.,1980). They are generally associated with rift basins formed in extensional, transtensional or strike – slip settings. Morley and Racey (2011) mentioned that Tertiary basin unlike from main area petroleum geology of Thailand. In Northern and Central Thailand have 42 intermontane basins varying in size from a few kilometers to over 150 km. (Polachan and Satayark, 1989; Uttamo et al.,2003). There is marked variation among the onshore basins in the timing of rifting and deposition. In general, basin formation and deposition occurred earlier in the western onshore basins (Late Oligocene – Early Miocene) and later in the eastern basins (Early to Middle Miocene). Moreover, there is often marked variation in basin-fill between the basins, although it is all alluvial-fluvial-lacustrine (Polachan et.al, 1991; Morley et al., 2001). The basins fall into two types: (1) smaller, intermontane basins in the Western Highlands, associated Mae Ping and Three Pagodas faults and (2) larger extensional basins located beneath the flat Central Plain region (Gibling, Ukakimaphan and Stisuk, 1985; O'Leary and Hill, 1989).

Burri (1989) summarized the petroleum potential of onshore basins of Thailand as follows;

 Basin with a thick organic-rich lacustrine fill, Central and Northern Thailand. Source rocks in these basins have generally reached the oil window at depths of 1.4 - 3 km.

2) Basins dominated by alluvial deposits generally lack petroleum source rocks. Even if potential source rocks are present, the total sediment thickness may be too thin to have permitted hydrocarbon generation. These basins are considered unprospective such as Sing Buri and Ayutthaya basins.

3) Basins dominated by swamp deposits with thick lignite, for example, the Mae Moh and Li basins near the Lampang Basin in Northern Thailand, generally have a limited sediment thickness. The main factor downgrading the prospective of these basins are the lack of thermally mature source rocks.

Burri (1989) and Racey (2011) concluded that depositional environment of Tertiary basins in Thailand are mainly lacustrine, alluvial and swamp. The lacustrine basins are located in Northern and Central Thailand and they are generally reached the oil window. Basins dominated by swamp deposit with thick coal are mostly found in Northern Thailand. They have a limited sediment thickness and the main factor downgrading the prospectively of these basins is the lack of thermally mature source rocks.

Onshore Tertiary basins having yielded significant hydrocarbon discoveries are Fang basin, Phisanulok basin, Phetchabun basin, Wichian Buri sub-basin and Suphan Buri/Kamphaeng Saen basin. The main petroleum and source rock associations are common in North Thailand. The largest petroleum potential in Chiang Mai province was found in Fang (Sethakul 1984; Burri 1989; Pradidtan 1989; Songtham, 2003). The similar other basins are Wiang Haeng and Mae Chaem (Na Hong) basin in Chiang Mai province, Ban Pa Kha, Li, Mae Than and Mae Teep basin in Lampang province, Mae Tun and Mae Lamao basin in Tak province (Morley and Racey, 2011; Ratanasthien, 2011).

However, most of onshore intermontane Tertiary basins in Thailand have been explored for coal resources, e.g. Chae Khon, Mae Chaem, Chiang Mai, Ngao, Lampang, Mae Tha, Mae Than, Mae Moh, Mae Teep, Li, Chae Hom, Wiang Haeng and Fang basins (Ratanasthien, 2011). There is only one coal deposit with oil shale is Khian Sa Basin in Surat Thani province (Morley and Racey, 2011). Mae Moh basin is the largest productive coal mine in Lampang provinces and Southeast Asia. The other Tertiary basins in the provinces are Wang Nua, Jae Kon, Jae Hom, Nago, Mae Teep, Mae Tha, Mae Than, and Serm Ngarm basin. In 2008 only four mines were in operation in Mae Moh, Mae Teep and Mae Than basin (Ratanasthien, 2011). Racey (2011) described onshore Tertiary basins of Northern Thailand as follows;

Fang Basin is in the northernmost Thailand, occupies an area of 670 km². The basin is divided by strike-slip faults into 3 sub-basins. The Miocene – Pliocene lacustrine sediments are main exploration target, with sediment in the main organic-rich shales and lignite and reservoir quality sandstone. The discovery was encountered a combined structural/stratigraphic trap with production from coarse fluvial-lacustrine sandstone of the inferred Mae Sot Formation, sourced and sealed by lacustrine shales of similar age.

Mae Sot Basin covers 700 km² in Northwestern Thailand extend westwards into Myanmar. No oil and gas have been discovered yet in this basin, but it had been estimated 18 billion tons of oil shale (Chaodumrong et al., 1983). The average total organic carbon (TOC) contents in the oil shale is 20% and reach peaks of 63%, while vitrinite reflectance at the surface is around 0.4%Ro (Gibling et.al., 1985).

Ratanasthien et al. (1992) presented the results of proximate and ultimate analysis of coal fields in Lamphun province. The coal samples were collected from Ban Pu, Ban Hong, Na Klang, Ban Pa Kha, Mae Long Bok and Na Sai coal field. The proximate results indicated 14 - 47 % moisture, 25 - 49 % volatile matter, 2.2 - 25 % ash, and 16 - 41 % fixed carbon. The ultimate results indicated 29 - 65% of carbon, .8 - 6.7% of hydrogen, 0.24 - 1.28 % of nitrogen, and 0.27 - 5.6 % of sulphur.

Petersen et al. (2006) investigated Thai oil shales and coals and his study results are showed in Table 2.1 and 2.2. Results of his study indicated that Thai oil shales were deposited in freshwater to brackish. They have total organic carbon (TOC) range from 371 to 44.18 wt.%. H/C ratios range from 0.80 to 0.90 which is corresponded to Type III kerogen. HI values range from 50 to 300 mg HC/g TOC and this is indicated a potential for oil/gas generation. Furthermore, the study of organic petrographic of the oil shales found that they were dominated by liptinite maceral. Most of the Li, Na Hong and Mae Lamao oil shale contain lamaginite. They are thermally immature (0.11 to 0.28 %Ro). Vitrinite reflectance values of most of Thai coals range from 0.38 to 0.47 %Ro, except the coal of Fang basin which has 0.59 %Ro. The oil window is estimated at 0.82 (Suphan Buri basin) to 0.98 %Ro (Fang basin).

	Moisture	Ash	С	Η	Ν	S	0	H/C	O/C
Basin	%	%		9	% (d.a.f	E)		Ato	mic
		(dry)		H				rat	tio
Fang	1.25	48.75	70.22	4.67	1.81	6.71	16.59	0.80	0.18
Li	11.04	2.66	77.12	5.12	1.40	0.44	15.92	0.80	0.16
Mae Lamao	12.77	21.33	70.84	5.54	2.38	1.79	19.45	0.94	0.21
Mae Ramat	15.50	7.04	68.02	4.67	2.01	1.79	19.36	0.81	0.21
Na Hong	9.87	8.76	69.36	5.20	1.61	5.94	23.24	0.90	0.25
Wiang	5.70 🥌	20.90	70.65	6.45	1.93	0.58	18.70	1.10	0.20
Haeng									

Table 2.1 Source rock data of coal (Peterson et al., 2006)

 Table 2.2 Source rock data of oil shale (Peterson et al., 2006)

	Moisture	Ash	С	Η	Ν	S	0	H/C	O/C
Basin	%	8%	uno	FuF	% (d.a.	f)		Ato	omic
		(dry)	711 Iri	IUN				ra	tio
Li	2.33	52.73	60.73	7.64	1.40	16.94	26.6	1.53	0.175
Mae	3.83	89.34	40.86	9.80	3.71	8.94	36.71	2.90	0.68
Lamao	2.75	54.38	66.32	8.72	1.81	1.82	21.33	1.57	0.25
Mae Sot	3.12	50.25	59.32	7.46	1.88	7.49	23.86	1.51	0.305
Na Hong									

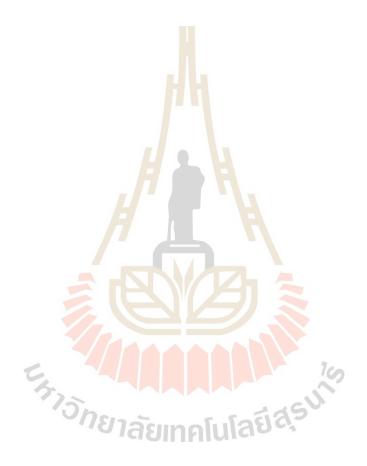
Ratanasthien (1997) studied algae type of oil source rock in northern Thailand and also classified them into alginite maceral consisting of telalginite and lamaginite. The telaginite consists of *Botroyococcus* brownie, *Botryococcus* sp., *Pila* sp. and *Reinschia*. Lamaginite is long shape algae and it is used to indicate depositional environment changing from lacustrine to temperate forested swamp.

Ratanasthien (1999) studied oil source rock in fang oil field, northern Thailand, using petrography study. Results of the study indicated that the lower part of Tertiary deposits succession contains only alginite A (*Botryococcus* sp.). The association of *Botryococcus braunii*, *Pila* algae, thick walled alginite B were found in the middle part of the studied sediment succession. The upper part of the studied sediment succession is dominated by alginite B with *Botryococcus*-related *Pila* algae, *Reinshia* and ferns. In Mae Sot basin, *Reinshia* is dominant in the northern part where as lamalginite is dominant in the south. Therefore, these evidences suggest the changes in depositional environments during Tertiary in northern Thailand.

2.2 Mae Teep basin

Coal in Mae Teep basin was first observed by Piyasin (1972). He found coal beds intercalated with shale along the Nam Mae Teep river. Their age is not known but they are presumed to be Tertiary by comparison with coal bearing strata elsewhere in Northern Thailand (Gibling and Ratanasthien, 1980; Gibling, Ukakimaphan and Srisuk, 1988; Ratanasthien, 1992).

The Mineral Fuels Division, Department of Mineral Resources (DMR) (1980) explored and drilled some exploration wells and found the Mae Teep basin trended north – south direction. The sedimentary strata on the western margin of the basin strike N10° – 30°E and dip eastwards at about 20° - 40°, with minor faulting and surrounded by Permian-Triassic rocks. The northern part of Mae Teep basin comprises Jurassic sandstone interbedded with shale and conglomerate (DMR, 1994) (Figure 2.1). The southern part of the basin comprises upper Triassic shale, sandstone, siltstone, mudstone, conglomerate, and limestone. The western part of the basin is bounded by the Triassic Pha Daeng



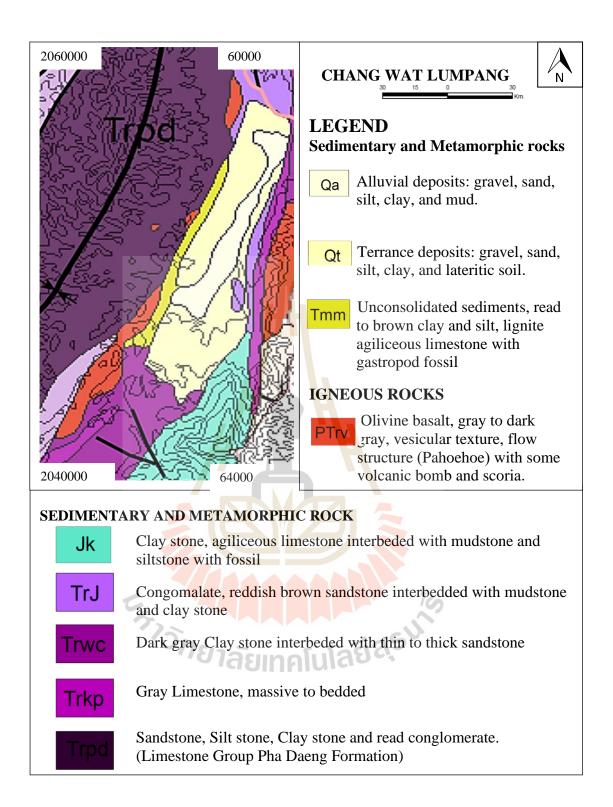


Figure 2.1 Geological map of Mae Teep basin and surrounding area (modified after

DMR, 1994; Charoenprawat et al., 1994)

Formation, consisting of sandstone, siltstone, conglomerate, and shale. The basement rock of Mae Teep basin is related to limestone of upper Permian - Triassic and bounded to the east of the basin. The volcanic rocks of Triassic-Permian exposed in the western part of the basin along the north to south (Piyasin, 1957; Chaodumrong et. al., 2002)... The descriptions of rocks in the vicinity of Mae Teep basin are shown in Table 2.3.

 Table 2.3 The rocks boundary around Mae Teep basin divided by age (Chaodumrong)

Age	Units				
Quaternary	Alluvial deposits: gravel, sand, silt, clay, and mud.				
	Terrace deposits: gravel, sand, silt, clay, and lateritic soil.				
	Erosional Surface				
Tertiary	ary Interbedded claystone, sandstone, mudstone, diatomite, and shale				
	with fossil leaves, stems, bone of fish, and Viviparus sp.				
	Unconformity				
Jurassic	Sandstone, purplish brown, fine-grained, calcareous, interbedded				
	with shale, reddish brown, limestone nodules; shale, gray,				
	intercalated with sandstone, fine-grained; and conglomerate.				
Triassic	Upper Triassic divided into 2 units are 1) limestone, gray, massive				
	to bedded; shale and sandstone, gray to greenish gray; with fossil				
	<i>Cassianella</i> sp. and brachiopods, and 2) shale and sandstone, gray				
	to greenish gray; siltstone; mudstone; conglomerate; and limestone;				
C	with fossils Halobia sp., Cassianella sp., Liostrea sp., Unionites				
	sp., and bivalves.				
	Middle to Upper Triassic: Pha Daeng Formation of Lampang				
	group (Piyasin, 1975) consists of sandstone, red to reddish brown,				
	cross-bedded; siltstone, conglomerate and shale.				
	Unconformity				
Permo-	Igneous rocks; Olivine basalt, gray to dark gray, vesicular texture,				
Triassic	flow structure (Pahoehoe) with some volcanic bomb and scoria.				
Permian	Limestone interbedded black shale, gray sandstone, dark gray				
	mudstone and gray limestone with chert nodules; intercalated with				
	fossiliferous limestone and mudstone, abundant fossils of				
	Paleofusulinasinensis (Sheng) and common Colaniella cf. lepida				
	(Wang). Assemblage with fragments of crinoid stems, bivalves, and				
	blue algae coated by oncolith.				

et. al., 2002).

According to the study of Ratanasthien (2011) Mae Teep Tertiary sediments have a total thickness approximately 100 m and can be divided into three units described in ascending order as follows;

1) Underburden

This unit consists mainly of gray claystone in the upper part and white to gray gravelly sandy claystone in the lower part. It is up to c. 50 m. thick.

2) Main Coal Seam

The lower part of unit consists of coal interbedded with carbonaceous shale. The coal is hard, dense and black in color. The middle part consists of coal and sheeted coal interbedded with carbonaceous mudstone, and the upper part consists of coal interbedded with oil shale. The thickness of unit is 30 m. The coal is hard, dense and black and its rank ranges from sub-bituminous to high-volatile bituminous C.

3) Overburden

The lower part of this unit is dark-gray to black oil shale with a thickness of 5-7 m. The upper part of the unit consists mostly of black shale and claystone with a thickness of 25 m. Beds of hard, dense, brown sandy mudstone, 15-20 cm. thick, occur in places.

Ratanasthien (1989) studied the stratigraphic unit of sediments in Mae Teep basin. Results of the study indicated that Mae Teep basin consists of 6 stratigraphic units in ascending order as topsoil unit, claystone, shale and conglomerate unit, oil shale unit, coal unit, claystone, shale, sandstone and conglomeratic sandstone unit and basement unit. The total thickness of the studied succession is about 91 m.

Petersen et al. (2006) reported that the Mae Teep coal field has TOC between 40-58 wt.% TOC. The maceral compositions are corpohuminite, densinite, suberinite

(Su) and exsudatinite (Ex) in association with suberinite. Study results indicated that maceral types are mainly of huminite (80 - 82%) and liptinite (18 - 19%) and some of inertinite group (less than 1%). The average vitrinite reflectance is 0.425 %Ro. This is indicated the thermally immature source.

The results of proximate and ultimate analysis of Mae Teep coal and oil shale samples from the study of DMR (1981), Enrich Consultants (2005) and Ratanasthien (2011) are compared and showed in Table 2.4

 Table 2.4 The results proximate and ultimate analysis of Mae Teep coal and oil shale samples.

Authors / Methods		DMR, 1981	Enrich Consultants, 2005		Ratanasthien, 2011
Authors	/ Methods	As- determined	As- determined	Dry basis	As-determined
	Moisture	2 <mark>6</mark> .22 – 8.57	25.55	-	13.7 - 23.3
Proximate analysis	Volatile Matter	41.78 – 28.79	31.20	41.91*	21.8 - 36.4
oxi nal	Ash	38.07 - 4.27	11.91	15.97*	8.16 - 39.7
Pr	Fixed carbon	54.58 – 20.77	31.33	42.12*	23.8 - 30.8
s e	Carbon		-	-100	17.7 – 58.9
Ultimate analysis	Hydrogen			-	5.39 - 8.58
ltir nal	Nitrogen	-	-	164	0.61 - 2.24
a	Sulfur	7.96 - 0.54	1.0225	1.37*	0.92-1.94

2.3 Source rocks classification and environment deposition

In petroleum geology, source rocks are fine-grained sedimentary deposited with organic materials and generating hydrocarbons (Law, 1999). The geological history shows main groups of biomass possible organic contribution to sediments in time with marine and non-marine are mostly of algae which were found since Precambrian to Paleozoic and Cenozoic with the adding of land plants which commencing mostly in Cenozoic (Tappan and Loeblich, 1970). The accumulation modes of organic material can be divided into 4 modes; sea water, brackish water, fresh water and on land (Stopes and Wheeler, 1918). They are many researchers studied in hydrological environments such as Cohen et al., 1989; Petersen and Nielsen, 1995; Roberts and McCabe, 1992; Sebag et al., 2006a; 2006b; Staub, 1991 and Wang et al., 2011.

The relationship among organic-rich rock, known precursors, rock types and environment of depositional can be illustrated as showed in Figure 2.2 (Hutton, 1982; Hurron, 1987; Sykes, 2001)

Four swamp types can be distinguished on the basis of plant communities: 1) open-water areas with water plants (in part submerged), 2) open reed swamps, frequently with sedges, 3) forest swamps, and 4) moss swamps (Stach, 1975).

Brook et al. (1987) and many authors (Durand and Paratte, 1983; Hunt, 1991; Thomas, 1982) distinguished source rocks in difference type. The characteristic of source rocks are based on amount and type of organic matters and their physical and chemical composition. The component of organic matter in petroleum source rocks are presented in form of maceral types. The classification of maceral components is established by the International Committee for Coal and Organic Petrology (ICCP, 1998, 2001 and Sýkorová et al., 2005). A similar system is also used in a rank-based international classification of hard coal and brown coal. The macerals can be divided into three groups which are vitrinite/huminite, liptinite/Exinite and inertinite.

The kerogen evolution presents the stage of burial of source rocks. The kerogen is classified into three basic types (Type I, II and III) based on carbon, hydrogen and oxygen ratio (Tissot and Welte, 1978; Selley, 1985). Van Krevelen

(1993) developed a simple diagram for kerogen type classification based on H/C and O/C atomic ratios. The successive evolutions are corresponded to composition and they can be indicated principal generated products in three stages of maturity; diagenesis, catagenesis and metagensis. The amount of petroleum generated and expelled from source rock increases as the increasing of hydrogen to carbon ratio (H/C) of the organic matter (Hunt, 1996).

Tissot and Welte (1984) modified Van Krevelen diagram to utilize pyrolysis parameters (oil yield, kerogen yield and CO_2 and CO product) and total organic carbon (TOC). The hydrogen content of kerogen is the controlling factor for oil and gas yields from the primary hydrocarbon-generating reactions. The modified van Krevelen diagram classifies kerogen type into four types, I, II, III and IV, based on the different amounts of hydrogen to carbon and oxygen atom.

Maceral types correspond to the fraction of organic matter in sedimentary rocks in term of kerogen. The maceral characteristics are related to the kerogen type which is determined by hydrocarbon parameters: oil yield (S1), kerogen yield (S2), amount of (S3) and Total Organic Carbon (TOC). This refers to the petroleum expelled as show in Table 2.5.

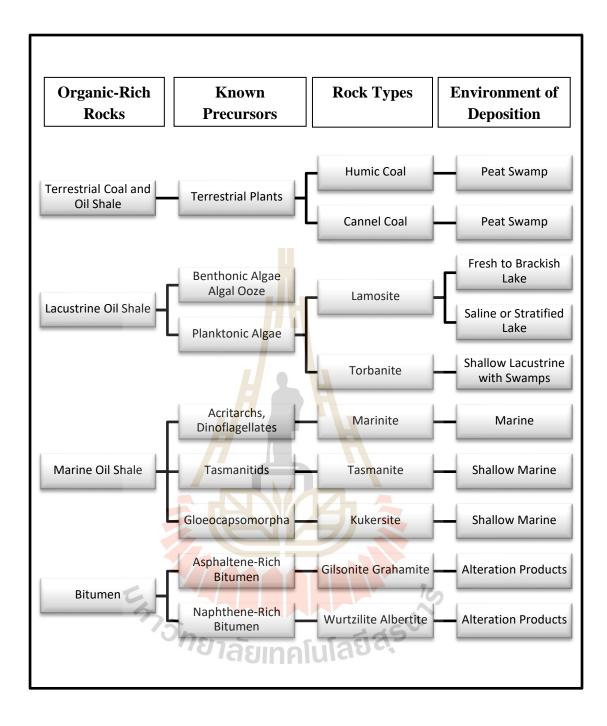


Figure 2.2 Relationship among organic-rich rock, known precursors, rock types and environment of depositional (modified after Hutton, 1982)

Table 2.5 Relationship among kerogen, maceral types, hydrocarbon index (HI), S2 to S3 ratio, and petroleum product expelled at maturity (modified after Peters and Cassa, 1994).

Kerogen type	Kerogen Composition (Marceral)	Hydrogen Index (HI)	S2/S3	Main Product
Ι	Amorphous/Alginate	>600	>15	Oil
II	Exinite	300 - 600	10 - 15	Oil
II/III	Exinite/Vitrinite	200 - 300	5 - 10	Mixed oil and gas
III	Vitrinite	50 - 200	1-5	Gas
IV	Inertinite	< 50	< 1	Gas

Pasley (1991), Jones (1987) and Tyson (1995) defined organic facies by geochemical, and optical data (microscopy). They integrated the organic petrography and organic geochemistry data not only to improve the better understanding of the occurrence of oil source rocks, but also to use it as a prediction tool. The seven organic facies defined by Jones (1987) are A, AB, B, BC, C, CD and D as presented in Table 2.6.

Petroleum source rock potential is directly related to its volume, organic richness and thermal maturity (Isaksen et. al., 1998). The potential of source rock is applied to a rock contains sufficient organic matter of suitable chemical composition to generate and expel hydrocarbons via biogenic or thermal processes (Miles, 1994). This is applied irrespective of whether its organic matter is mature or immature (Durand, 1993; Belaid et al., 2010).

The type of petroleum source rocks potential can be divided into four major categories: potential, effective, relic effective and spent source rock (Jeffrey, 1993;

Law, 1999; Ronald, Wikins and George, 2002). Each type refers to the stage of thermal maturity (immature, mature, and over/post mature).

 Table 2.6 The relationship among palynofacies, geochemical and environment factors

(after Jone,	1987;	Tyson,	1995).
--------------	-------	--------	--------

Organic Facies	Α	AB	B	BC	С	CD	D
Palynofacies							
<i>characteristics</i>							
% AOM of kerogen	Do	om <mark>in</mark> ant		Mod	Usua	ally low/a	bsent
AOM matrix	High	est	Mod-	weak	Weak	Usuall	y absent
fluorescence				-			
% prasinophytes of	Highest	Mod	Rare		Usually	very rar	e
plankton							
% phytoclasts of	Low (dil	ution)	Mod		Usually	dominar	nt
kerogen						-	
Opaque: translucent	Oft	en high	1	Usua	lly low	incr	eases
phytoclasts							
Geochemical	F						
characteristics (for							
immature sediments)							
Hydrogen Index (HI)	≥ 850	2	\geq	\geq	≥125	50 -	\leq 50
		650	400	250		125	
Kerogen type	I	I/II	II	II/III	III	III/IV	IV
TOC %	5 - 20 +	3 –	10+	3 –	≤ 3	<	0.5
				3+			
Environment factors					10		
Proximal-distal trend	I	Distal		Pro	ximal	Di	stal
Oxygen regime	Anoxic	Ano	xic-dys	oxic	О х	kic	Very
	ปาลัยเ	nal	ula	90,-			Oxic
Sediment	Low	Va	ries	Н	ligh	Mod	Low
accumulation rate							

*AOM = Algal Organic Matter

Dow (1977) reported the petroleum generative windows which related to temperature as the oil generation (oil window) at 50 - 150 °C and the gas generation (gas windows) at 150 - 200 °C. This is depended on how quickly the source rock is heated. Generally, the onset of oil generation is also correlated with vitrinite reflectance of 0.5-0.6%Ro and the termination of oil generation with vitrinite reflectance of 0.85-

1.1%Ro. The onset of gas generation (gas window) is typically associated with values of 1.0-1.3%Ro and terminated around 3.0% Ro.

Cook and Kantsler (1982) modified the source rocks maturation range chart by elevated temperature associated with physic-chemical coalification and hydrocarbon generation. The maturity range is corresponded to hydrogen content (kerogen type).

2.4 Petroleum source rock evaluation and maturity

According to Law (1999) source rocks are referred to the stage of thermal maturity (Immature, Mature, and Over/Postmature). The potential of petroleum source rocks are usually assessed both in term of quantity and quality. Quantity and quality are commonly assessed by a measure of the total organic carbon (TOC), kerogen types contained in source rock, prevalence of hydrocarbons can be measured by ultimate analysis and elemental compositions, including the hydrogen and carbon ratio. They are related to the quantity of oil and gas windows of each kerogen type with temperature and depth.

There are many methods to identify oil and gas generation potential, thermal maturity and the organic matter type (Tissot and Welte, 1978). This part presents two of petroleum source rock evaluation methods, geochemical analysis and petrographic analysis.

2.4.1 Geochemical analysis

Most geochemical studies of source rocks belongs to one of the following types: elemental analysis, oxidation, hydrogenolysis and pyrolysis (Hutton, 1982). The determination for proximate and ultimate analyses follow the guide line of American Standards for Testing of Materials [ASTM]. The chemical classification of source rocks is based on chemical properties and elemental composition of organic rocks. The most commonly employed systems of methods are:

- ASTM D3302/D3302M for total moisture and instrumental procedures (ASTM, 2011d)

- ASTM D5142-09 for proximate analysis of the analysis sample of coal and coke by instrumental procedures (ASTM, 2010)

- ASTM D7582 for proximate analysis of coal and coke by Macro Thermogravimetric analysis (ASTM, 2011e) and used percentages of C, H and O to plot the composition of coal

- ASTM D2013/D2013M-1 and Practice D346-04 for preparing coal samples for analysis (ASTM, 2011c).

The total organic carbon method is used to determine the concentration of total organic carbon in sediments or in soil samples and inorganics are removed by digestion in hydrochloric solution (McKee and Goodwin, 1923; Lewis and McConchie, 1937).

The classification of organic matter based on H/C and O/C atomic ratios (Van Krevelen, 1993). Exponents of the modified Van Krevelen diagrams recognize up to 4 types of kerogen; Type I, Type II, Type III and Type IV (Tissot and Welte, 1978; Durand, 1993). Type I is aliphatic kerogen with high initial H/C (1.5) and low initial O/C (1.0). Type II has relatively high H/C and low O/C. Type III kerogen is H/C 1 and O/C 0.2 to 0.3, derived from terrestrial plant. Type IV kerogen corresponds with inertinite. Type I, II and III are plotted in the same zone as alginate, higher plant exinite and vitrinite in coal on the van Krevelen diagram (Tissot and Welte, 1978).

Van Krevelen (1950) mapped the natural pathways of the major groups of coals (sapropelic and humic) as they thermally mature by using elemental analysis data on a plot of H/C vs. O/C (Figure 2.3). The various macerals of coal follow distinct pathways with distinct changes in H/C and O/C as they thermally mature (but all with decreasing H/C and O/C). Van Krevelen's work laid the foundation for the geochemical assessment of kerogens. However, as coals are terrestrial in origin, the thermal evolutionary pathway of marine macerals is still unknown.

The introduction to organic geochemistry by Killops (2005) and the biomarker guide by Peters, Walters and Moldowan (2005) indicated that the thermal maturation pathways of petroleum source rocks are approach specifically to kerogen that they contain. Tissot plotted data for kerogens that were falling on trend line (Figure 2.4). The labeled trend lines were foundation of the kerogen classification scheme that most geochemists use today with Type I kerogens being of lacustrine origin, Type II of marine origin, and Type III of terrestrial origin.



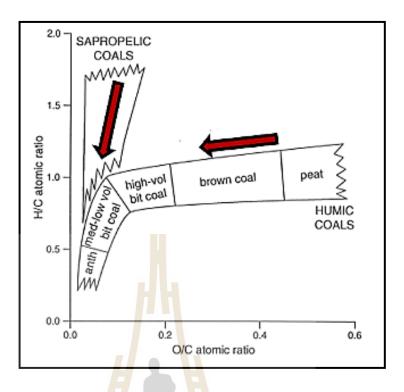


Figure 2.3 Van Krevelen diagram showing the evolutionary trends of dominant coal types (Van Kervelen, 1950).

Type I kerogen is the rarest of the three types and usually forms in oxygen-deficient, relatively fine-grained, shallow-water environments, with abundant freshwater algae (e.g. lagoons and lakes).

Type II kerogen can potentially be formed in a variety of environments, but generally in marine settings where the major source of organic matter is autochthonous phytoplankton from the water column.

Type III kerogen is formed from vascular plants and often contains identifiable plant debris, thus proximity to land is mandatory.

The major difference between what Tissot developed in the 1970's and what we use today is that we no longer use the hydrogen, carbon, and oxygen elemental composition of kerogen (which is required to achieve the H/C and O/C ratios plotted on the van Krevelen diagram), instead we use the Hydrogen Index (HI) and Oxygen Index (OI) achieved through Rock-Eval Pyrolysis as developed (Figure 2.4).

Based on methods developed during the early 20th century for coal science, kerogens (and thus petroleum source rocks) are most commonly typed based on their relative abundance of hydrogen, carbon, and oxygen. Traditionally, the amount of H, C and O were determined via elemental analysis (ultimate analysis) of chemically purified kerogen and plotted in terms of H/C and O/C on a van Krevelen diagram. Since the late 1970, Rock-Eval pyrolysis has been used to determine the HI and OI of source rock kerogens which are proxies for the H/C and O/C, respectively. The results HI vs OI are then plotted on the modified Van Krevelen diagram. The beauty of Rock-Eval is that it's cheap, fast, and does not require the lengthy, hazardous, expensive procedure of chemically purifying the kerogen from the source rock prior to analysis. The work by Van Krevelen, Tissot, and Espitalie have resulted in the lumping of kerogen into three main groups, Type I (lacustrine), Type II (marine), and Type III (terrestrial). Moreover, kerogen type can be classified into 4 types based on palynology and chemical composition related to maceral type (Mendonca Filho et al., 2012) (Table

2.7).

⁷ว*ิกยาลั*ยเทคโนโลยีสุร^ง

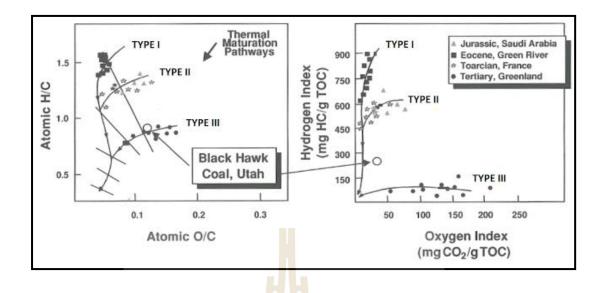


Figure 2.4 Van Krevelen diagram (left) showing thermal maturation trends of the different kerogen types on a plot of H/C vs. O/C. The modified Van Krevelen diagram (right) showing the same kerogen as that on the left, but analyzed using rock-Eval pyrolysis and plotted in terms of Hydrogen Index and Oxygen Index (Peters et al., 2005).

 Table 2.7
 The main type and evolution paths of kerogen occurred in difference type of palynology. (Mendonca Filho et al., 2012)

Palynology	Algal	Amorphous	Herbaceous	Woody	Coaly
Macerals	5	Liptinite (Ex	inite)	Vitrinite	Inertinite
Evolutionary	Ту	pe I or II	Type II	 Type III 	Type IV
Pathway					
H/C	1	.7 – 0.3	1.4 - 0.3	1.0 - 0.3	0.45 - 0.3
O/C	0.	.1 - 0.02	0.2 - 0.02	0.4 - 0.02	0.3 - 0.02
Hydrogen	9	000 - 50	600 - 50	200 - 50	< 50
Index					
Source	Lac	ustrine and	Terrestrial	Terrestrial	Terrestrial
Material		Marine			and
					Recycled
Hydrocarbons	Μ	lostly Oil	Oil and Gas	Mostly Gas	Very little
Generated					gas

2.4.2 Petrographic analysis

The basis of organic petrography is optical microscopy that includes reflected and transmitted light, fluorescence and polarized light analysis of the organic matter in a broad sense. Maceral are microscopical organic entities derived from terrestrial, lacustrine and marine plant remains and modified by deposition processes, early diagenesis and subsequent thermal evolution. There are three maceral groups: huminite/vitrinite, liptinite/exinite and inertinite (Teichmuller, 1975; Teichmuller and Durand, 1983). Over the last two decades the International Committee for Coal and Organic Petrology (ICCP) has defined the description of maceral and revised their nomenclature (Suarez-Ruiz et al., 2012). Macerals classification based on ICCP (1995 and 2001) and Australian Standard (AS) (1986) and ASTM (1996) are compared and presented in Table 2.8.

The microscical determination of polished surfaces of vitrinite and other macerals can be measured their light reflectance in both the mean maximum and mean random reflectance. The vitrinite reflectance is determined by the percentage of incident light reflected from the surface ($\[mathcal{R}_0\]$) based on vitrinite particles measured in an individual grain (Tissot et al., 1987).

According to vitrinite determination was became a skilled operation to both distinguish maceral of autochthonous and allochthonous vitrinite. It was the autochthonous or primary vitrinite that measurements should be made on and the values were derived from primary vitrinite that should be recorded. False values of maturity will result if unsuitable particles are measured (Matchette-Downes, 2009). Table 2.8 Classification of maceral based on International Committee for Coal and

Organic Petrology (ICCP) (after ICCP, 1995 and 2001; Stracher, Prakash and Ellina V. Sokol, 2012)

Maceral Group	Maceral Subgroup	Maceral (ICCP, 1995)	Maceral (AS 3856, 1986)	Maceral (ASTM D2799, 1996)
Vitrinite	Telovitrinite	Telinite Collotelinite	Textinite* Texto- Ulminite* Eu-Ulminite* Telocollinite	Vitrinite
	Detrovitrinite	Vitrodetrinite Collodetrinite	Attrinite* Densinite* Desmocollinite	
	Gelovitrinite	Gelinite Corpogelinite	Corpogelinite Porigelinite* Eugelinite	
Liptinite			Sporinite Cutinite Resinite Liptodetrinite Alginite Suberinite Fluorinite Exsudatinite Bituminite	Sporinite Cutinite Resinite Alginite
Inertinite	Telo-Inertinite		Fusinite Semifusinite Sclerotinite	Fusinite Semifusinite Sclerotinite
	Detro- Inertinite Gelo-Inertinite	บเทคโนโลรี	Inertodetrinite Micrinite Macrinite	Inertodetrinite Micrinite Macrinite

*Maceral mostly in Tertiary basin

Levine (1993) compiled to report the evolution of coal as source rock and reservoir rock for oil and gas that the term maturation is commonly used synonymously with coalification. However, maturation is a broader term that refers more accurately to the complete set of compositional changes influencing sedimentary organic matter (OM) during burial, some of which occur in the near- surface environment prior to and/or after diagenesis. The importance of this distinction lies in the fact that the various organic micro constituents in a single coal, having all experienced the same digenetic history, are technically of the same rank, but may exhibit widely varying degrees of compositional maturity. Inertinite macerals, for example, are compositionally mature even at low rank, having many of the same characteristics as vitrinite at much higher rank. As a consequence of coal being comprised of a mixture of materials of differing maturities, rank determination can be problematical for coals having unusual petrographic composition. For example, volatile matter yields of inertinite-rich Gondwana coals are abnormally low at low rank, giving them the appearance of a higher rank coal as compared with vitrinite- rich Euro-American Carboniferous age coals; or vitrinite reflectance of some alginite- rich coals can be suppressed at moderate rank, giving them the appearance of lower rank coals. Both of these examples are relevant to the present paper, as they specifically relate to the generation and partial retention of molecular hydrocarbons in coal.



CHAPTER III

METHODOLOGY

Research methodology in this study can be divided into 3 main parts; fieldwork, sampling methods and sample analysis (Figure 3.1). Fieldwork had been conducted to study geology and litho-stratigraphic units of the study area. The organic sediments sampling comprises samples collecting and preservation, samples description, and samples preparation for analyses. Geochemical analysis in this study comprises proximate analysis, ultimate analysis, heating value and pyrolysis analyses. Petrographic analysis comprises maceral identification and vitrinite reflectance measurement. Details of each work step are described as follows.

3.1 Fieldwork

Fieldwork is an important part of geological investigation as it provides many of data of environment conditions and petroleum potential source rocks of the studied organic sediments.

In this study fieldworks had been conducted during 15-17 June 2015 and 3-6 October 2015 at the studied sediment succession in the vicinity of Mae Teep coal mine, especially at mine-front. The objectives of this fieldworks are: 1) to study the lithology and stratigraphy of the studied sediment succession, and 2) to collect organic sediment samples for geochemical analysis and petrography study in laboratory. During conducting fieldwork, the necessary information including thickness of each rock layer, rock type, and location of rock sample are noted in field-note (Figure 3.2).

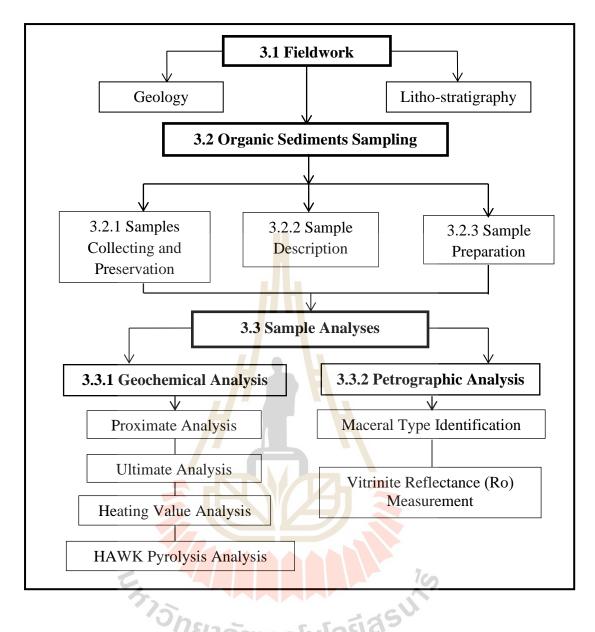


Figure 3.1 Steps of work and methodologies conducted and used in this study.



Figure 3.2 Fieldwork activities: measuring thickness of each layer by measuring tape (A), note taking everything on field note book (B), samples collecting (C).

3.2 Organic sediments sampling

Organic sediments sampling in this study comprises 3 main parts; sample collecting and preservation, sample description, and sample preparation. Details of each part are given as follows.

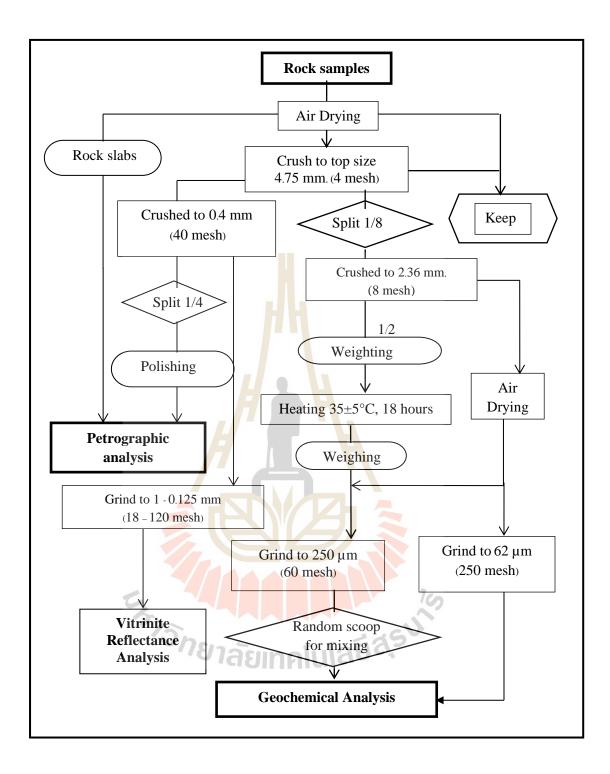
3.2.1 Samples collecting and preservation

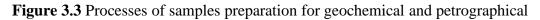
Sample collecting and sample preservation from contamination are importance for laboratory work. Fresh rock samples about 5 kg from each sampling point were collected following the ASTM D 4596 – 09 standard (ASTM, 2011b) and stored in plastic bags.

3.2.2 Sample preparation

All of samples required air drying before feeding properly through the crushing, washing and dividing equipment. The air-dried samples were prepared following standard practice for preparing coal samples for geochemical analysis of ASTM D2013/D2013M-11 and Practice D346 – 04. The samples were air dried for 1-3 days to remove free moisture and were then crushed into the size less than 4.75 mm (4 mesh). After that, the samples were split into 8 parts by a dividing equipment machine, and then they were grinded to size smaller than 2.36 mm (8 mesh). Some of samples was ovened at 40 °C for 18 hours. Each sample was weighted before and after ovened. The lost weight of samples after ovened was recognized as the free moisture. Samples were then grinded to smaller than 1 mm (20 mesh) for vitrinite reflectance analysis and the rest were grinded to smaller than 250 μ m (60 mesh) and 62 μ m (250 mesh) for geochemical analysis. Steps of samples preparation are showed graphically in Figure 3.3.

Oil shale and other hard rock samples were prepared for microscopic analysis by cutting as polished rock slab specimens. The slabs were cut perpendiculars and parallel to the bedding plane approximately 2 cm wide, 3 cm long and 1.5 cm thick. Coal, clays, soft or brittle rock samples were grinded to smaller than 4 mm (20 mesh) to make resin mounting polished specimens. The mounting polished specimens were made up by mixing liquid epoxy resin with hardener and pour over the samples in molds for 12 hours. Next step, molded and slap samples were polished on the glass plate with aluminum oxide size No. 200, 400, 600 and 1000 with water as a lubricant. After that they were polished with 1-5 microns chrome oxide and 0.005 microns γ -alumina on the rolling table over the polishing pad or chamois cloth.





analysis.

3.3 Methodology of sample analysis

In this research geochemical and petrographical analysis were applied. The geochemical analysis was used to determine composition and quality of coal samples. The chemical contents of elements and compositions in organic source rocks samples in this study were examined by proximate, ultimate, heating value and HAWK pyrolysis methods. Whereas the physical property of organic source rocks samples was examined by reflected light microscopic in petrographic analysis. This technique was used to determine the depositional environments and to classify organic rock samples maceral type; vitrinite, liptinite and inertinite, which hint to indicate the quality of source rocks. In addition, the composition of source rocks was also considered together with results from maceral analysis and values of vitrinite reflectance (Ro).

3.3.1 Geochemical analysis

Proximate analysis, ultimate analysis, heating value analysis and hydrocarbon source rock analysis, were conducted for geochemical analysis in this study. The procedure details of each method are as follows:

3.3.1.1 Proximate analysis

In this study the rock samples were analyzed their moisture, volatile matter, fixed carbon and ash content by the Leco TGA-701 (an automatic instrument for proximate analysis) (Figure 3.4) at the Laboratory Section of Geology Department, Mae Moh Mine Planning and Administration Division.



Figure 3.4 Leco TGA-701 (an automatic instrument for proximate analysis).

These instrumental test methods cover the determination sequentially of moisture, volatile matter, and ash in a single instrumental procedure whereas the fixed carbon can be determined by calculation. Theoretically, the instrumental of proximate analysis is recorded repeatedly as a function of temperature and time (Figure 3.5). The sequentially process for moisture, volatile and ash content determination can be listed as follows;

A) Prepared rock powder sample was dried up by heating at 35
 °C for 18 hours and grinding to smaller than 60 mesh.

B) Put rock sample powder into the 18 sample slots (1 gram/sample slot).

C) The temperature was elevated up to $107 \pm 3^{\circ}$ C in nitrogen gas and measure the weight of the samples for moisture calculation. Then the temperature was elevated up to 950 °C for 7 min to measure the volatile matter of the

samples. Decrease the temperature down to 750 ± 10 °C in oxygen gas for ash analysis until the combustion completed and weight what left over as the ash content.

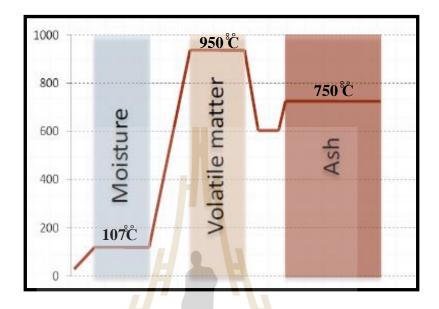


Figure 3.5 The temperate process during conducting the proximate analyses for moisture, volatile matter and ash content determination.

D) The total moisture of the rock sample can be calculated according to the ASTM D3302/D3302M standard (ASTM, 2011d) by equation 3-1.

$$M_{ar} = [M_{ad} \times 100 - Mf_{(-2.36 \text{ mm})}] + Mf_{(-2.36 \text{ mm}.)}$$
(3-1)
100

where

 M_{ar} = moisture content by weight at As-Received (percentage)

M_{ad} = moisture content by weight at As-Determined (percentage)

 $M_{f(-2.36 \text{ mm})}$ = free moisture content (percentage)

E) The fixed carbon percentage of the samples can be calculated from equation 3-2.

%Fixed Carbon =
$$100 - (\%M + \%VM + \%Ash)$$
 (3-2)

Where

%Fixed carbon = fixed carbon content (percentage)

%M	= moisture content (percentage)
%VM	= volatile matter content (percentage)
%Ash	= ash content (percentage)

3.3.1.2 Ultimate analysis

In this study the ultimate analysis was conducted to determine carbon, hydrogen, nitrogen and sulfur content of the studied samples by LECO Model Tru Spec CHN following the ASTM D5373 – 08 standard (ASTM, 2011f). Carbon, hydrogen and nitrogen content were determined by the automatic calculation of the instrument while sulfur and nitrogen were released in solution form. The quantity of elements in form of their corresponding gases (CO₂, H₂O, and NO_x) were then detected by the Infrared detector (IR) and thermal conductivity detector cell. The steps of the ultimate analysis as illustrated in Figure 3.6 are listed as follows;

A) Place the studied samples (0.1 gram) in the sample hole of the instrument for combustion at 950° C in oxygen to form oxides forms of carbon, hydrogen and nitrogen. Combustion products which can be interfered with the subsequent gas analysis were removed by specific reagent, especially SO₂.

B) Water vapor and carbon dioxide were detected and removed from the gas stream at the Infrared detector (IR) cell while oxides of nitrogen (NO_x) was separated to be N_2 before sending to the thermal conductivity detector cell to detect the nitrogen.

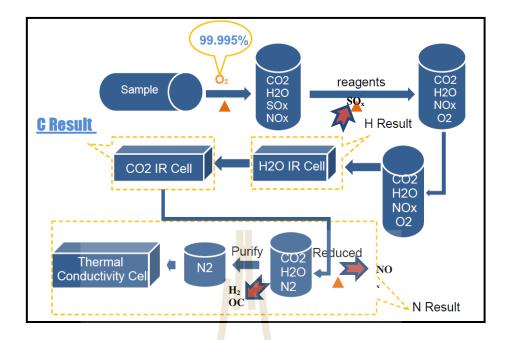


Figure 3.6 The process of the ultimate analysis to detect carbon, hydrogen and nitrogen content by IR cell and thermal conductivity detector cell.

Sulfur content determination was obtained from the total sulfur spectrum produced by complete burning to flame of sulfur compounds (ASTM 4239 – 12, 2011g). The process to detect sulfur content of the studied samples as showed in Figure 3.7 are listed as follows;

A) A 0.3 gram of sample was burned in a furnace tube at 1350 °C

in a stream of oxygen.

B) During combustion, the sulfur and sulfur compounds were decomposed and oxidized to be sulfur dioxide (SO₂).

C) Moisture and particulates were removed from the gas stream

by filters.

D) Sulfur dioxide was then detected and absorbed at IR cell by a

precise wavelength filter.

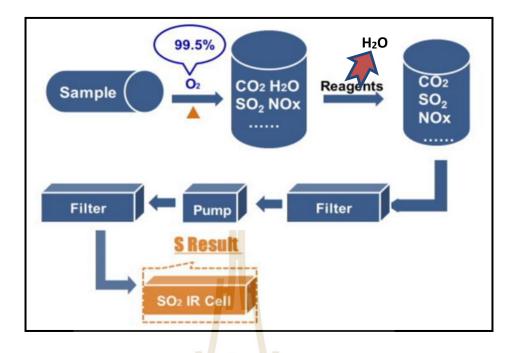


Figure 3.7 The process of ultimate analysis for sulfur detection.

Oxygen content can be determined by subtraction the sum of the percentage of C, H, N, and S, and ash from 100 as expressed in equation 3-3. The ash content can be got from proximate analysis.

$$\text{\%Oxygen} = 100 - (\text{\%C} + \text{\%H} + \text{\%N} + \text{\%S} + \text{\%Ash})_{ad}$$
(3-3)

Where

%Oxygen = oxygen content (percentage)

- %C = carbon content (percentage)
- %H = hydrogen content (percentage)
- %N = nitrogen content (percentage)
- %S =sulfur content (percentage)

3.3.1.3 Heating Value analysis

The gross calorific values measurement of the studied coal samples in this study had been conducted following the ASTM D5865 – 10a standard.

The bomb calorimeter Leco AC-350 at geochemical laboratory of Mae Moh Mine (Figure 3.8) was used in this study. The heat capacity in the calorimeter is determined by burning a specified mass in oxygen and measuring the increase temperature of water in the calorimeter. The steps start with mass of specimen around 1 g was accurately weighed in to specific cup, weight of wire length 10 cm. (fuse) before burned. Electricity per with cylindrical container which connect fuse for burning ensure some part of wire contact with sample for completely burning, then put the sample into the close cylindrical which connect to electrode and filled oxygen combustion in to it. A comparable amount of the analysis sample is burned under the same conditions in the calorimeter. The equipment detected water temperature change by burning of coal. The last step is to weigh of remain wire after burned and titration nitrogen. The calorific value of the analysis sample is computed by multiplying the corrected temperature rise, adjusted for extraneous and fuse heat effects, deducting value of sulfur, nitrogen, and other composition, by the heat capacity and dividing by the mass of the sample.

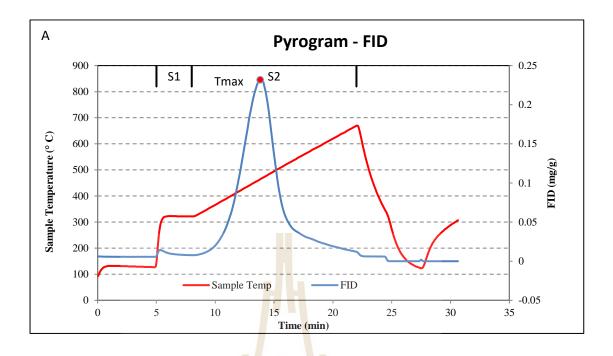


Figure 3.8 The bomb calorimeter Leco AC-350.

3.3.1.4 HAWK pyrolysis analysis

HAWK (Hydrocarbon Analyzer with Kinetics) system was used in this study to measure TOC, oil and kerogen yields as well as thermal maturity. Selected organic sediments were sent to the Energy Resources Consulting Pty. Ltd., Australia, to conduct the HAWK pyrolysis analysis. The amounts of hydrocarbons were measured by a flam ionization detection (FID) while CO and CO₂ were measured by an infrared (IR) detector cell of the HAWK instrument during the temperature was elevated at each step. The relationship among oil yield (S1), kerogen yield (S2), CO₂ (S3), CO, elevated temperature and time during the pyrolysis process of the HAWK instrument is illustrated graphically in Figure 3.9.





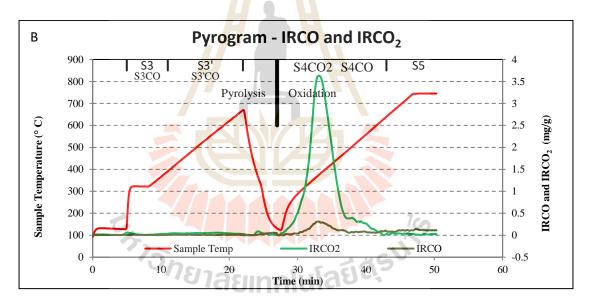


Figure 3.9 The relationship among S1, S2, S3, CO2, CO generating and elevated temperature and time during the pyrolysis process of the HAWK instrument: the FID detector to detect S1, S2 and Tmax (A) and the IR detector to detect CO on S3, CO2 and CO on S4 (B).

3.3.2 Petrographic analysis

In this study the petrographic analysis was conducted on polished specimens made from rock slabs, cutting both perpendicular and parallel sections and crushed samples mounting in epoxy resin to identify maceral and mineral composition and to determine the vitrinite reflectance pf the studied organic samples. The basis of organic petrography is optical microscopy that includes reflected and transmitted white light, fluorescence (UV and blue light excitation), and polarized light analysis of the organic matter (Ruiz *et al.*, 2012).

The identification of maceral types conducted in this study was based on the simplified classification and volume percent of organic composition and mineral matter by composition from petrography. The determinations were point counting procedure to obtain the volume percent of the various macerals. The petrography can also be used to determine contaminants and to detect the sample oxidation. The maturation of the studied organic samples was determined by using maximum vitrinite reflectance (VR) which present in unit of %Ro.

10

3.3.2.1 Maceral composition

The maceral compositions and types of the selected polished specimens were identified under a microscope based on their light reflectance, optical properties and morphology by using reflected light microscope equipped with polarizer and UV-excitation, follow the maceral nomenclature as described in Stach *et al.* (1975), ASTM D2799 – 11 (2011) and ICCP (1994; 1998; 2001). Under 10x10magnification, four observed area were selected from each of the studied sample. Maceral and mineral matter were then identified under Plane Polarized Light (PPL), Cross-Polarized Light (XPL) and the Ultraviolet (UV) excitation and were counted up to 100 points from each observed area (400 observed points for each of the studied sample).

3.3.2.2 Vitrinite reflectance (Ro)

The vitrinite reflectance analysis is the major method to determine the thermal maturity of the organic sediments. It is determined by illuminating a polished surface in immersion oil. In this study the vitrinite reflectance analysis was made using a Leica MP4500P system with Hilgers DISKUS software of ERC Pty. Ltd., Australia. The microscopic system measures amount of light which recorded in percent reflectance and calibration of photometric by calculated from their refractive indices.

The 2 samples from Coal A and Coal B, were prepared by crushing the samples to smaller than 1 mm (18 mesh). The samples were sub-sampled by evenly spreading the coal and taking between 10 and 15 scoops using 5 mm wide spatula. Ensuring the samples obtained evenly spreading was about 10 g of sample. Then, these samples were mounted in epoxy resin and polished for microscopic. The polished sample was desiccated at least 12 hours prior to analysis. The microscopic examination is using polished in oil in reflected light. Place the polished in mechanical stage to traverse the sample at regular intervals. Reflectance was determined of a 20 μ m² area at the wavelength of 546 nm using a total magnification of 500X. The determinations are mean maximum and random in term of vitrinite reflectance (Ro) which Ro_{max} and range of Ro with point count number. A minimum of 50 measurements per sample were made. The vitrinite reflectance measurement was identified by a Leica MP4500P system with Hilgers DISKUS software following the Maceral classification of the Australian Standard AS2856-1986 by Energy Resources Consulting Pty Ltd. The result of mean and maximum reflectance measured in oil are to be reported.

CHAPTER IV

RESULTS AND DISCUSTION

According to the objectives of this research, results of the study and experiments can be categorized into 4 main parts as geology of the studied sedimentary succession, organic petrological analysis, geochemical analysis, and discussion, respectively.

4.1 Geology of studied sedimentary succession

Mae Teep basin is a small half-graben basin. The basin trends north-northeast – south-southwest direction. Results from fieldwork at the mine front indicate that the strata on the western margin of the basin strike N10° – 30°E with monocline dipping eastward at 40° for lower sequences, and less than 20° for the upper sequences (Figure 4.1). The main rock units in the Mae Teep coal mine consist of Tertiary sequences, which are overlain by Quaternary deposits. Quaternary sediments are unconsolidated sediments including gravel, sand, silt, clays, mud, and lateritic soil with the total thickness about 5 meters. The Tertiary sedimentary deposited in the studied coal mine can be classified (Cook and Sherwood, 2003) by their distinguished characters into 3 main depositional environments (Fluvial, Lacustrine and Swamp), 5 rock units (Fluvial sequences, Fine-grained sedimentary sequences, Oil Shale, Coal, and Leonardite), and 7 sub-units (Upper Oil Shale, Lower Oil Shale, Oil Shale in Coal A, Coal A, Coal B, Coal C, and Leonardite) as showed in Table 4.1 and Figure 4.2

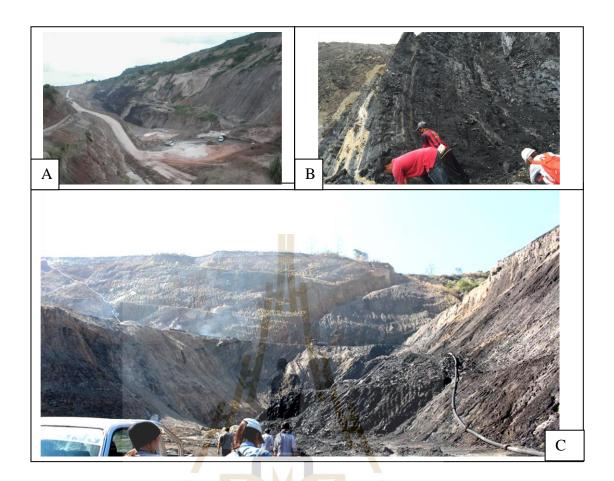


Figure 4.1 Overview of Mae Teep coal mine (A) (look south-west), the strata

showing bedding plane strike NE direction (B) and dip eastwards (C)

(look south).

Unit	Sub-units	Thickness (m)			
Fluvial sequences	(semi-consolidated)	65.50			
Fine-grained sedin	5.50				
Oil Shale	3.14				
Lower Oil Shale		2.16			
Oil Shale in Coal A					
Coal	Coal A	9.26			
	Coal B	3.95			
	Coal C	4.65			
Leonardite	>3.00				
	Fluvial sequences Fine-grained sedir Oil Shale Coal	Fluvial sequences (semi-consolidated) Fine-grained sedimentary sequences Oil Shale Upper Oil Shale Lower Oil Shale Oil Shale in Coal A Coal Coal B Coal C			

Table 4.1 Tertiary rock units of Mae Teep coal mine deposits.

The uppermost part is the youngest Tertiary fluvial deposits. The boundary of the Quaternary and Tertiary deposits is clearly seen by its color. This deposit is made up mainly of greenish gray to gray and reddish-brown sandstone and gravel bed sequences. They consist of semi- consolidated quartz, feldspar and volcanic rock fragments with calcite cement locally. Figure 4.2 A shows difference color and feature of sediments sequences of fluvial (light color) and lacustrine deposits (dark color). Moreover, the lacustrine sequences show the distinguished laminated layers. At the west wall of the Mae Teep coal mine shows darker color organic rocks of the swampy environment (Figure 4.2 B).

The lower part of the Tertiary sequences is the organic sediments which deposited in lacustrine and swamp environment. The 3 main units consist mainly of oil shale, coal, and leonardite. The bedding shows several sub-units striking in the SSW direction and the clear boundary of lacustrine and swampy environments.

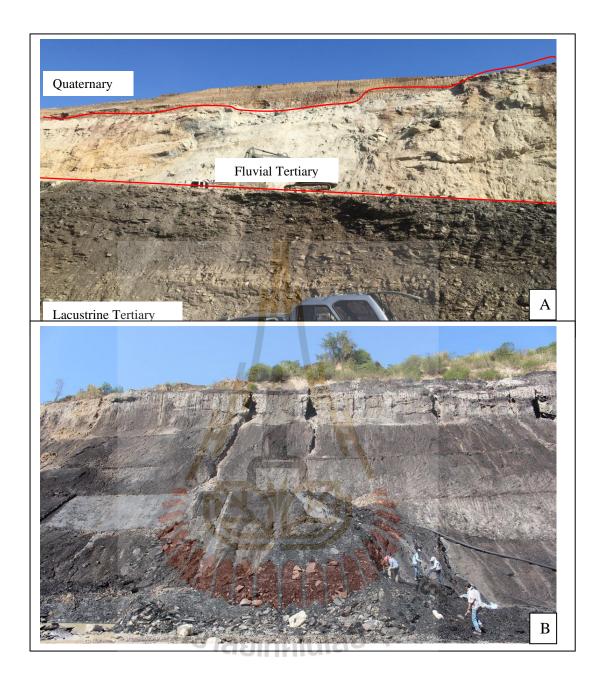


Figure 4.2 The western wall of the Mae Teep coal mine showing units boundary between the Quaternary, fluvial, and lacustrine sequences(A) (look east), the feature of coal and leonardite in the swampy environment at the western wall of mine (B) (look west).

Based on lithology, the lacustrine environment can be divided into 2 units; the Fine-grained sedimentary sequences unit in the upper part which are rare organic material, and the Oil Shale units in the lower part. Deposits of the swampy environment consist of Coal units in the upper part and Leonardite unit in the lower part (Figure 4.3).

The boundaries of the possible petroleum source rock according to their depositional environments from the bottom to the top are depicted in Figure 4.4. The oil shale units in lower lacustrine can be divided into 2 sub-units as the Lower and the Upper Oil Shale sub-unit. The coal formations in the swampy environment deposits can be divided into 3 sub-units; Coal C, Coal B and Coal A sub-unit. All these coal sub-units show the coal bearing sequences starting from the carbonaceous clays or leonardite, sapropelic coal and end up with humic coal (Francis, 1961; Bertrandd, 1984). The Coal A sub-unit has 2 parting of oil shale which deposits in lacustrine environment. The lithostratigraphic units of Mae Teep deposits at the Mae Teep coal mine are sequenced and illustrated in Figure 4.5.

The lithologic details of each unit and sub-units are described in ascending order as follows.

53

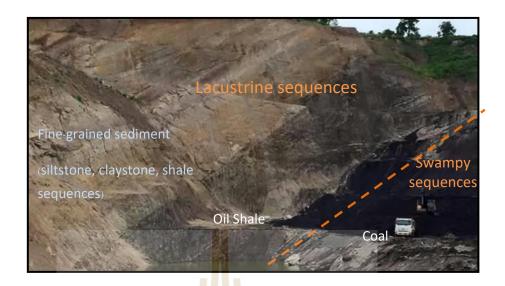


Figure 4.3 The contact boundary between oil shale unit (dark color) and the Finegrained sediment unit (light color) can be observed at the Mae Teep coal mine front (look south).



Figure 4.4 Contact boundaries of the swamp environment deposits (Leonardite, Coal C, Coal B, and Coal A sub-unit) and lacustrine environment deposits (Oil shale) at the Mae Teep coal mine (look south).

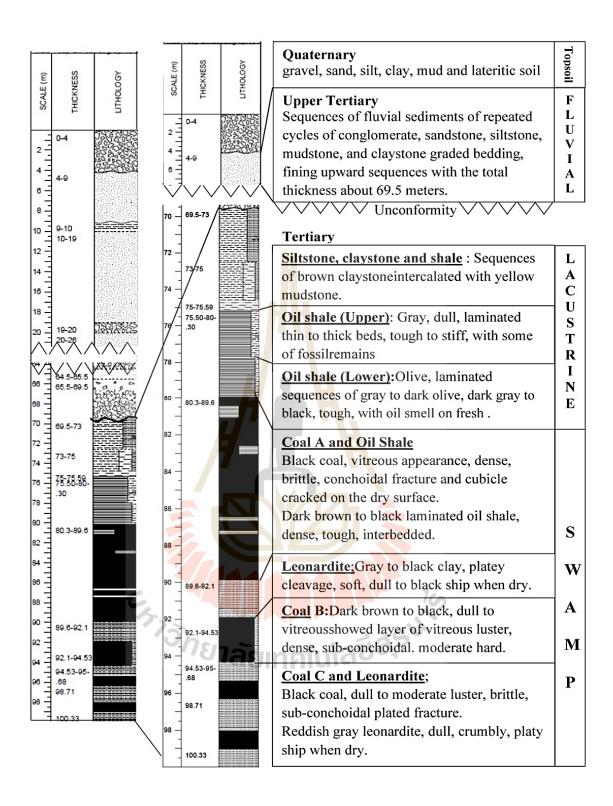


Figure 4.5 Lithostratigraphic column of Mae Teep deposit at the Mae Teep coal mine showing the sedimentary sequences and their related depositional environment.

4.1.1 Leonardite sub-unit

The leonardite sub-unit is the lowermost organic layer deposited in the swamp environment of the studied sedimentary succession at Mae Teep coal mine. Leonardite is carbonaceous clay of various amount of organic contents, dark gray to black, clay sized, platy cleavage, and approximately 5 - 10 m thick. The lower leonardite appears as a thick bed with clay features at the surface (Figure 4.6). It is also found in the lower part of all coal sub-units. This indicates that the depth of water prior to coal deposits starting from deep water and then gradually shallower with having more plants before the ending up of the sequences. It is noticed that the leonardite parting in coal sub-units show feature of less clays than the lowermost leonardite unit.

4.1.2 Coal C sub-unit

Coal C is the lowest coal sub-unit. It is impure coal, dark gray to black, dull to moderate glossy luster, dense, sub-conchoidal to conchoidal, and shows platy cleavage. The lower part of the sub-unit is interbedded with clay- to silt- sized leonardite, unconsolidated, dull, crumbly and platy cleavage (Figure 4.7). The upper part shows moderate glossy luster to dull interbedded with claystone of 1-2 cm thick (Figure 4.8 A). The total thickness of the Coal C sub-unit with leonardite parting is 4.65 m.

4.1.3 Coal B sub-unit

Coal B is the sub-unit in between the Coal C and Coal A. It is separated from Coal A and Coal C by the upper and lower leonardite respectively. It is dark brown to black coal, dense, hard, sub-conchoidal fracture. The coal in this sub-unit still deposited with clays or organic sediments that showed moderate dull to moderate glossy luster (Figure 4.8 B). Coal B are dark brown to black, dull to vitreous, dense, moderate hard with sub-conchoidal fracture. The lower part starting from leonardite, sapropelic coal, show clay- to silt- sized, unconsolidated, dull, crumbly and platy cleavage. The thickness of this coal sub-unit with leonardite is 3.95 m.

4.1.4 Coal A sub-unit

Coal A is the uppermost unit of the coal sub-units. In the lower part, it is dull coal seating on leonardite and sapropel coal of the Coal B sub-unit. It displays clay- to silt- sized, unconsolidated, dull, crumbly and platy cleavage, gradually increases to moderate glossy luster upwards to the higher layer. The lowermost part of the Coal A siltstone is interbedded with siltstone. In the upper part, coal shows moderate glossy to glossy luster. It consists of 2 parting of dark gray to black oil shale (Figure 4.9). This part is massive, black color, vitreous luster, brittle, conchoidal fracture, cubicle cracked on the dry surface. The total thickness of the Coal A sub-unit with leonardite and oil shale parting layers is 9.26 m.

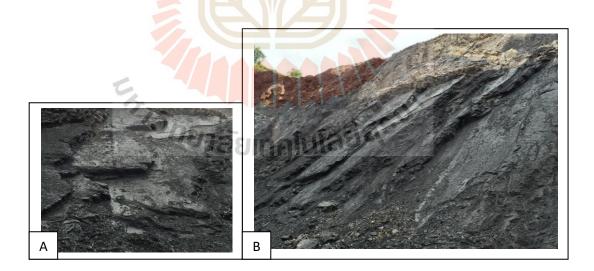


Figure 4.6 The western wall of Mae Teep coal mine showing the bedding plane of leonardite sub-unit: the layer of the lower leonardite sub-unit (A) (look west), leonardite showing surface character of clays (B) (look south-west).

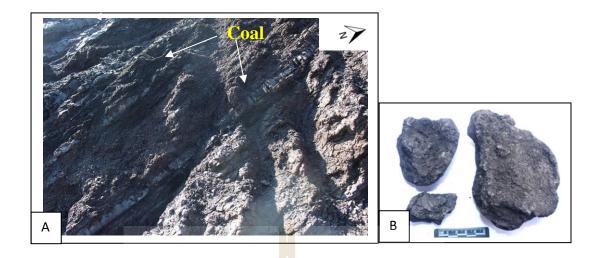


Figure 4.7 Thin layer of coal interbedded in the leonardite (A), the platy cleavage and crumbly surface of leonardite (B).



Figure 4.8 Thin layer claystone with impure coal interbedded in the Coal C (A), glossy luster and conchoidal fracture of the Coal B (B).



Figure 4.9 The Coal A sub-unit showing the oil shale parting in the upper part (A), Coal A massive texture (B) and Coal A conchoidal fracture with cubicle crack (C).

4.1.5 Oil shale in Coal A sub-unit

This sub-unit is the parting layers of oil shale in the Coal A sub-unit (Figure 4.10). They are made up of fine-grained sediments deposited together with organic material. It was occurred during high stand deep water in forested swamps. The characters of oil shale are likely black shale which is gray to black, dull, dense, fine-sand to clay- sized, tough to break, and stiff (Figure 4.11). Some parts of oil shale show laminated shale layers which are interbedded with some thin yellowish-brown siltstone partings of 1-5 cm thick (Figure 4.11). Mineral matters are coarse-grained

sand to clay sized, poor sorted with sub-round to sub angular. Boundaries of oil shales, coals and siltstone are very clearly seen. The thickness of the lower and upper oil shale in the Coal A sub-unit are 0.60 and 0.53 m respectively.

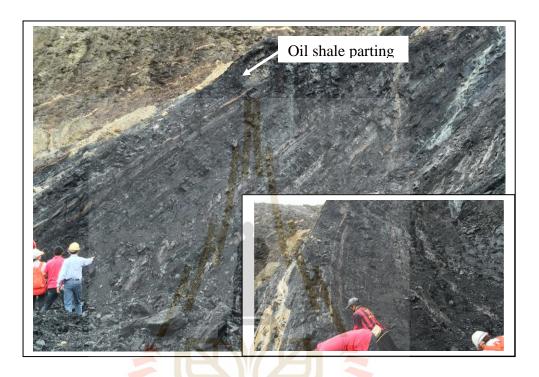


Figure 4.10 The oil shale parting layers in Coal A (look west).

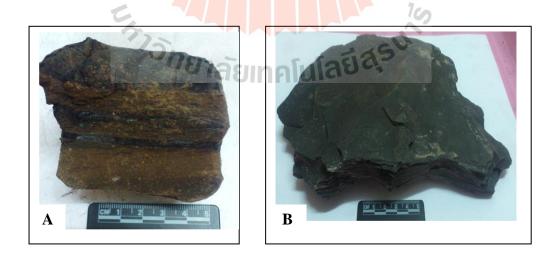


Figure 4.11 The samples show both character of oil shale, dark brown oil shale with thin layer of coal and siltstone (A) and laminated black shale (B).

4.1.6 Lower Oil Shale sub-unit

They are deposited in the lacustrine environment and laid conformably over the Coal A. It is indicated the environmental conditions changing suddenly from the shallow water of forest-peat swamp to the high stand water by successive unit from coal to oil shale. These oil shales show character of pale gray to yellowish brown, and dark gray to dark brown, dull, tough, consolidated, sub-conchoidal fracture in very thin laminated bed with platy cleavage to the thick bed (Figure 4.12 A and B). They have smell of oil in fresh rocks and some layers show shell fossil (Figure 4.12 C). The thickness of the lower oil shale sub-unit is 2.16 m.

4.1.7 Upper Oil Shale sub-unit

The Upper Oil Shale is overlain conformably to the Lower Oil Shale sub-unit and they can be separated from each other by a thick bed of lacustrine sediments. They are brownish black to dark olive laminated oil shale with characters of dull, massive, stiff and hard to break (Figure 4.13). Some layers show remains of shell fossil and platy cleavage. The upper part of this sub-unit has more clay to silt sized particles than the lower part. It is interbedded with brown to yellowish brown siltstone of 1-3 cm thick. The color of uppermost layer is the key to separate fined-grained sedimentary sequences from this oil shale sub-unit. It is reddish brown to brownish black, dull, massive and very hard. The environment of deposition of this sub-unit is the high stand stagnant water and nutrient rich led to thick algal deposit and gradually recedes before the strong current with large amount of fine-grained sediments flooding into the basin and end of organic matter accumulation.

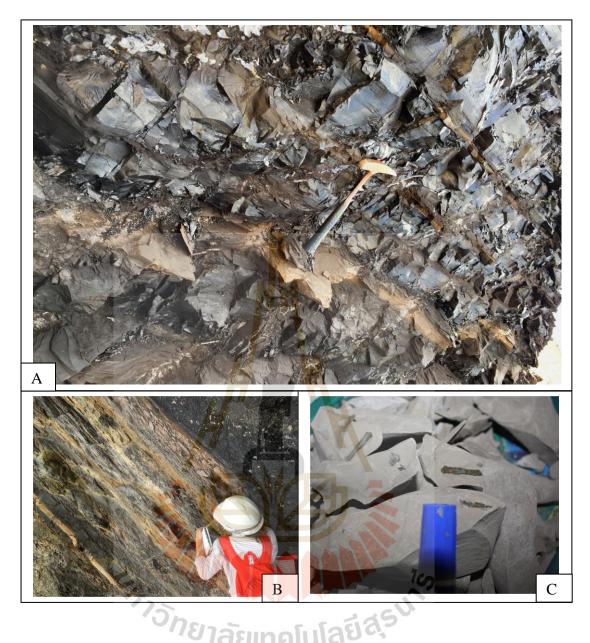


Figure 4.12 The character of the oil shale in fresh rock show dark gray to yellowish brown (A), weathered laminated oil shale show yellowish brown and pale gray (B), and fossils remains found in the Lower Oil Shale sub-unit (C).

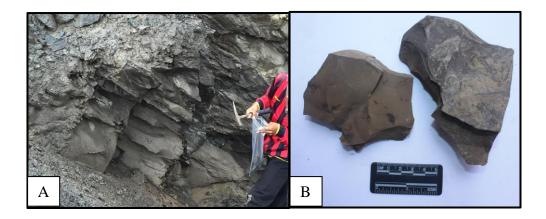


Figure 4.13 Out crop of the upper sub-unit oil shale interbedded with siltstone (A) and brown oil shale with fossils remains (B).

4.1.8 Fine-grained sediment unit

The fine-grained sediment unit is the uppermost part of the lacustrine deposits. It is overlain by fluvial deposits. It is made up of variegated sequences of thin fining upward sediments laying conformably on oil shale (Figure 4.14 A). The total thickness of this unit is 5.5 m. The characters of this unit are varied color and graded bedding of silt to very fine-grained sandstone interbedded with fine-grained mudstone. In figure 4.14 the pale-yellow layers are siltstone and pale gray layers are claystone. Weathered sample shows desiccation cracks perpendicular to the bedding plane (Figure 4.14 B). Moreover, there is a parting of fossil about 1-5 cm thick which is deposited with mudstone and shows same remains of leaves and shells (Figure 4.14 C).

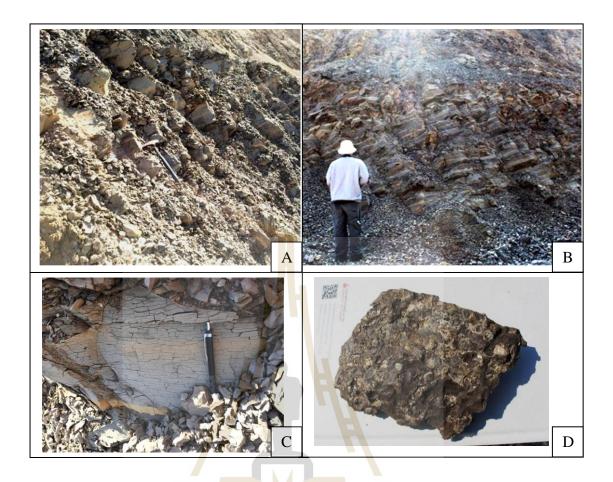


Figure 4.14 The Fine-grained sediment unit from mine front. The outcrop shows intercalated siltstone and mud rock sequences (A and B), the weathered sample displaying desiccation cracks (C) and fossil remains of leaves and shells in the mud rocks (D).

4.1.9 Fluvial deposits

The fluvial sediments are the overburden of Mae Teep deposits at the Mae Teep coal mine. They consist mainly of semi-consolidated of conglomerate, sandstone, siltstone, mudstone, and claystone (Figure 4.15). They are pale gray color, granule to pebble size, poorly sorted, sub-rounded of sandstone clast, conglomeratic limestone cemented by fine to coarse sand matrix (Figure 4.16). They are interbedded

with gravel bed, sandstone and limestone, fine to coarse sand, very poorly sorted, sub angular matrix. The total thickness of the fluvial sediments is 65.50 m and they can be divided into 3 main sequences as follows:

- The lower sequence shows graded bedding, fining upward sequences of conglomerate and sandstone, pale gray to greenish gray and gray, poorly sorted, sub-round to round, very coarse to fine sand. Matrix is white, pale gray to gray with layer of various sized coal fragments. The sequence displays cross bedding of coal with coal lens (Figure 4.17).

- The middle sequence consists of conglomerate and sandstone, reddish brown to purple, medium sorted, sub-round to round, coarse to fine sand. The faulting systems found in sediment beds are both normal and reverse faults striking NW-SE (Figure 4.18).

- The upper sequence consists of reddish-brown sandstone and gravel bed layers. They are fine to medium sand size, moderately sorted, sub-rounded to subangular, composed of quartz, feldspar and volcanic rock fragments with calcite cement.

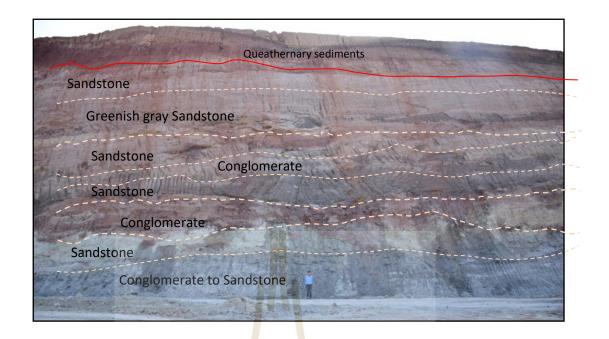


Figure 4.15 Overburden fluvial sedimentary sequences at the Mae Teep coal mine.

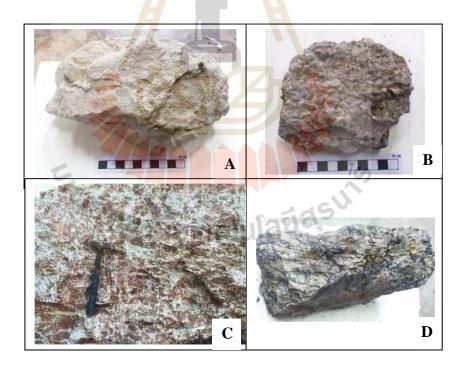


Figure 4.16 Overburden sedimentary rocks: gray sandstone (A), conglomerate (B), reddish mottled sandstone calcite cement (C)and conglomeratic sandstone with coal fragments (D).



Figure 4.17 Conglomerate and sandstone deposited with coal lens (A) and planar cross bedded and laminar of coal (B) at the lower part of the fluvial sequences (look north-earth).



Figure 4.18 Reverse faults trending N 10 - 38 W cut conglomerate and sandstone sequences of the fluvial sediment sequences (look east).

In order to conduct geochemical and petrographic analysis, 14 oil shale samples of lacustrine environment, 26 coal and 4 leonardite samples of swampy environment had been collected. The 26 coal samples were collected from the lower to the upper coal unit consisting of 11 samples from the Coal C sub-unit, 4 samples from the Coal B sub-unit and 11 samples from the Coal A sub-unit. The oil shale samples are 4 samples of Oil Shale in Coal A sub-unit, 6 samples of the Lower Oil Shale sub-unit and 4 samples of the Upper Oil Shale. Number of collected samples, organic rock unit and sub-unit are summarized and showed in Table 4.2. Details of collected organic rock samples from each sub-unit are summarized and showed in Table 4.3. As a result, the correlation among lithostratigraphic unit, environment of deposition and locations of collected organic rock samples of the studied organic sedimentary succession can be illustrated graphically in Figure 4.19.



 Table 4.2 Environment of deposition, rock units, sub-units and number of samples

Environments	Rock Unit	Sub-units	Number of collected samples
Fluvial	Fluvial sequences (se	mi-consolidated)	-
Lacustrine	Fine-grained sedimen	tary sequences	-
	Oil Shale	Upper Oil Shale	4
		Lower Oil Shale	6
		Oil Shale in Coal A	4
Swamp	Coal	Coal A	11
	, 1	Coal B	4
	H	Coal C	11
	Leonardite	Leonardite	4

collected from each sub-unit.



Sub- units	Sample NO.	Descriptions	Thickness (cm)
	OH10	Reddish brown to light brown oil shale, clay- to silt- sized particles, dull, very hard, consolidated, tough with calcite cement, laminated thin to medium beds.	24
il Shale	OH 9	Black to brownish black oil shale, dull, moderately hard, semi-consolidated, laminated wavy thin bed, with shell remains interbedded with 1 cm. thick brown siltstone.	107
Upper Oil Shale	OH 8	Black oil shale, dull, dense, moderate hard, clay- sized particles, tough, semi-consolidated, platy cleavage laminated wavy to parallel very thin beds.	96
	OH 7	Brownish black and dark green oil shale, clay- to silt- sized particles, dull, dense, hard, tough, laminated thin beds, sub-consolidated fracture with fossil remains.	87
	OH 6	Yellowish gray to grayish green oil shale, dull, hard, tough, uneven laminated layers, with fossil remains.	56
Lower Oil Shale	OH 5	Grayish green to greenish black oil shale, dull, tough, moderate hard, semi-consolidated, sub- conchoidal fracture, wavy to curved lamination.	28
	OH 4	Yellowish gray to grayish green oil shale, dull, hard, tough, laminated curve with fossil remain.	32

 Table 4.3 Organic rock sample descriptions of the studied organic sedimentary succession.

Sub-	Sample	Descriptions	Thickness
units	NO. OH 3	Dark grouich vallow to groopich grou oil shale, alow	(cm)
<u>ව</u>	00 3	Dark grayish yellow to greenish gray oil shale, clay- to silt- sized particles, dull, hard, sub-conchoidal fracture, platy cleavage, laminated to very thin beds, with smell of oil shown in fresh rocks.	27
Lower Oil Shale	OH 2	Black gray to greenish black oil shale, dull, hard, tough, wavy laminated to thin beds, with fossil remain. Smell of oil shown in fresh rocks.	39
	OH 1	Greenish gray oil shale, dull, hard, tough, sub- conchoidal fracture, platy cleavage, laminated to very thin beds, with fossil remains.	34
ıle in Coal A	AS 4	Dark brown to black oil shale, clay- to silt- sized particles, dull, very hard, stiff, consolidated, platy cleavage, micro lens in places, very fine to fine lamination, with yellowish brown siltstone interbedded 3-5 cm. thick.	23
Oil sha	AS 3	Dark gray to black oil shale, clay- to silt- sized particles, dull, tough, hard, semi-consolidated, even, platy cleavage, micro lens in places, very thin to thin laminated beds.	30

Sub- units	Sample NO.	Descriptions	Thickness (cm)
	AS 2	Dark gray and yellow oil shale, clay-to silt- sized particles, dense, platy cleavage, micro lens in places, wavy very thin to thin laminated beds.	28
Oil shale in Coal A	AS 1	Dark gray to black interbedded with yellowish brown oil shale, dull, dense, waxy luster, tough, platy cleavage, very thin laminated layers.	32
	A 11	Black coal, moderately glossy luster, brittle, conchoidal fracture with sub-cubic cracking, semi- consolidated, very thin lamina siltstone interbedded.	143
	A 10	Dark gray to black coal, moderately dull to moderate glossy luster lamination, brittle to stiff, sub-cubicle cracked, 0.5 – 1 cm. thick beds.	51
Coal A	A 9	Black coal, glassy luster, dense, brittle, conchoidal fracture, cubicle cracked.	56
	A 8	Dark brown to black coal, dull, moderately hard, tough, platy cleavage, alternate siltstone 2 mm. to 1 cm. thick interbedded.	21
	A 7	Black coal, dull, dense, moderately hard, moderately brittle, sub-conchoidal fracture to plate cleavage.	89

Sub- units	Sample NO.	Descriptions	Thickness (cm)
	A 6	Dark brown to black coal, moderately glossy luster, dense, moderately brittle, sub-conchoidal fracture to platy cleavage.	58
	A 5	Black coal, glossy luster, brittle, dense, conchoidal fracture with sub-cubicle cracked.	84
1A	A 4	Black coal, moderately glossy, dense, moderately brittle, sub-conchoidal fracture to platy cleavage, with brown to yellowish brown siltstone 0.3-2 cm. thick interbedded.	97
Coal A	A 3	Black coal, moderately dull to moderately glossy luster band of $0.3 - 0.5$ cm. thick, moderately brittle, sub-conchoidal fracture to platy cleavage.	63
	A 2	Dark gray to black coal, dull, dense, moderately hard, tough, semi- consolidated, platy cleavage, thin to medium lamination.	78
	A 1	Black coal, dull to moderately glossy luster in discontinuous wavy very thin lamination, dense, moderately brittle, sub-conchoidal fracture.	94
Leonardite	L19	Black leonardite, clay- sized particles, sticky, waxy luster and platy cleavage when fissile.	137

Sub-	Sample	Descriptions	Thickness
units	NO.	Dark gray to black coal, discontinuous dull to	(cm)
	B18	moderately glossy luster band, moderate brittle, platy cleavage, sub- conchoidal fracture, sub- cubical cracking.	87
Coal B	B17	Black coal, moderately dull, dense, moderately brittle, sub-conchoidal fracture to platy cleavage.	47
	B16	Black coal, moderately glossy luster, brittle, sub- conchoidal fracture, cubical cracking.	39
	B15	Black coal, dull, moderate brittle, dense, sub- conchoidal fracture to platy cleavage.	35
Leonardite	L14	Black leonardite, clay- to silt- sized particles, sticky, waxy luster, crumble and platy cleavage, fissile.	50
C	C13	Dark brown to black coal, moderately dull to moderately glossy luster band of $0.1 - 0.3$ cm. thick, dense, moderately brittle, sub-conchoidal fracture, sub-cubical cracking.	58
Coal C	C12	Brown to black coal, dull to moderately glossy luster band of 1 cm. thick, moderate brittle, sub-conchoidal, sub- cubical cracking to platy cleavage, alternate siltstone 0.1 cm. laminated layer.	23

Sub- units	Sample NO.	Descriptions	Thickness (cm)
	C11	Black coal, dull to glossy luster band of $0.5 - 2$ cm. thick, dense, brittle, sub-conchoidal to conchoidal fracture, sub-cubicle cracked.	34
Coal C	C10	Black coal, discontinuous dull to moderately glossy luster, dense, moderate brittle, sub- conchoidal to platy cleavage, fissile.	31
	C 9	Black coal, discontinuous dull to moderate dull luster, dense, moderately brittle, sub-conchoidal to platy cleavage.	22
	C 8	Dark gray to black coal, dull, stiff to lightly sticky, moderately brittle, platy cleavage, fissile.	27
Leonardite	L 7	Reddish black to dark gray leonardite, dull, dense, sticky, crumble when dry.	67
	C 6	Black coal, moderately glossy luster, moderately brittle, sub-conchoidal fracture to platy cleavage.	46
Coal C	C 5	Black and brown coal, dull with glossy locally luster, brittle, platy cleavage with sub-conchoidal fracture locally.	37
	C 4	Black coal, dull, moderately brittle, platy cleavage, fissile.	41

Sub-	Sample	Descriptions	Thickness
units	NO.		(cm)
	C 3	Dark gray to black coal, dull to moderately glossy locally luster, sub- conchoidal fracture with platy	23
Coal C		locally.	
0	C 2	Dark gray to black leonardite, dull, dense, stiff, platy cleavage, lightly sticky, with crumble when dry.	56
Leonardite	L 1	Reddish gray leonardite, dull, dense, clay- to silt- sized particles, sticky, crumble when dry.	N/A



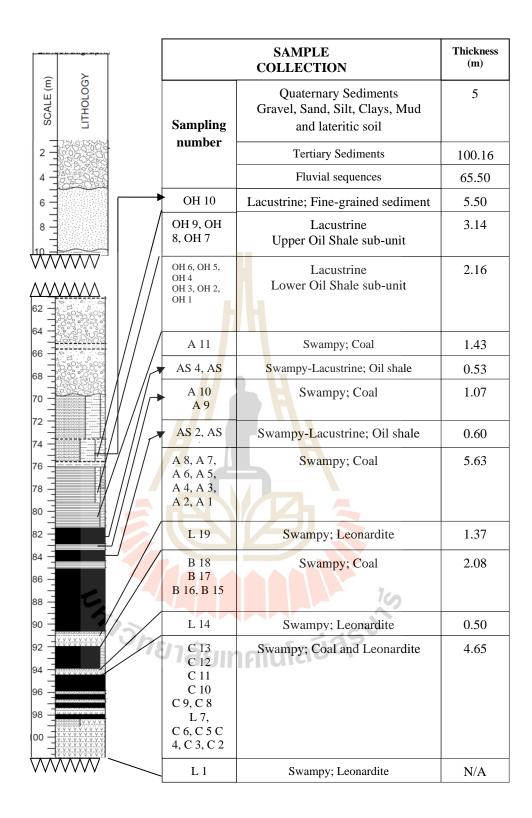


Figure 4.19 Correlation among lithostratigraphic unit, environment of deposition, and locations of the collected organic rock samples of the studied organic sedimentary succession at the Mae Teep coal mine.

4.2 Organic petrological results

Under microscopy, characters of macerals in organic sediments of Mae Teep deposits can be observed. Details of macerals and their depositional environment of each sub-unit can be summarized in ascending order as follows.

4.2.1 Leonardite sub-unit

Leonardite was found at the lowermost of the organic bearing formation in the swampy unit and it was also found at the lower part of coal sub-units. They are carbonaceous clays which are made up of fine-grained sediments deposited with small number of organic compounds. This formation shows characters of high supply of finegrained sediments which were transported into deep water and deposited with small amount of detrital or colloidal organic sediments. Depositional processes occurred under water during slowly subsidence or rising of water level in the basin. The associated organic matter causes them to display dark brown to black in color, moderately soft and stiff to moderate hard, mild fissile, with platy cleavage when dry.

Under microscopy, leonardite shows maceral groups mainly of vitrinite and liptinite which are associated with fine-grained sediments. The percentage of vitrinite varies from 12 – 25%. It consists of decomposed organic matter in form of gel (gelovitrinite) and minor organic fragments. The percentage of liptinite varies from 12 – 24%. It consists mainly of resinite, sporinite, and liptodetrinite, which are the oxidation products of other liptinitic macerals. Lamalginite was found only in sample L7-4 and L14-1. Cutinite, fluorinite, suberinite, and telalginite were not found in these leonardite samples. Details of macerals; vitrinite (V), liptrinite (L), inertinite (I), and mineral matter (MM) under petrographic study of 7 leonardite samples are summarized and showed in Table 4.4 and Figure 4.20 to Figure 4.26.

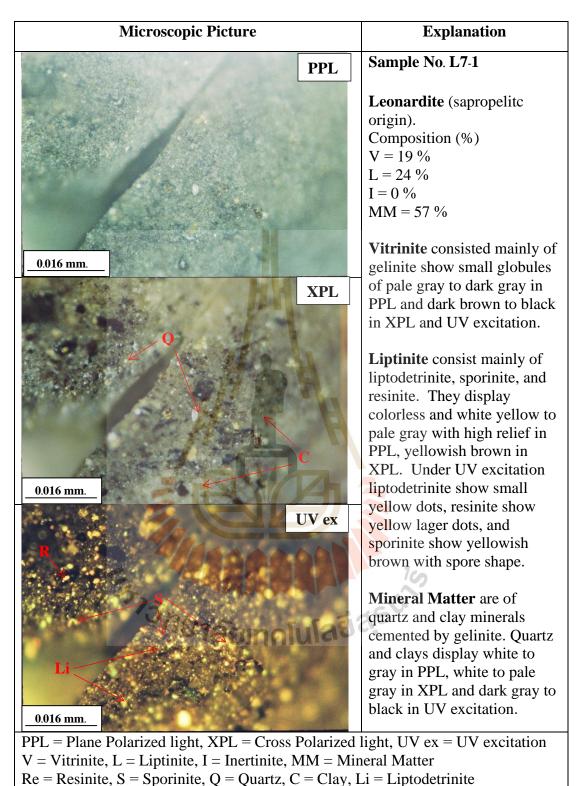
		Vi	trinite			Liptinite									
				Total				Algi	nite				Total		
Sample	Telo	Detro	Gelo		Sp	Cu	Lip_	Lam	Te	Re	Fl	Su		In	MM
L7-1	1	5	13	19	3	0	17	0	0	4	0	0	24	0	57
L7-3	0	0	25	25	1	0	9	0	0	3	0	0	13	0	62
L7-4	0	2	19	21	2	0	8	12	0	1	0	0	23	0	56
L14-1	0	7	18	25	2	0	10	1	0	1	0	0	14	0	61
L14-2	3	1	17	21	1	0	17	0	0	0	0	0	18	0	61
L14-3	0	3	9	12	4	0	11	0	0	2	0	0	17	0	71
L19-1	0	2	19	21	0	0	9	0	0	3	0	0	12	0	67
min	0.00	0.00	9.00	12.00	0.00	0.00	8.00	0.00	0.00	0.00	0.00	0.00	12.00	0.00	56.00
max	3	7	25	25	4	0	17 -	12	0	4	0	0	24	0	71
%	0.57	2.86	17.14	20.57	1.86	0.00	11.57	1.86	0.00	2.00	0.00	0.00	17.29	0.00	62.14

 Table 4.4 Composition in percentage of leonardite samples.

Tel = Telovitrinite, Det= Detrovitrinite, Gel = Gelovitrinite, In = Inertinite, MM. = Mineral Matter

Sp = Sporinite, Re = Resinite, Lip = Liptodetrinite, Cu = Cutinite, Fl= Fluorinite, Su = Suberinite, Lam = Lamalginite and Te = Telalginite





Re Resnine, 5 Sporinite, & Quartz, e Ciay, Er Elptodeurina

Figure 4.20 The microscopic picture of leonardite sample No. L7-1.

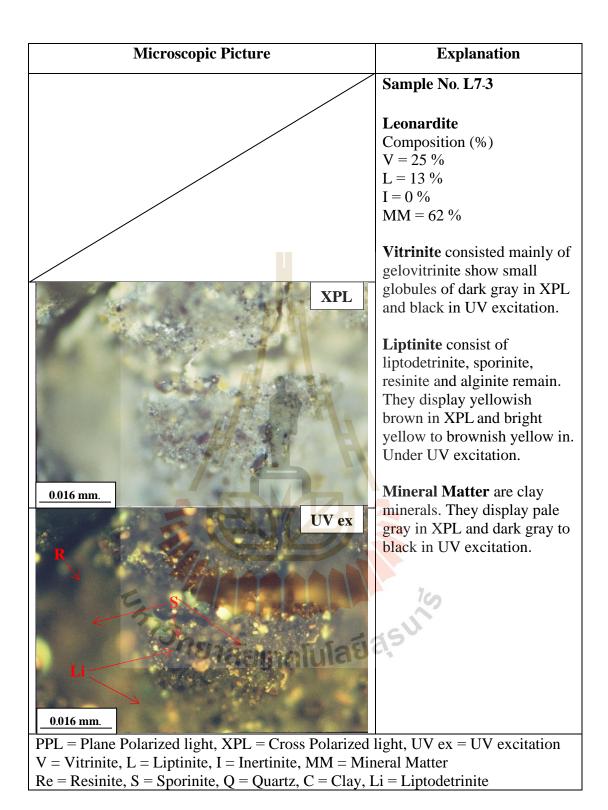


Figure 4.21 The microscopic picture of leonardite sample No. L7-3.

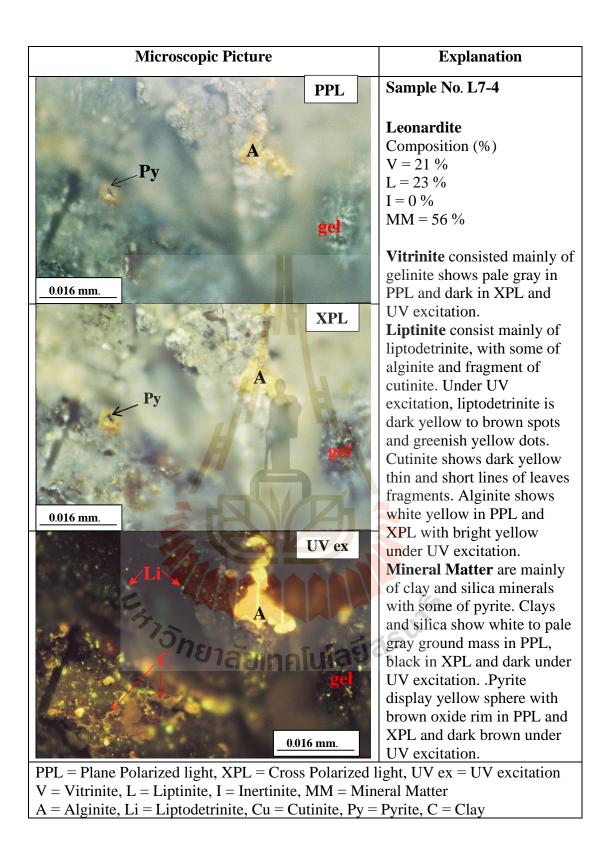


Figure 4.22 The microscopic picture of leonardite sample No. L7-4.

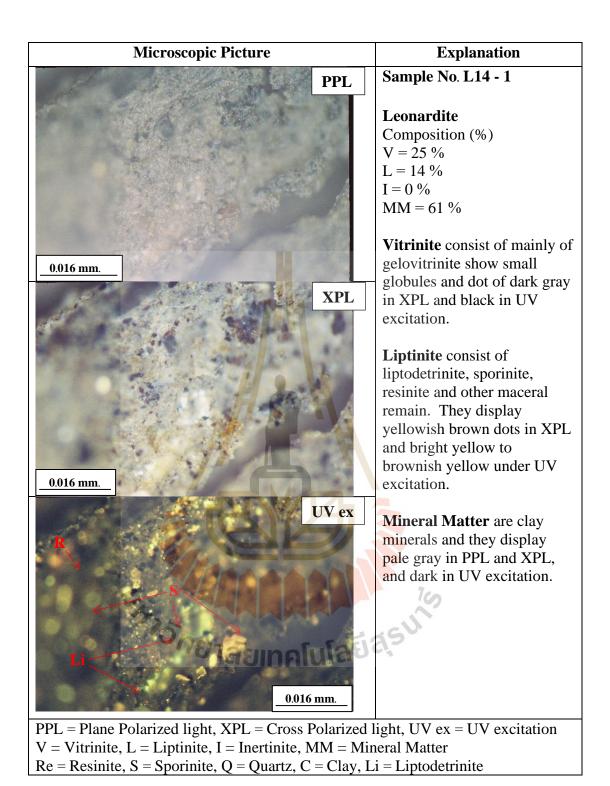


Figure 4.23 The microscopic picture of leonardite sample No. L14-1.

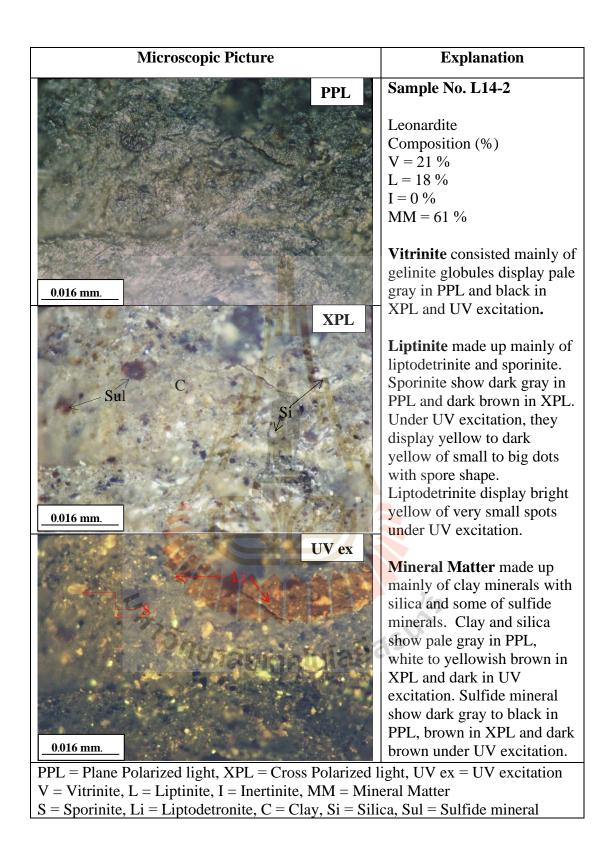


Figure 4.24 The microscopic picture of leonardite sample No. L14-2.

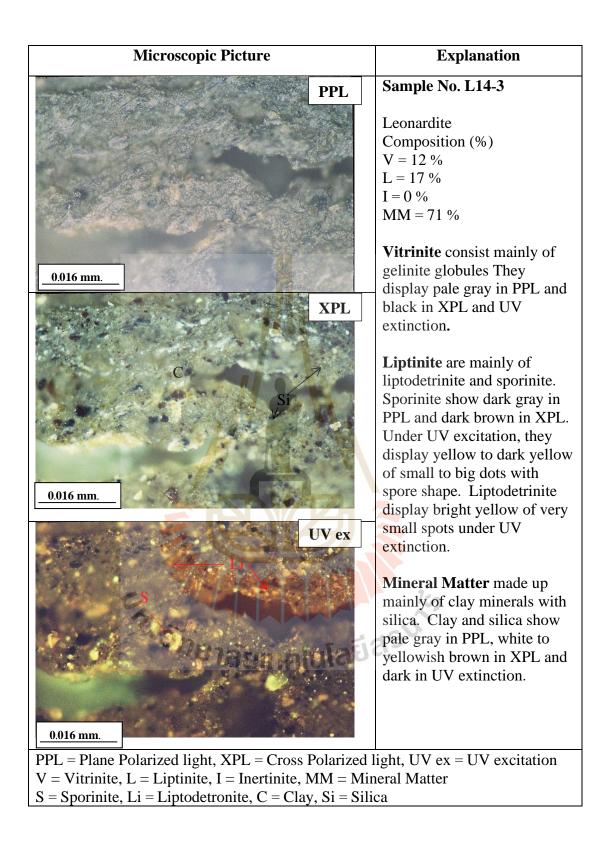


Figure 4.25 The microscopic picture of leonardite sample No. L14-3.

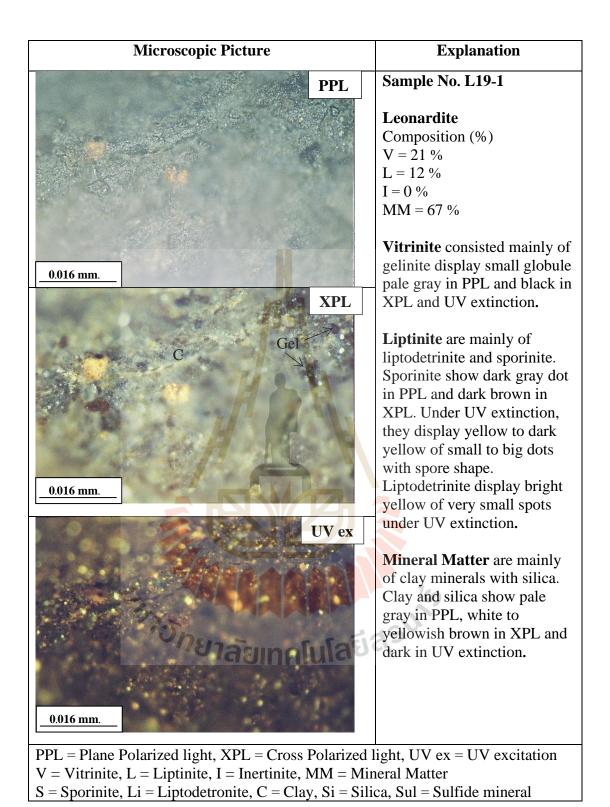


Figure 4.26 The microscopic picture of leonardite sample No. L19-1.

4.2.2 Coal C sub-unit

The Coal C is the lowest sub-unit of coal succession laid on the leonardite sub-unit. They display both organic and inorganic rich layers. The impure coal layers (high mineral matters) are in the lower part while more pure coal layers (low mineral matter) are in the upper part. The vitrinite maceral group (sapropelic origin) is varied from 21% (Sample C2-10) to 100% (Sample C4-7) (Table 4.5). Vitinite are mainly of texto-ulminite, densinite, gelinite and phlobaphinite. The mineral matters contents are varied from 0 (Sample C4-7 and C13-2) to 73% (Sample C12-5). The sapropelite is the dominant character of these coals. This suggests that they were deposited under water and consisted of densinite, gel globules and mineral matters. Vitrinite found in the lower part of the Coal C sub-unit consist mainly of texto-ulminite and gelovitrinite with some of detrovitrinite. These vitrinites indicate the less oxidized to mild reducing condition shallow water where reed peat with other submerged plant are deposited and produced vitrinite. The texto-ulminite resembles the original cell walls characterized by open cell lumens and fill up by ulmin gel and mineral matter (Figure 4.27). The upper part of the Coal C sub-unit layer shows layers of sapropel. They display telinite and densinite (Figures 4.27). Gelinite are mostly show gel cracking and cloudy structure of cork tissue which indicated porigelinite or textinite and texto-ulminite (Figures 4.27). These could imply the water level changing from deep stagnant water to shallow water. The top layer of peat bog could have been highly oxidized and led to highly decomposed of plant tissue and form gel which prevent the access of oxygen to the lower part of Coal C sub-unit. The more reducing condition occurred, the more well preserved. This led to the presence of undecomposed plant tissue such as cuticles with essential structure and cell walls of wood, barks, or roots

which indicated the preservation under the protection from air by oxidized gel layer (Figure 4.28).

The liptinite maceral group vary from 0 - 68 %. They consist mainly of liptodetrinite, sporinite, cutinite, resinite and suberinite. They are high resistance from oxidation maceral. The water level changing significantly affected the amount of oxygen dissolved in water. The shallow water or forest swamp could completely preserve cutinite (Figure 4.28), suberinite (Figure 4.29), telovitrinite and gelovitrinite. The cutinite and suberinite display in pale gray with highly relief in PPL and dark in XPL. Under UV excitation cutinite and suberinite show cuticle ledge structure and cell walls. They fluoresce yellow to dark brown (Figure 4.30). Most of sporinite was often found as a group of bright yellow and some were associated with thick cutinite which could be spores in sporangium. The liptodetrinite are the degradation remains of sporinite, cutinite, resinite and suberinite which are concentrated in subaquatic, especially in sapropelic coals. Under microscopy, liptodestinite display in yellow to yellowish brown irregular shape, whereas resinite and sporinite display in globule and various shapes and ornaments respectively.

The inertinite found in Coal C sub-unit samples is vary from 0 to 24 %. They consist mainly of funisite-pyrofusinite and a few of sclerotinite. The mineral matters are mainly clay minerals which are filled in cell lumens and textinite voids and in the groundmass. The mineral materials replace organic matter (gelinite) which are also found as autogenic minerals associated with woody tissue. The found minerals are marcasite and siderite (Figure 4.31 and 4.32) which are intergrowth or replaced by pyrite.

	Vitrinite				Liptinite									In	MM.
								Alginite							
Sample	Tel	Det	Gel	Total	Sp	Cu	Lip	Lam	Te	Re	Fl	Su	Total		
C2-1	77*	0	0	77	0	0	0	0	0	0	0	0	0	0	23
C2-2	3	17	48	68	3	0	9	0	0	5	0	0	17	0	15
C2-4	86*	0	0	86	0	0	0	0	0	0	0	0	0	0	14
C2-7	84*	0	0	84	0	0	0	0	0	0	0	0	0	0	16
C2-8	27	17	35	79	0	0	0	0	0	0	0	0	0	0	21
C2-9	27	9	35	71	0	0	7 0	0	0	0	0	0	0	0	29
C2-10	0	0	21	21	0	0	9	0	0	2	0	0	11	0	68
C3-1	1	10	37	48	5	0	40	0	0	0	0	0	45	0	7
C4-1	0	2	48	50	12	0	6	0	0	2	0	0	20	0	30
C4-2	0	0	51	51	12	0	12	0	0	2	0	0	26	0	23
C4-3	43	0	12	55	1	0	8	0	0	0	0	0	9	1	35
C4-5	53	4	8	65	10	3	13	-0	0	1	0	0	27	0	8
C4-6	28	43	14	85	0	0	0	0	0	0	0	0	0	0	15
C4-7	94	0	6	100	0	0	0	0	0	0	0	0	0	0	0
C5-1	68	0	0	68	0 4	6	13	0	0	0	0	0	19	0	13
C6-1	48	0	5	53	20	16	2	0	0	0	0	0	38	0	9
C6-2	4	0	18	22	21	44	3	0	0	0	0	0	68	0	10
C6-4	0	5	43	48	24	80 -	8	5.0fa	50	0	0	0	32	0	20

Table 4.5 Composition in percentage of Coal C sub-unit samples.

* = Texto-Ulminitel, Tel = Telovitrinite, Det= Detrovitrinite, Gel = Gelovitrinite, In = Inertinite, MM. = Mineral Matter Sp = Sporinite, Re = Resinite, Lip = Liptodetrinite, Cu = Cutinite, Fl= Fluorinite, Su = Suberinite, Lam = Lamalginite, Te= Telalginite

		Vit	Liptinite												
								Algini	te						
Samples	Tel	Det	Gel	Total	Sp	Cu	Lip	Lam	Te	Re	Fl	Su	Total	In	MM.
C8-1	32	11	17	60	6	2	12	0	0	0	0	0	20	0	20
C8-2	20	12	18	50	7	0	31	0	0	2	0	0	40	0	10
C8-3	0	0	38	38	18	0	12	0	0	0	0	0	30	0	32
C8-4	0	0	29	29	38	8	0	0	0	12	0	0	58	0	13
C9-1	94	2	1	97	0	0	0	0	0	0	0	0	0	0	3
C9-2	83*	0	9	92	0	0	0	0	0	0	0	0	0	0	8
C10-1	91	0	0	91	0	0	0	0	0	0	0	0	0	4	5
C10-3	84	0	2	86	0	0	0	0	0	0	0	0	0	1	13
C10-4	68	0	6	74	0	0	0	0	0	0	0	0	0	0	26
C10-5	95	0	3	98	0	0	0	0	0	0	0	0	0	0	2
C11-1	0	0	67	67	8	-8	5	0	0	0	0	0	21	0	12
C11-2	0	0	56	56	6	4	8	-0	0	2	0	0	20	0	24
C11-3	95	0	1	96	0	0	0	0	0	0	0	0	0	0	4
C11-5	0	0	20	20	4	0	3	0	0	0	0	0	7	0	73
C11-6	25	0	19	44	0	0	0	0	0	0	0	42	42	0	14
C11-7	86	0	3	89	3	0	4	0	0	0	0	0	7	0	4
C11-8	96	0	0	96	0	0	0	0	0	0	0	0	0	0	4

Table 4.5 Composition in percentage of Coal C sub-unit samples (Con.).

* = Texto-Ulminitel, Tel = Telovitrinite, Det= Detrovitrinite, Gel = Gelovitrinite, In = Inertinite, MM. = Mineral Matter Sp = Sporinite, Re = Resinite, Lip = Liptodetrinite, Cu = Cutinite, Fl= Fluorinite, Su = Suberinite, Lam = Lamalginite, Te= Telalginite

		Vitri	inite			Liptinite									
Samples								Alginite							
_	Tel	Det	Gel	Total	Sp	Cu	Lip	Lam	Te	Re	Fl	Su	Total	In	MM.
C12-1	94	0		94	0	0	0	0	0	0	0	0	0	0	6
C12-2	0	0	43	43	0	0	0	0	0	0	0	0	0	0	57
C12-3	0	0	75	75	0	0	0	0	0	0	0	0	0	0	25
C12-5	0	0	29	29	0	0	0	0	0	0	0	0	0	0	71
C12-6	0	0	67	67	0	0	0	0	0	0	0	0	0	0	33
C12-7	71	0	0	71	0	0	0	0	0	0	0	0	0	24	5
C13-2	82	0	6	88	7	0	0	0	0	0	0	0	12	0	0
C13-3	96	0	0	96	0	0	- 0	0	0	0	0	0	0	0	4
C13-5	0	0	90	90	0	0	0	-0	0	0	0	0	0	0	10
min	0	2	1	20	1	0	2	0	0	1	0	42	0	0	0
max	96	43	90	100	38	44	40	0	0	12	0	42	68	24	73
average	34.66	3.01	22.32	67.59	4.67	2.07	4.62	0.00	0.00	0.64	0.00	0.96	12.96	0.68	19.00

Table 4.5 Composition in percentage of Coal C sub-unit samples (Con.).

Tel = Telovitrinite, Det= Detrovitrinite, Gel = Gelovitrinite, In = Inertinite, MM. = Mineral Matter

Te= Telalginite

ะ รัววักยาลัยเทคโนโลยีสุรบาร

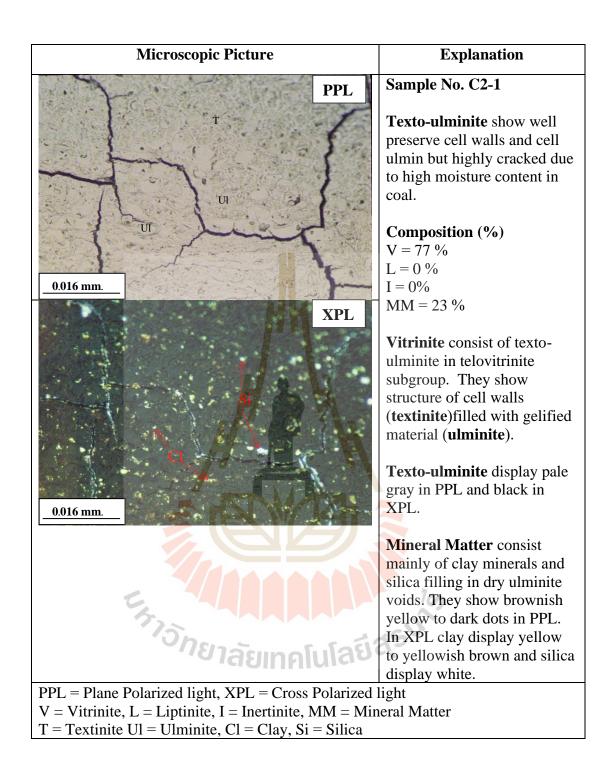
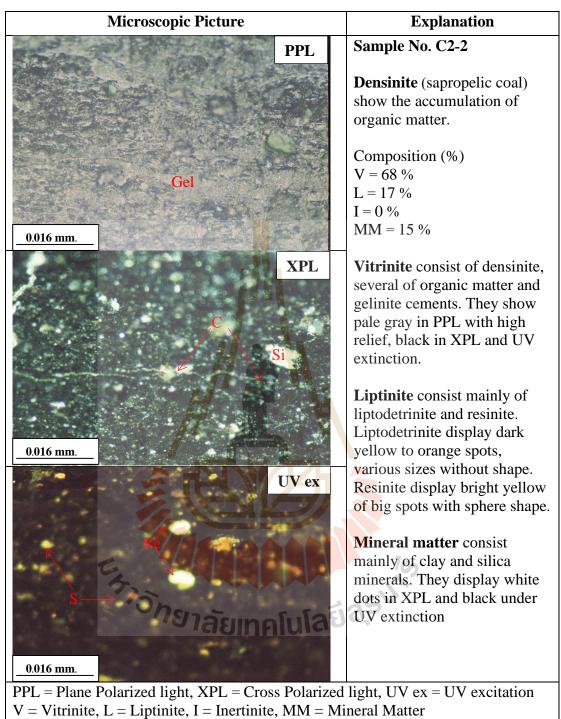


Figure 4.27 The microscopic picture of coal sample No. C2-1.



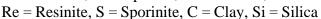


Figure 2.28 The microscopic picture of coal sample No. C2-2

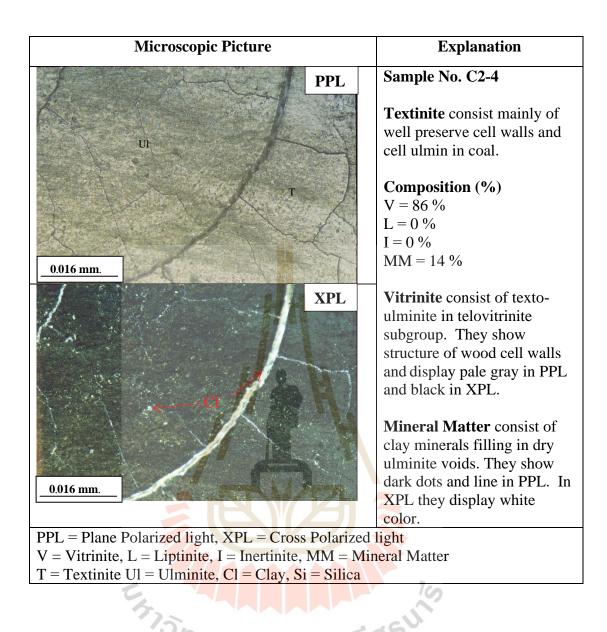


Figure 2.29 The microscopic picture of coal sample No. C2-4.

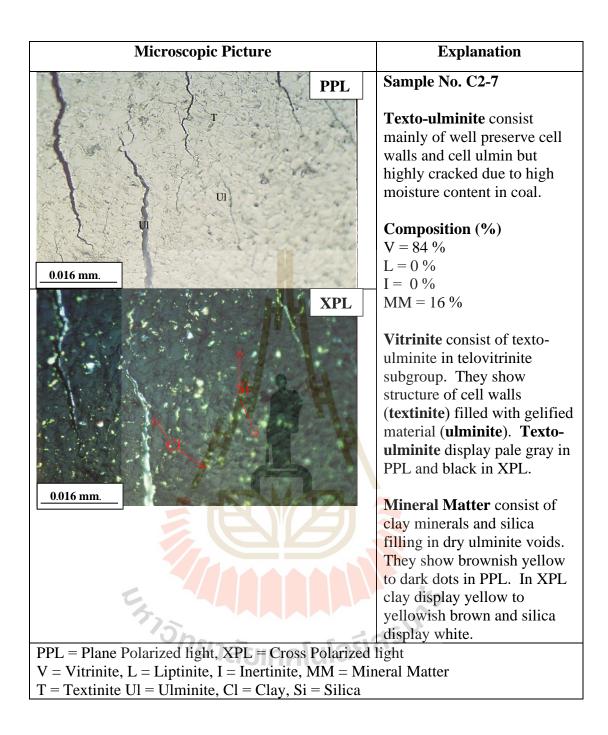
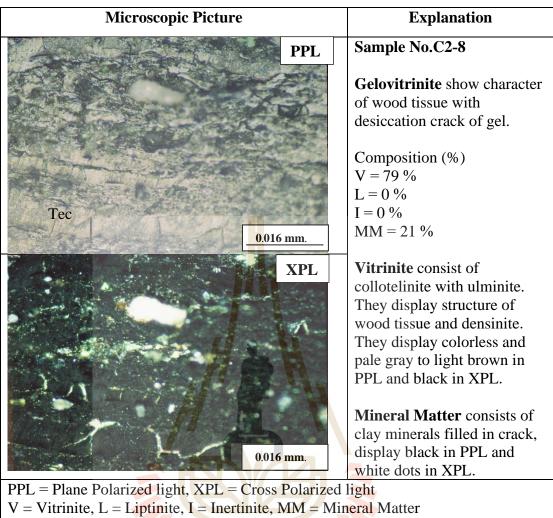


Figure 4.30 The microscopic picture of coal sample No. C2-7.



Co

Gel = Gelinite, Cl = Clay, Tec = Telocollinite, Ul = Ulminite

Figure 4.31 The microscopic picture of coal sample No. C2-8.

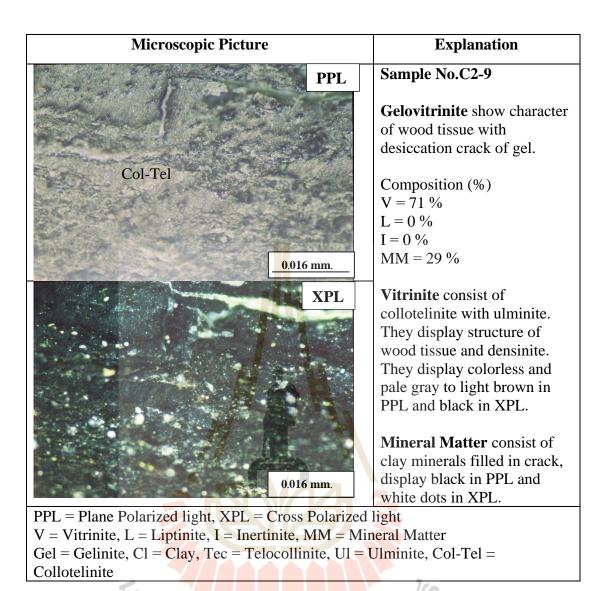
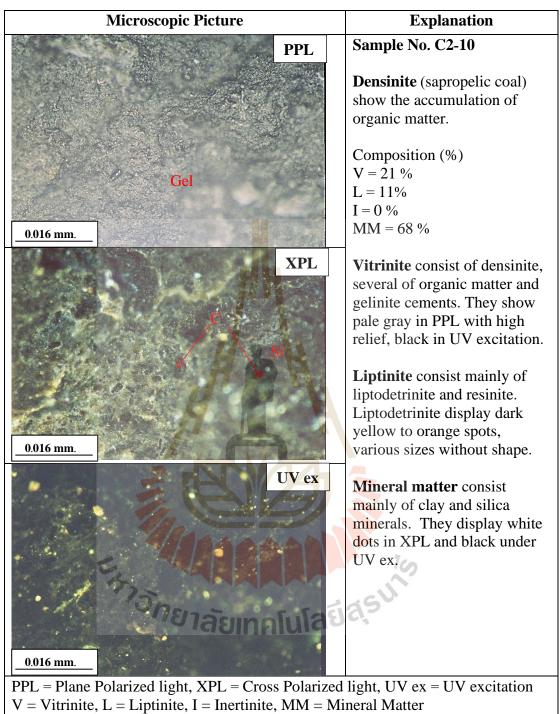
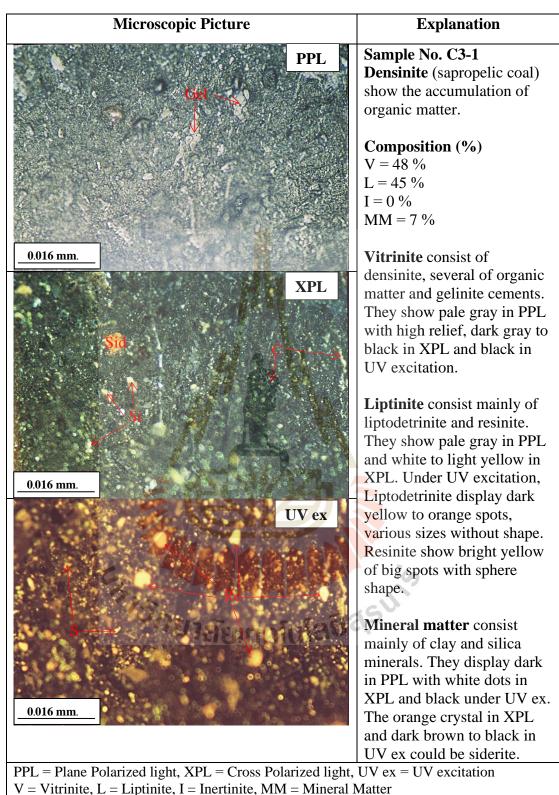


Figure 4.32 The microscopic picture of coal sample No. C2-9.



Re = Resinite, S = Sporinite, C = Clay, Si = Silica

Figure 4.33 The microscopic picture of coal sample No. C2-10.



V = V infinite, L = Liptimite, I = Inertifite, MM = Mineral MatterRe = Resinite, S = Sporinite, C = Clay, Sid = Siderite, Si = Silica

Figure 4.34 The microscopic picture of coal sample No. C3-1.

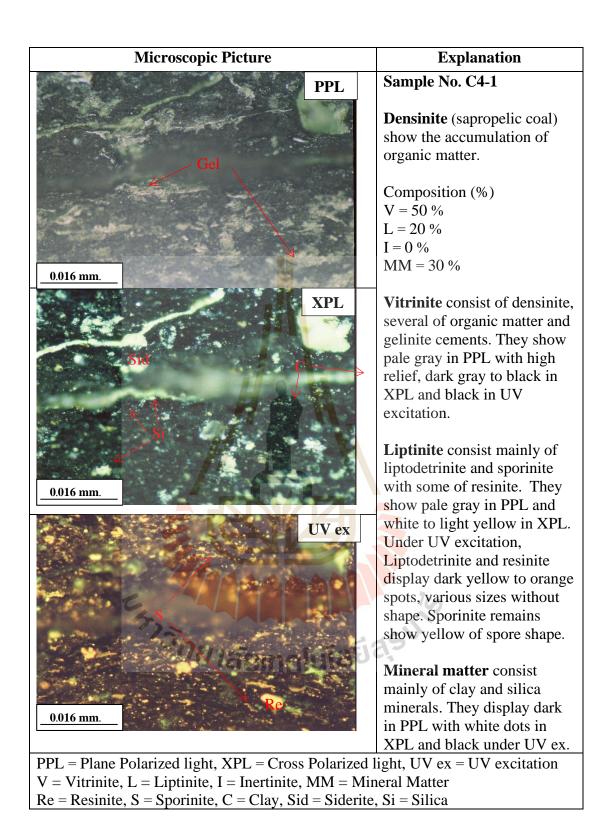
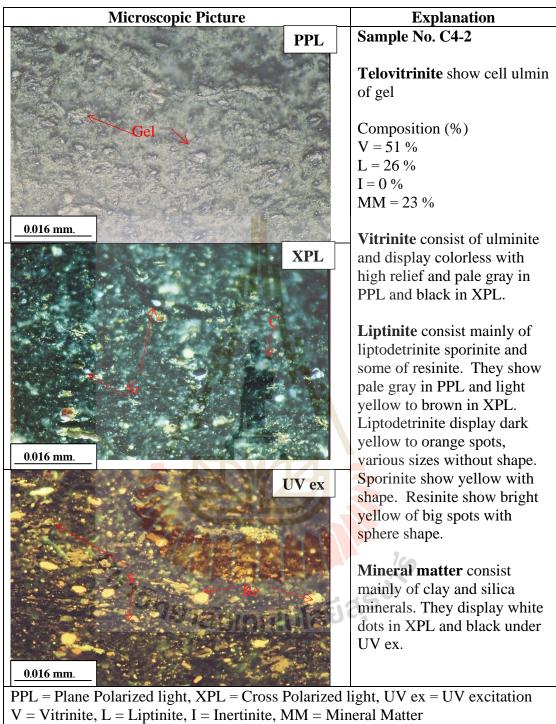


Figure 4.35 The microscopic picture of coal sample No. C4-1.



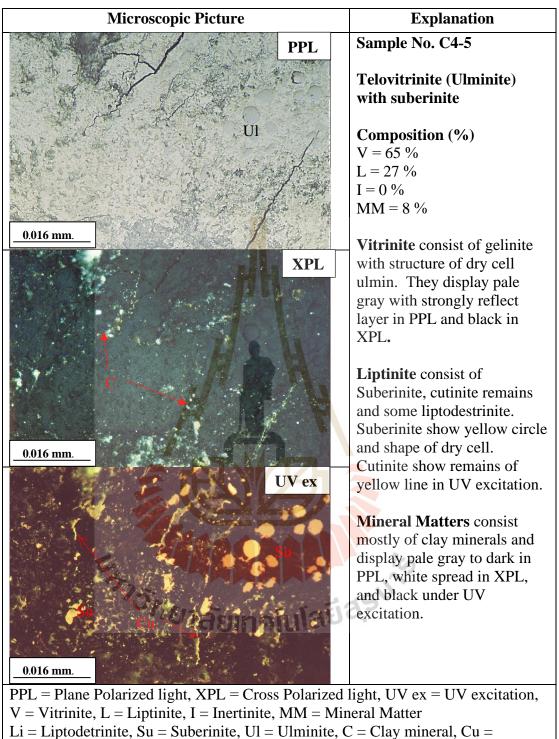
Re = Resinite, S = Sporinite, C = Clay

Figure 4.36 The microscopic picture of coal sample No. C4-2.

Microscopic Picture	Explanation
PPL	Sample No. C4-3
PPL	
A CONTRACT OF A	Telovitrinite with
	gelovitrinite and Resinite
Sc	
and the second se	Composition (%)
	V = 55 %
Tex-Ul	L =9 %
the second second second second	I = 1 %
	MM = 35 %
0.016 mm.	Vitninita consist of colinita
XPL	Vitrinite consist of gelinite with structure of ulmin and
AIL	gel dry. They display pale
and the second s	gray with strongly reflect
and the second	layer in PPL and black in
	XPL and UV ex.
H ANG	Liptinite consist of resinite,
	with some sporinite. Resinite
	show colorless to light
	yellow in PPL, white to
0.016 mm.	orange in XPL, bright yellow
UV ex	with sphere shape and highly
Ovex	orange rim, and small sphere
	shape in UV excitation.
A MARTIN AND A MARTIN	
Re	Inertinite is a sclerotinite in
	gelovtrinite.
A CONTRACTOR OF A CONTRACTOR OFTA CONTRACTOR O	Minoral Matters consist
• A Contraction of the contracti	Mineral Matters consist mostly of clay minerals and
S. COMPANY	display pale gray to dark in
	PPL, white spread in XPL
0.016 mm.	and black under UV
	excitation.
PPL = Plane Polarized light, XPL = Cross Polarized	
V = Vitrinite, L = Liptinite, I = Inertinite, MM = Min	

V = Vitrinite, L = Liptinite, I = Inertinite, MMRe = Resinite, S = Sporinite, Sc = Sclerotinite

Figure 4.37 The microscopic picture of coal sample No. C4-3.



Cutinite

Figure 4.38 The microscopic picture of coal sample No. C4-5.

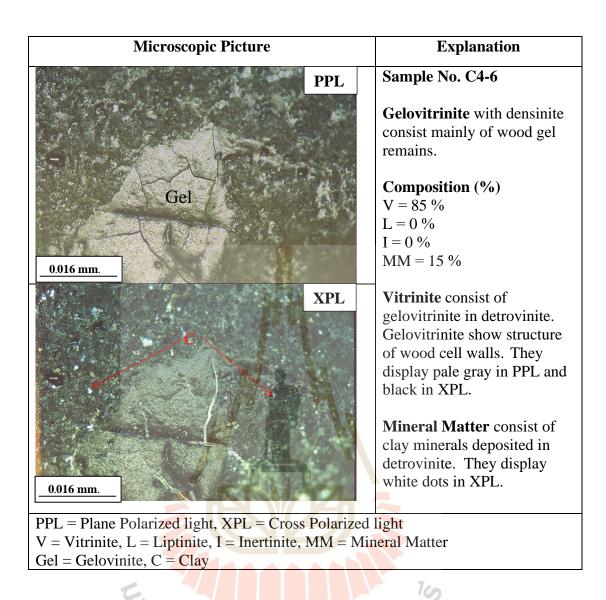


Figure 4.39 The microscopic picture of coal sample No. C4-6.

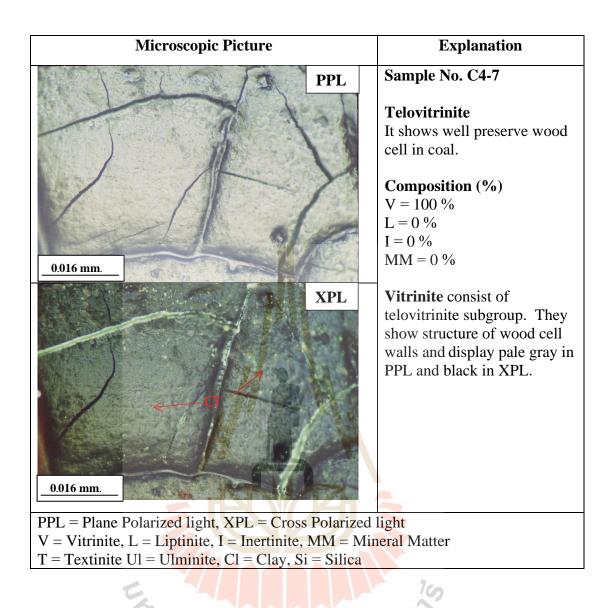
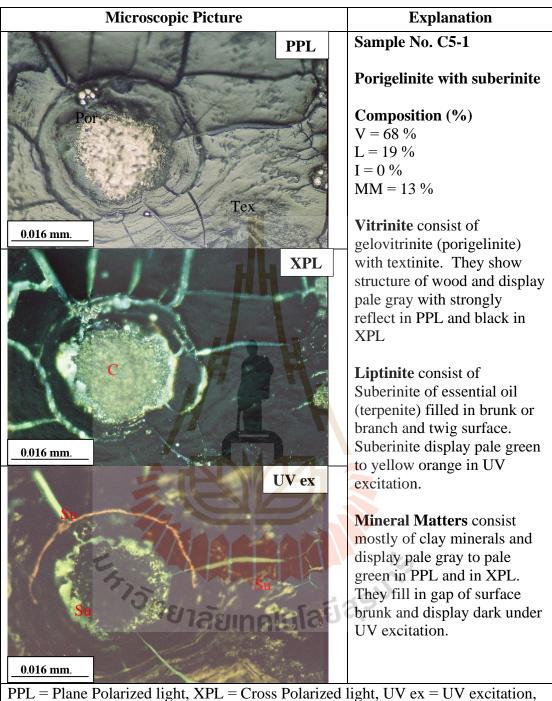
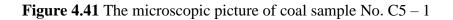


Figure 4.40 The microscopic picture of coal sample No. C4-7.



V = Vitrinite, L = Liptinite, I = Inertinite, MM = Mineral MatterSu = Suberinite, C = Clay mineral, Por = Porigelinite, Tex = Texinite



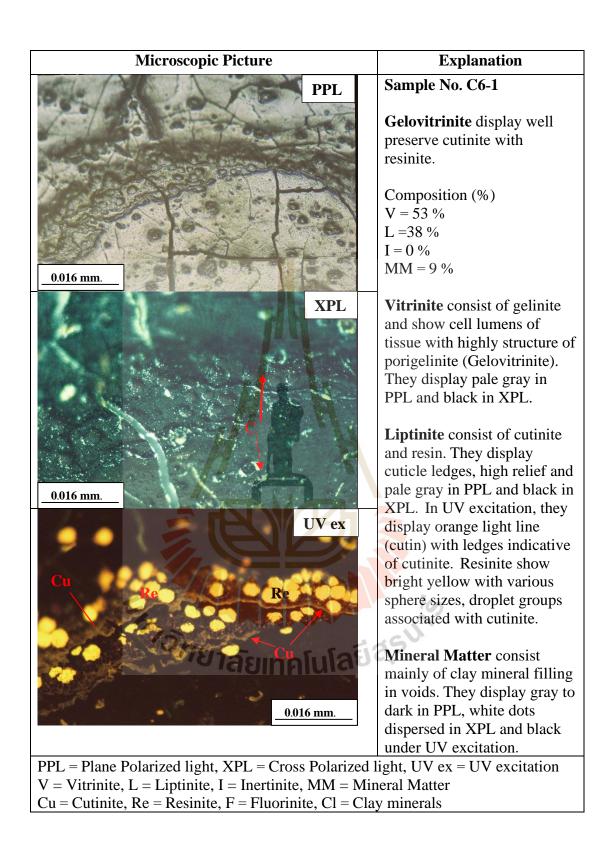


Figure 4.42 The microscopic picture of coal sample No. C6 – 1

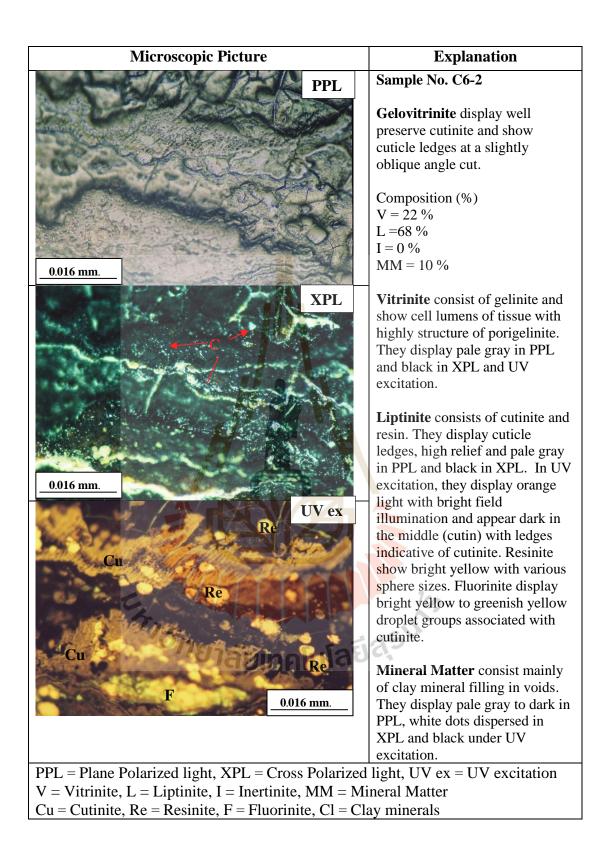
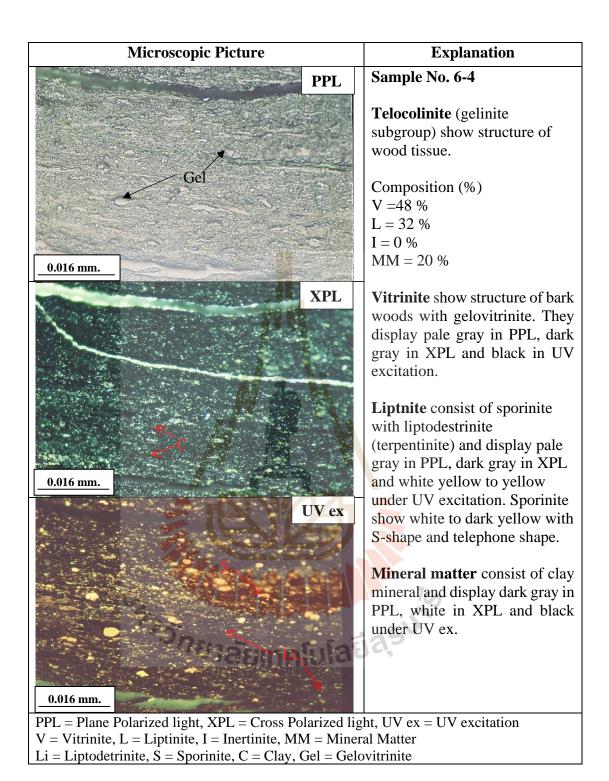
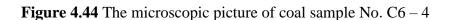


Figure 4.43 The microscopic picture of coal sample No. C6 - 2





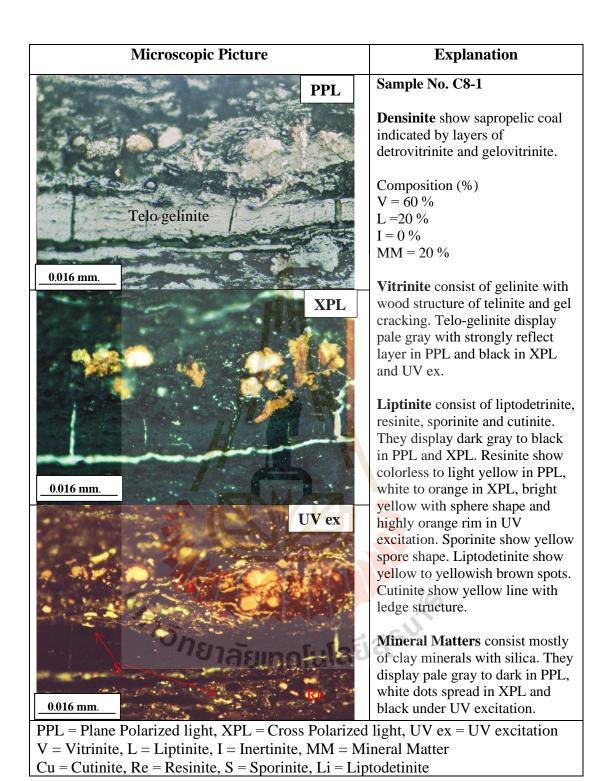


Figure 4.45 The microscopic picture of coal sample No. C8 – 1

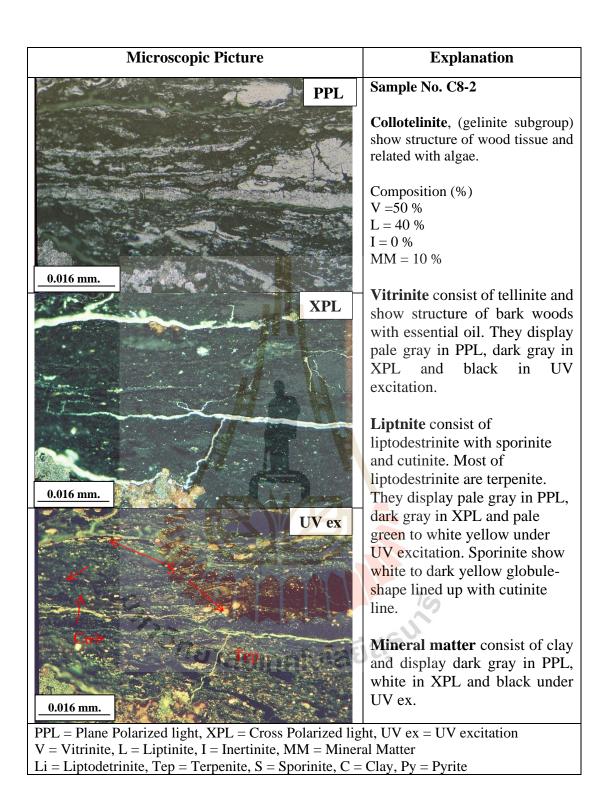


Figure 4.46 The microscopic picture of coal sample No. C8 – 2

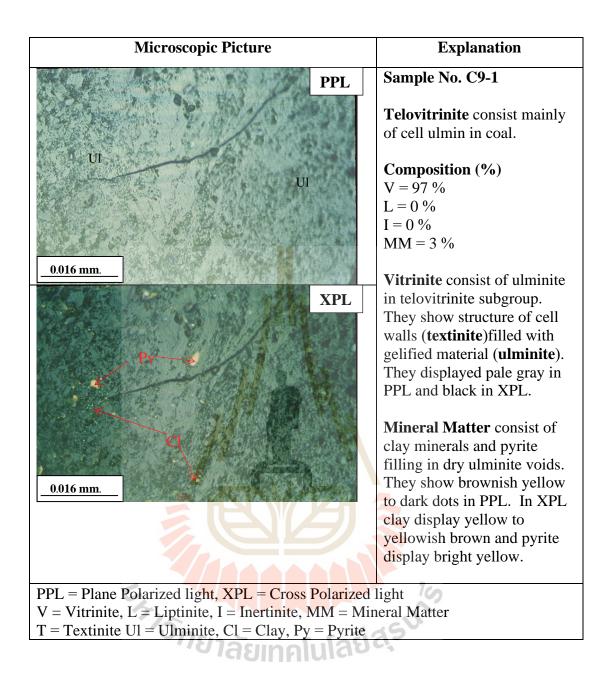


Figure 4.47 The microscopic picture of coal sample No. C9 – 1

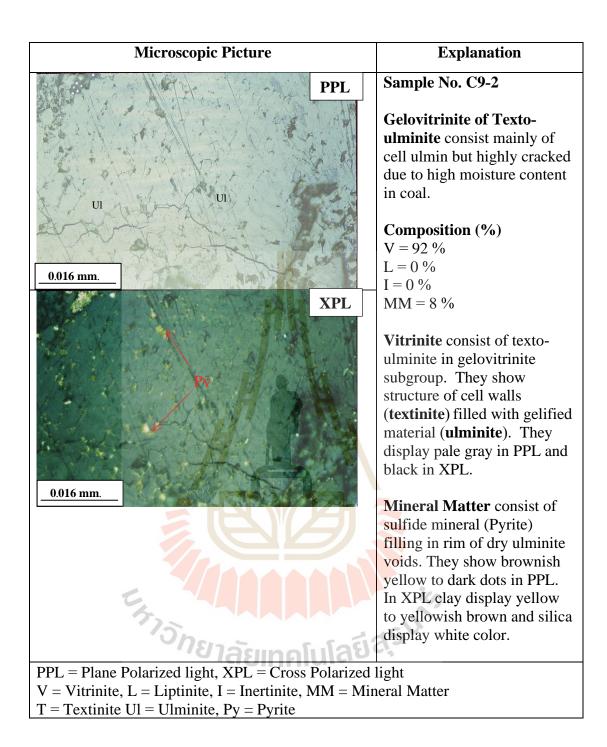


Figure 4.48 The microscopic picture of coal sample No. C9 – 2

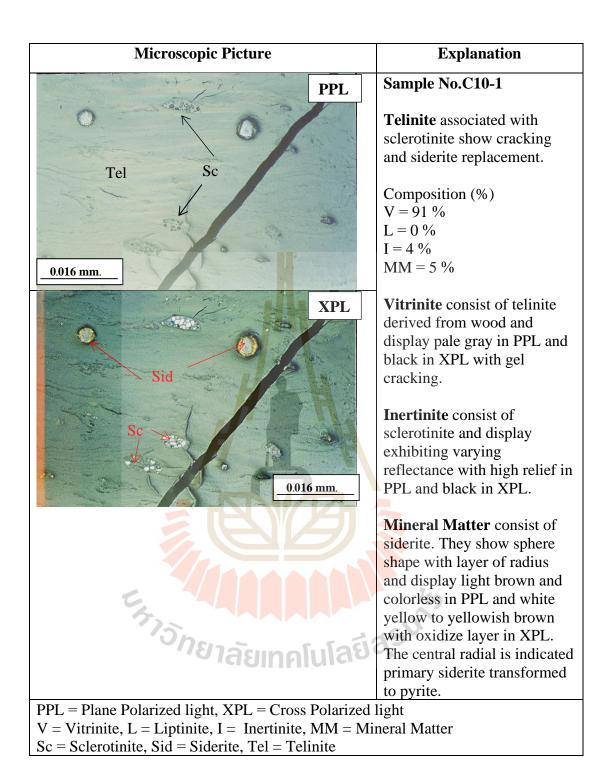


Figure 4.49 The microscopic picture of coal sample No. C10 - 1

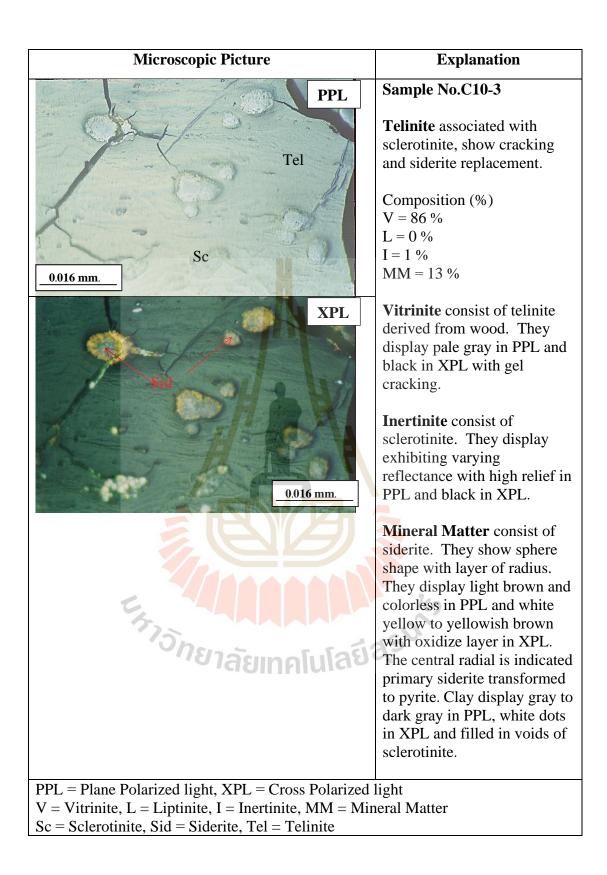


Figure 4.50 The microscopic picture of coal sample No. C10 - 3

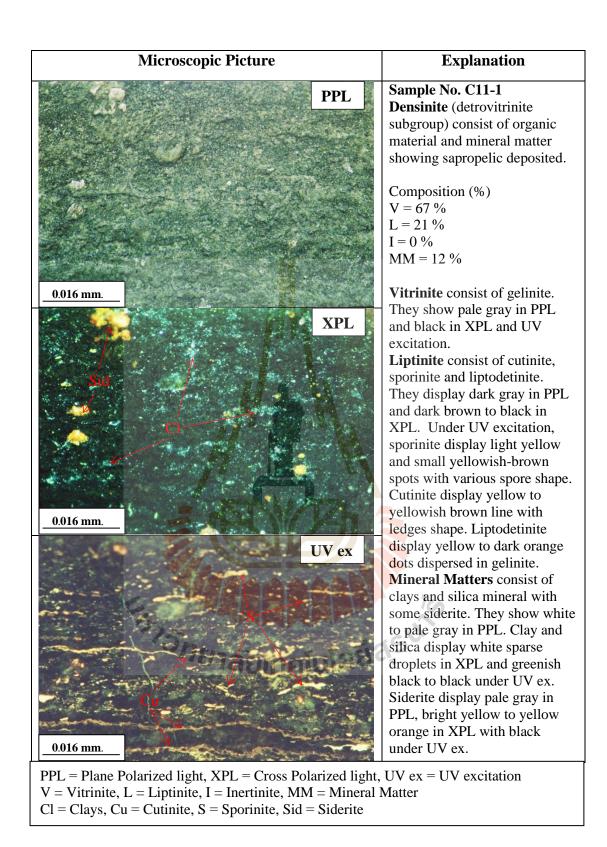


Figure 4.51 The microscopic picture of coal sample No. C11 - 1

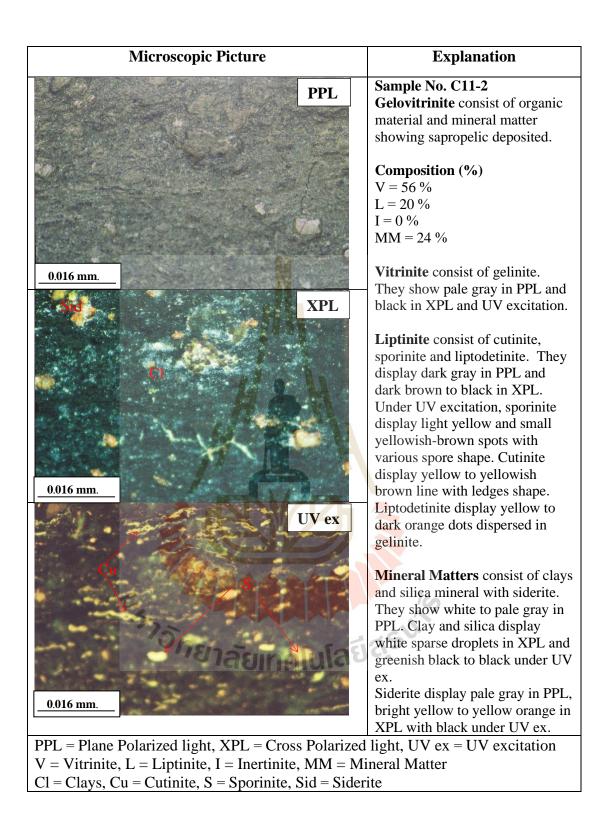


Figure 4.52 The microscopic picture of coal sample No. C11 - 2

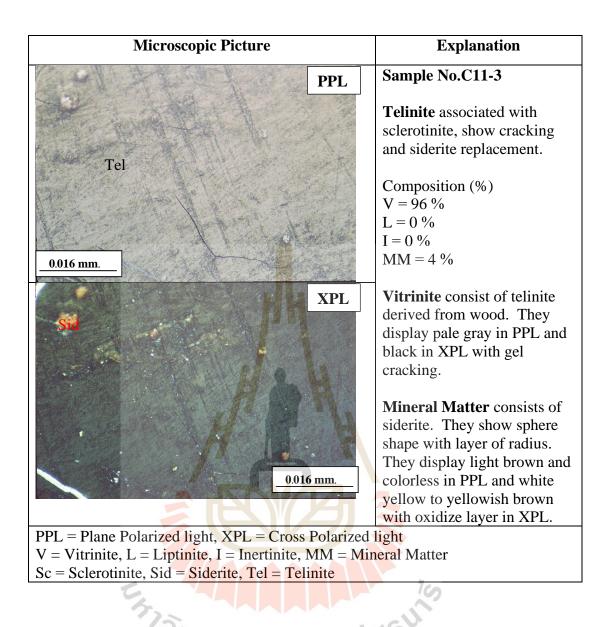
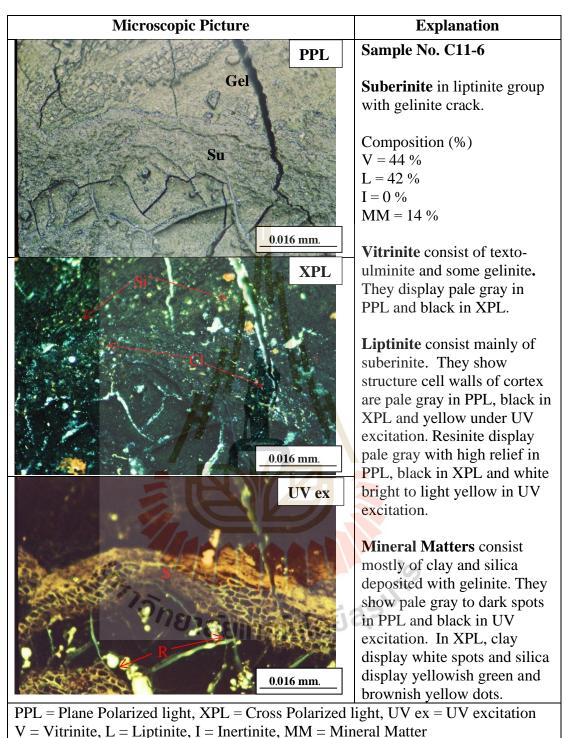
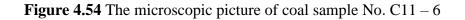


Figure 4.53 The microscopic picture of coal sample No. C11 - 3



Cl = Clay, Si = Silica, Su = Suberinite, Re = Resinite, Cg = Gel = Gelinite



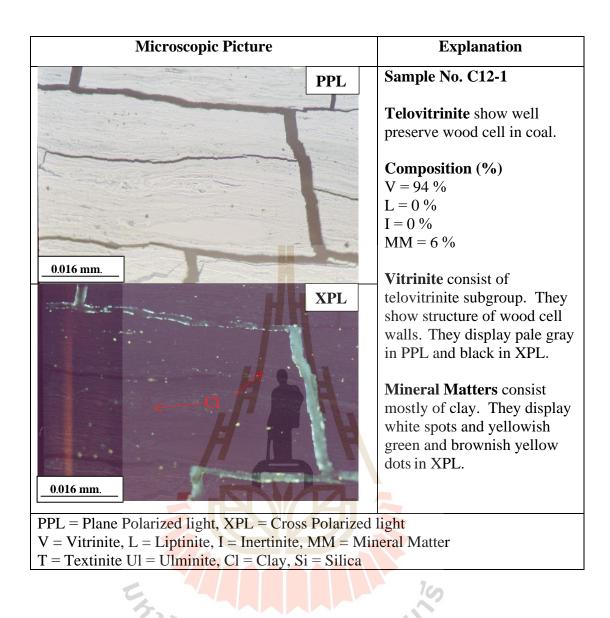


Figure 4.55 The microscopic picture of coal sample No. C12 – 1

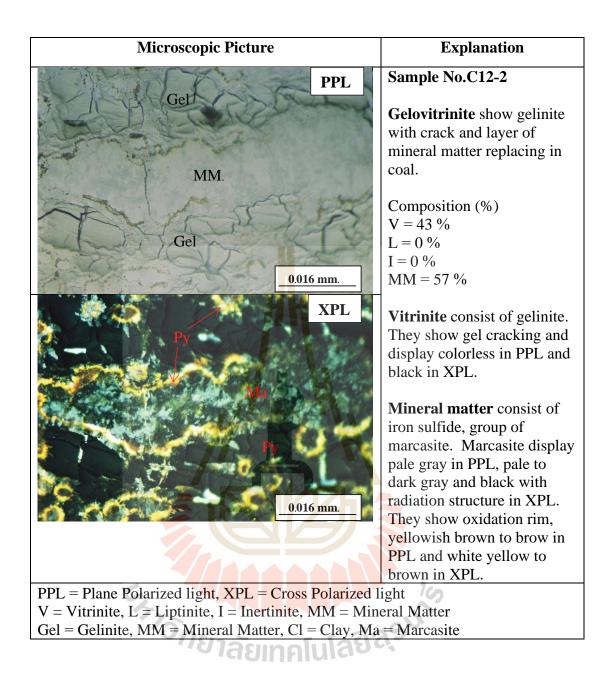


Figure 4.56 The microscopic picture of coal sample No. C12 - 2

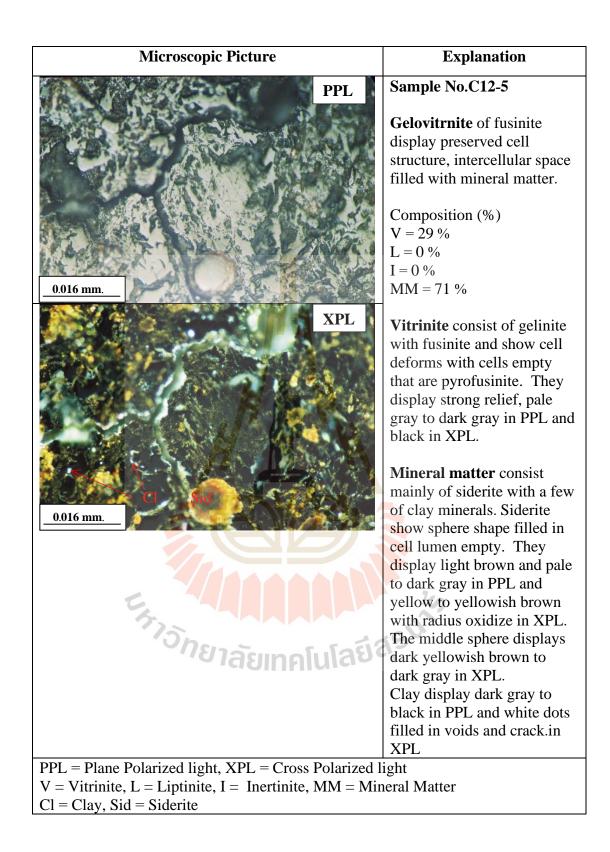


Figure 4.57 The microscopic picture of coal sample No. C12 - 5

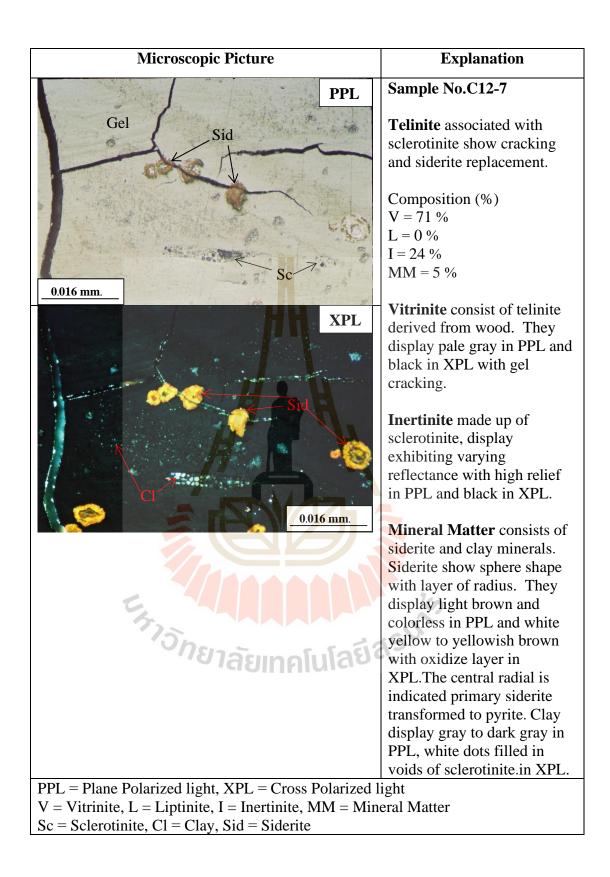


Figure 4.58 The microscopic picture of coal sample No. C12 – 7

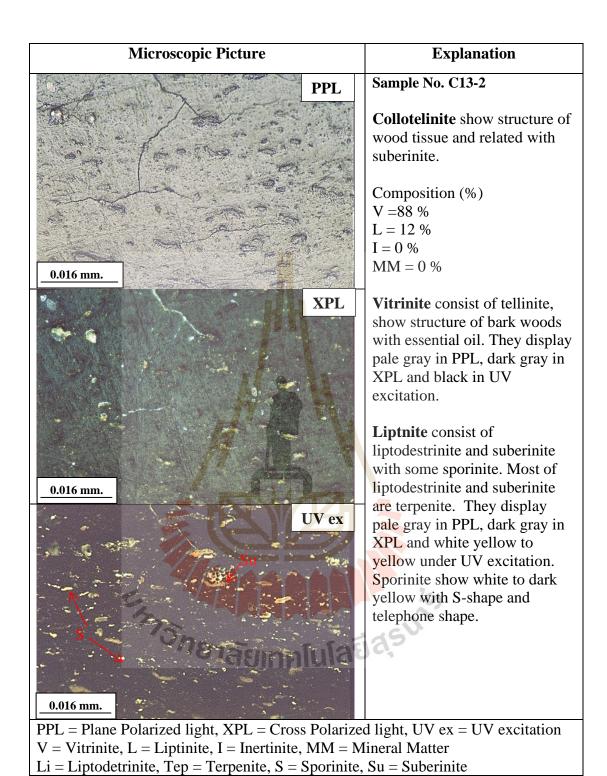


Figure 4.59 The microscopic picture of coal sample No. C13 - 2

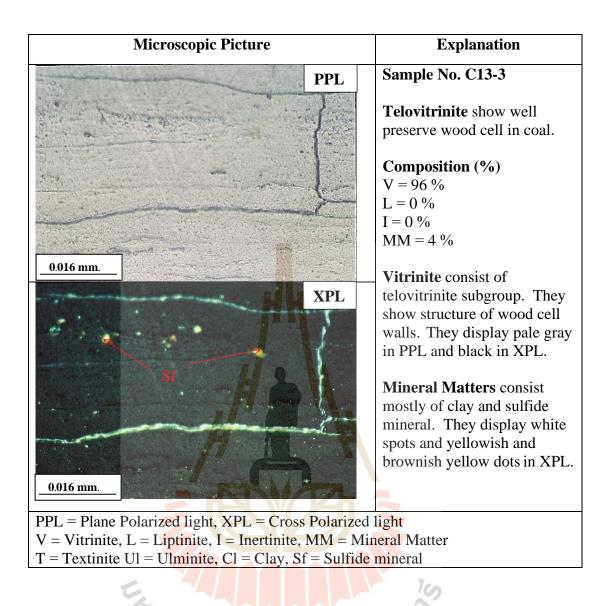


Figure 4.60 The microscopic picture of coal sample No. C13 – 3

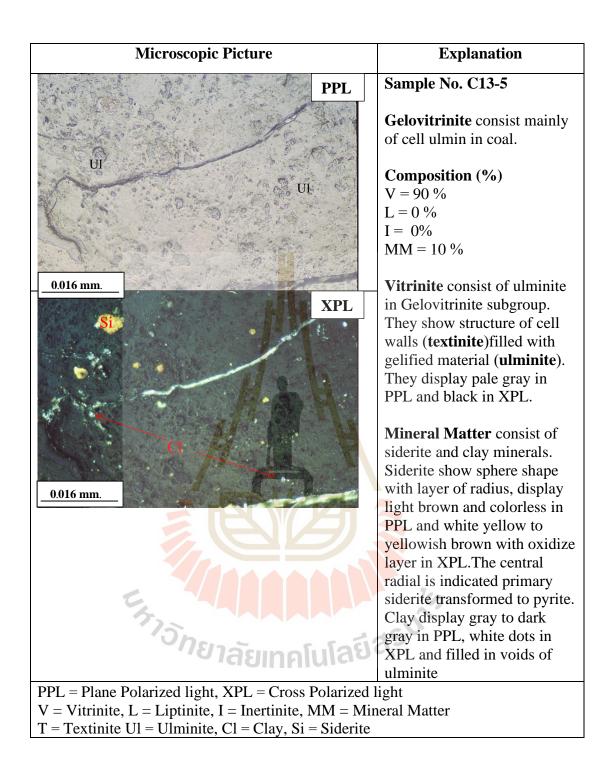


Figure 4.61 The microscopic picture of coal sample No. C13 – 5

4.2.3 Coal B sub-unit

Coal B sub-unit deposits between the coal C and coal A. The Coal B sub-unit is characterized by banded luster of moderate dull to glossy luster. The Coal B consists mainly of vitrinite 75.29%, liptinite 11.88% with a few of inertinite 0.12%, and mineral matter 12.71% (Table 4.6). The vitrinite consist of telovitrinite (38.47%) and gelovitrinite (44.71%). Telovitrinite shows characters of plant tissue which are telinite, texto-ulminite or porigelinite. Some of them show discernible characters of woods and barks displaying faint outline structure so called telinite. Some of them are highly decomposed and undergone gelification processes led to gelinite of gelovitrinite. Both gelinite and textinite usually display bright banded coals of vitrain and clarain (Figure 4.63 - 4.67). They display white to pale gray in PPL and dark gray to black in XPL. They occurred preferentially through oxidation of peat in abundant of water and near surface where oxygen easily contact the surface of peat deposit or in subaquatic environment. The coal consists mainly of vitrinite vary from 35 - 97% and they are particularly liptinite poor less than 42%. This represents forest peat origin and lack of terpenite associated in wood structure. The sclerotinites of inertinite group was also found in this Coal B sub-unit (Figure 4.63).

Liptinite found in this coal sub-unit consist mainly of resisted to oxidation maceral i.e. sporinite, resinite and liptodetrinite. Some of samples are dominated by sporinite which are deposited into humic gel and transformed to gelinite by absorption of water. They are cannel coal where the sporinite are more dominated than alginate. They should be represented the reed peats in the forest swamp. They display bright to dark yellow in fluorescence light with the character of spore shape (Figure 4.72). The resinite in gelovitrinite could be derived from leaf tissues which generally tend to be very rich in resin, especially conifers found in the Tertiary flora. There are also isolated resinite bodies which are original cell excretion when the tissues are destroyed. They remain as individual entities that are commonly found in Tertiary coals. They display pale gray in PPL with high relief and brown to black in XPL. Under UV excitation they display bright yellow with rodlets bodies which resin embedded in cell tissues (Figure 4.69 and 4.71). The liptodetrinite together with sporinite should indicate the extension of reed swamp to subaquatic area where 'gyttja' deposit with organic mud. They display pale gray to dark gray in PPL and brown to black in XPL, and yellow to yellowish brown in irregular shape and other fine-grained clearly distinguished under the UV excitation

The small amount of mineral matters is found in this sub-unit, but in some layers there are silica diatomite, deposited with sporinite and a few of other materials. Diatomite display pale gray to white in PPL, white in XPL and fluorescence in white yellow to greenish yellow under UV excitation (Figure 4.70). The present of diatomite in coal layers could be indicated the prevailing contribution of high silica volcanic ash from distant volcanic eruption

		Vitr	inite			Liptinite										
								Algi	nite					In	MM.	
Sample	Tel	Det	Gel	Total	Sp	Cu	Lip	Lam	Te	Re	Fl	Su	Total			
B15-4	96	0	0	96	0	0	0	0	0	0	0	0	0	2	2	
B15-5	75*	0	18	93	0	0	0	0	0	0	0	0	0	0	7	
B15-7	93	0	2	95	0	0	0	0	0	0	0	0	0	0	5	
B15-8	90*	0	5	95	0	0	0	0	0	0	0	0	0	0	5	
B16-2	94	0	3	97	0	0	-0	0	0	0	0	0	0	0	3	
B16-4	95	0	0	95	0	0	0	0	0	0	0	0	0	0	5	
B17-2	0	0	35	35	2	5	17	0	0	2	0	0	26	0	39	
B17-4	0	0	65	65	2	0	13	0	0	9	0	0	24	0	11	
B17-8	0	0	37	37	3	0	12	0	0	4	0	0	19	0	44	
B17-7	0	0	48	48	0	0	4	0	0	0	0	0	4	0	48	
B17-10	0	0	49	49	3	14	4	0	0	2	0	0	23	0	28	
B17-11	0	0	50	50	0	20	9	0	0	13	0	0	42	0	8	
B17-14	96*	0	0	96	0	0	0	0	0	0	0	0	0	0	4	
B17-12	0	0	87	87	9	0	4	0	0	0	0	0	13	0	0	
B18-2	0	0	69	69	7	0	22	0	0	2	0	0	31	0	0	
B18-4	15	0	79	94	0	0	0	0	0	0	0	0	0	0	6	
B18-5	0	0	79	79	4	0	15	0	0	1	0	0	20	0	1	
min	0	0	2	35	2	75	- 4	0	0	9 1	0	0	0	0	0	
max	96	0	87	97	9	20	22	0	0	13	0	0	42	2	48	
Average	23.12	0.00	36.82	75.29	1.76	2.29	5.88	0.00	0.00	1.94	0.00	0.00	11.88	0.12	12.71	

Table 4.6 Composition in percentage of Coal B sub-unit samples.

* = Texto-Ulminitel, Tel = Telovitrinite, Det= Detrovitrinite, Gel = Gelovitrinite, In = Inertinite, MM. = Mineral Matter Sp = Sporinite, Re = Resinite, Lip = Liptodetrinite, Cu = Cutinite, Fl= Fluorinite, Su = Suberinite, Lam = Lamalginite, Te= Telalginite

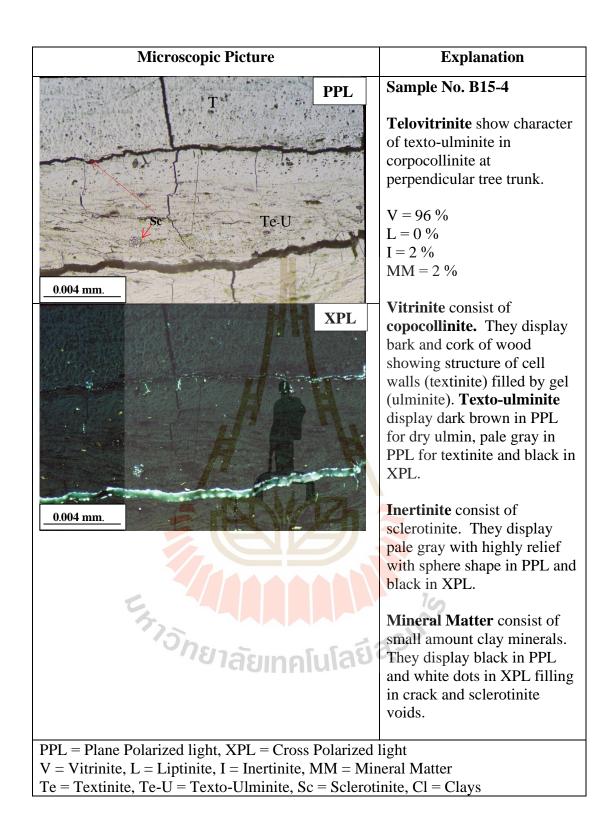


Figure 4.62 The microscopic picture of coal sample No. B15 – 4

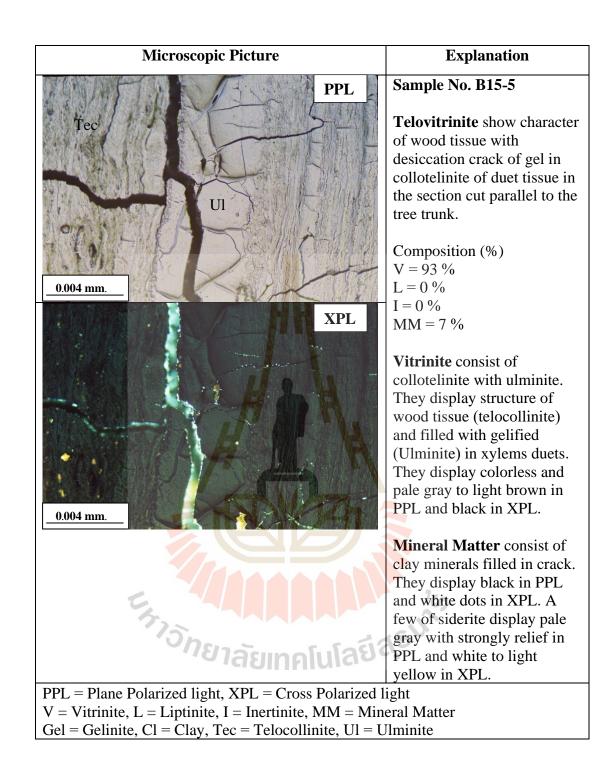


Figure 4.63 The microscopic picture of coal sample No. B15 – 5

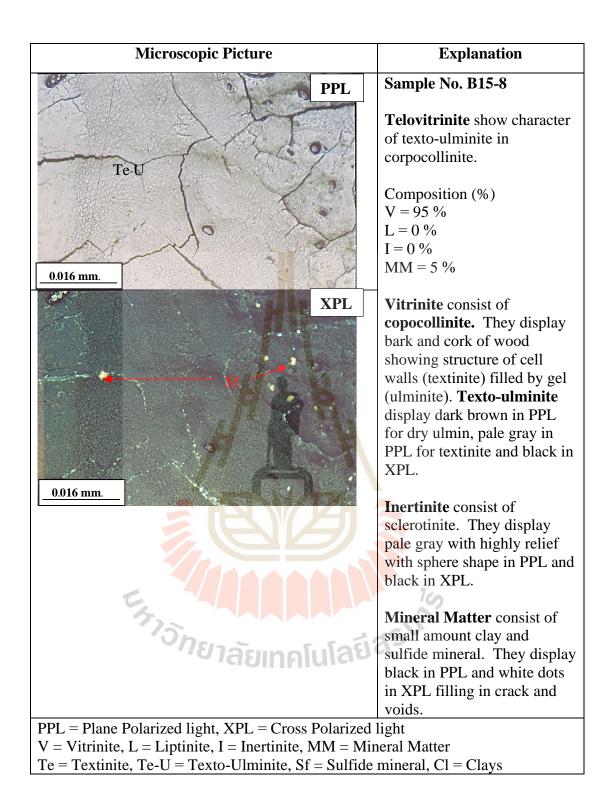


Figure 4.64 The microscopic picture of coal sample No. B15 - 8

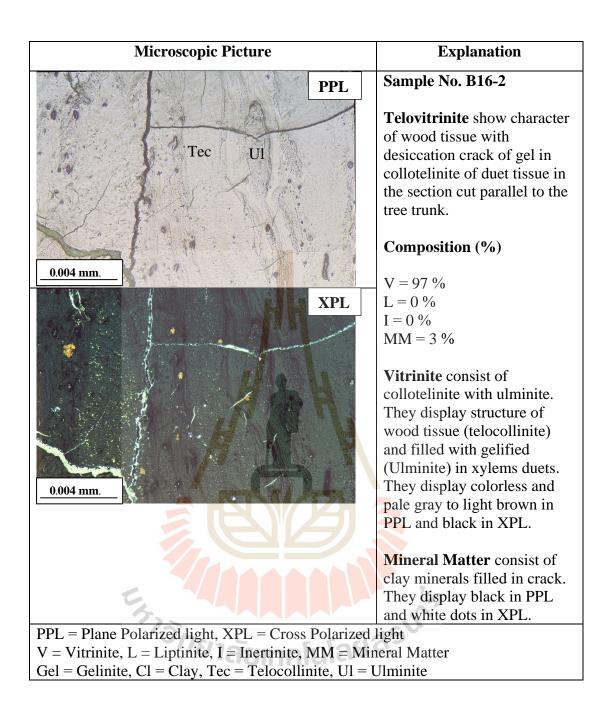


Figure 4.65 The microscopic picture of coal sample No. B16 – 2

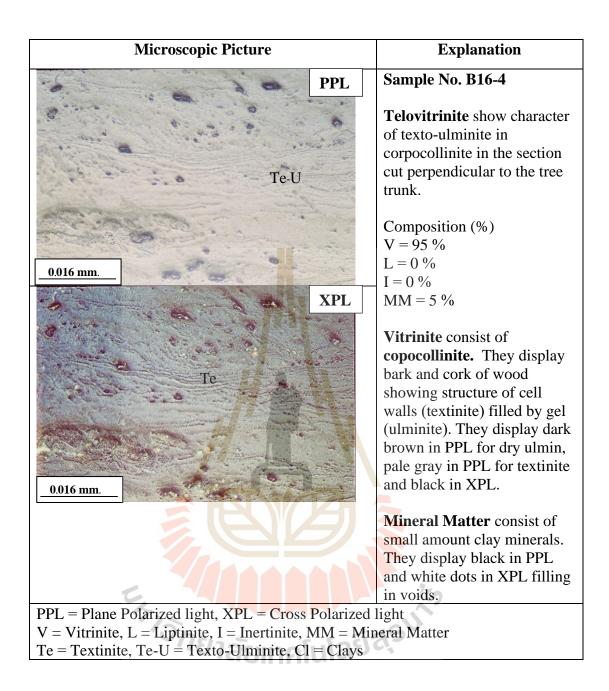


Figure 4.66 The microscopic picture of coal sample No. B16 – 4.

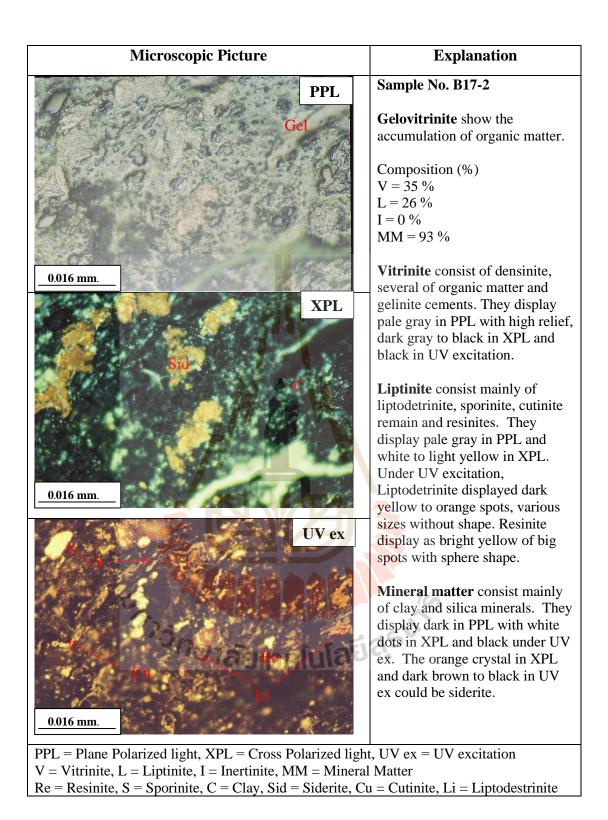
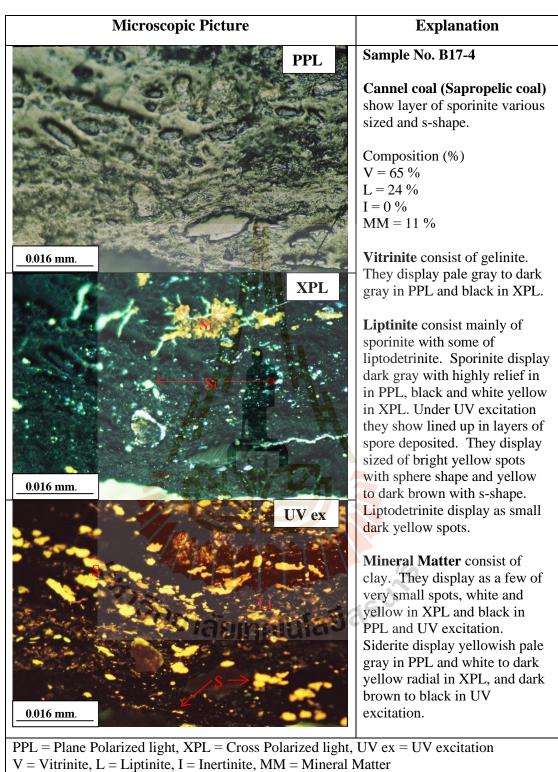
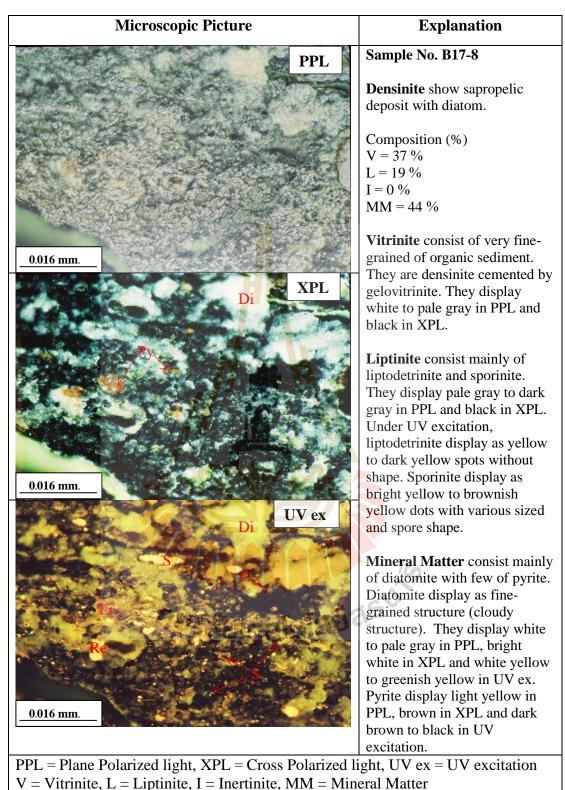


Figure 4.67 The microscopic picture of coal sample No. B17 - 2.



S = Sporinite, Li = Liptodestinite, Cl = Clay, Si = Siderite

Figure 4.68 The microscopic picture of coal sample No. B17 – 4.



V = Vitilite, L = Liptilite, I = Institute, With = Witherar With

Figure 4.69 The microscopic picture of coal sample No. B17 - 8.

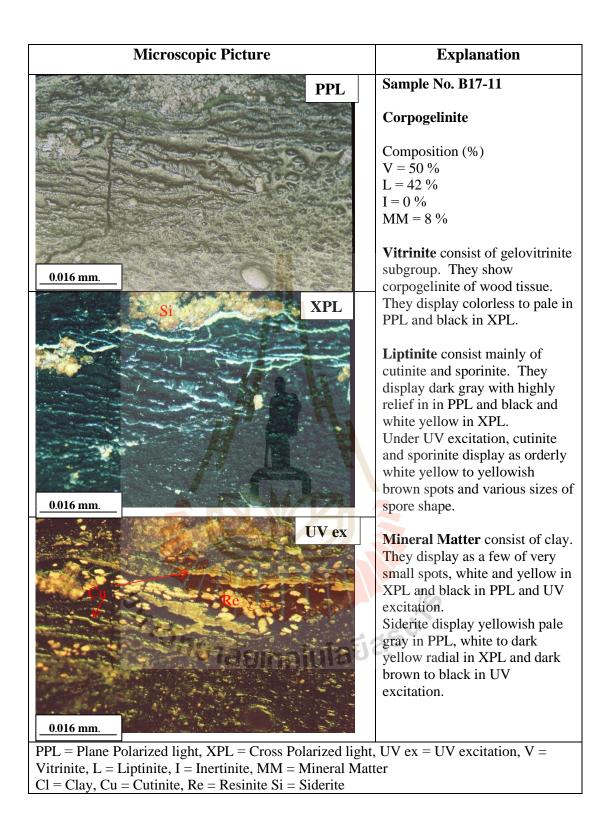


Figure 4.70 The microscopic picture of coal sample No. B17 – 11

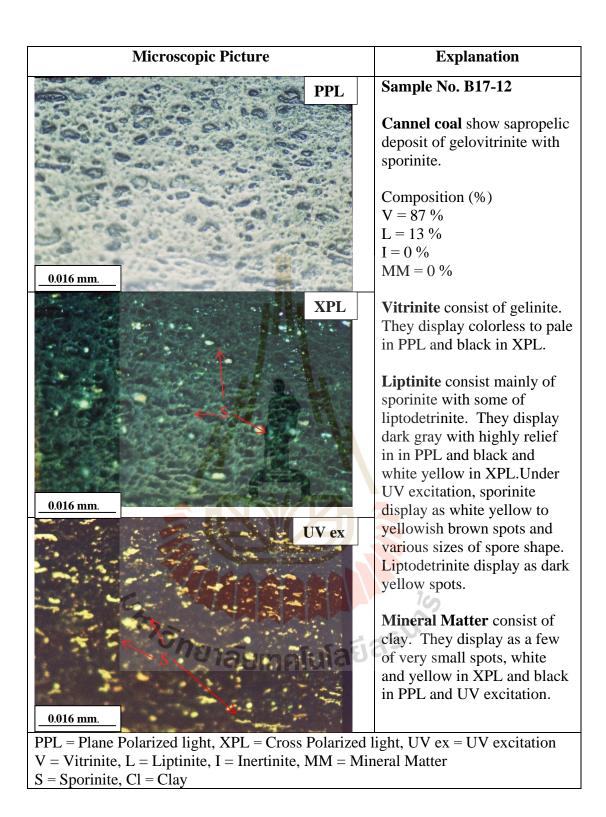


Figure 4.71 The microscopic picture of coal sample No. B17 – 12

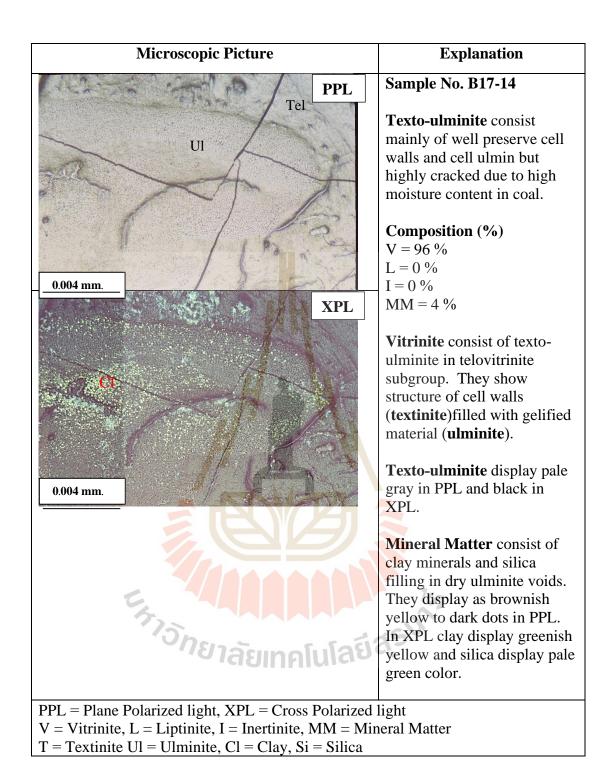


Figure 4.72 The microscopic picture of coal sample No. B17 – 14.

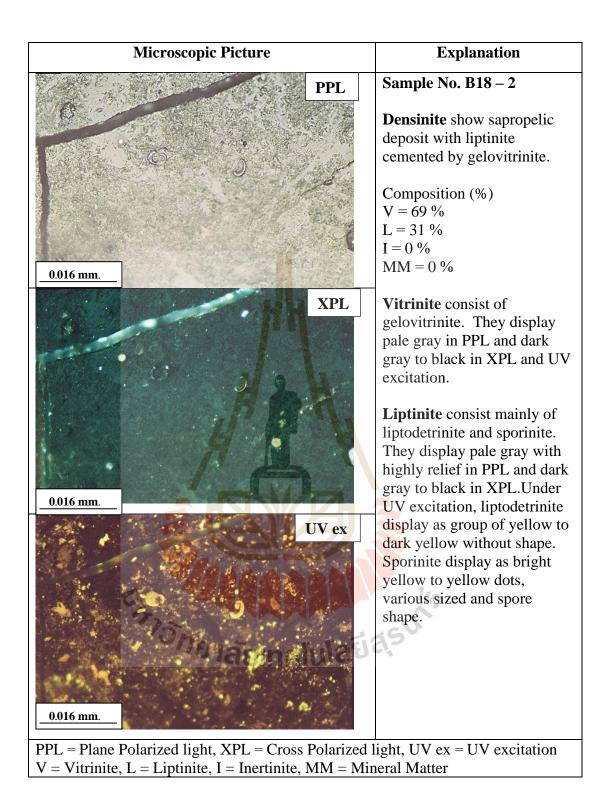


Figure 4.73 The microscopic picture of coal sample No. B18 – 2.

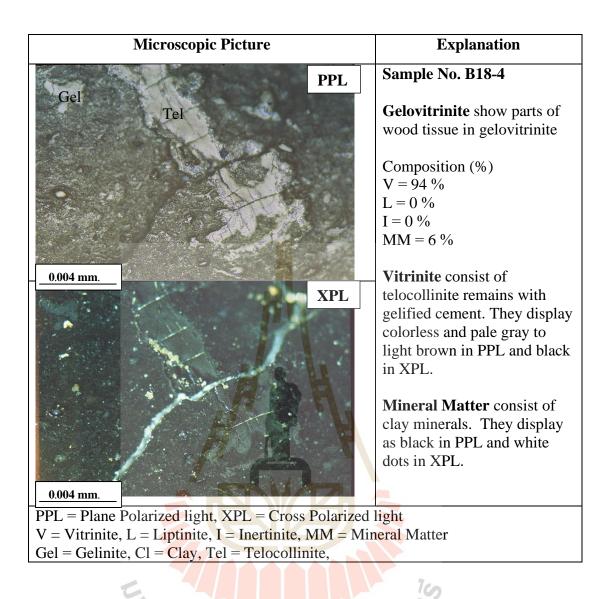


Figure 4.74 The microscopic picture of coal sample No. B18 – 4.

4.2.4 Coal A sub-unit

Coal A is the uppermost layer of the coal sub-units. The characters of this sub-unit show the coal bearing sequences from the lower part consisting of leonardite, sapropelic coal, and the upper part which is ended up with humic coal and preserved plant tissue. The vitrinite are vary from 28 - 100%. They consist mainly of telovitrinite (48.17%) and gelovitrinite (20.94%) which are represents the forest-peat swamp environment (Table 4.7). The sapropelic coal consists mainly of detrovitrinite deposited with liptinite group in gelovitrinite. They display difference fluorescence character of various liptinite in dark background of gelovitrinite under UV excitation (Figure 4.75 – 83). The coal derived from plant tissues as originate mainly from wood part show the ongoing processes that the lignin and cellulose of plant-cell walls and peatification are transformed to humic substance. They display dark color under microscope.

Telovitrinite consist of telinite, collotelinite and porigelinite which show character of wood structure (Figure 4.84). The vitrinite found in this coal sub-unit are believed to deposit in high water since they show character of gel associated with liptinite and a few of inertinite. Liptinite are filled in lacuna of porigelinite, collotelinite or dry cell and well preserve of plants (Figure 4.88, 4.95 and 4.96). The telovitrinite in gel can preserve plant tissues which are derived from wood stems, roots and barks (Figure 4.86 and 4.88). They also show difference fluorescing color under microscope with UV excitation. A few of sclerotinite which derived from fungal (a minor inertinite group) was found associated with telinite (Figure 4.101).

The liptinite display white or pale gray in PPL, black in XPL. The wellpreserved leaf layers coal show cutinite with fluorinite (chlorophyllinite) which indicate strongly reducing environment. Under UV excitation, the well preserved cutinite display as long wavy thin line, with cuticle ledges high relief in PPL. The fluorinite (chlorophyllinite) display as arrayed small bright white, yellow to greenish yellow dots under cutinite strips (Figure 4.95 and 4.99) which indicate the well preservation under reducing condition. The sporinite can be observed a typical structural feature of the exine, which are noticeable by double lines, yellow to brownish yellow under UV excitation (Figure 4.95, 4.96 and 4.99). Exsudatinite are presented in vitrinite and filled cracks of gelinite. They display as white-yellow to greenish-yellow fluorescing mass filled in void and fine cracks (Figure 4.94). The small amount of mineral matters in this Coal A sub-unit consist of framoidal pyrite, clay minerals, quartz, and other silica minerals. Framoidal pyrite display as white dots in PPL and XPL and dark under UV excitation. They are fill in crack of gelinite associate with exsudatinite (Figure 4.94, 104 and 4.106). Marcasite display colorless in PPL and white, gray to black with radiated structure in XPL which indicate the siderite intergrowth associated with pyrite (Figure 4.102, 4.103 and 4.109).

ะ รัว_{วั}กยาลัยเทคโนโลยีสุรุบา

		Vitr	inite			Liptinite											
								Algi	nite						In.	MM.	
Sample	Tel	Det	Gel	Total	Sp	Cu	Lip	Lam_	Te	Re	Fl	Su	Ex	Total			
A1-1	0	4	55	59	0	16	7	0	0	3	11	0	0	37	0	4	
A1-3	0	2	69	71	0	2	12	0	0	1	0	0	0	15	0	14	
A1-4	0	8	68	76	2	0	15	0	0	0	0	0	0	17	0	7	
A1-5	19	1	36	56	0	9	5	0	0	9	11	0	0	34	0	10	
A1-7	56	0	0	56	1	18	9	0	0	0	16	0	0	44	0	0	
A2-3	50	8	19	77	6	6	7	0	0	0	4	0	0	23	0	0	
A2-4	15	0	76	91	3	0	0	0	0	0	0	0	4	7	0	2	
A2-5	0	0	28	28	0	0	5	64	0	0	0	0	0	69	0	3	
A2-6	0	0	70	70	0	0	0	29	-0	0	0	0	0	29	0	1	
A2-7	2	1	27	30	6	0	8	35	0	0	0	0	0	49	0	21	
A2-8	49	4	9	62	2	16	6	10	0	0	3	0	0	37	0	1	
A2-1	87	0	3	90	0	0	0	-0	0	0	0	0	0	0	0	10	
A3-1	97*	1	0	98	0	0	0	0	0	0	0	0	0	0	0	2	
A5-2	40*	0	29	69	0	15	6	0	0	7	3	0	0	31	0	0	
A5-3	58	0	4	62	1	18	5	1	0	0	0	0	0	25	0	13	
A5-4	100	0	0	100	0	0	0	0	0	0	0	0	0	0	0	0	
A5-5	10	0	57	67	4	0	29	0	0	0	0	0	0	33	0	0	
A5-6	95	0	0	95	0	0	0	0	0	0	0	0	0	0	0	5	
A6-1	28	0	18	46	6	0	25	13	4	0	0	0	0	48	0	6	
A6-2	49	0	12	61	0	0	10	0	0	9	0	0	0	19	0	20	

Table 4.7 Composition in percentage of Coal A sub-unit samples.

* = Texto-Ulminitel, Tel = Telovitrinite, Det= Detrovitrinite, Gel = Gelovitrinite, In = Inertinite, MM. = Mineral Matter, Sp = Sporinite, Ex=Exsudatinite, Re = Resinite, Lip = Liptodetrinite, Cu = Cutinite, Fl= Fluorinite, Su = Suberinite, Lam = Lamalginite, Te= Telalginite

		Vitr	inite													
								Algi	nite						In.	MM.
Sample	Tel	Det	Gel	Total	Sp	Cu	Lip	Lam	Те	Re	Fl	Su	Ex	Total		
A6-3	76	0	0	76	0	0	0	3	0	0	0	0	0	3	0	21
A7-2	72	0	26	98	0	0	0	0	0	0	0	0	0	0	0	2
A7-4	81	0	13	94	0	0	0	0	0	0	0	0	0	0	0	6
A7-5	0	0	88	88	0	0	0	0	0	0	0	0	7	7	0	5
A9-1	1	0	57	58	4	8	8	0	-0	0	22	0	0	42	0	0
A9-3	82	0	0	82	5	0	6	0	0	0	7	0	0	18	0	0
A9-6	0	0	50	50	9	0	23	18 -	0	0	0	0	0	50	0	0
A9-9	24	0	30	54	5	0	17	22	2	0	0	0	0	46	0	0
A9-11	74	0	0	74	6	3	6	-0	0	0	5	0	0	20	0	6
A9-13	59	0	0	59	5	12	2	0	0	0	12	0	0	31	0	10
A10-1	89	0	0	89	0	0	0	0	0	0	0	0	0	0	5	6
A10-3	96	0	0	96	0	0	0	0	-0	0	0	0	0	0	0	4
A10-4	90	0	0	90	0	0	0	0	0	-0	0	0	0	0	6	4
A10-6	68	0	0	68	0	0	0	0	0	0	19	0	0	19	1	12
A10-8	75	0	7	82	2	1	7	0	0	0	6	0	0	16	0	2
A10-9	63	0	2	65	2	4	25	0	0	1	3	0	0	35	0	0
A10-10	17	0	37	54	1	24	9	0	0	0	8	0	0	42	0	4
A10-11	10	0	46	56	0	14	8	0	0	0	8	0	5	35	0	9
A11-3	88	0	0	88	0	0	0	0	0	0	12	0	0	12	0	0
A11-5	73	0	21	94	1	0	0	3	0	0	0	0	0	4	0	2
A11-7	0	0	69	69	0	0	1	0	0	0	14	0	0	15	0	16
* = Texto-U	lminitel,	Tel = T	elovitrin	ite, Det=	Detrov	itrinite,	Gel = 0	Gelovitr	inite, In	= Inert	inite, N	$\mathbf{M} = \mathbf{N}$	/lineral	Matter, S	$\mathbf{p} = \mathbf{S}\mathbf{p}$	orinite,

 Table 4.7 (Con.) Composition in percentage of Coal A sub-unit samples.

* = Texto-Ulminitel, Tel = Telovitrinite, Det= Detrovitrinite, Gel = Gelovitrinite, In = Inertinite, MM. = Mineral Matter, Sp = Sporinite, Re = Resinite, Lip = Liptodetrinite, Cu = Cutinite, Fl= Fluorinite, Su = Suberinite, Ex=Exsudatinite, Lam = Lamalginite, Te= Telalginite

		Vitı	rinite		Liptinite											
								Alginite							In.	MM.
Sample	Tel	Det	Gel	Total	Sp	Cu	Lip	Lam	Te	Re	Fl	Su	Ex	Total		
A11-8	88	0	0	88	0	0	0	0	0	0	0	0	0	0	0	12
A13-1	98	0	0	98	0	0	0	0	0	0	0	0	0	0	1	1
A13-2	87	0	0	87	5	0	6	0	0	0	1	0	0	12	0	1
A13-3	98	0	0	98	0	0	0	0	0	0	0	0	0	0	0	2
A13-4	96	0	0	96	0	0	0	0	0	0	0	0	0	0	1	3
min	0.00	1.00	2.00	28.00	1.00	1.00	1.00	1.00	2.00	1.00	1.00	0.00	4.00	0.00	0.00	0.00
max	100	8	88	100	9	24	29	64	4	9	22	0	7	69	6	21
%	48.33	0.63	22.30	74.24	1.65	3.61	5.80	4.30	0.13	0.65	3.59	0.00	0.35	20.09	0.30	5.37

Table 4.7 (Con.) Composition in percentage of Coal A sub-unit samples.

* = Texto-Ulminitel, Tel = Telovitrinite, Det= Detrovitrinite, Gel = Gelovitrinite, In = Inertinite, MM. = Mineral Matter Sp = Sporinite, Re = Resinite, Lip = Liptodetrinite, Cu = Cutinite, Fl= Fluorinite, Su = Suberinite, Ex = Exsudatinite, Lam = Lamalginite, Te= Telalginite



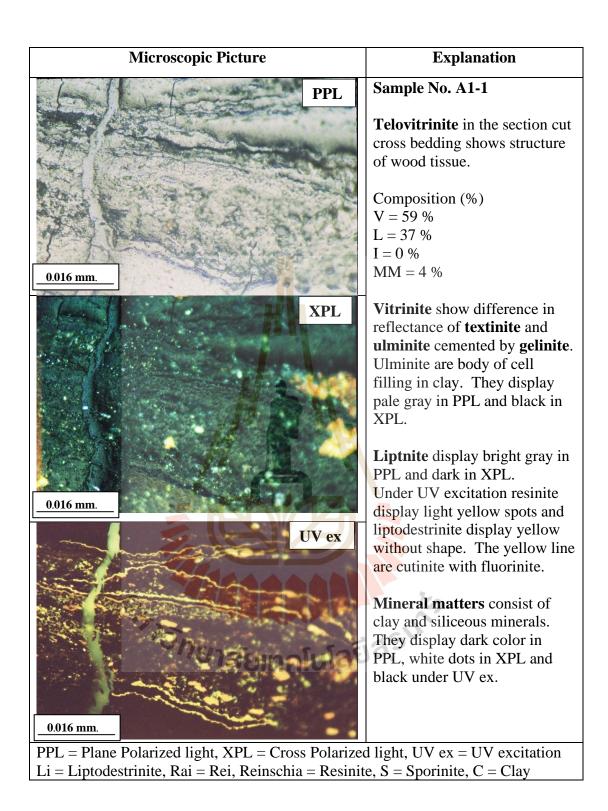


Figure 4.75 The microscopic picture of coal sample No. A1 - 1.

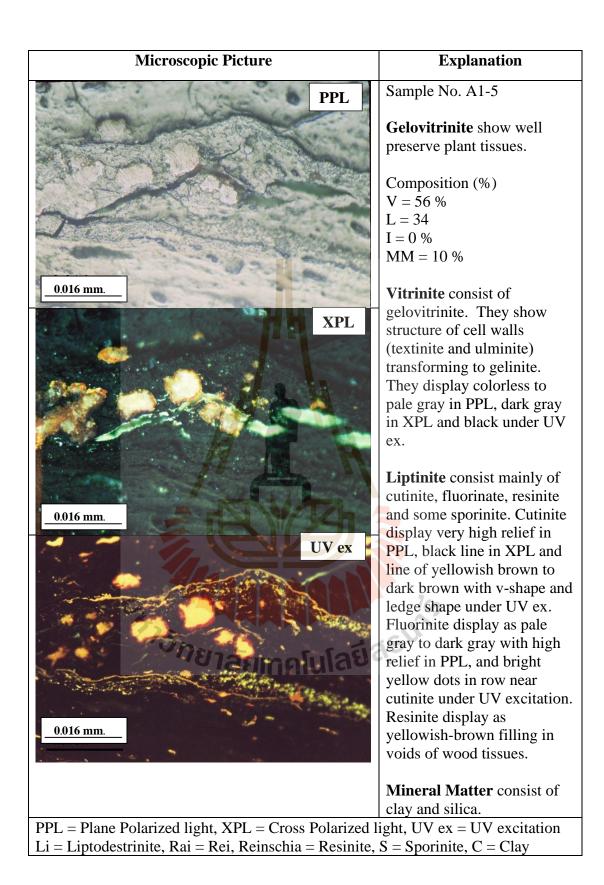


Figure 4.76 The microscopic picture of coal sample No. A1 - 5.

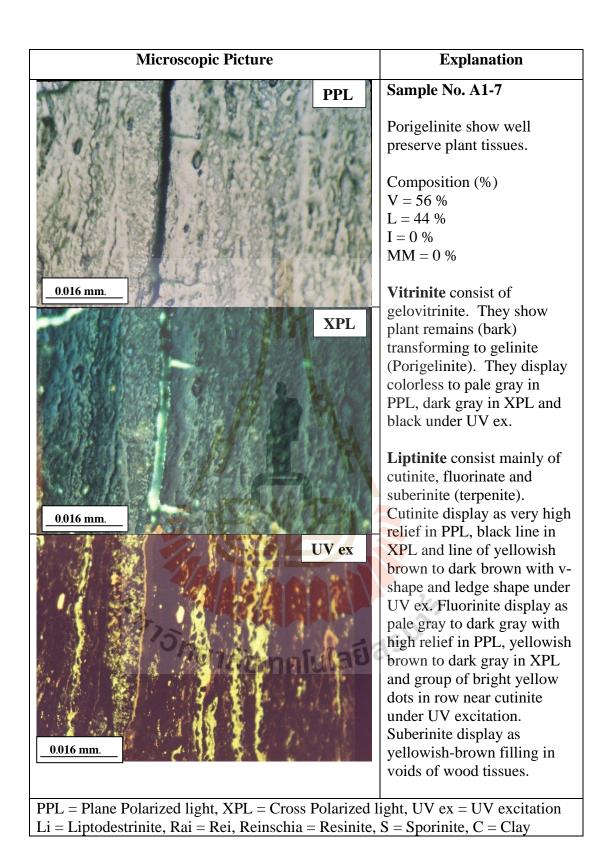


Figure 4.77 The microscopic picture of coal sample No. A1 - 7.

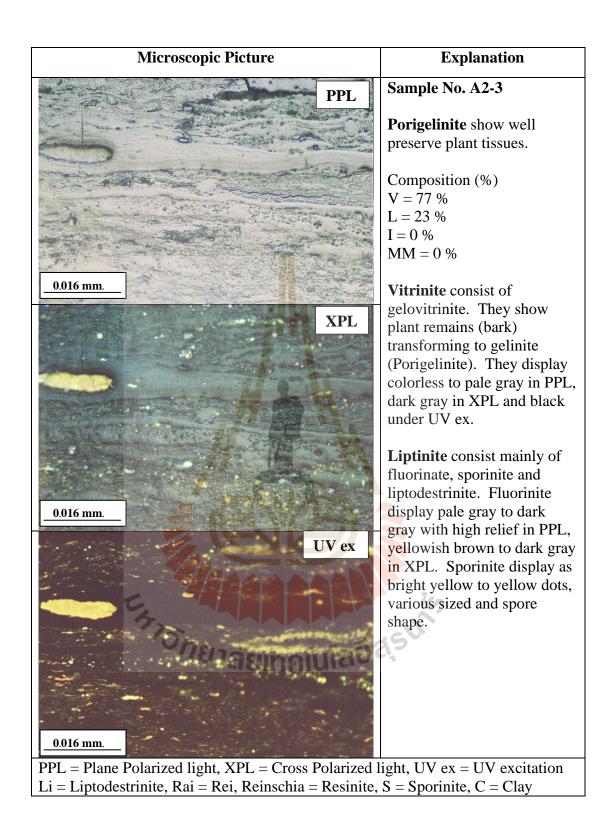
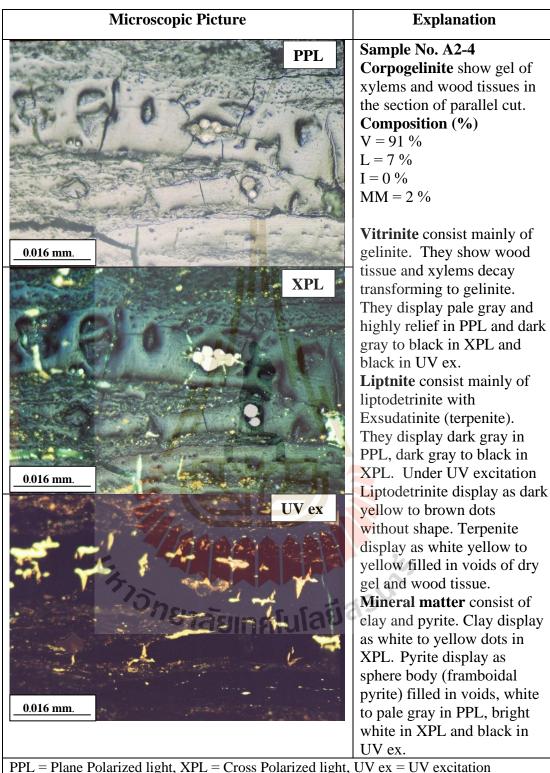
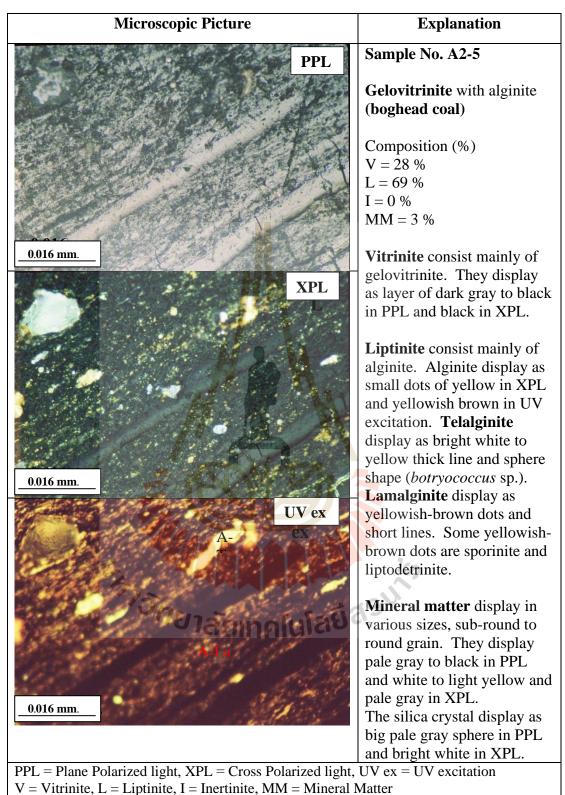


Figure 4.78 The microscopic picture of coal sample No. A2 - 3.



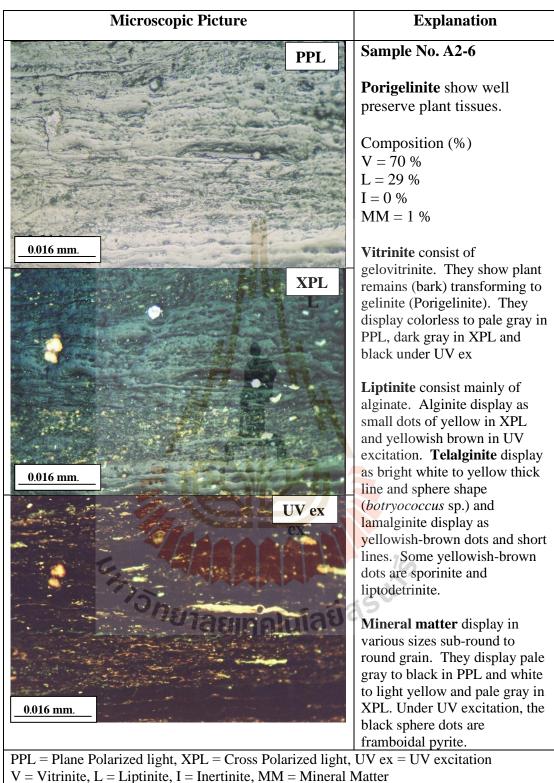
PPL = Plane Polarized light, XPL = Cross Polarized light, UV ex = UV excitation V = Vitrinite, L = Liptinite, I = Inertinite, MM = Mineral Matter Li = Liptodestrinite, Ex = Exsudatinite, Py = Pyrite, C = Clay

Figure 4.79 The microscopic picture of coal sample No. A2 - 4.



Li = Liptodestrinite, A-Te = Telalginite, A-La = Lamaginite, = Pyrite, C = Clay

Figure 4.80 The microscopic picture of coal sample No. A2 - 5.



Li = Liptodestrinite, A-Te = Telalginite, A-La = Lamaginite, Py = Pyrite, C = Clay

Figure 4.81 The microscopic picture of coal sample No. A2 - 6.

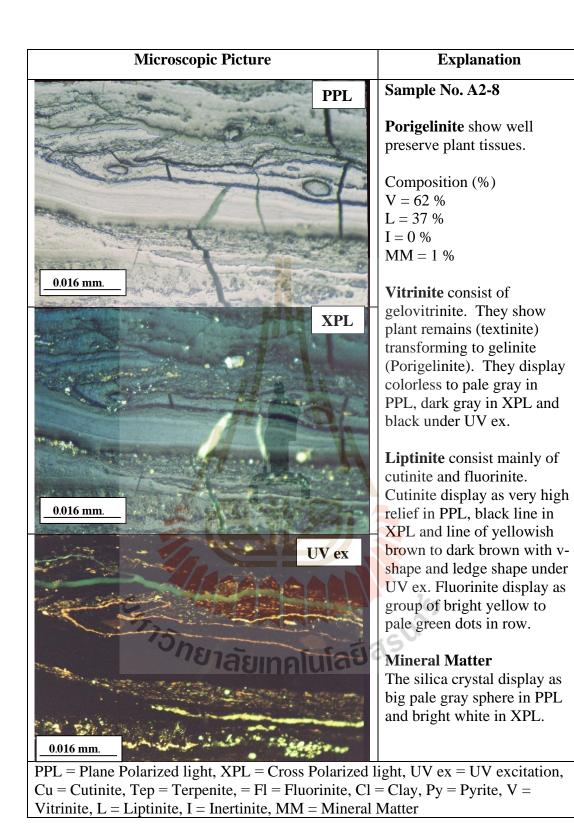
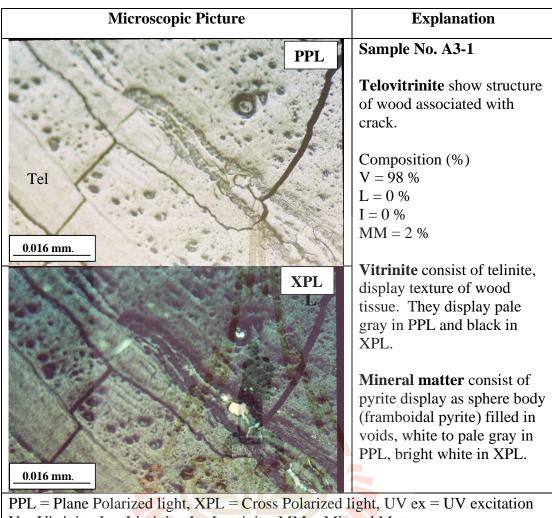
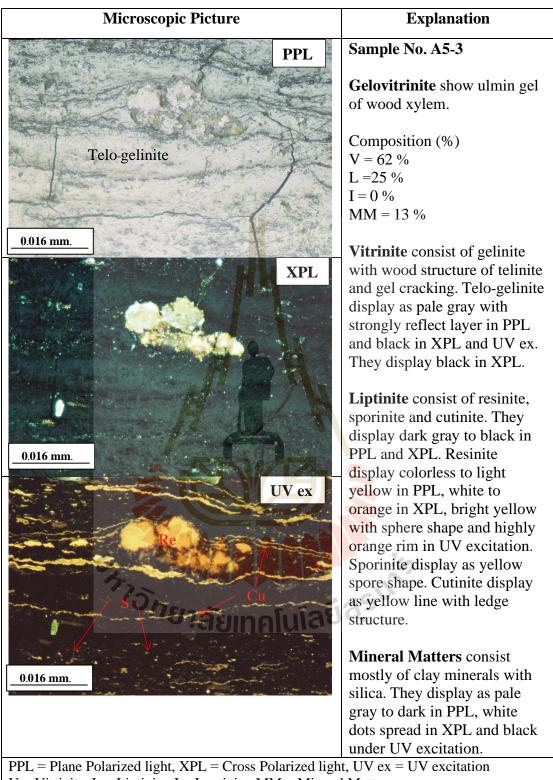


Figure 4.82 The microscopic picture of coal sample No. A2 - 8.



PPL = Plane Polarized light, XPL = Cross Polarized light, UV ex = UV excitatio V = Vitrinite, L = Liptinite, I = Inertinite, MM = Mineral Matter Tel = Telovitrinite, Te = Telinite, Ul = Ulminite, Cl = Clay, Py = Pyrite

Figure 4.83 The microscopic picture of coal sample No. A3 - 1.



V = Vitrinite, L = Liptinite, I = Inertinite, MM = Mineral MatterCu = Cutinite, Re = Resinite, S = Sporinite, Li = Liptodetinite

Figure 4.84 The microscopic picture of coal sample No. A5 - 3.

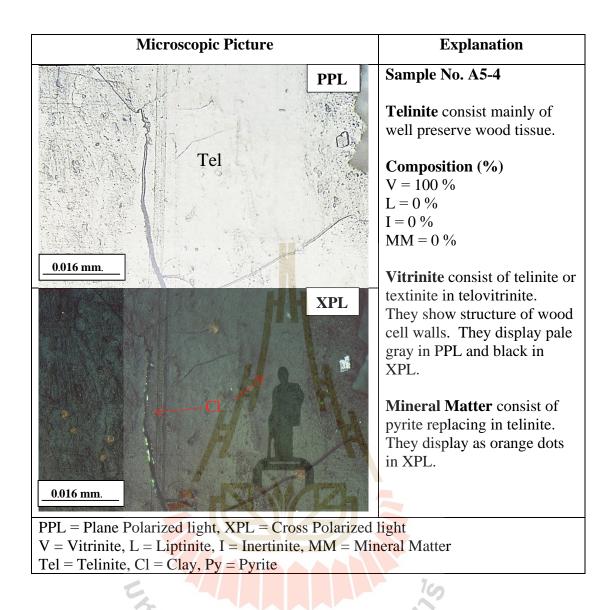


Figure 4.85 The microscopic picture of coal sample No. A5 - 4.

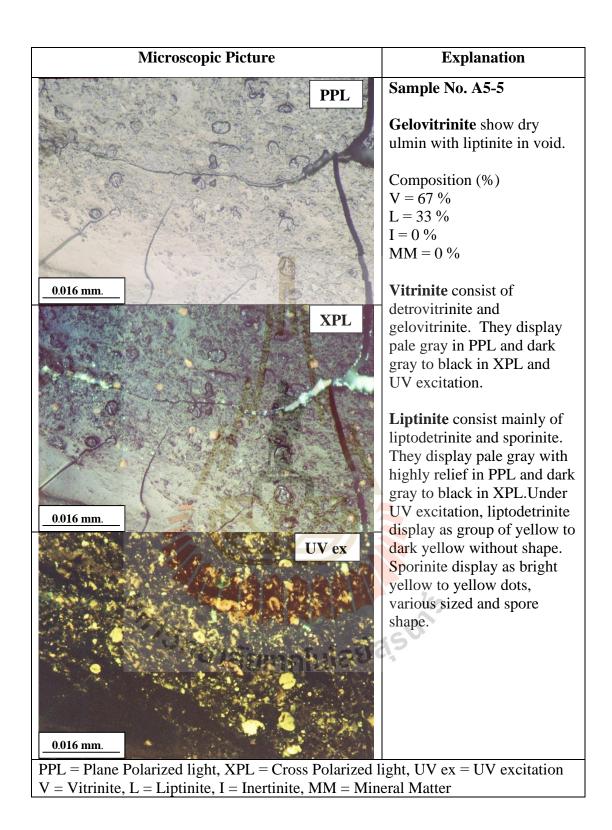


Figure 4.86 The microscopic picture of coal sample No. A5 - 5.

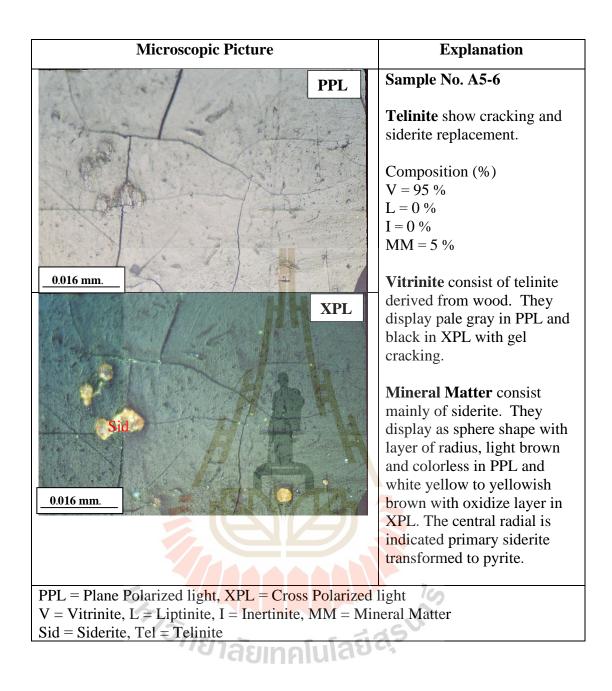


Figure 4.87 The microscopic picture of coal sample No. A5 - 6.

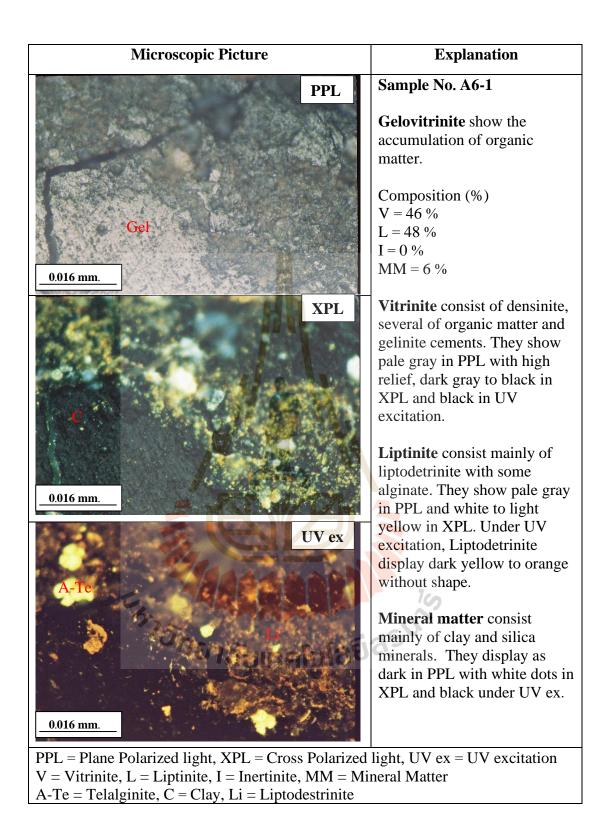


Figure 4.88 The microscopic picture of coal sample No. A6 - 1.

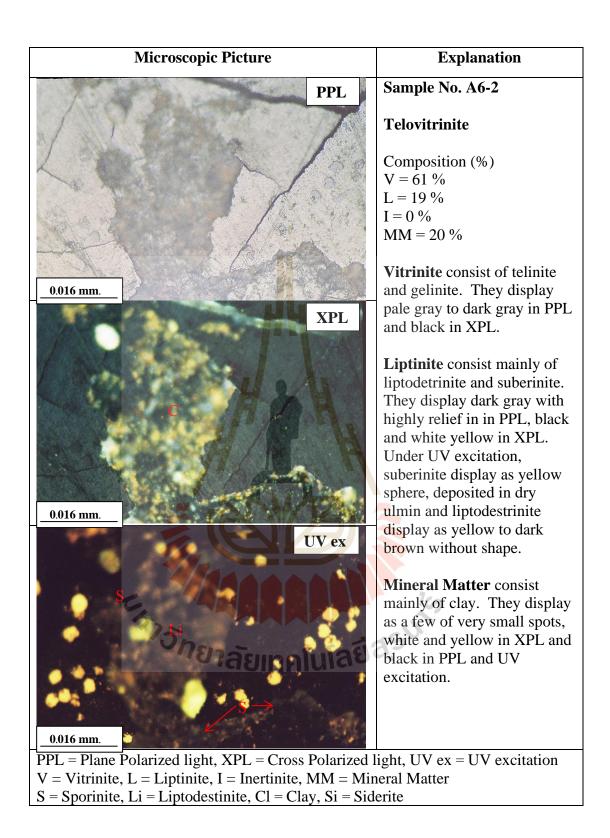


Figure 4.89 The microscopic picture of coal sample No. A6 - 2.

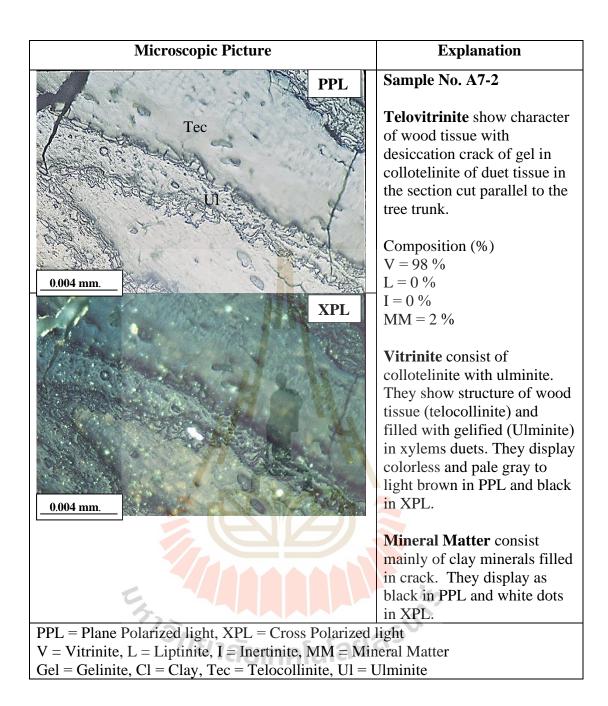


Figure 4.90 The microscopic picture of coal sample No. A7 - 2.

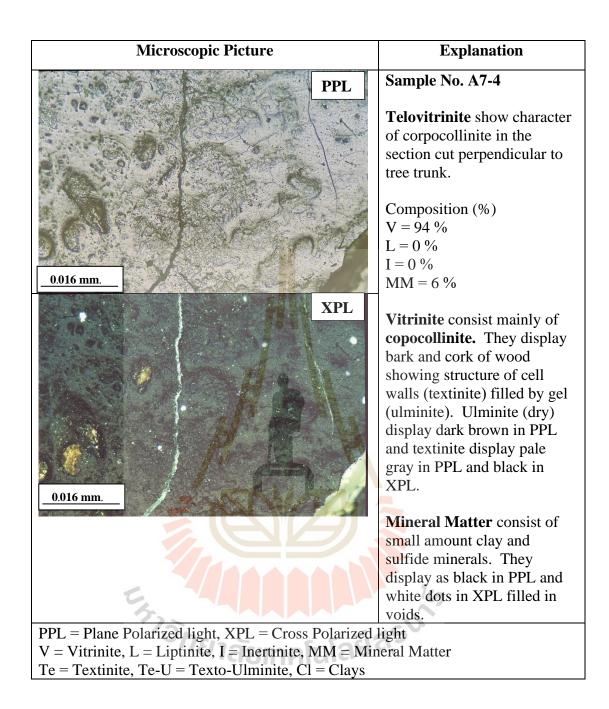
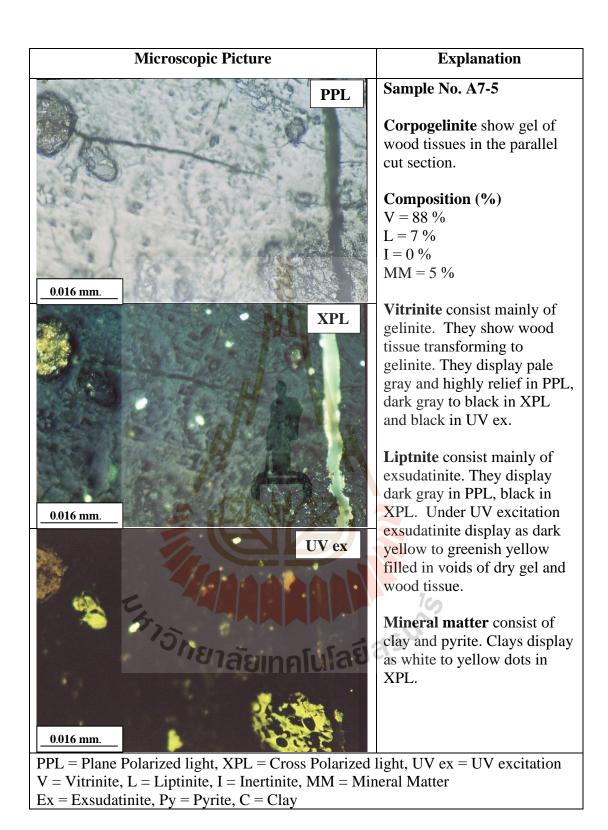
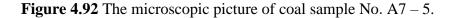
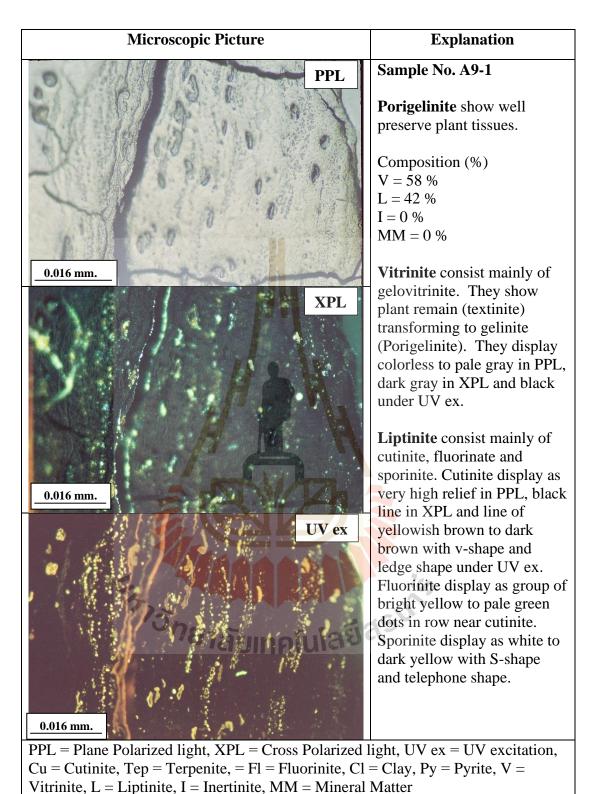


Figure 4.91 The microscopic picture of coal sample No. A7 – 4.







Vitilite, E – Elptilite, I – Incruite, Wivi – Winerar Watter

Figure 4.93 The microscopic picture of coal sample No. A9 - 1.

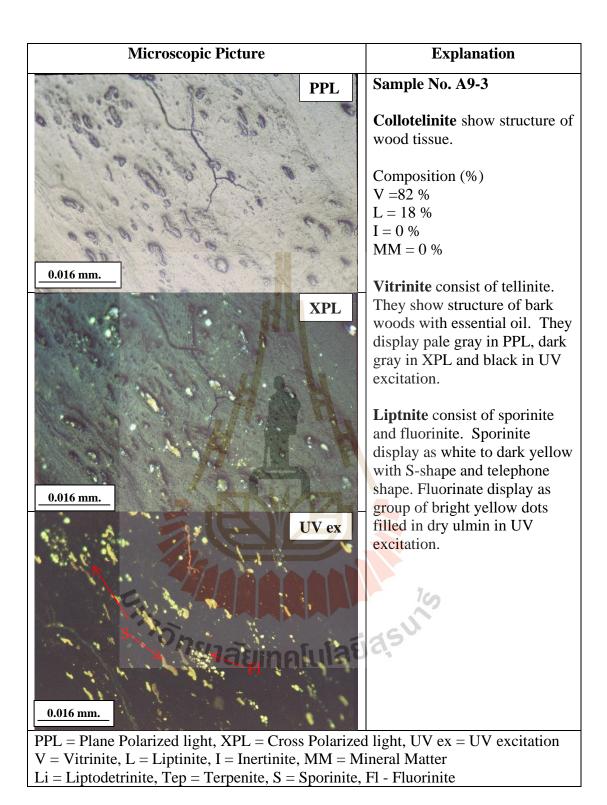


Figure 4.94 The microscopic picture of coal sample No. A9 - 3.

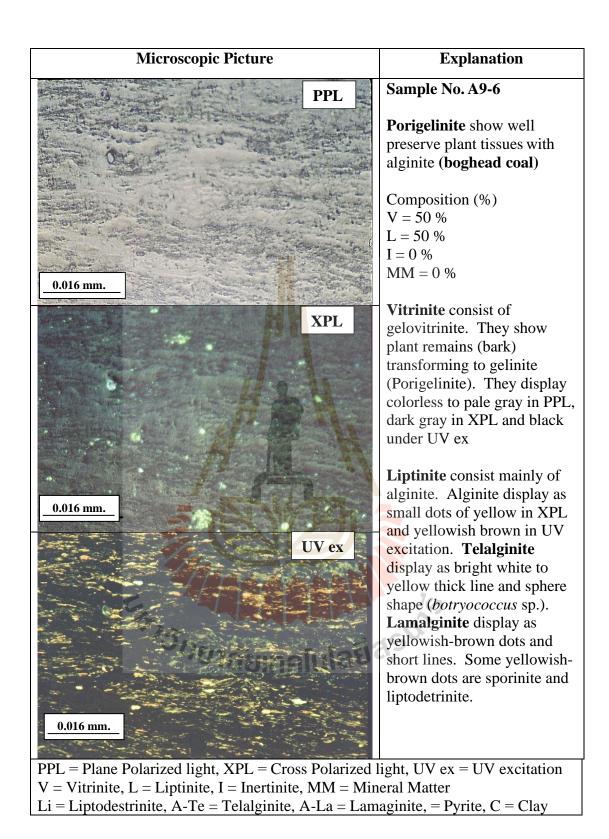
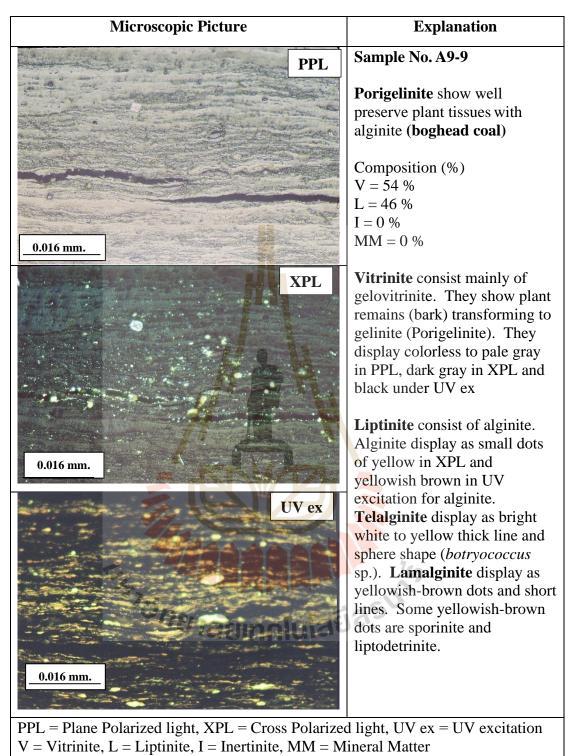


Figure 4.95 The microscopic picture of coal sample No. A9 - 6.



Li = Liptodestrinite, A-Te = Telalginite, A-La = Lamaginite, = Pyrite, C = Clay

Figure 4.96 The microscopic picture of coal sample No. A9 - 9.

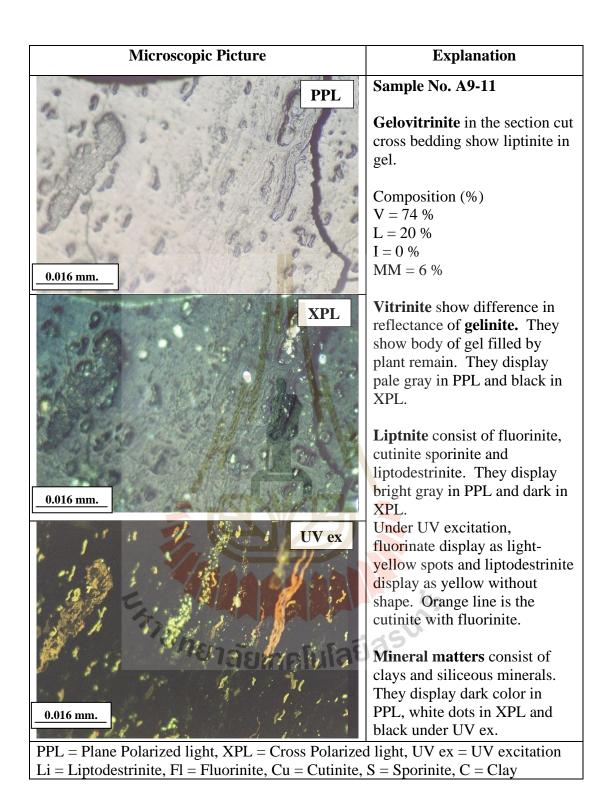


Figure 4.97 The microscopic picture of coal sample No. A9 – 11.

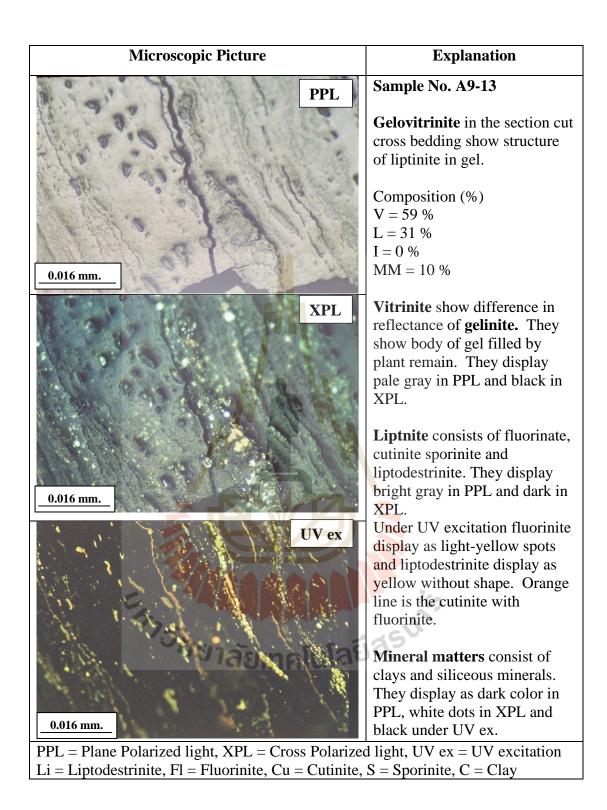


Figure 4.98 The microscopic picture of coal sample No. A9 – 13.

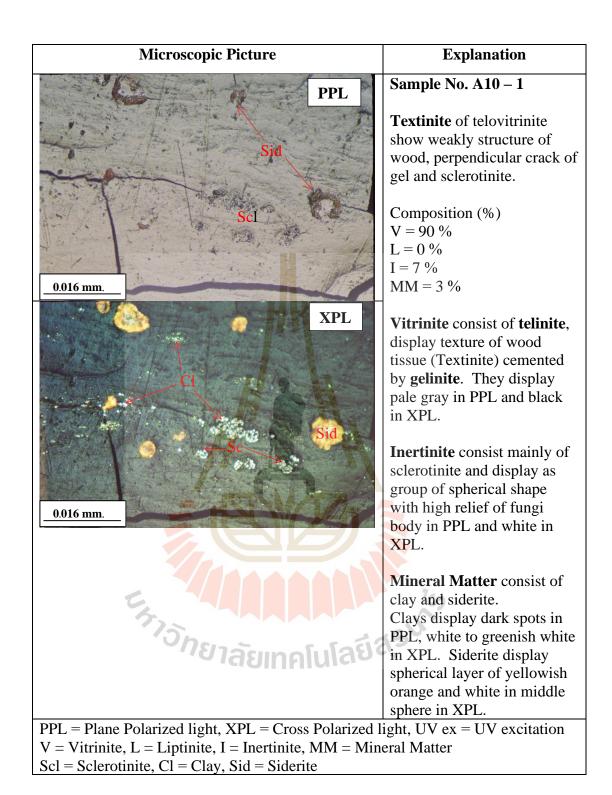


Figure 4.99 The microscopic picture of coal sample No. A10 - 1

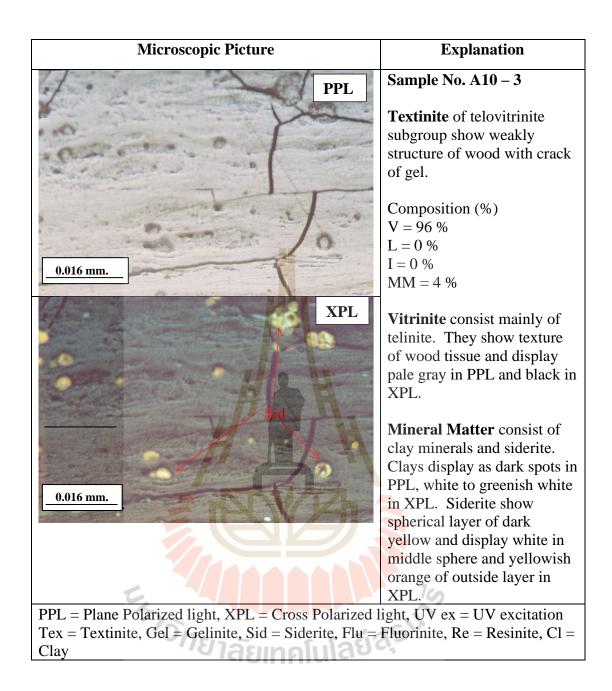
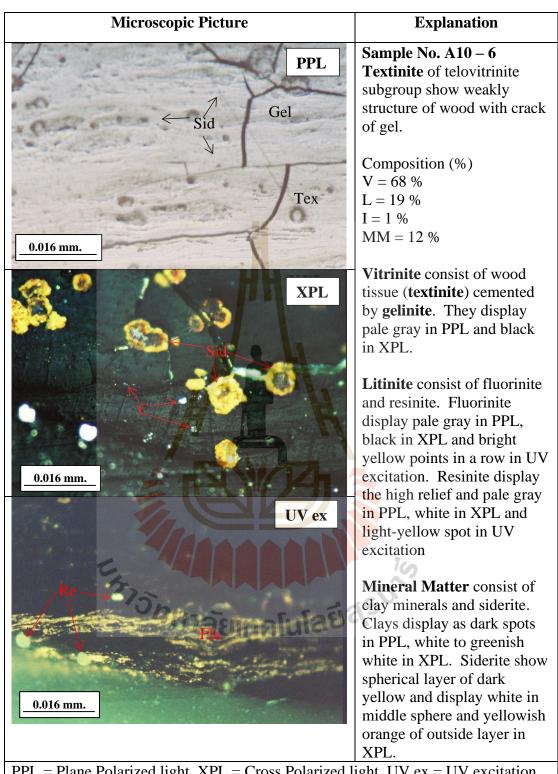
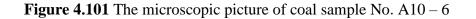


Figure 4.100 The microscopic picture of coal sample No. A10 - 3



PPL = Plane Polarized light, XPL = Cross Polarized light, UV ex = UV excitation Tex = Textinite, Gel = Gelinite, Sid = Siderite, Flu = Fluorinite, Re = Resinite, Cl = Clay



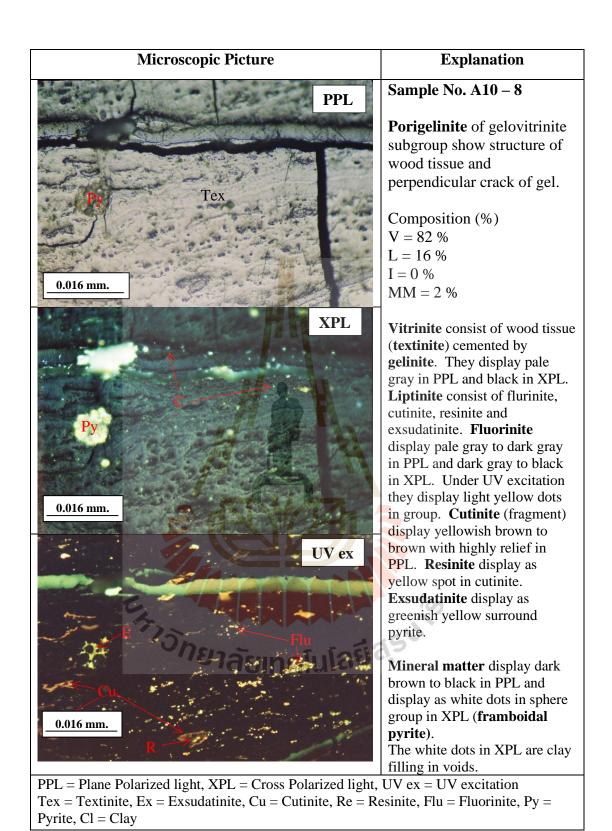
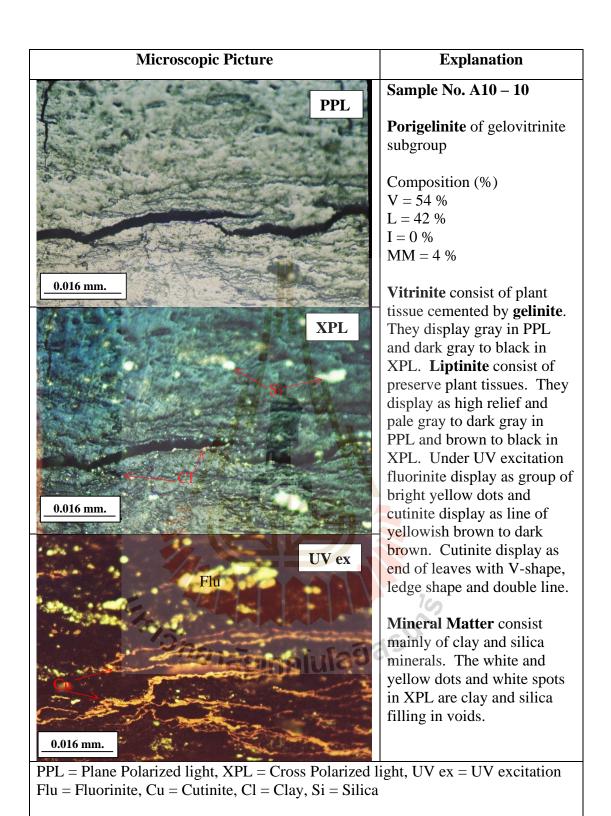


Figure 4.102 The microscopic picture of coal sample No. A10 - 8



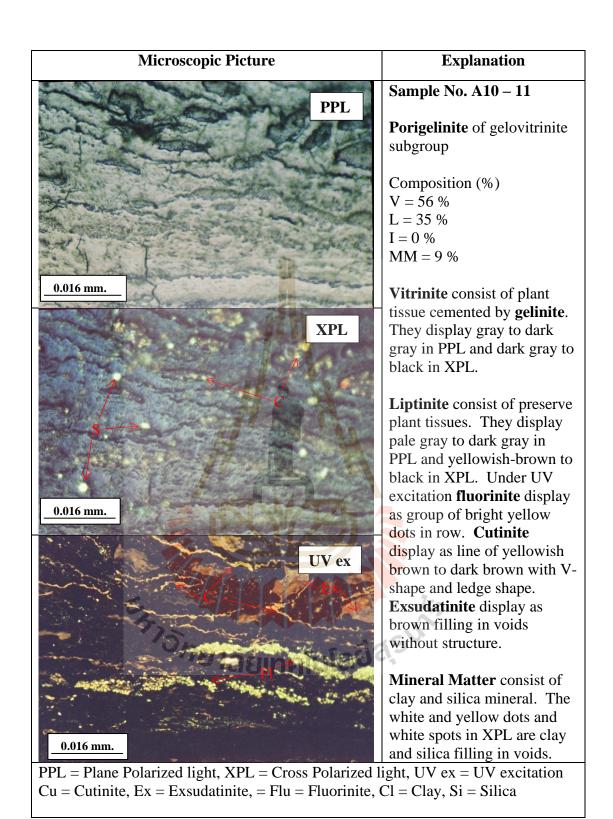
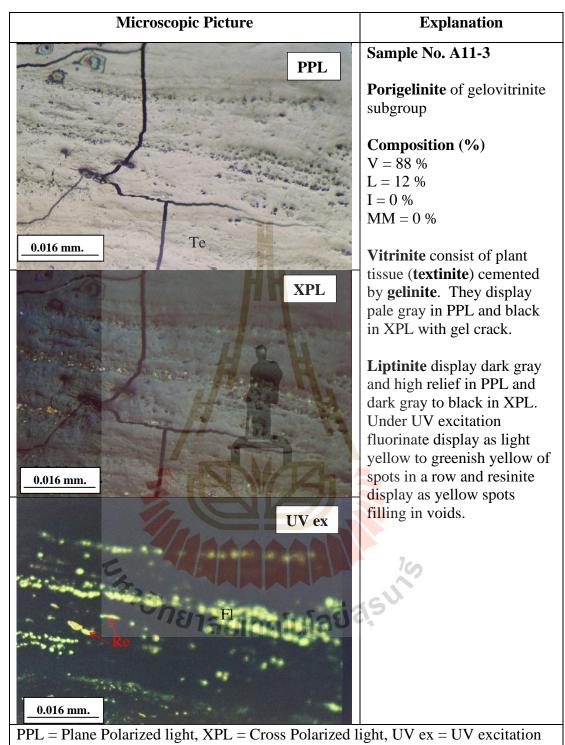
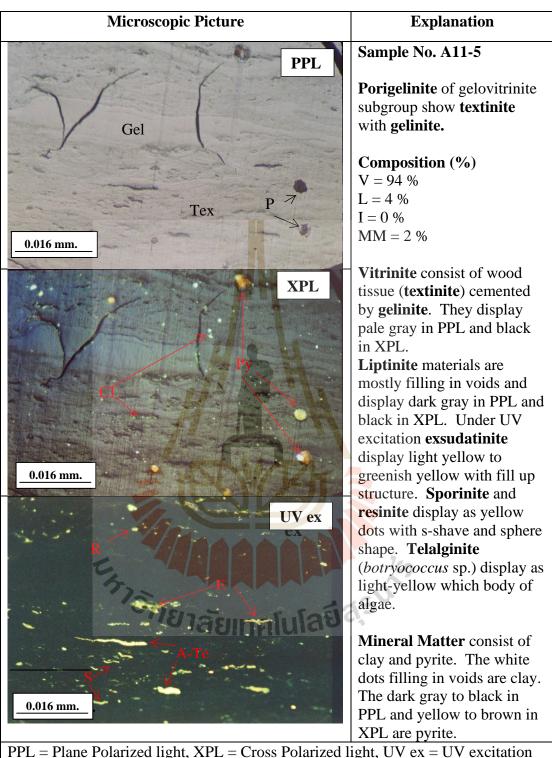


Figure 4.104 The microscopic picture of coal sample No. A10 – 11



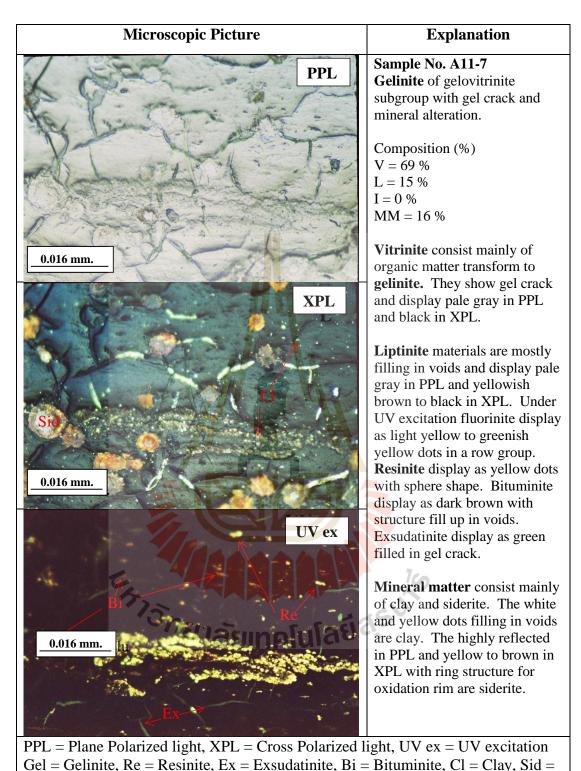
Tex = Textinite, Flu = Fluorinite, Re = Resinite,

Figure 4.105 The microscopic picture of coal sample No. A11 – 3



PPL = Plane Polarized light, XPL = Cross Polarized light, UV ex = UV excitation Te = Textinite, Gel = Gelinite, Re = Resinite, Ex = Exsudatinite, A-Te = Telalginite, S = Sporinite, Cl = Clay, Py = Pyrite

Figure 4.106 The microscopic picture of coal sample No. A11 - 5



Siderite

Figure 4.107 The microscopic picture of coal sample No. A11-7

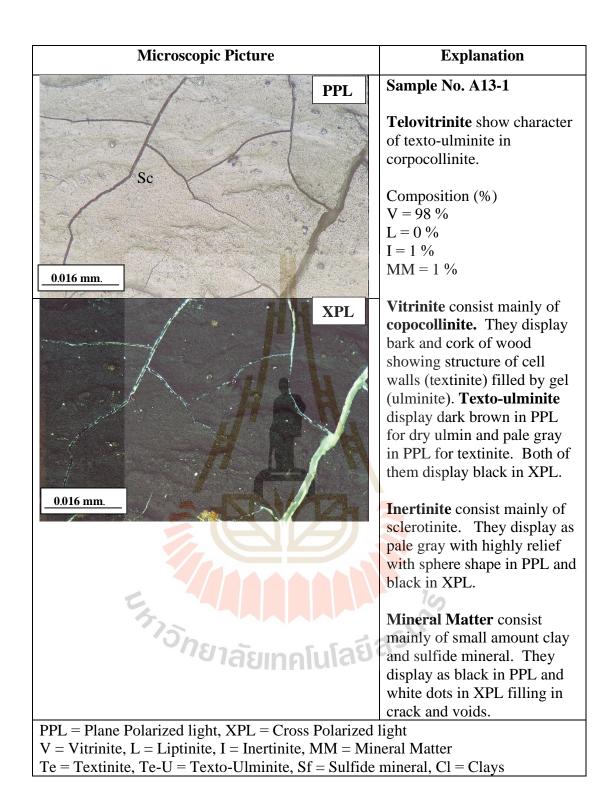
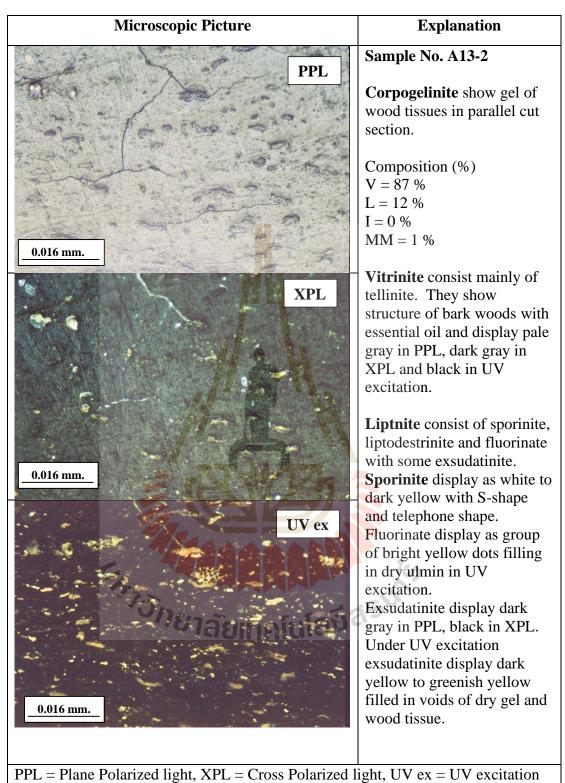


Figure 4.108 The microscopic picture of coal sample No. A13-1



Gel = Gelinite, Re = Resinite, Ex = Exsudatinite, Bi = Bituminite, Cl = Clay

Figure 4.109 The microscopic picture of coal sample No. A13 –2

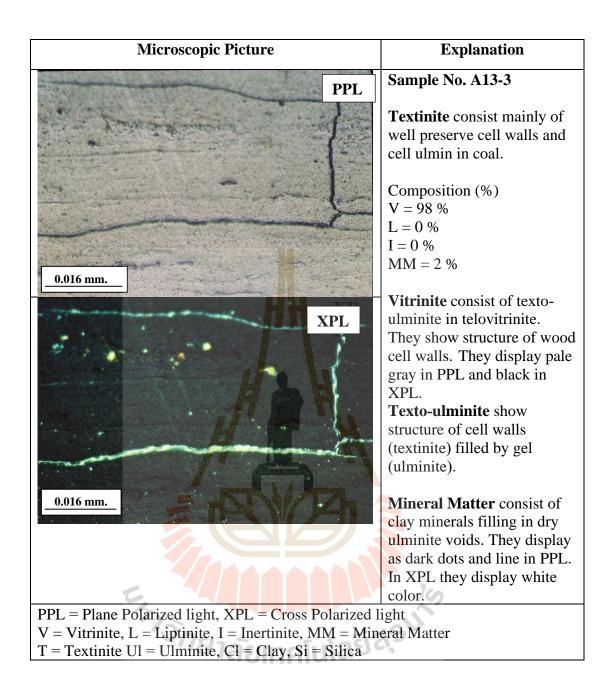


Figure 4.110 The microscopic picture of coal sample No. A13 –3

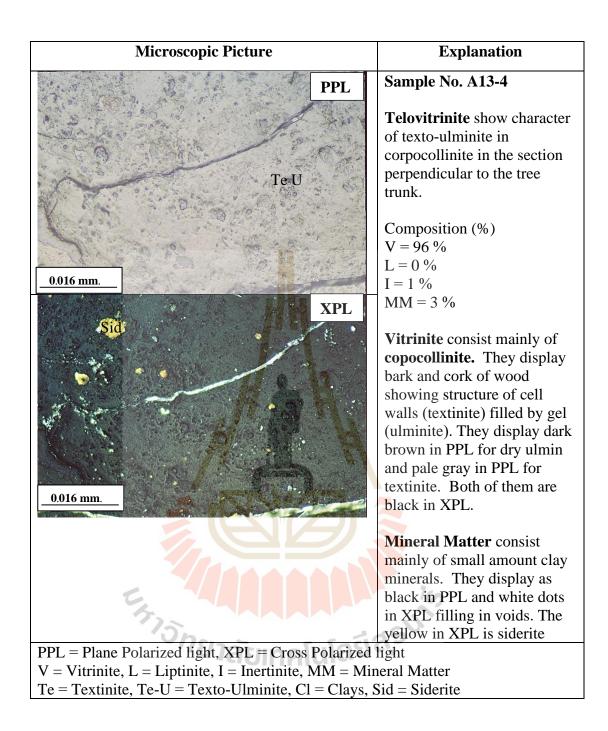
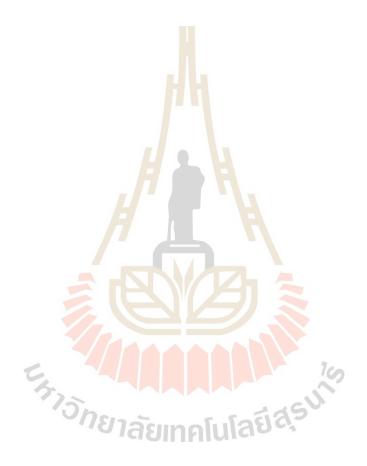


Figure 4.111 The microscopic picture of coal sample No. A13-4

4.2.5 Oil Shale in Coal A sub-unit

These oil shales consist of fine-grained sediments deposited together with algae and were cemented by gelinite. They are laminated black shale interbedding in Coal A sub-unit. Their major compositions are mineral matter deposit associated with liptinite (mostly of alginate) and some of vitrinite (Table 4.8). The vitrinite (1 – 25%) consist mainly of gelinite with some telovitrinite. They display essential oil filled in wood tissues, white yellow and greenish yellow to orange under UV-excitation (Figure 4.115 and 4.116). Alginite show difference layers of algae which consist mainly of lamalginite (63.81%) and telalginite (3.14%). The difference of algae abundance both number and size could reflect to the level of nutrients in water. The stagnant of coming up water for a long time with rich of nutrient led to algae booms and produced thick bed of algal mats. Under microscopic of the perpendicular section, various sizes of lamalginite with limited recognizable structure can be observed. Liptodestrinite display as the groundmasses without structure and show dark brown under UV excitation. The mineral matter consists of coarse diagenetic crystals of sand to silt sizes deposited with groundmass of clay minerals.

Alginite in this sub-unit is dominated by lamalginite type. They display yellow to orange with lamellar shape. They show different character and abundant in 2 types: the long form (0.004 to 0.016 mm) and the short form (0.001 to 0.004 mm) with the thickness of 0.001 to 0.006 mm in the perpendicular section (Figure 4.119, 4.125, 4.126 and 4.127). The sizes of the algal could depend on the pH and nutrient of the swamp water. From the photosynthesis, different conditions of water have different nutrients in them. Algae take waste (dead animal and plant) in water and provide oxygen and nitrogen. Some parts of oil shale consist of telalginite (*Botryococcus* sp.), fluorescing greenish yellow to white yellow. Most of colonies are *Pila* algae which live in freshwater lakes. They show ovoid to circular with 0.004 to 0.024 mm long and 0.004 to 0.005 mm thick. The parallel cross-sections show the circular colonies with shapes which is the significant morphological features used to identify the algae as *Pediastrum* (Tsukii, 2014) (Figure 4.120 and 4.129).



	Liptinite												Mineral Matter			
Sample	Alginite										Total	Vitrinite				Total
	Lam	Tela		Lip	Sp	Cu	Fl	Re	Su	Ex	(%)	v iti iiite	Clay	Q+Si	Ру	(%)
	Laill	Botry	Pila								(70)					(70)
AS1-1	66	0	0	0	2	0	0	0	0	0	68	13	3	16	0	19
AS1-2	67	0	0	0	3	0	0	0	0	0	70	15	10	5	0	15
AS1-3	73	0	0	0	1	0	0	-0	0	0	74	9	16	0	1	17
AS2-1/1	67	3	2	12	4	0	0	-0	-0	0	88	1	10	0	1	11
AS2-1/2	85	2	0	0	0	0	0_	0	0	0	87	7	6	0	0	6
AS2-2	83	5	0	1	0	0	0	0	0	0	89	2	6	0	3	9
AS2-3	60	0	0	1	1	0	0	0	0	0	62	18	16	0	4	20
AS3-1	50	6	0	5	3	0	0	1 -	-0	0	65	9	23	3	0	26
AS3-2	55	9	0	1	1	0	0	0	0	0	66	25	4	4	1	9
AS3-3	56	0	0	12	0	0	0	0	0	0	68	14	10	7	1	18
AS3-4	45	0	0	12	11	0	0	3	0	0	71	18	8	1	2	11
A11-1	73	4	0	0	0	0	0	0	0	0	77	10		13	0	13
A11-2/1	74	2	0	3	0	0	0	0	0	0	79	9	8	4	0	12
A11-2/2	61	1	0	19	4	0	0	2	0	0	87	3	6	1	3	10
A11-3	54	4	0	0	5	0	0	2	0	0	65	23	11	0	1	12
A11-4	52	12	0	6	4	0	0	0	0	0	74	16	5	5	0	10
max	85	12	2	19	11	0	60	3	0	0	89	25	23	16	4	26
min	45	0	0	0	0	0	0	0	0	0	62	1	3	0	0	6
%	63.81	3.00	0.13	4.50	2.44	0.00	0.00	0.50	0.00	0.00	74.38	12.00	8.88	3.69	1.06	13.63

Table 4.8 Composition in percentage of Oil Shale in Coal A sub-unit samples.

Lam = Lamalginite, Tela = Telalginite, Bot = Botryococcus brounii, Pil = Pila algae, Lip = Liptodestrinite, Sp = Sporinite, Cu = Cutinite, Fl= Fluorinite, Re = Resinite, Su = Suberinite, Ex = Exsudatinite, V = Vitrinite (consist of telovitrinite, detrovitrinite and gelovitrinite) Q = Quartz, Si = Silica, Py = Pyrite

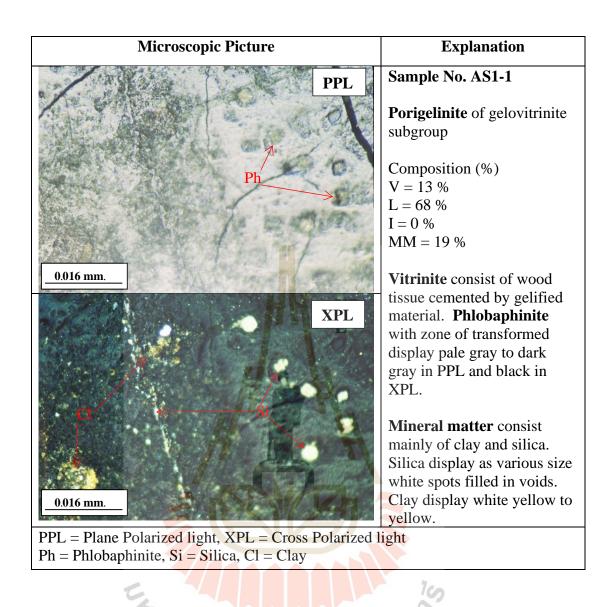


Figure 4.112 The microscopic picture of oil shale sample No. AS1 – 1

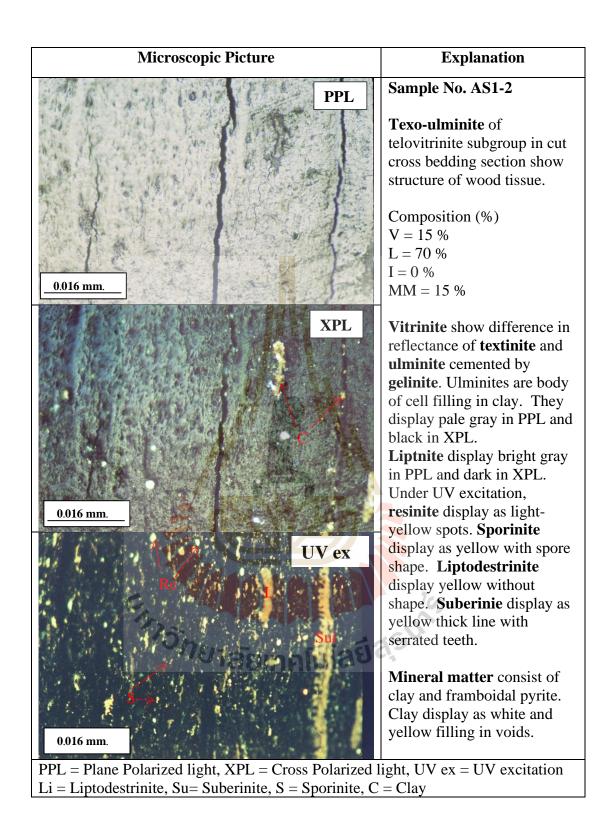
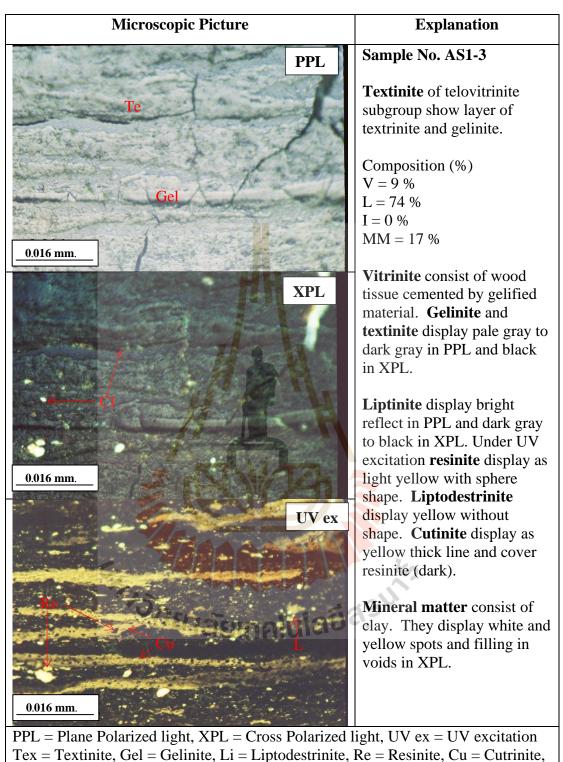


Figure 4.113 The microscopic picture of oil shale sample No. AS1 – 2



C = Clay

Figure 4.114 The microscopic picture of oil shale sample No. AS1 - 3

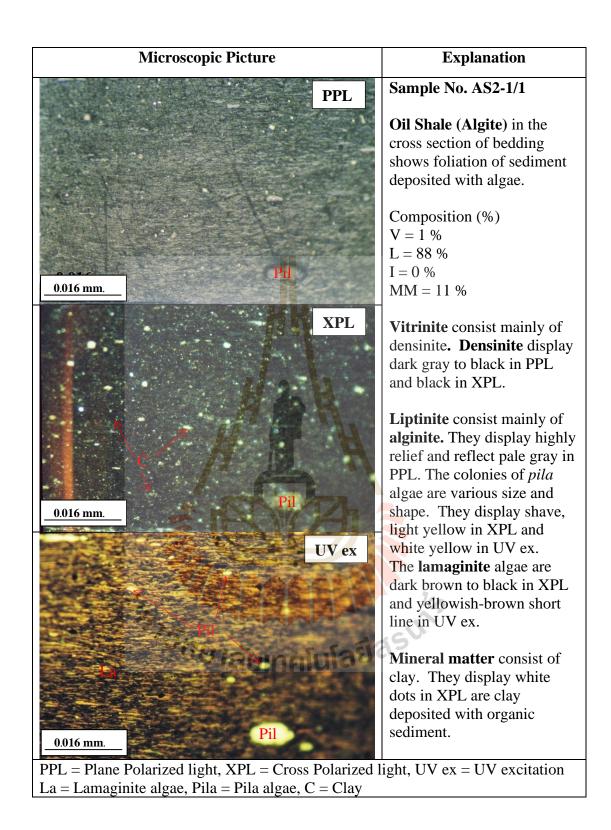


Figure 4.115 The microscopic picture of oil shale sample No. AS2 - 1/1

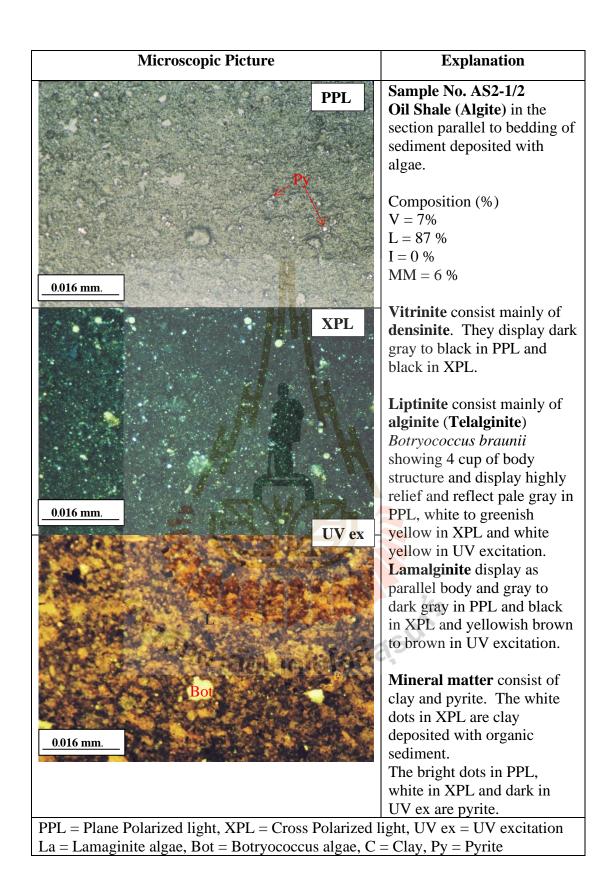


Figure 4.116 The microscopic picture of oil shale sample No. AS2 - 1/2

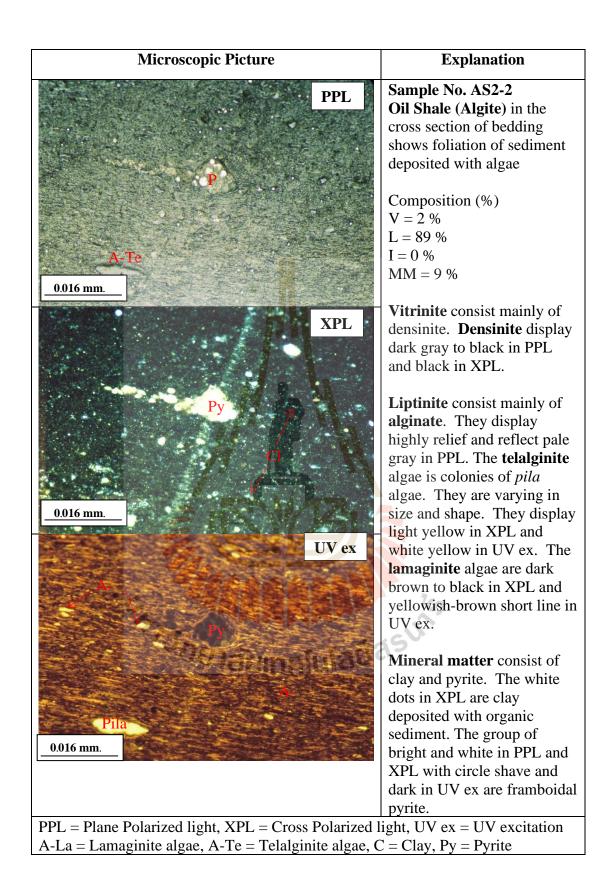
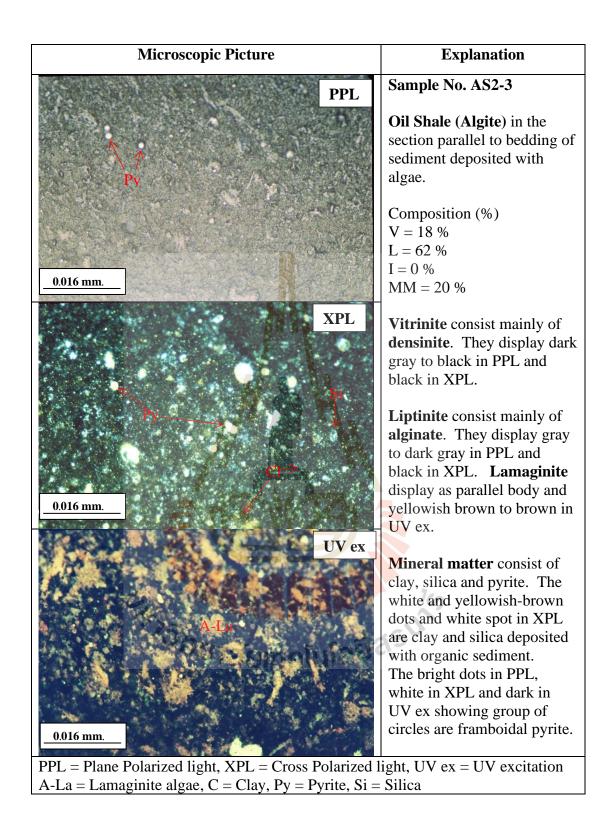
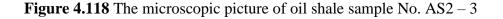


Figure 4.117 The microscopic picture of oil shale sample No. AS2 – 2





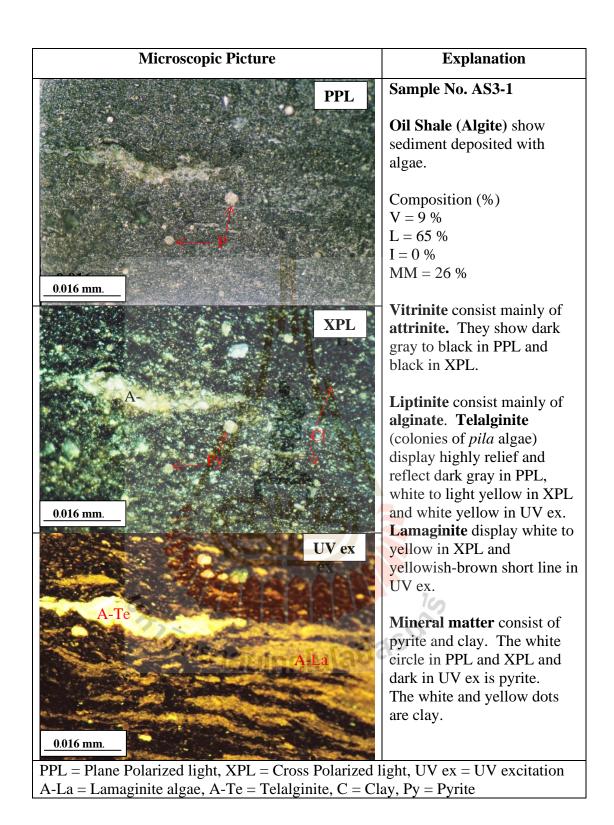


Figure 4.119 The microscopic picture of oil shale sample No. AS3 – 1

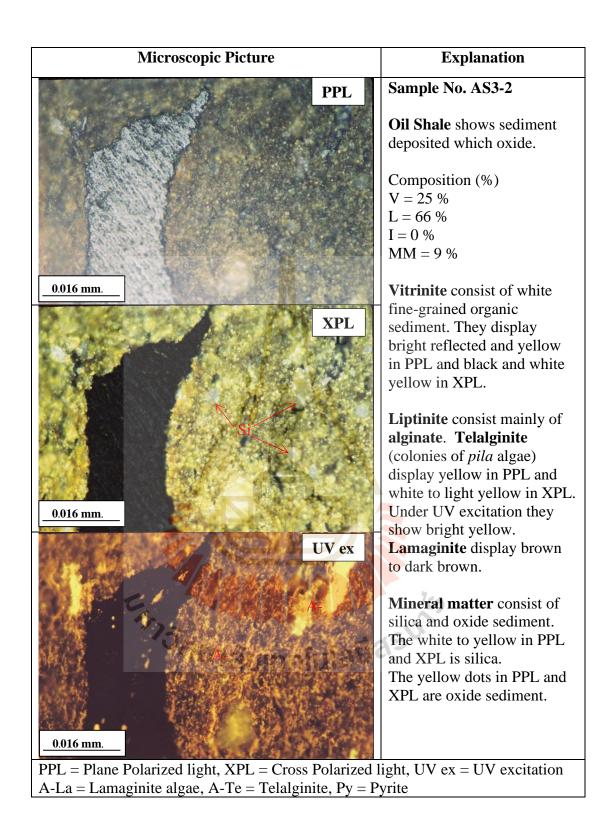


Figure 4.120 The microscopic picture of oil shale sample No. AS3 – 2

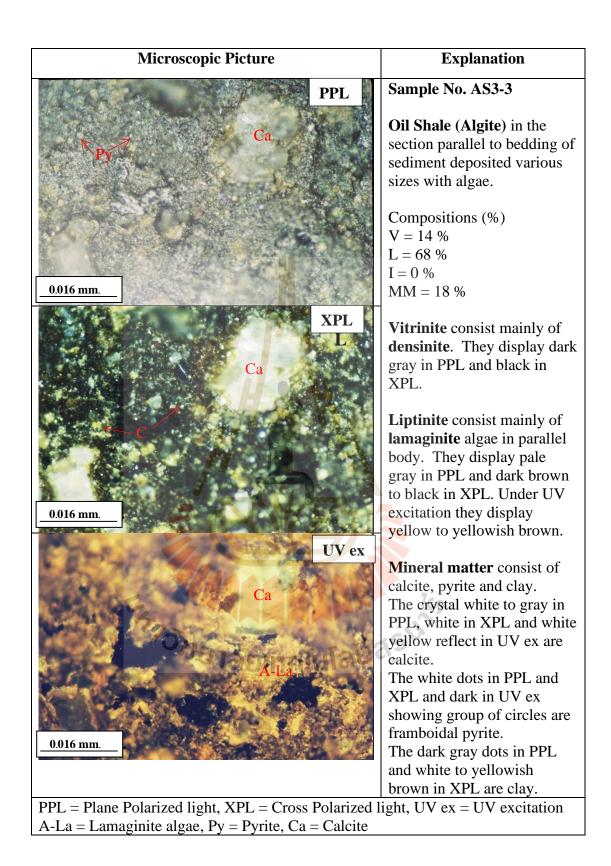
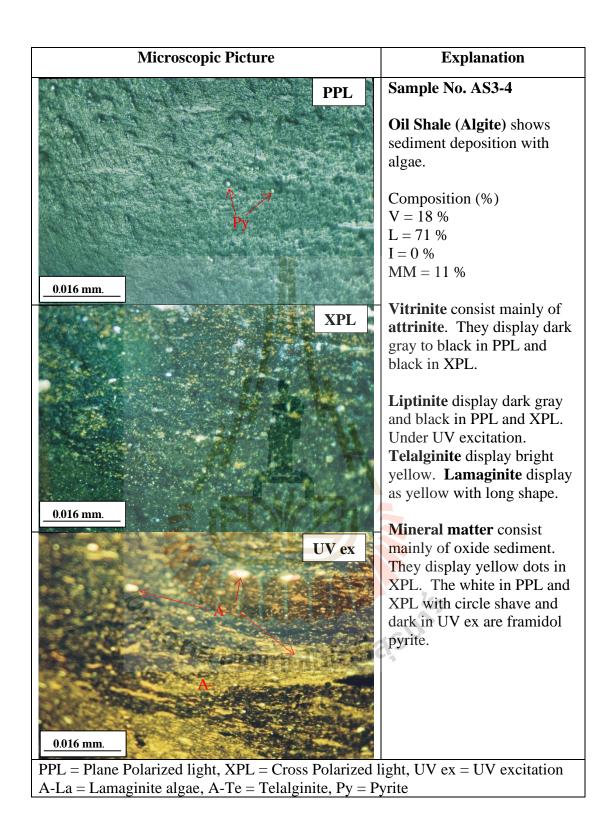
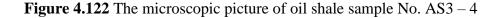
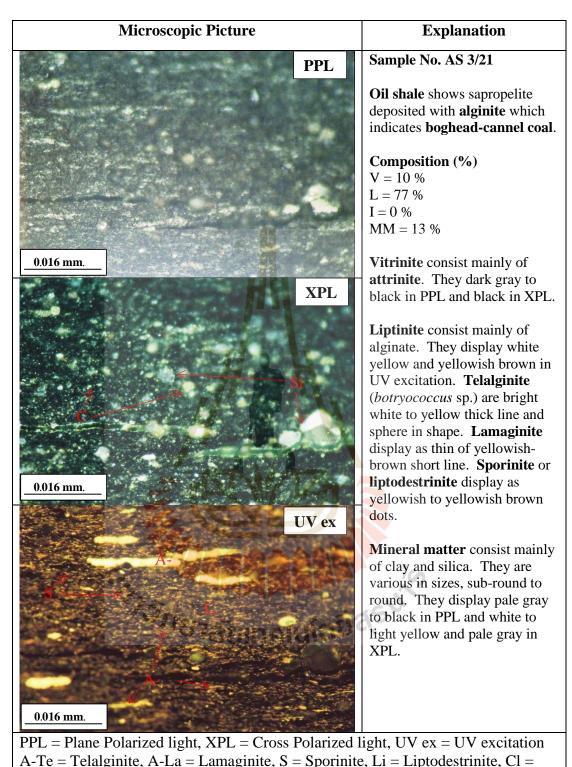


Figure 4.121 The microscopic picture of oil shale sample No. AS3 – 3







Clay, Silica

Figure 4.123 The microscopic picture of oil shale sample No. AS3/21

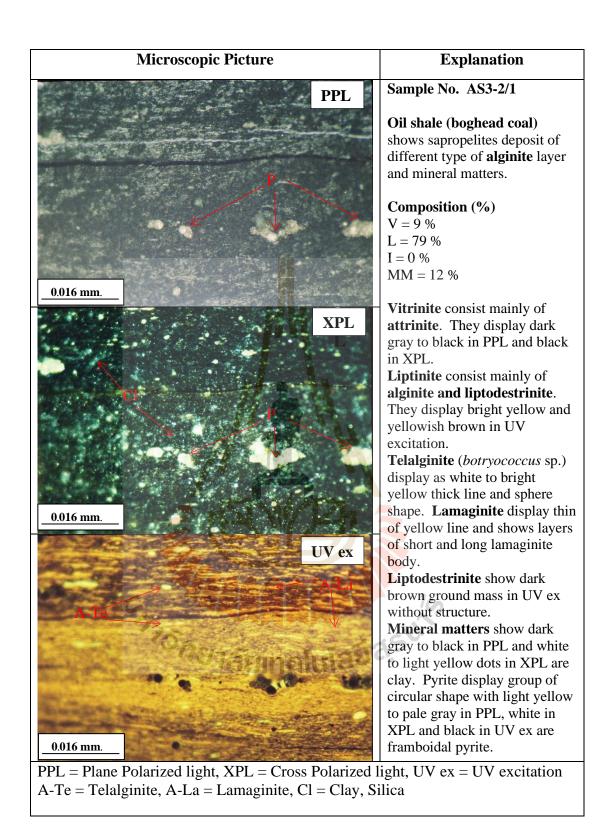


Figure 4.124 The microscopic picture of oil shale sample No. AS3 - 2/1

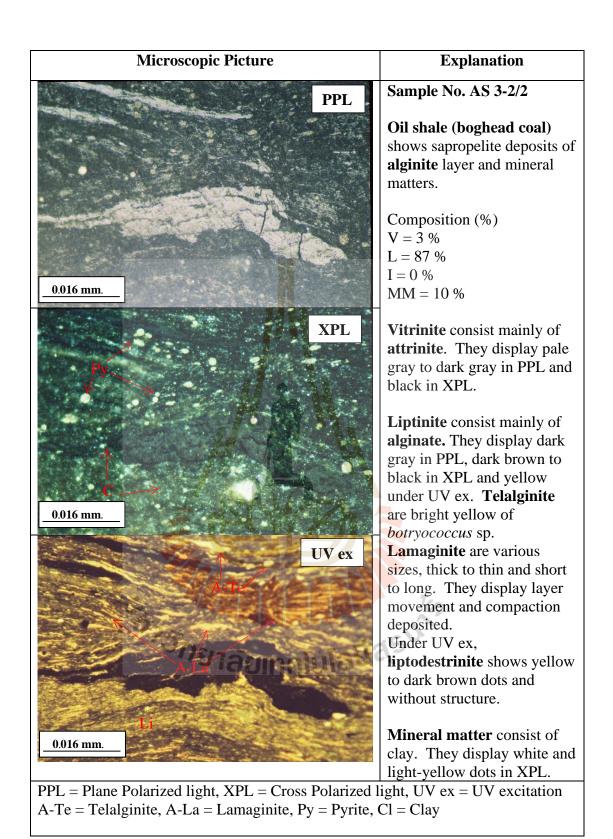
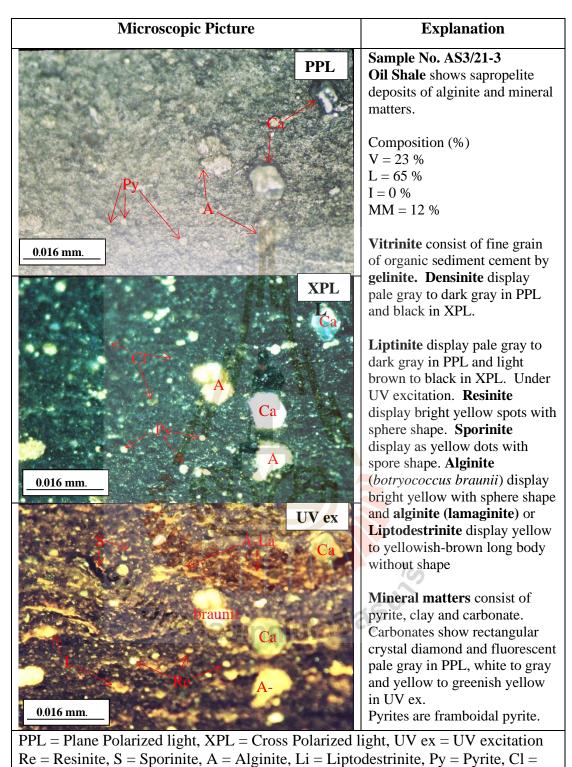


Figure 4.125 The microscopic picture of oil shale sample No. AS3 - 2/2



Clay, Ca = Carbonate

Figure 4.126 The microscopic picture of oil shale sample AS3/21 - 3

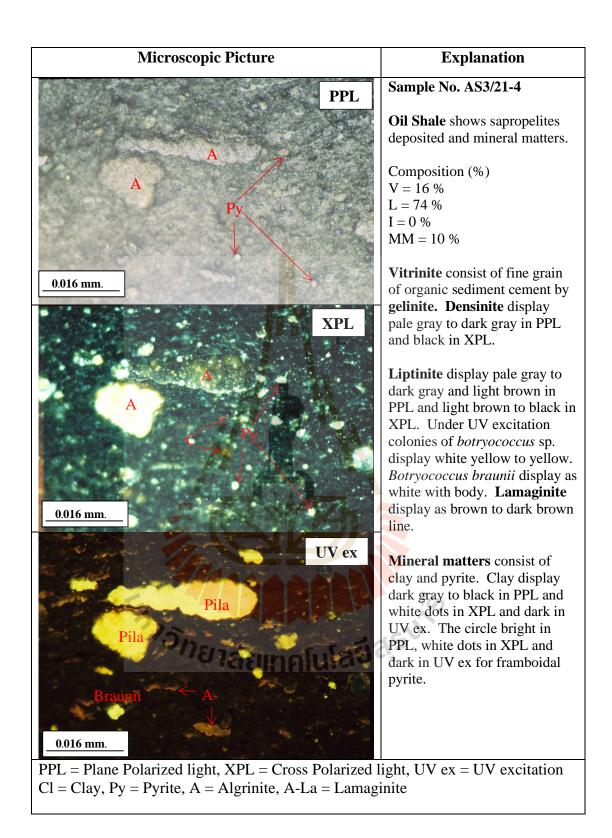


Figure 4.127 The microscopic picture of oil shale sample No. AS3/21 - 4

4.2.6 Lower Oil Shale sub-unit

The Lower Oil Shale sub-unit is a successive sequence above the Coal A. The unit indicates the environmental conditions changing suddenly from the shallow water in forest-peat swamp (Coal A sub-unit) to high stand water (Oil Shale unit). The high stand deep water with high nutrient result in the accumulation of thick algae deposited with gelinite and fine-grained sediments. Under microscopy, the composition of the lower oil shale sub-unit consists mainly of mineral matter vary from 62 - 87% (Table 4.7). Most of sediments are clay mineral which display fluffy character with white in PPL and XPL. Some layers consist of pyrite displaying as metallic bright spots in PPL with dark in XPL and under UV excitation.

Maceral is mainly of liptinite and vitrinite. Liptinite consist mainly of alginite deposited together with fine-grained sediments cemented by gelinite. The alginite consist mainly of lamalginite (3 - 23%) and some telalginite (4%). The lamalginite in this sub-unit display as both long and short bodies, but they are thinner and shorter than those of the other sub-units. The thick and thin algal mats indicated the algal booms related to the seasoning nutrient supply and the flavoring temperature conditions which led to the different character of algae (Tsukii, 2014). Both of long and short body lamalginite in this oil shale sub-unite are very small and thin. Therefore, this could indicate the lower nutrients supply than other sub-units. The other liptinite are liptodetrinite and sporinite.

The long and short body of lamalginite display dark brown to black in XPL and white yellow to greenish yellow under UV-excitation. The long body has length vary from 0.001 to 0.003 mm while the short body has the length less than a half of the long body (less than 0.001 mm) (Figure 4.132). The short lamalginite look like

sporinite, but lamalginite have shape on both of nibs while the sporinite have bend on the end of body. In addition, the color of sporinite often brighter than lamalginite and display. White yellow to orange in fluorescence. The telalginite is mostly of *Pila* algae which display spheroid, ovoid to circular shape in massive colony. *Pila* colony is 0.016 to 0.024 mm long and 0.002 to 0.008 mm thick in the perpendicular section. They might be *Botryococcus* sp. and the related algae of telalginite (Figure 4.130 and 4.131).

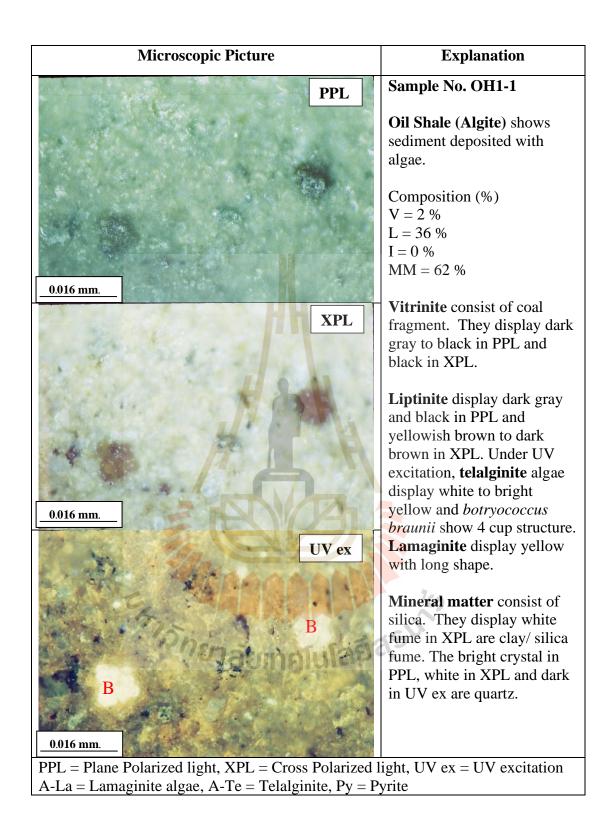


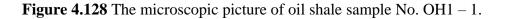
	Liptinite												Mineral Matte				
		Alginite	9														
Sample		Tela							Π.			Vitrinite					
_	Lam	Bo	Pil	Lip	Sp	Cu	Fl	Re	Su	Ex	Total	(%)	Clay	Q+Si	Py	Total	
OH1-1	23	8	0	5	0	0	0	0	0	0	36	2	45	13	4	62	
OH2-1	3	15	0	12	0	0	0	0	0	0	30	5	57	6	2	65	
OH2-2	9	13	0	2	0	0	0	0	0	0	24	3	62	10	1	73	
OH3-1	8	2	0	5	0	0	0	0	0	0	15	1	68	15	1	84	
OH3-2	13	2	0	2	0	0	0	0	0	0	17	5	68	5	5	78	
OH4-1	7	3	0	3	0	0	0	0	0	0	13	0	79	6	2	87	
OH4-2	9	0	1	3	0	0	0	0	0	0	13	2	76	7	2	85	
OH4-3	13	0	0	4	0	0	0	0	0	0	17	2	77	2	2	82	
OH5-1	14	1	0	3	0	0	-0	0	0	0	18	5	76	1	0	77	
OH5-2	17	1	0	3	1	0	0	0	0	0	22	8	65	3	2	70	
OH5-3	14	0	0	0	1	0	0	0	0	-0	15	8	62	5	10	77	
OH6-1	3	3	2	5	4	0	0	0	0	0	17	4	78	1	0	81	
OH6-2	6	3	0	8	2	0	0	0	0	0	19	7	72	2	0	74	
Max	23	15	2	12	4	0	0	0	0	0	36	8	79	15	10	87	
Min	3	1	1	2	17	0	0	0	0	0	13	1	45	1	1	62	
%	10.69	3.92	0.231	4.231	0.615	0	0 -	0	0	0	19.69	4	68.08	5.846	2.385	76.31	

 Table 4.9 Composition in percentage of the Lower Oil Shale sub-unit.

Vitrinite (consist of telovitrinite, detrovitrinite and gelovitrinite), Q = Quartz, Si = Silica, Py = Pyrite

Lam = Lamalginite, Tela = Telalginite, Bot = Botryococcus brounii, Pil = Pila algae, Lip = Liptodestrinite, Sp = Sporinite, Cu = Cutinite, Fl= Fluorinite, Re = Resinite, Su = Suberinite, Ex = Exsudatinite





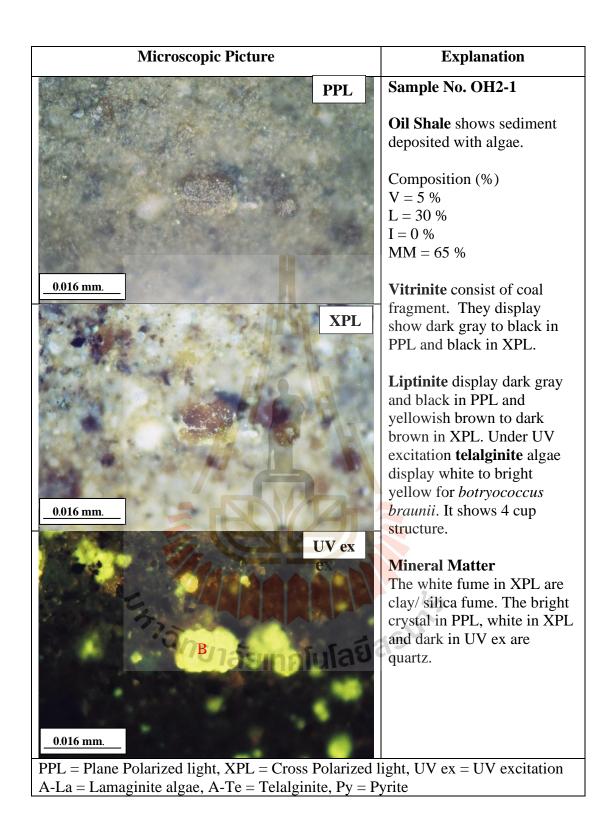
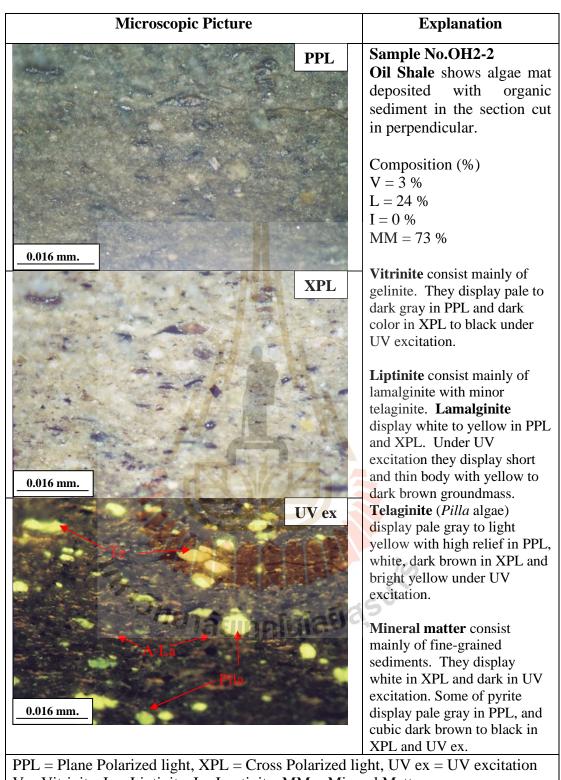


Figure 4.129 The microscopic picture of oil shale sample No. OH2 – 1.



V = Vitrinite, L = Liptinite, I = Inertinite, MM = Mineral Matter A-La = Lamaginite algae, A-Te = Telalginite, Py = Pyrite

Figure 4.130 The microscopic picture of oil shale sample No. OH2 - 2.

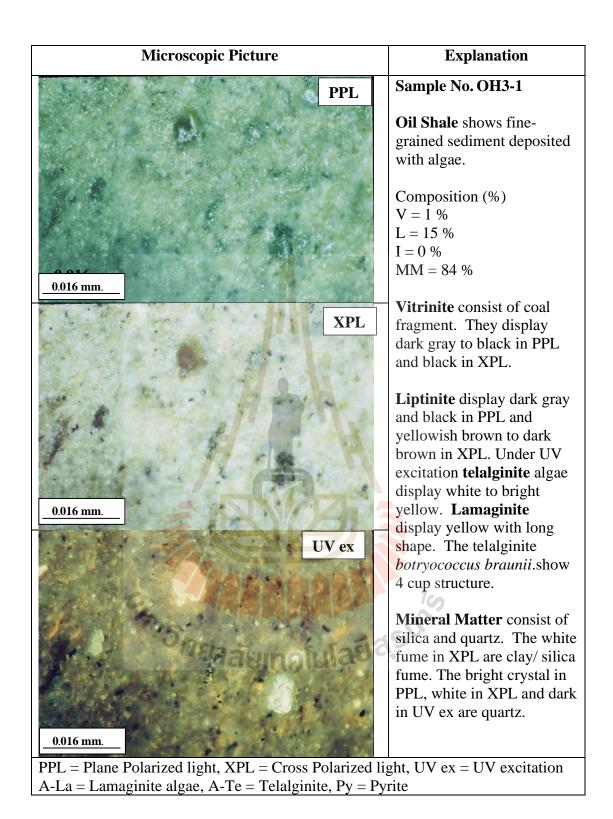


Figure 4.131 The microscopic picture of oil shale sample No. OH3 – 1.

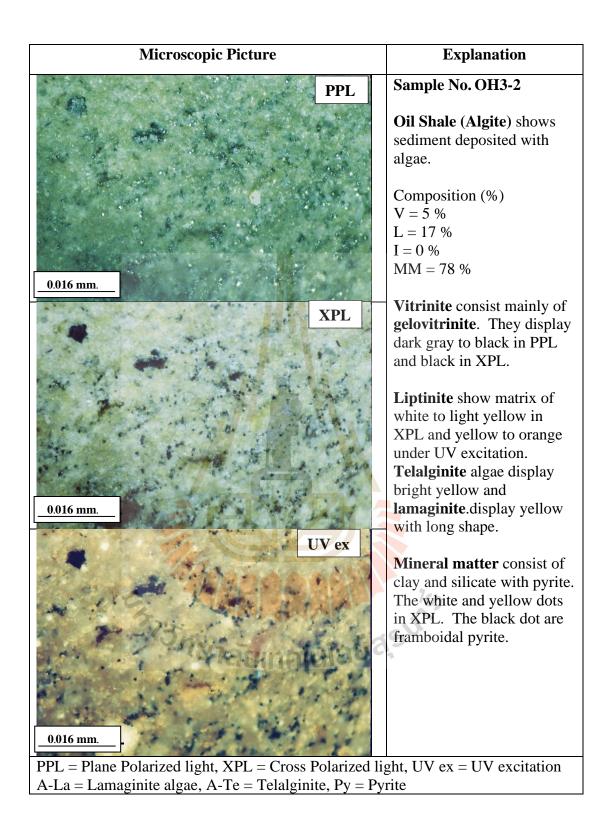


Figure 4.132 The microscopic picture of oil shale sample No. OH3 - 2.

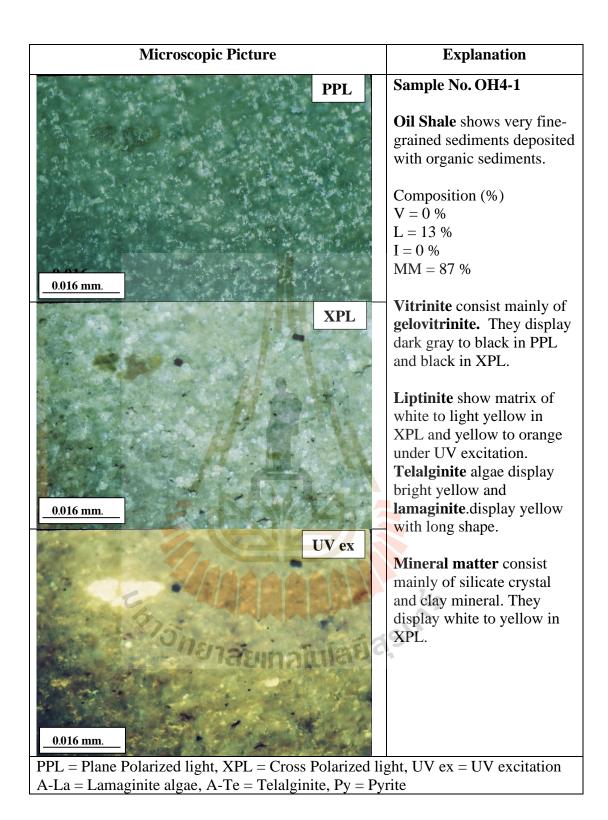


Figure 4.133 The microscopic picture of oil shale sample No. OH4 – 1.

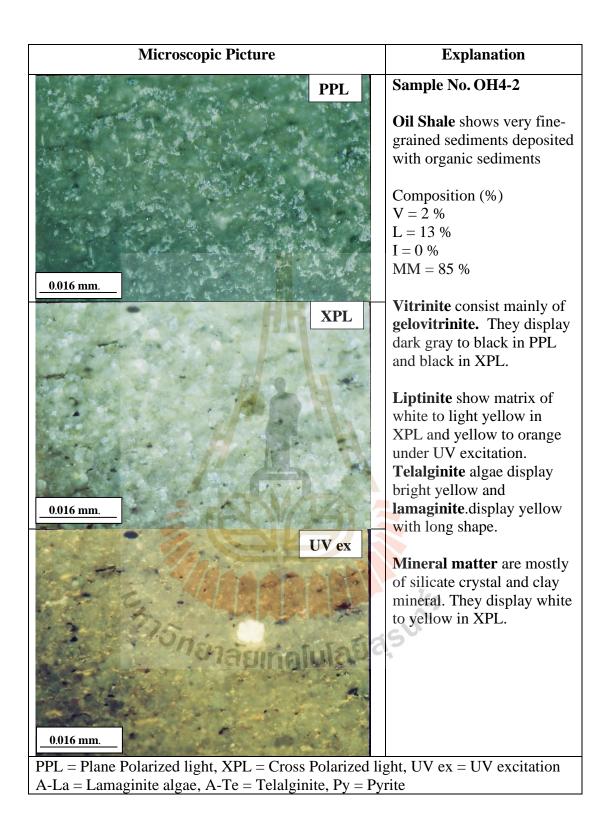


Figure 4.134 The microscopic picture of oil shale sample No. OH4 - 2.

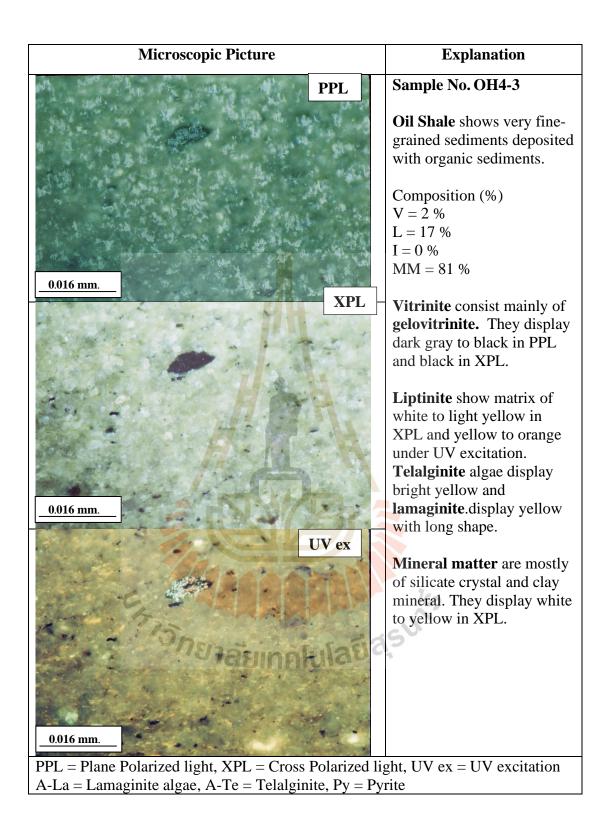


Figure 4.135 The microscopic picture of oil shale sample No. OH4 - 3.

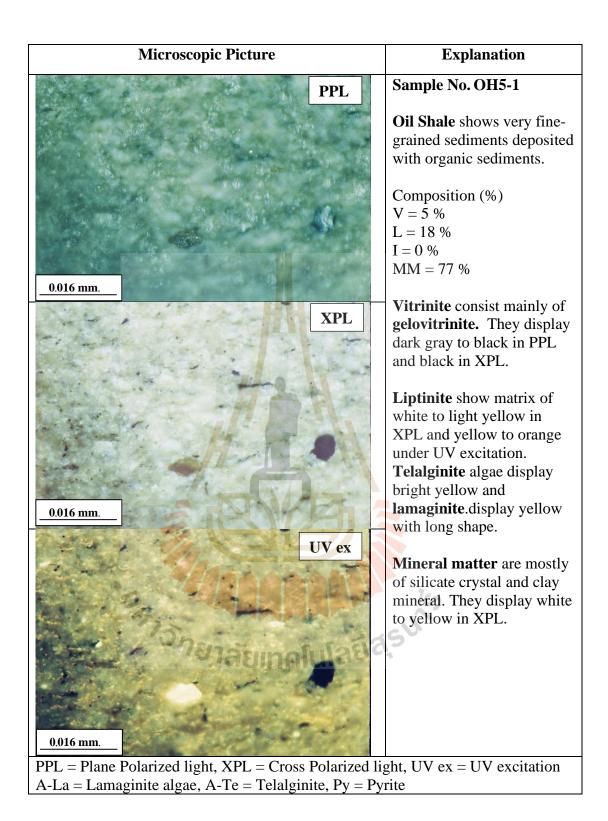


Figure 4.136 The microscopic picture of oil shale sample No. OH5 – 1.

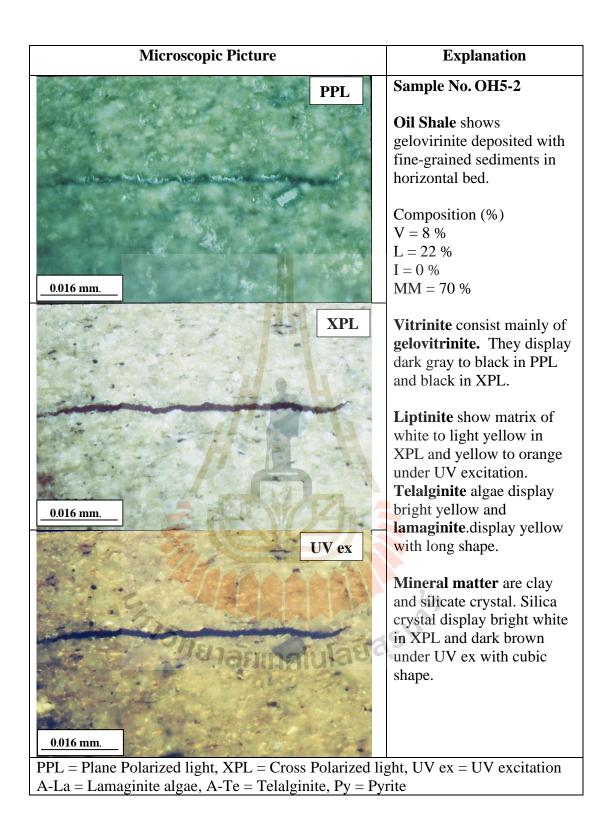


Figure 4.137 The microscopic picture of oil shale sample No. OH5 - 2.

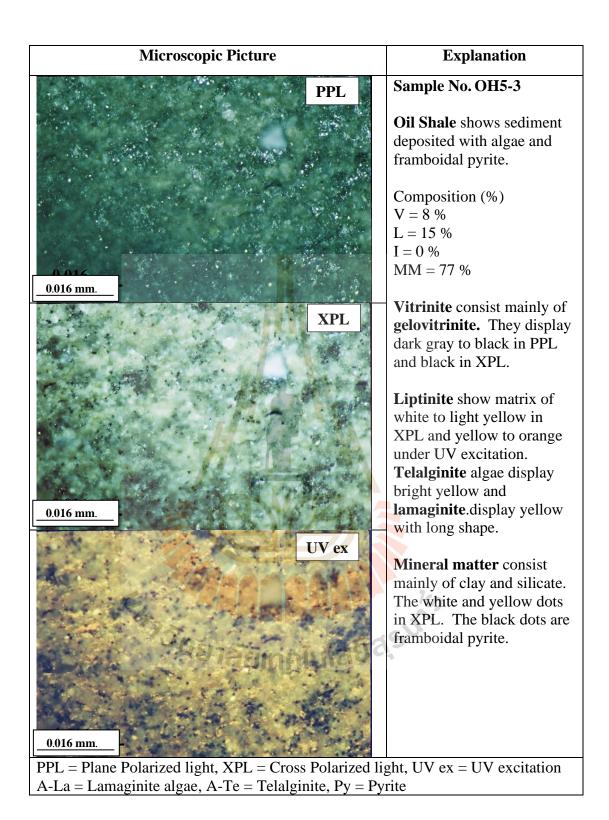


Figure 4.138 The microscopic picture of oil shale sample No. OH5–3.

Microscopic Picture	Explanation
	PPL Sample No.OH6-1
	Oil Shale shows fine-
	grained sediments deposited
Carlos and Sector in	with algae.
	Composition (%)
and the second	V = 4%
	L = 17%
7	I = 0%
the second s	MM = 79 %
and the second sec	
0.016 mm.	Vitrinite consist mainly of
	gelinite. They display
PERSONAL PROPERTY AND A	XPL white to pale gray in PPL
ANTE OF A CONTRACT OF A CONTRACT. CONTRACT OF A CONTRACT. CONTRACT OF A CONTRACT OF A CONTRACT OF A CONTRACT OF A CONTRACT. CONTRACT OF A CONTRACT. CONTRACT OF A CONTRACT OF A CONTRACT OF A CONTRACT. CONTRACT OF A CONTRACT OF A CONTRACT. CONTRACT OF A CONTRACT OF A CONTRACT. CONTRACT OF A CONTRACT OF A CONTRACT OF A CONTRACT. CONTRACT OF A CONTRACT. CO	and black in XPL and UV
the second s	excitation.
	Liptinite consists mainly of
and the second of the second s	lamaginite. They display
and the state of the set of the	short and thin body. Under
	UV excitation, they display
	light yellow to orange
	groundmass with some
0.016 mm.	telalginite colony.
	Telalginite display pale
	UV ex gray to light yellow in PPL,
A CAR AND A	white to light brown in XPL
	and bright white to light
	yellow under UV ex.
175	Mineral matter consist
18 Tasunali	mainly of fine-grained
- identifie	clays. They display white
	in XPL and dark in UV
the second second	excitation. Some of pyrite
	display dark gray in PPL,
0.016 mm.	yellowish brown in XPL
	with cubic dark brown to
	black under UV excitation.
PPL = Plane Polarized light, XPL = Cross Po	

PPL = Plane Polarized light, XPL = Cross Polarized light, UV ex = UV excitation V = Vitrinite, L = Liptinite, I = Inertinite, MM = Mineral Matter A-La = Lamaginite algae, A-Te = Telalginite, Py = Pyrite

Figure 4.139 The microscopic picture of oil shale sample No. OH6 – 1.

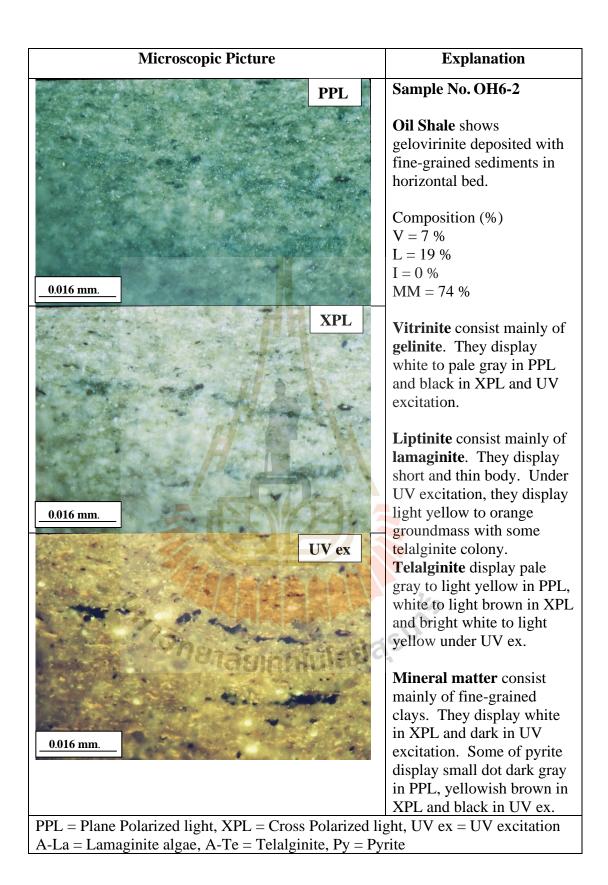


Figure 4.140 The microscopic picture of oil shale sample No. OH6 - 2.

4.2.7 Upper Oil Shale sub-unit

Upper Oil Shale sub-unit overlay conformably to the Lower Oil Shale sub-unit. They show character of clays. The environment of deposition was high stand quiet water with nutrient rich. This led to thick algal deposited and gradually receded before the strong current with large amount of inorganic sediments flooding into the basin and end of organic accumulation. The algal mat accumulated in the Upper Oil Shale sub-units are similar to those deposited in the Lower Oil Shale, but the seams are slightly longer and denser. These could be the result of better nutrients supply which led to richer algal booms and deposited as thicker oil shale beds and more uniform.

From petrographic study, the Upper Oil Shale consist of inorganic sediments (67.85%), liptinite (26.62%) and vitrinite (5.54%). The sediments are mostly of clay (55.15%) and the rest are quartz, silica and carbonate mineral and pyrite (Table 4.10). The liptinite macerals are mainly of lamalginite with some of telalginite. They display dark in PPL and pale gray to white in XPL (Figure 4.143 – 4.144). The coarser inorganic sediments of silt size were found at the contact between the Lower and the Upper oil shale sub-unit. The lamalginite (18.85%) is short to medium with thicker body. They are 0.0032 to 0.0048 mm long in the perpendicular section. They display dark yellow to orange fluorescence in UV-excitation.

The upper part of this sub-unit shows algal mats found associated only with lamalginite. They show paler color and thinner body. This layer is rich in lamalginite with minor telalginite (*Botryococcus* sp.) colony which are varying in size and shape. Framboidal pyrite was also found in this part. The lamalginite bodies become thinner and longer than 0.0032 mm. They display lighter yellow fluorescence in UV-excitation, than those of the lower sub-unit.

	Liptinite												Mineral Matter			
		Tela														
Sample	Lama	Bo	Pila	Lip	Sp	Cu	Fl	Re	Su	Ex	Total	Vitrinite	Clay	Q+Si	Ру	Total
OH7-1	2	4	0	9	0	0	0	0	0	0	15	5	74	5	1	80
OH7-2	4	15	0	7	0	0	0	0	0	0	26	4	58	12		70
OH8-1	28	7	0	3	0	0	0	0	0	0	38	6	45	9	2	56
OH8-2	31	7	0	4	2	0	0	0	0	0	44	4	38	9	5	52
OH8-3	31	1	0	1	2	0	0	- 0	0	0	35	28	27	10		37
OH8-4	40	4	0	0	0	0	0	-0	0	0	44	7	35	9	5	49
OH9-1	16	3	0	8	0	0	0	0	0	0	27	6	57	10		67
OH9-2	16	4	0	1	0	0	0	0	0	0	21	1	69	6	3	78
OH9-3	20	0	0	3	0	0	0	0	0	0	23	4	65	7	1	73
OH9-4	17	2	1	2	0	0	0	0	0	0	22	3	60	10	5	75
OH10-1	16	2	2	3	0	0	0	0	0	0	23	2	64	9	2	75
OH10-2	11	1	0	0	0	0	0	0	0	0	12	1	77	10		87
OH10-3	13	1	0	2	0	0	0	0	0	0	16	1	65	17	1	83
Max	40	15	2	9	2	0	0	0	0	0	44	28	77	17	5	87
Min	2	0	0	0	0	0	0	0	0	0	12	21	27	5	1	37
average	18.85	3.92	0.23	3.31	0.31	0.00	0.00	0.00	0.00	0.00	26.62	5.54	56.46	9.46	1.92	67.85

Table 4.10 Composition in percentage of the Upper Oil Shale sub-unit samples.

Vitrinite (consist of telovitrinite, detrovitrinite and gelovitrinite), Q = Quartz, Si = Silica, Py = Pyrite

Lam = Lamalginite, Tela = Telalginite, Bot = Botryococcus brounii, Pil = Pila algae, Lip = Liptodestrinite, Sp = Sporinite, Cu = Cutinite, Fl= Fluorinite, Re = Resinite, Su = Suberinite, Ex = Exsudatinite

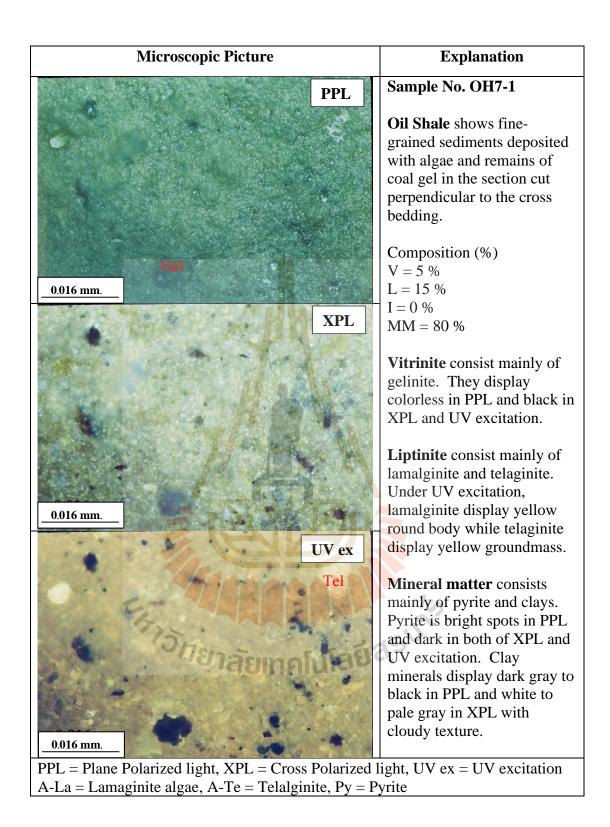


Figure 4.141 The microscopic picture of oil shale sample No. OH7 – 1

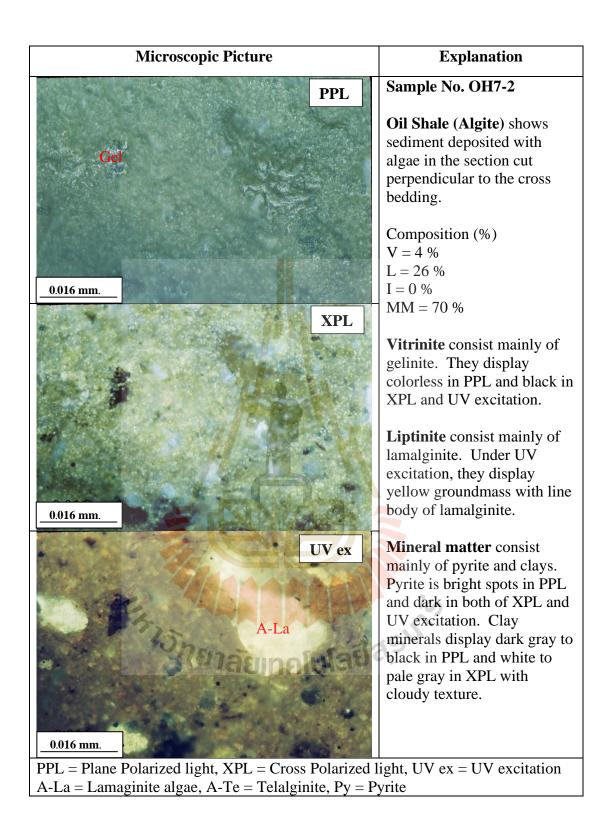


Figure 4.142 The microscopic picture of oil shale sample No. OH7 - 2

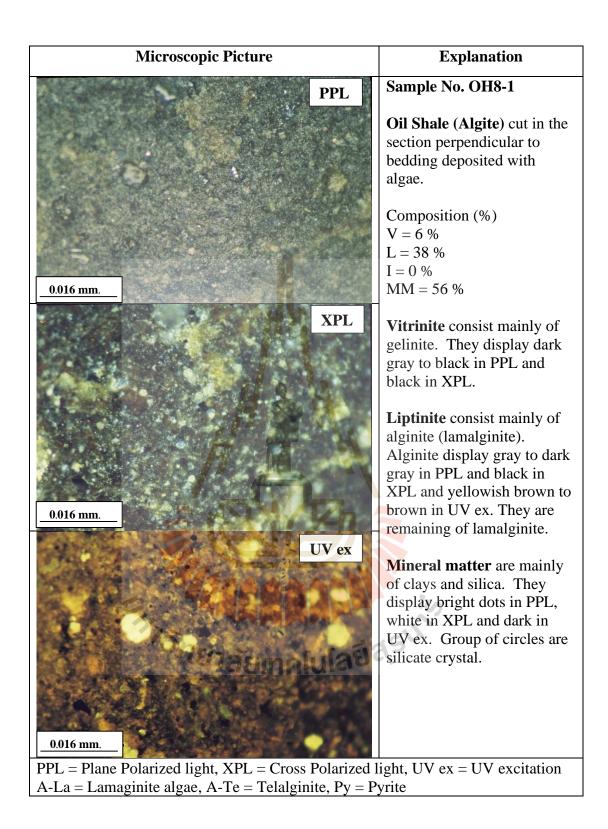


Figure 4.143 The microscopic picture of oil shale sample No. OH8 – 1

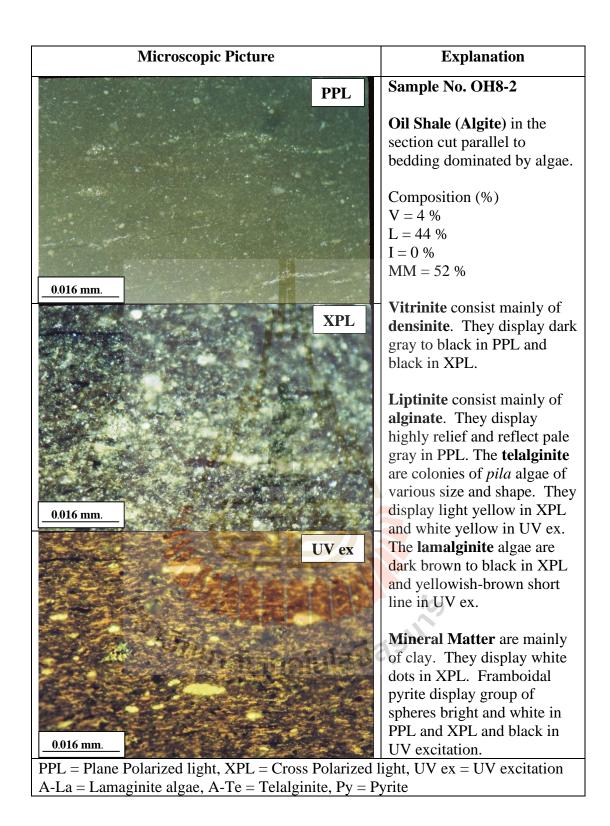


Figure 4.144 The microscopic picture of oil shale sample No. OH8 – 2

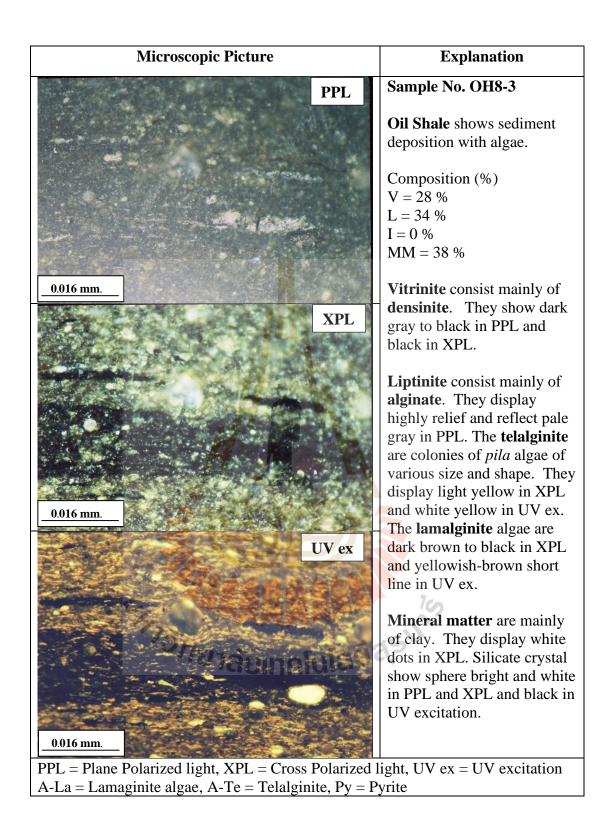


Figure 4.145 The microscopic picture of oil shale sample No. OH8 – 3

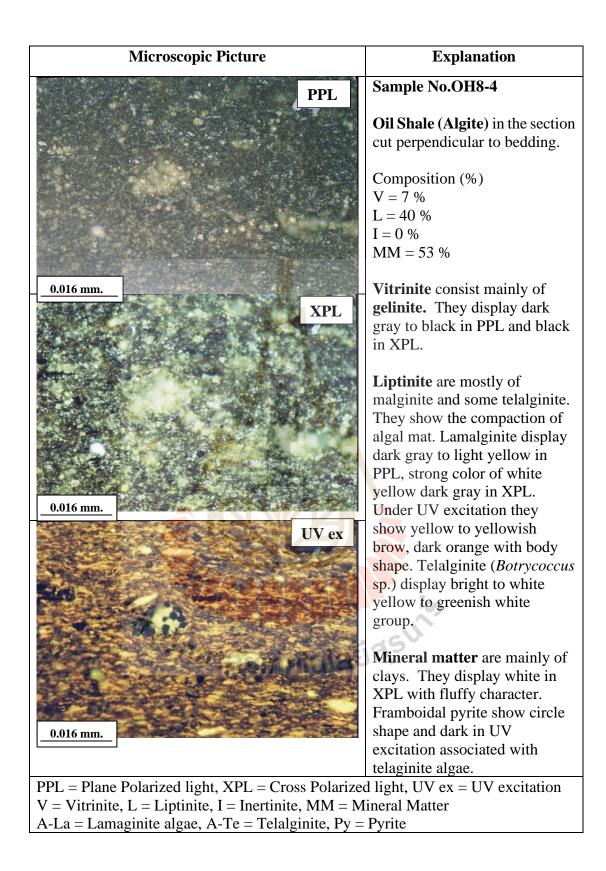


Figure 4.146 The microscopic picture of oil shale sample No. OH8 – 4

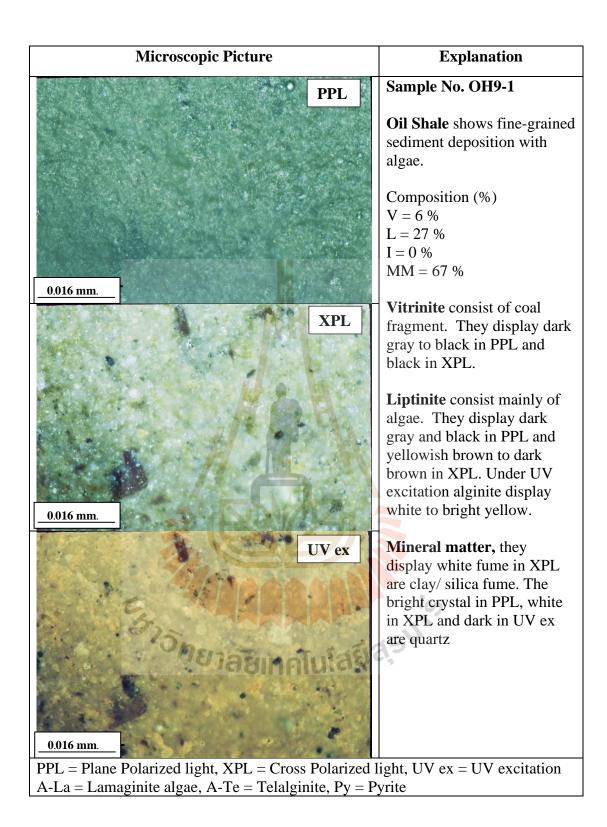


Figure 4.147 The microscopic picture of oil shale sample No. OH9 – 1

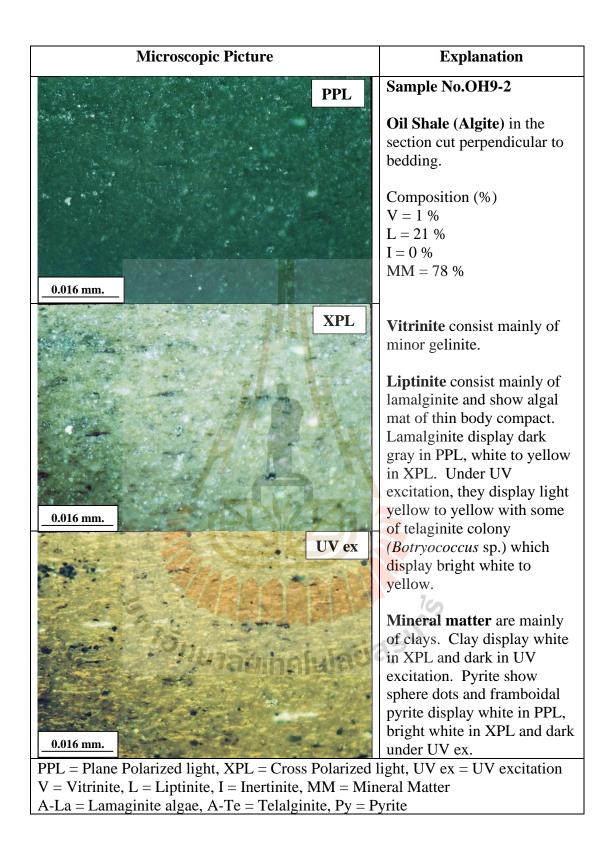


Figure 4.148 The microscopic picture of oil shale sample No. OH9 -2

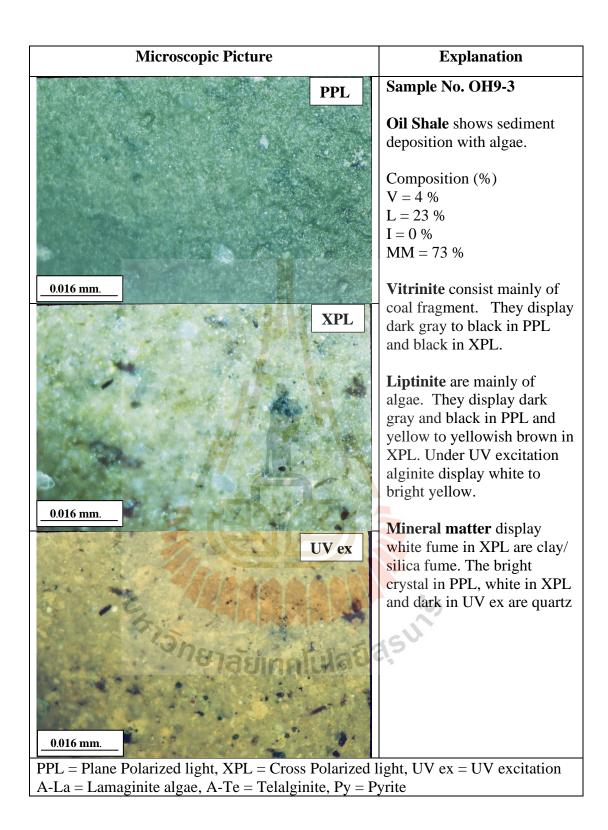


Figure 4.149 The microscopic picture of oil shale sample No. OH9 – 3

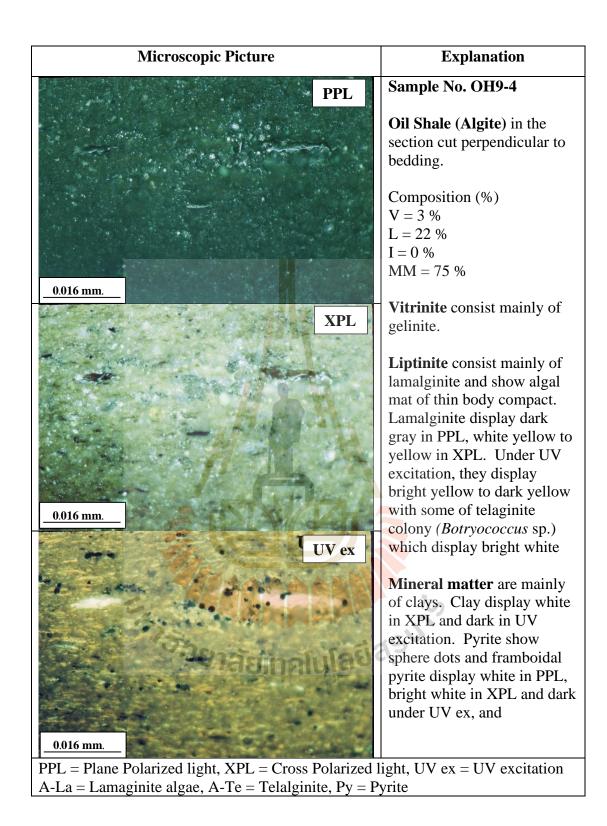


Figure 4.150 The microscopic picture of oil shale sample No. OH9 – 4

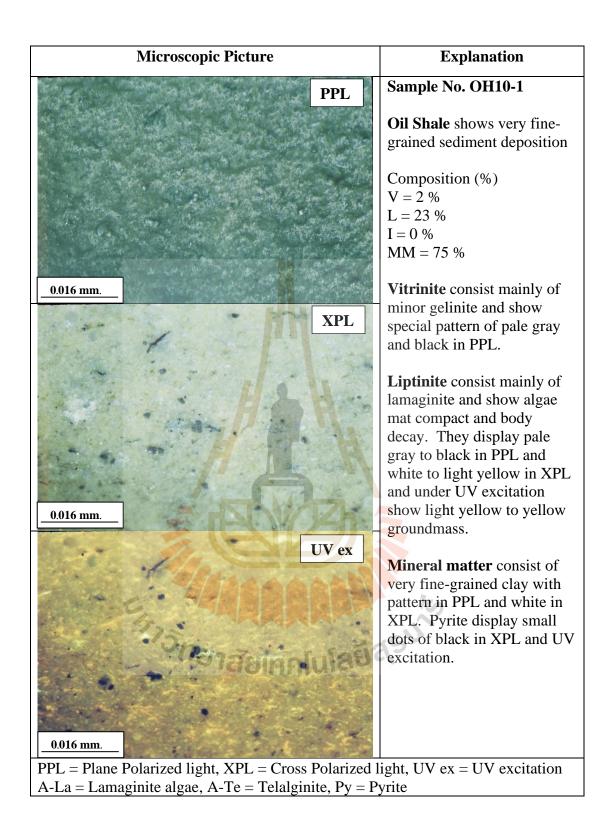


Figure 4.151 The microscopic picture of oil shale sample No. OH10 - 1

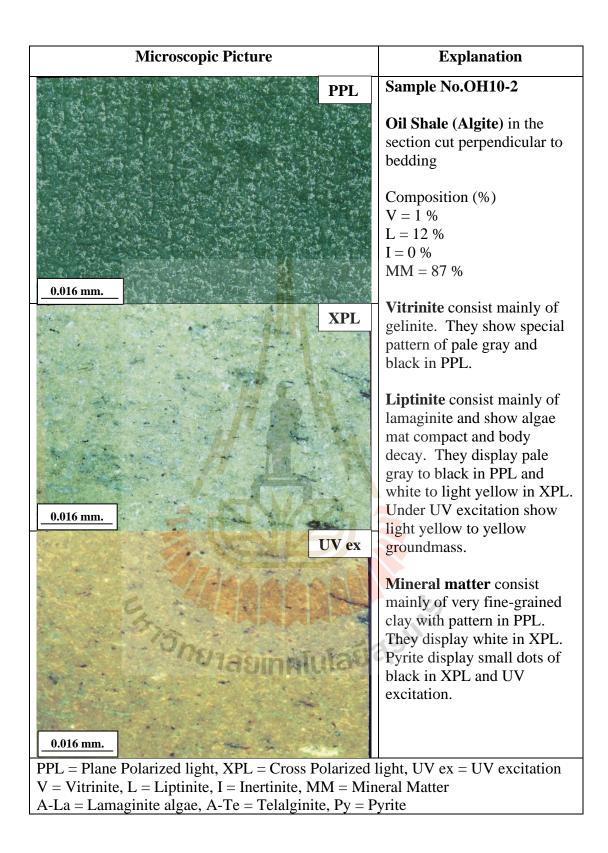


Figure 4.152 The microscopic picture of oil shale sample No. OH10 - 2

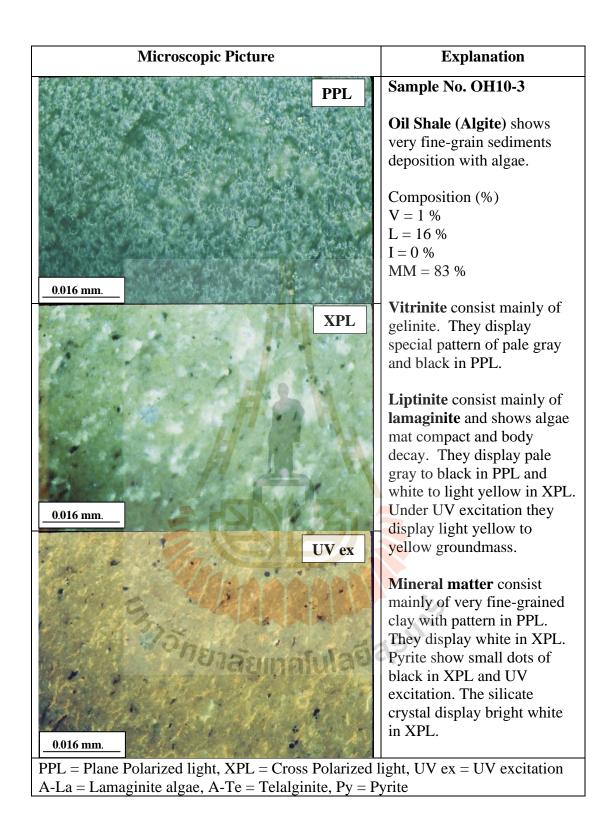


Figure 4.153 The microscopic picture of oil shale sample No. OH10 - 3

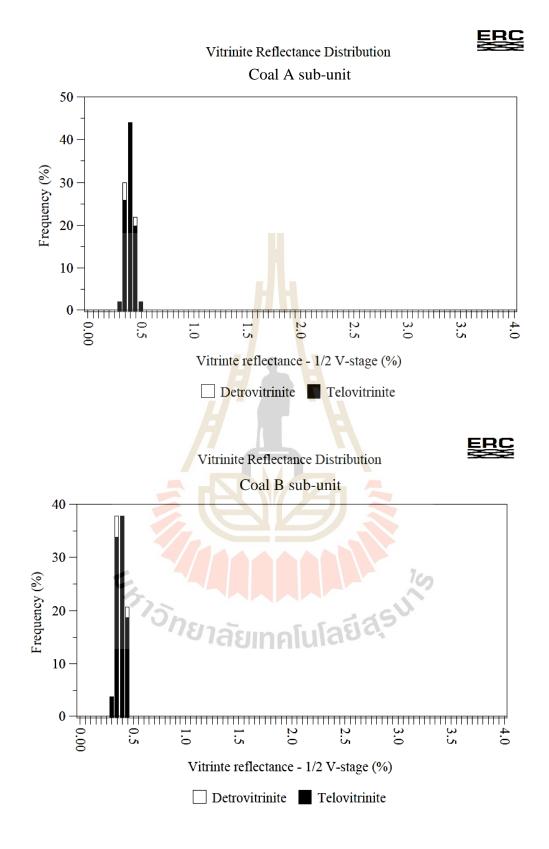
4.2.8 Vitrinite reflectance

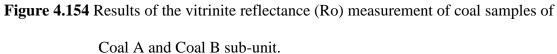
In this study, Coal A and Coal B sub-unit samples were conducted vitrinite reflectance (Ro) measurement under microscopic study using a Leica MP4500P system with Hilgers DISKUS software of ERC Pty. Ltd., Australia. Results of the measurement show that Ro of the studied samples varies from 0.31 - 0.50 %Ro. Results of Ro measurement are presented in Table 4.11 and Figure 4.154.

Sub-units	Maceral	Ro max	Range	n*
Coal A	Telovitrinite	0.41	0.31 - 0.50	47
	Detrovitrinite	0.41	0.36 - 0.49	3
	Total Vitrinite	0.41	0.31 - 0.50	50
Coal B	Telovitrinite	0.41	0.34 - 0.49	50
	Detrovitrinite	(A)	-	-
	Total Vitrinite	0.41	0.34 - 0.49	50

Table 4.11 Vitrinite Reflectance (Ro) of Coal A and Coal B sub-unit.

*n = Number of test samples





4.3 Geochemical analysis

In this study, the studied organic matter compositions were analyzed by proximate and ultimate method to determine the content of fixed carbon, volatile matter, ash and other elements such as sulfur, nitrogen, and oxygen. In addition, they were also measured their heating value and vitrinite reflectance (Ro). The hydrocarbon potential of the studied organic sediments was analyzed by pyrolysis technique in term of oil yield, kerogen yield, carbon and total organic carbon. Results of geochemical analysis conducted in this study can be summarized as follows.

4.3.1 Result of proximate, ultimate and heating value analysis

4.3.1.1 Leonardite unit

Four leonardite samples, which were collected from the lowest part of the studied organic sediment succession (L1), the interbedded part of Coal C sub-unit (L7), the upper part of Coal C (L14) and Coal B sub-unit (L19), were chosen for conducting geochemical analyses.

Results of proximate analysis (moisture, volatile matter, ash and fixed carbon content in wt.%), ultimate analysis (carbon, hydrogen, nitrogen, sulfur and oxygen content in wt.%), and heating value (kcal/kg) of each leonardite sample were presented in Table 4.12.

Results from proximate analysis show that the average value of moisture, volatile matter, ash and fixed carbon content of the studied leonardite samples is 7.22, 13.49, 78.66 and 0.63 wt.% respectively. It was remarkable that the ash content of all leonardite sample was very high (more than 77 wt.%). And results from ultimate analysis indicate the average content of carbon, hydrogen, nitrogen, sulfur and oxygen of the studied leonardite samples is 7.24, 1.95, 0.19, 0.30 and 11.65 wt.% respectively.

The heating value of sample L1, L7, L14 and L19 is 302.8, 277.9, 303.0 and 355.4 kcal/kg respectively.

L1	L7	L14	L19	Average
5.14	7.64	8.23	7.86	7.22
12.57	13.17	13.61	14.60	13.49
81.28	78.51	77.82	77.04	78.66
1.01	0.68	0.34	0.50	0.63
7.08	6.86	7.15	7.88	7.24
1.43	2.03	2.12	2.22	1.95
0.24	0.20	0.19	0.13	0.19
0.30	0.31	0.30	0.30	0.30
9.67	12.09	12.41	12.42	11.65
302.8	277.9	303.0	355.4	309.8
	5.14 12.57 81.28 1.01 7.08 1.43 0.24 0.30 9.67	5.14 7.64 12.57 13.17 81.28 78.51 1.01 0.68 7.08 6.86 1.43 2.03 0.24 0.20 0.30 0.31 9.67 12.09	5.14 7.64 8.23 12.57 13.17 13.61 81.28 78.51 77.82 1.01 0.68 0.34 7.08 6.86 7.15 1.43 2.03 2.12 0.24 0.20 0.19 0.30 0.31 0.30 9.67 12.09 12.41	5.14 7.64 8.23 7.86 12.57 13.17 13.61 14.60 81.28 78.51 77.82 77.04 1.01 0.68 0.34 0.50 7.08 6.86 7.15 7.88 1.43 2.03 2.12 2.22 0.24 0.20 0.19 0.13 0.30 0.31 0.30 0.30 9.67 12.09 12.41 12.42

Table 4.12 Results of proximate, ultimate and heating value analysis of the studied leonardite samples (Air dry basis).

4.3.1.2 Coal unit

The 26 coal samples, 11 samples from Coal C sub-unit, 4 samples from Coal B sub-unit, and 11 samples from Coal A sub-unit, were collected and conducted geochemical analysis and were assessed their heating value in this study.

Results in range and an average value of proximate, ultimate and heating analysis of coal samples were presented in Table 4.13. It is noticeable that all of proximate, ultimate analysis results and heating value of coal samples are higher than those of leonardite samples, especially the heating value.

 Table 4.13 Results of proximate, ultimate and heating value analysis of the studied coal samples (Air dry basis).

Geochemical methods	Coal C		Coal B		Coal A	
	Range	Avg.	Range	Avg.	Range	Avg.
Proximate analysis (wt.%)		L	1	I	
Moisture	10.48 – 17.97	14.14	10.42 - 20.38	14.74	4.28 – 17.86	10.52
Volatile Matter	25.17 – 42.18	32.45	31.53 - 36.08	33.31	25.94 - 41.32	31.51
Ash	17.06 – <mark>53.3</mark> 8	32.35	8.28 - 43.64	28.70	12.00 - 65.56	30.33
Fixed Carbon	10.61 – 28.97	21.06	13.79 – 35.26	23.26	4.22 - 34.84	22.63
Ultimate analysis (wt.%)						
Carbon	27.87 – 44.72	35.01	28.19 - 35.27	31.73	19.34 - 50.48	42.19
Hydrogen	3.53 - 5.09	4.54	4.01 - 4.84	4.43	3.10 - 5.56	4.84
Nitrogen	0.92 - 1.26	1.08	0.75 – 1.17	0.96	0.48 - 1.72	1.30
Sulfur	0.38 - 3.31	1.87	0.64 – 3.53	2.09	0.30 - 0.58	0.44
Oxygen On	20.22 – 29.28	24.75	19.88	19.88	28.46 - 30.96	30.12
Heating Value (kcal/kg)	2565 – 4170	3179	4689.1	4689.1	4581 - 4588	4584

4.3.1.3 Oil Shale unit

In this study oil shale samples collected from oil shale in Coal A sub-unit, Lower Oil Shale sub-unit, and Upper Oil Shale sub-unit were conducted proximate, ultimate, and heating value analysis. Results of analyses are presented in Table 4.14. It is found that the ash content of oil shale samples is quite high as those of leonardite samples and the heating value of these oil shale samples is in between leonardite and coal.

Table 4.14 Results of proximate, ultimate and heating value analysis of the studied oil shale samples (Air dry basis).

Geochemical methods	Oil Shale in Coal A		Lower C	Dil Shale	Upper Oil Shale			
	Range	Average	Range	Average	Range	Average		
Proximate analysis (wt.%)								
Moisture	6.25 – 7.65	6.76	1.98 – 4.97	3.90	1.21 – 3.86	2.80		
Volatile Matter	31.80 – 34.08	33.27	16.05 – 30.32	19.47	19.38 – 29.65	23.04		
Ash	45.78 – 58.23	50.77	67.77 – 80.29	76.92	70.15 – 76.33	73.73		
Fixed Carbon	9.97 – 20.14	15.96	1.91 – 5.28	3.61	0.20 – 5.90	3.22		
		Ultimate ar	nalysis (wt.	%)				
Carbon	24.	02	11.	.73	12.50			
Hydrogen	3.1	13	2.13		2.30			
Nitrogen	0.0	52	0.17		0.19			
Sulfur	0.68		0.94		0.30			
Oxygen 💋	16.46		8.91		10.00			
Heating Value (kcal/kg)	1534.2		946.3		1161.8			
181201011289								

ารเสยเทคเนเลอง

4.3.2 HAWK pyrolysis

The HAWK pyrolysis was conducted in this study to determine values of total organic carbon (TOC), oil yield (S1), kerogen yield (S2), amount of CO₂ (S3), amount of CO (S4 and S5) and maximum temperature (Tmax) of the studied organic sediment samples. In addition, results from pyrolysis analysis can be used for calculating hydrogen index (HI) and oxygen index (OI) which are used to identify kerogen type on the modified van Krevelen's diagram. The results of the HAWK pyrolysis analysis of organic sediments samples from each sub-unit are presented in Table 4.15.

Table 4.15 Results of HAWK pyrolysis analysis of studied organic sediment samples

Sub-units	Oil Yield; (S1) (mg/g)	Kerogen Yield; (S2) (mg/g)	Amount of CO ₂ ; (S3) (mg/g)	TOC (wt.%)	Tmax (°C)	HI	OI
Leonardite	0.64	21.49	1.33	6.37	432	337	20
Coal C	2.11	59.14	9.35	39.18	426	150	23
Coal B	2.32	69.80	8.8 <mark>8</mark>	36.43	424	191	24
Coal A	2.19	69.77	12.30	46.65	427	149	26
Oil Shale in Coal A	1.49	67.80	5.25	19.13	422	371	31
Lower Oil Shale	0.58	42.59	0.72	5.98	434	712	12
Upper Oil Shale	0.96	40.39	1.19	7.57	425	533	15
Average	1.47	53.00	5.57	23.04	427.14	349	21.57

from each sub-unit.

HI; Hydrogen Index = (S2*100)/TOCOI; Oxygen Index = (S3*100)/TOC

Oil yield (S1) of all samples are less than 3 mg/g and vary from 0.64 - 2.32 mg/g. The Leonardite sample shows very low S1 value (0.64 mg/g). All coal samples have similar S1 values around 2.11 - 2.32 mg/g. The oil yield (S1) of all oil shale samples is lower than 2 mg/g. The S1 value of Oil Shale in Coal A is the highest among the oil shale samples (1.49 mg/g).

Kerogen yield (S2) of all samples are vary from 21.49 - 69.80 mg/g. Leonardite has the lowest S2 value (21.49 mg/g) while the highest S2 value is of the Coal B sub-unit sample (69.80 mg/g).

 CO_2 (S3) content of all samples are less than 13 mg/g. The highest CO_2 content is of the Coal A sub-unit samples (12.30 mg/g) while the lowest CO_2 content is of the lower oil shale sub-unit samples (0.72 mg/g).

Total organic carbon (TOC) (wt.%) of all samples are vary from 5.98 – 46.65 wt.%. TOC of the Coal A sub-unit samples is the highest (46.65 wt.%) while TOC of the lower oil shale sub-unit samples is the lowest (5.98 wt.%).

The maximum temperature (Tmax) of all studied sample varies from 422 – 434 °C. The highest Tmax is of the Lower Oil Shale sub-unit samples (434 °C).

Hydrogen Index (HI) of all samples are between 149 and 712. Lower Oil Shale sub-unit samples have the highest HI (712) while Coal A sub-unit samples have the lowest HI (149)

Oxygen Index (OI) of all samples are lower than 31 of the oil shale samples of the Coal A sub-unit. The lowest OI is of the Lower Oil Shale sub-unit sample (12).

Jarvie *et al.* (2001) proposed the correlation between Tmax and vitrinite reflectance as the following equation.

$$Ro = 0.018 (Tmax) - 7.16 \tag{4.1}$$

Therefore, Tmax values from HAWK pyrolysis analysis (Table 4.14) were used to calculate Ro based on the equation 4.1. The results of the calculated Ro are showed in Table 4.16. The evolution of volatile matter begins with the expel of H₂O, CO₂ and CO before large amounts of CH₄ are released. In contrast to during coalification, low molecular weight hydrocarbons, especially methane and other volatiles are generated. Moreover, some methane is liberated from liptinite at relatively low rank (0.2 – 0.5%Ro) (Petersen *et al.*, 2006). While the first volatile products liberated in coal at temperature below 100 °C are mainly H₂O and CO₂ and small amounts of CH₄ (Petersen, 2006). The oil window for the source rocks are depending on the geothermal which is estimated oil window from 0.82 to 0.98 %Ro and burial depths of \sim 1300 – 1400 m. are necessary for efficient oil expulsion to occur (Petersen *et al.*, 2006).

The effective oil window is estimated to occurs at 0.7%Ro for type I, 0.5 %Ro for type II and 0.6 %Ro for type III and kerogen type I and II are early 0.5%Ro for generating dry gas (Tissot and Welte, 1984; Tissot, Pelet and Ungerer, 1987).

Therefore, the organic source rock maturation based on the calculated Ro, kerogen type and Tmax for each studied organic matter sub-unit can be estimated and showed in Table 4.16. Consequently, results of the source rock maturation study based on kerogen type, Tmax and calculated vitrinite reflectance (%Ro) indicate that all of organic matter sub-unit of the Mae Teep organic succession are in between immature and early mature stage.

Table 4.16 The organic source rock maturation estimation based on kerogen type,

Sub-units	Kerogen	Tmax	Ro	Maturation
	Types	(°C)	(%)	
Leonardite	II and III	432	0.616	Early Mature
Coal C	II and III	426	0.508	Immature to Early
				Mature
Coal B	II and III	424	0.472	Immature
Coal A	II	427	0.526	Immature to Early
				Mature
Oil Shale in Coal A	I and II	422	0.436	Immature
Lower Oil Shale	Ι	434	0.652	Immature to Early
				Mature
Upper Oil Shale	I	425	0.490	Immature

Tmax and Ro.



4.4 Discussions

The implication of the petrographical and geochemical results reveal the history of the depositional environments, the source rocks quality for petroleum generation and/or expulsion, the type of organic matter (kerogen), and source rock potential of the Mae Teep organic sediment succession. In this study, the thermal maturation of source rocks was considered by maximum temperature (Tmax), Quality Index (QI) and vitrinite reflectance (%Ro).

4.4.1 Depositional environment of the Mae Teep organic sediment succession.

Depositional environment appearances in lithological source rocks indicated that the organic deposits in the Mae Teep basin had been involved with the water fluctuation. The change of water levels led to the organic matter and fine-grained sediments depositing, maceral types and geochemical composition in the Mae Teep basin. These situations caused the deposition of leonardite at the high-water stand, impure coal (Coal C sub-unit) at the intermediate water stand to coal beds (Coal B subunit and Coal A sub-unit) at the low water stand and toward the forest swamp. The water level changing significantly affected the amount of oxygen dissolved in water which caused the level of oxidization. Since, leonardite is interbedded with coal in the lower part of coal units, this may refer to continuality submergence of organic sediments in Mae Teep basin. The encounter of liptodetrinite together with sporinite may indicate the extension of grass swamp to subaquatic area where organic mud is deposited. The environment of deposition and its related macerals can be summarized as follows. The environment of deposition of the lower part of the Mae Teep organic succession could be lake. It was deep water in the middle part, and gradually shallower along the bank slope and the swampy toward the land. Macerals of this part consists mainly of vitrinite and liptinite groups with some inertinite group and mineral matters. Later on, the coal sub-units were deposited starting from the water dwelling plants such as reed and grass in the marshland or salt marsh that edging the lake and followed by forest swamp on land with woods and ferns. These coals are mainly impure coal with high mineral matter in the lower part and less mineral matter in the upper part.

In general, the ash content in organic sediments can be used to predict the water level during their accumulation. Sapropelic deposits (leonardite and oil shale) having high ash contents may indicate the high-water level environment. Results from geochemical analyses indicate that leonardite samples have the highest ash content but has the lowest carbon and fixed carbon content. Results from coal petrography study of the studied leonardite samples show that the studied samples comprise mineral matter presents (less than 60%) and organic macerals (liptodetrinite, resinite and sporinite with minor alginate). The sapropelic leonardite is subaquatic deposited in high level or open water slowly to the bottom by floating plant debris including algae together with muds.

The Coal C sub-unit is a humic coal which deposited both in reed marsh and forest swamp environments. Results of proximate and ultimate analysis indicate that this coal has low ash content but the highest fixed carbon and carbon. This is agreeable to the highest vitrinite maceral in petrography study results. This vitrinite consists mainly of detovitrinite and gelovitrinite with some of telovitrinite. They were derived from wood stems, root leaves and barks that represents the swampy forest peat environment and refer to low level of water. The ratio of plant cell structure and gel can reflect the association of water/moisture and oxidizing environments. In high moisture and oxidation condition vitrinite would be gelovitrinite from gelification process. In lower moisture and oxidation condition vitrinite would be detrovitinite while in very low moisture and/or oxidizing condition some discernible characters of woods and barks would display only their cell structure outline.

The volatile matter and hydrogen contents show the same direction of the percentage of liptinite content in coal petrography. The liptinite macerals in oil shale are mostly of alginite which deposited with fine-grained sediments while the liptinite in the coals are dominated by several of liptinite derived from plant remains or wood tissues. In the reducing condition, the plant tissues are almost completely preserved e.g. cell wall of bark or root structure, cutical and chlorophyllinite (fluorinite) (Table 4.17).

In mild reducing condition, some of liptinite containing relatively large amounts of fat-wax group can display their shape which can be easily identified. Beside the liptinite, alginite in oil shale, sporinite, cutinite, resinite and suberinite can be distinguished by their shape and ornament. Sporinite dominated coal (cannel coal) may indicate the higher oxidizing condition where all structural tissues are gelified. Resinite were usually found associated with cutinite especially in conifer leave in the temperate Tertiary flora in northern Thailand.

				Composition			
Environments	Unit	Sub-units	Macer <mark>al</mark> Type	V (%)	L (%)	In (%)	MM. (%)
Fluvial	Fluvial seque consolidated)		N/A	N/A	N/A	N/A	N/A
	Fine-grained sequences	sedimentary	N/A	N/A	N/A	N/A	N/A
Lacustrine	Oil Shale*	Upper Oil Shale	Alginite and liptinite	5.54	26.62	0	67.84
		Lower Oil Shale	Alginite and liptinite	4.33	19.54	0	76.46
		Oil Shale in Coal A	Alginite liptinite and sporinite	12.00	74.36	0	13.62
	Coal*	Coal A	Telovitrinite, gelinite, alginite, cutinite, sporinite, fluorinate, liptinite, resinite, and some of extinite	70.45	23.18	0.29	5.04
Forest-Swamp		Coal B	Telovitrinite, gelinite, cutinite, sporinite liptinite, resinite	75.29	11.88	0.12	12.71
		Coal C	Telovitrinite, detrovitrinite and gelinite, cutinite, sporinite, liptinite, resinite	67.59	12.96	0.68	19.00
	Leonardite*	Leonardite	Detrovitrinite, gelinite, sporinite, liptinite resinite and some of alginite	20.57	17.29	0	62.14

Table 4.17 Depositional environments of each Mae Teep deposit sub-unit based on maceral type and petrography study results.

*organic sub-units in this study, V = Vitrinite, L = Liptinite, In = Inertinite, MM. = Mineral Matter

Two oil shale parting in the Coal A sub-unit may indicate the temporary long period deep-water flooding in the forest swamp. The stagnant of water for a long time with rich of nutrient led to algae booms and produced thick bed of algal mats. This part of the Coal A sub-unit indicated the environmental conditions changing suddenly from the shallow water in forest-peat swamp to high stand water by successive unit from Coal A to the above Oil Shale sub-unit.

The oil shale deposit is normally restricted in the lacustrine environment. They have high inorganic sediments and ash content which derived from fine-grained sediment deposited together with algae during the algal boom period. This is related to the seasoning nutrient supplied and the flavoring temperature conditions which led to the variety of the algae characters. In general, alginite maceral cause both of high volatile matter and hydrogen contents in oil shale sub-unit.

Layers of algae in oil shale consist mainly of lamalginite and telalginite. Under microscopic, lamalginite in the Lower oil shale show both long and short bodies, but they are thinner and shorter than those of other sub-units. The size of the algae normally depends on the pH and nutrient of the swamp water. In general algae can be better absorb nitrogen and grow faster in warmer temperature. Later on, the oil shale deposition was terminated by waterflooding. After waterflooding, the fluvial process had been developed and fluvial sediments have been deposited.

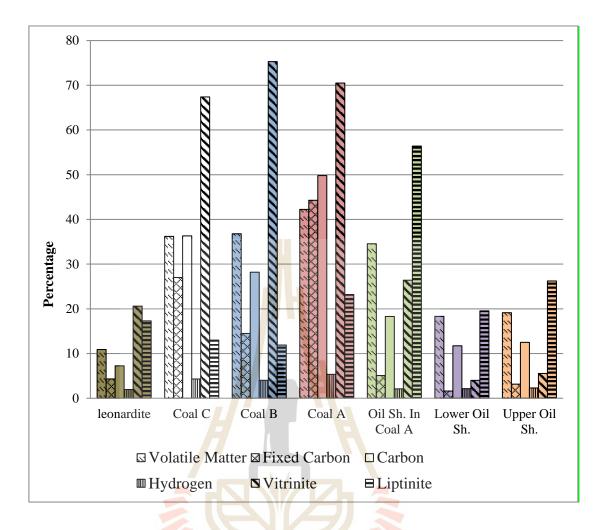


Figure 4.155 Geochemical compositions and dominated maceral type of each sub-unit.

4.4.2 The thermal maturation of petroleum source rocks potential of Mae Teep organic sediments.

According to the depositional environment from high to shallow water led to the component of organic sediments in form of maceral types. The rate of organic matter transformation during burial normally related to compositions of source rocks and the stage of evolution.

Results of the study indicate that in the pyrolysis stage the oil yield (S1) is low and carbon are in form of carbon dioxide while the kerogen yield (S2) is high in

Coal B, Coal A and Oil Shale in Coal A sub-unit. The oil yield (S1), kerogen yield (S2) and total organic carbon (TOC) are low in leonardite and oil shale. However, Oil Shale in Coal A has kerogen yield (S2) as high has those of the coal units.

The carbon contents (S3) indicates carbon in form of CO₂ and CO which are normally low in organic sediments such as leonardite and oil shale. Hydrogen index (H) and oxygen index (OI) can be calculated from the kerogen yield (S2), carbon contents (S3) and total organic carbon (TOC). In this study, the calculated HI and OI were cross-plotted on the modified Van Krevelen diagram to classify the kerogen type of the studied samples (Figure 4.156). Results of the plots indicate that the of oil shale, leonardite and coal studied samples are classified as kerogen type I, type II and type II respectively. However, oil shale samples from coal A sub-unit are classified as both kerogen type II and type III.



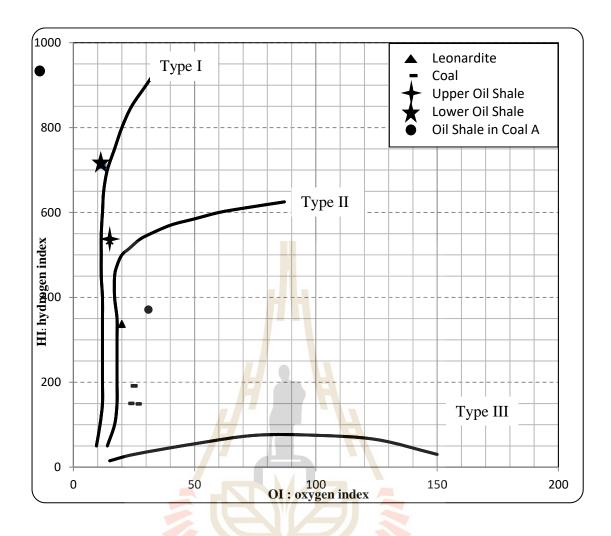


Figure 4.156 Kerogen type classification of the studied samples by the HI and OI

cross-plot on the Modified Van Krevelen diagram.

The amount of free hydrocarbon (S1) and the quantity of remaining hydrocarbon which has not yet been transformed to hydrocarbons (S2) can be measured in mg/g of rock. Therefore, the genetic potential (S1+S2) which relate to production index or productivity index (PI) can be derived from the relationship of S1/(S1+S2). As a result, the calculated PI of the studied samples are between 0.1 and 0.3 mg HC/g TOC and this indicates the immature stage of the source rock. Coal and leonardite samples have high

PI while the lowest PI is of the Lower Oil Shale sub-unit samples. The highest PI is show at the coals and leonardite and lowest at the Lower Oil Shale sub-unit. Results of the cross-plot between S2 and TOC indicate that the studied samples have good to excellent hydrocarbon generation potential (Figure 4.157).

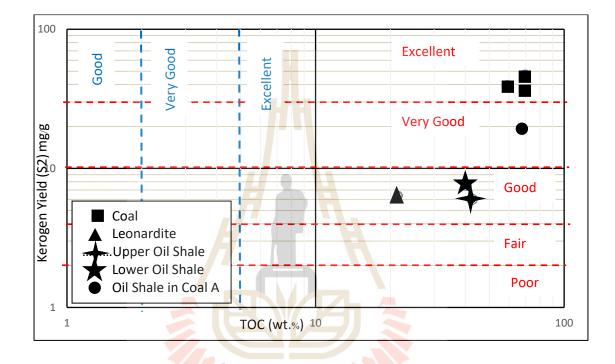


Figure 4.157 Cross-plot of remaining hydrocarbon potential (S2) and TOC (wt.%) show good to excellent potential hydrocarbon generation of the studied samples.

The maturation of the organic matter can be estimated by the maximum temperature (Tmax). In general, a Tmax of 430°C is the boundary between immature and mature (oil production zone). In this study, leonardite samples have Tmax over 430°C and the highest Tmax (434 °C) is of the Lower Oil Shale sub-unit sample (Figure 4.158A).

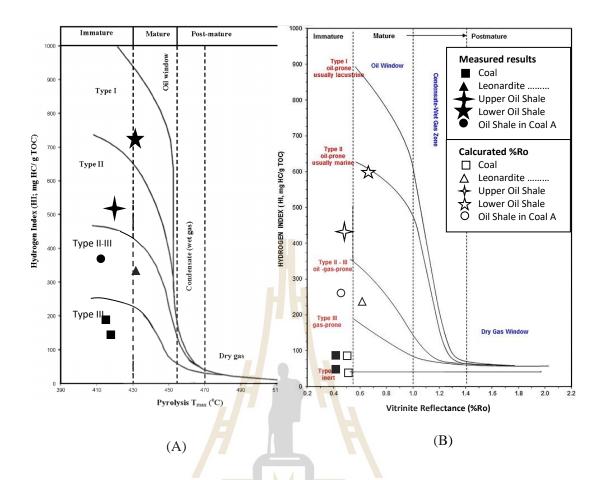


Figure 4.158 Evaluation of the thermal maturity stage of the studied organic samples based on HI vs Tmax cross-plot (A) and HI vs measured vitrinite reflectance cross-plot (B).

Results of the HI vs Tmax cross-plot indicate that the thermal maturity of the studied leonardite, oil shale and coal samples are mostly fallen in the immature stage. However, there are a sample of Lower Oil Shale and a sample of Leonardite fall in the early mature stage (Figure 4.158A).

The vitrinite reflectance (Ro) is an optical method for measuring the source rock maturity (Tissot and Welte, 1984). The maturity ranges for generated hydrocarbons can be start at vitrinite reflectance of 0.4 %Ro (or Tmax of~420°C) is onset of petroleum

generation (Petersen, 2002., Sykes *et al.*, 2002). In this study, the calculated vitrinite reflectance are between 0.436 - 0.652 %Ro (Table 4.16) while the average measured vitrinite reflectance is 0.41 %Ro. The results of the HI vs measured vitrinite reflectance cross-plot indicate that the studied organic samples are all in the immature stage. However, results of the HI vs calculated vitrinite reflectance indicate that the Lower Oil Shale and Leonardite samples are fallen in the early mature stage (Figure 4.158B).

Productivity index (PI) and maximum temperature (Tmax) cross-plot can be used to identified the generated hydrocarbon type of the source rock. Results of the PI vs Tmax cross-plot of the studied samples in this study are depicted in Figure 4.159. The cross-plot indicate that all of studied organic samples are fallen in the oil zone generation.

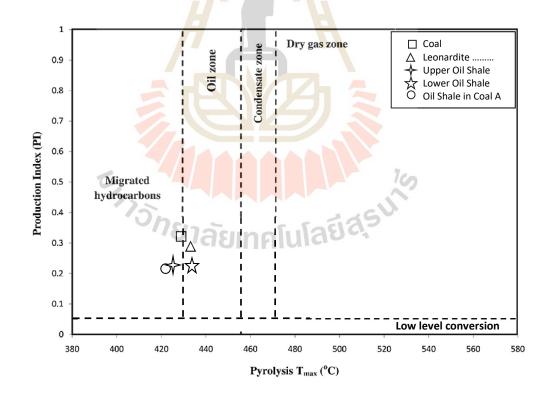


Figure 4.159 Cross-plot of Productive Index (PI) versus Tmax of the studied organic

samples.

CHAPTER V

CONCLUSION AND RECOMMENDATION

In this study, the depositional environment and petroleum potential of Mae Teep organic sediments had been studied and evaluated. Field work, petrography study and geochemical analyses had been conducted to achieve the objectives of this study. Some conclusions from this study can be drawn as follows.

5.1 Depositional environment and characteristics of Mae Teep organic sediments

Mae Teep basin is the small terrestrial Cenozoic basin located in northern of Thailand. There are 3 environments of depositional systems in this basin including fluvial depositional system in the upper part, lacustrine depositional system in the middle part and swamp depositional system in the lower part of basin. The common organic sediments found in this basin are oil shale, coal and leonardite, and the main factor to directly control of these rocks' deposition is the changing of water level in the basin. Based on lithology, organic sediments in Mae Teep basin can be subdivided into 7 sub-units from the lower part to the upper part of basin as Leonardite, Coal C, Coal B, Coal A, Oil Shale in Coal A, Lower Oil Shale and Upper Oil Shale, respectively.

The investigations regarding to organic compositions of Mae Teep deposits and their depositional environments based on the results of the petrographic and geochemical analyses indicate three types of depositional environment in the ascending order as: (a) swampy to forest swamp environment, (b) lacustrine environment, and (c) fluvial environment.

The sediments accumulation in Mae Teep basin began deposit concurrently with the rising of water level in basin due to the basin subsidence. This event induced the deposit of fine-grained particles that were absence or low organic matter, consisting of clays and organic mud (gyttja) in the near shore. Later, leonardite was deposited in low water level. When water became shallower, reed peat and peat from forest swamp were deposited, increasing organic contents in the deposits, making coal sequences as the Coal C, Coal B and Coal A sub-units at the lower part of basin as swamp environmental area, and then the sediments of low energy lacustrine were accumulated in the middle part. These depositional processes regular supply of clay particles and organic material accumulation together especially resulted from rich algal boom. The oil shale with more uniform and richer organic matter bed was formed in this event. The main rock subunits in this process are oil shale in Coal A, the Lower Oil Shale and the Upper Oil Shale sub-unit, Finally, sediments from high energy fluvial environment had been deposited at the upper part.

Results of the study indicate that leonardite sub-unit deposited in the high-water level swamp environment with a few of plant growth. It presents large amount of finegrained inorganic matter with some of organic contents dominated by gelovitrinite which indicates moderately oxidizing environment. In the Coal C, Coal B, and Coal A sub-units, the present of detrovitrinite, liptodetrinite and moderately high ash contents indicates the low-water level swamp environment with moderately oxidized of reed peat. The low ash coal with good preservation of plant tissues, some cutinite, fluorinite, sporinite, and resinite association indicates the reducing condition in the forest swamp environment. In the addition, the maceral composition of these coal units corresponds to type II and type III kerogen.

The product of lacustrine environment deposition in Mae Teep basin is mainly oil shale with uniform, rich organic matter and containing plenty of algal deposit. These fine-grained sediments are high ash contents with alginite maceral which indicates the high stand, deep water and undisturbed environment. Moreover, this alginite rich thick algal mat also indicates the availability of nutrient which is resulted in good oil source rocks of type I kerogen.

5.2 Potential of petroleum source rocks

According to chemical compositions, Mae Teep coals contain large quantity of carbon and hydrocarbon contents but the ash volume is quite low. This characteristic presents the high heating values as a good potential fuel. Moreover, the present of high vitrinite and liptinite content may contribute these coals to have the high potential for gas generation.

The heating values of leonardite and oil shale are lower than those of the Mae Teep coals because the organic carbon content in both rocks is low volumes. However, leonardite might be a potential petroleum source since it has high TOC (6.37 wt.%). Therefore, based on the genetic potential, leonardite can be classified as a moderate quality source rock.

Oil shales in Mae Teep basin contain lower carbon but higher ash contents than the Mae Teep coals. They also have high TOC and kerogen yield. The Lower Oil Shale characteristics are similar to those of the Upper Oil Shale, except having larger the volume of alginite.

Results form HI vs OI cross-plot on the modified Van Krevelen diagram indicate that organic sediments of both the Lower and the Upper Oil Shale sub-unit are Type I kerogen. Therefore, based on the kerogen type, Mae Teep oil shales have a potential for oil generation.

Results of the HI vs Tmax cross-plot indicate that the thermal maturity of the studied leonardite, oil shale and coal samples are mostly fallen in the immature stage. However, there are a sample of Lower Oil Shale and a sample of leonardite fall in the early mature stage.

In this study, the calculated vitrinite reflectance are between 0.436 - 0.652 %Ro while the average measured vitrinite reflectance is 0.41 %Ro. The results of the HI vs measured vitrinite reflectance cross-plot indicate that the studied organic samples are all in the immature stage. However, results of the HI vs calculated vitrinite reflectance indicate that the Lower Oil Shale and leonardite samples are fallen in the early mature stage.

Though the results of pyrolysis analysis of the studied samples show low oil yields (S1) (0.58 – 2.32 mg/g), they are considered to be the high potential hydrocarbon source rock since they have high kerogen yield (S2) (up to 69.8 mg/g). They also have high total generated petroleum potential (22.13 - 72.12 mg/g). These may contribute them to be a good - very good source rock. Moreover, the encounter of the associated macerals of resinite, i.e. suberinite with small amount of exsudatinite in these studied

organic sediments could indicate the early expel of heavy petroleum generation from these immature - early mature source rocks.

5.3 Recommendation

This research covered the study of depositional environments and petroleum potential of organic sediments of the Mae Teep deposits which showed the possibility to be the good petroleum potential source rocks. The study methodologies used in this study could be applied to study the depositional environment and to evaluate the petroleum potential of the expected petroleum source rocks in other petroleum province where has the similar source rocks, successive tectonics and geological setting, especially Tertiary basins in Thailand.

Therefore, it is recommended to apply these study methodologies to Thai Tertiary basins which were setting at the same time of Mae Teep basin but were offset by tectonic and deeper burial (Chinbunchorn et. al., 1989), such as Phrae, Ngao, Chiang Muan, Mae Moh, Lampang, Chae Hom, Na Noi, Fak Tha, Wang Nua, Mae Suai, Wiang Pa Pao and Phraw basin.

REFERENCES

- ASTM International (2011a) Standard practice for collection of channel samples of coal in amine. In: Bailey S.J., Baldini N.C., Emery S. (eds) Annual Book of ASTM Standards: section 5 Petroleum Products, Lubricants, and Fossil Fuels, Gaseous Fuels; Coal and Coke 05.06, pp.560 562.
- ASTM International (2011b) Preparing coal samples for analysis. In: Bailey S.J., Baldini N.C., Emery S. (eds) Annual Book of ASTM Standards: section 5
 Petroleum Products, Lubricants, and Fossil Fuels, Gaseous Fuels; Coal and Coke 05.06, pp.420 - 436.
- ASTM International (2011c) Collection and preparation of coke sample for laboratory analysis. In: Bailey S.J., Baldini N.C., Emery S. (eds) Annual Book of ASTM Standards: section 5 Petroleum Products, Lubricants, and Fossil Fuels, Gaseous Fuels; Coal and Coke 05.06, pp.367 371.
- ASTM International (2011d) Standard test method for total moisture in coal. In: Bailey S.J., Baldini N.C., Emery S (eds) Annual Book of ASTM Standards: section 5 Petroleum Products, Lubricants, and Fossil Fuels, Gaseous Fuels; Coal and Coke 05.06, pp.506 - 512.
- ASTM International (2011e) Proximate Analysis of coal and coke by Macro Thermogravimetric Analysis. In: Bailey S.J., Baldini N.C., Emery S. (eds) Annual Book of ASTM Standards: section 5 Petroleum Products,

Lubricants, and Fossil Fuels, Gaseous Fuels; Coal and Coke 05.06, pp.600, 814 - 822.

- ASTM International (2011f) Instrumental determination of carbon, hydrogen, and nitrogen in laboratory samples of coal. In: Bailey S.J., Baldini N.C., Emery S. (eds) Annual Book of ASTM Standards: section 5 Petroleum Products, Lubricants, and Fossil Fuels, Gaseous Fuels; Coal and Coke 05.06, pp.613 621.
- ASTM International (2011g) Sulfur in the analysis sample of coal and coke using high temperature tube furnace combustion. In: Bailey S.J., Baldini N.C., Emery S.(eds) Annual Book of ASTM Standards: section 5 Petroleum Products, Lubricants, and Fossil Fuels, Gaseous Fuels; Coal and Coke 05.06, pp.542 549.
- ASTM International (2011h) Preparing coal sample for microscopical analysis by reflected light. In: Bailey S.J., Baldini N.C., Emery S.(eds) Annual Book of ASTM Standards: section 5 Petroleum Products, Lubricants, and Fossil Fuels, Gaseous Fuels; Coal and Coke 05.06, pp.454-458.
- ASTM International (2011i) Microscopical determination of the maceral composition of coal. In: Bailey SJ, Baldini NC, Emery S (eds) Annual Book of Astm Standards: section 5 Petroleum Products, Lubricants, and Fossil Fuels, Gaseous Fuels; Coal and Coke 05.06, pp.464-469.
- Bertrand, P. (1984) Geochemical and petrographic characterization of humic coals considered as possible oil source rocks. In : Schenck, P.A., de Leeuw, J.W. and Lijmbach, G.W.M (eds) **Organic Geochemistry**, pp. 481-488.

- Belaid, A., Krooss, B.M., and Littke, R. (2010). Thermal history and source rock characterization of a Paleozoic section in the Awbari Trough, Murzuq Basin, SW Libya. Marine and Petroleum Geology 27, pp. 612-632.
- Brook, J., Conford, C., Archer, R. (1987) The role of hydrocarbon source rock in petroleum exploration. In: Brooks, J., Fleet, A.J. (eds.), Marine Petroleum
 Source Rocks Geological Society Special Publication No. 26, pp. 17 46.
- Buffetaut, E., Helmcke-Ingavat, R., Jaeger, J.-J., Jongkanjanasoontorn, Y. and Suteethorn, V. (1988) Mastodon remains from the Mae Teep basin (nortern Thailand) and their boistratigraphic significance. Competes Rendus Acadamie Scientifique Paris 306, 249 254.
- Burri, P., (1989). Hydrocarbon potential of tertiary intermontane basins in Thailand.
 In T. Thanasuthipitak, and P. Ounchanum (eds.), Proceedings of the the International Symposium on Intermontane Basins: Geology and Resources. Department of Geology Sciences, Chiang Mai University, Chiang Mai, Thailand, January 30 February 2, 3 12.
- Chaodumrong, P., Ukakimapan, Y., Sansieng, S., Janmaha, S., Pradidtan, S., and Sae Leow, N. (1983). A Review of the Tertiary Sedimentary Rocks of Thailand. *In*P. Nutalaya (eds.), Proceeding of the Workshop on Stratigraphic
 Corrlation of Thailand and Malaysia, HaadYai, Thailand, September 8 10, 159 187.
- Chaodumrong P., Chaimanee Y. (2002) Tertiary Sedimentary Basins in Thailand. **The Symposium on Geology of Thailand**, 26-31 August, 156 – 169.

- Charoenprawat, S. Chuaviroj, C. Hinthong and C. Chonglakmani (1994): Geology of Changwat Lampang (NE 47-7), scale 1:250,000. Geological Survey Division, Department of Mineral Resources, (in Thai)
- Chinbunchorn, N., Pradidtan, S., and Sttayarak, N. (1989). Petroleum potential of Tertiary intermontane basins in Thailand. In T. Thanasuthipitak, and P. Ounchanum (eds.), Proceedings of the Internaltional Symposium on Intermontane Basin: Geology and Resources. Department of Geology Sciences, Chiang Mai University, Chiang Mai, Thailand, January 30 February 2, 29 41.
- Cohen, A.D., Raymond, R., Ramirez, A., Morales, Z., Ponce, F. (1989) The Changuinola peat deposit of northwestern Panama: a tropical, back-barrier, peat (coal)- forming environment. International Journal of Coal Geology 12, pp.157-192.
- Cook, A. C. and Kantsler, A.J. (1982) The Origin and petrology of organic matter in coals, oil shales and petroleum source rocks. Geology Department, University of Wollongong.
- Cook, A.C. and Sherwood, N.R. (2003) Classification of oil shales, coals and other organic-rich rocks. **Organic Geochemistry 17(2)**, pp. 211 222.
- Department of Mineral Resources (1964) Report on the Geology of Oil, Oil Shale, and Coal in the Tertiary Basin of Northern Thailand. Bangkok.
- Department of Mineral Resources (1981) Report on the Geology of Oil, Oil Shale, and Coal in the Tertiary Basin of Northern Thailand. Bangkok.

- Department of Mineral Fuels (2007). Geology of Thailand. Department of Mineral Fuels, Bangkok, (in Thai). Available from internet, http://www.dmf.go.th/bid20/petro_province.html
- Dow, W.G. (1977). Kerogen studies and geological interpretations. Journal of Geochemical Exploration, V.7, pp. 79 99.
- Durand, B. (1993). Composition and structure of organic matter in immature sediments. In: Bordenave, M.L., (eds.). Applied Petroleum Geochemistry, Paris. pp. 77-100.
- Durand, B. and Paratte, M. (1983) Oil potential of coals. In: Brooks, J. (eds.)
 Petroleum Geochemistry and Exploration of Europe, Blackwell Scientific
 Publication, Oxford, pp.285-292.
- Francis W. (1961) Coal: Its Formation and Composition. Edward Arnold (Publishers) Ltd., London.
- Gibling, M. and Ratanasthien, B. (1980). Cenozoic basins of Thailand and their coal deposits: A preliminary report. Bulletin of the Geological Society of Malaya 13, pp. 27 42.
- Gibling MR, Ukakimaphan Y, Stisuk S (1985) Oil shale and coal in intermontane basins of Thailand, American Association of Petroleum Geologists, Bulletin 69, pp. 760-766
- Gibling, M.R., Tantisukrit, C., Uttamo, W., Thanasuthipitak, T. and Haraluck, M. (1985) Oil Shale sedimentology and geochemistry in Cenozoic Mae Sot Basin, Thailand. American Association of Petroleum Geologists Bulletin 69, pp. 767 780.

- Gibling MR, Ukakimaphan Y, Srisuk S (1988) Facies change of coal and oil shale strata in the Cenozoic Mae Tip basin, Northern Thailand. Open-file Report, Geological Science, ChiangMai University 8105-2, 1-15.
- Hunt, J.M., (1991). Generation of gas and oil from coal and other terrestrial organic matter. Organic Geochemistry, 17, No.6, pp. 673-680. Pergamon Press. Oxford.
- Hunt, J.M. (1996). Petroleum geochemistry and geology. New York, Second Edition. pp. 743.
- Hutton, A.C. (1982) Organic petrology of oil shales [Dissertation]. University of Wollongong
- Hutton, A.C. (1987) Petrographic classification of oil shales. International *Journal of* **Coal Geology V.8**, pp. 203 – 231.
- International Committee for Coal and Organic Petrology; ICCP. The new vitrinite classification (ICCP System 1994). Fuel 1998; 77 No.5, pp. 349 358.
- International Committee for Coal and Organic Petrology; ICCP. The new inertinite classification (ICCP System 1994). Fuel 2001. 80, pp. 459 471.
- Isaksen, H.G., Curry, J.D., Yeakel, D.J. and Jenssen, I.A. (1998) Controls on the oil and gas potential of humic coals. Organic Geochemistry Vol 29 (Bi, 1-3) Elsevier Science. Ltd., pp 23 – 44
- Jeffrey R. Levine (1993) Coalification: The Evolution of Coal as Source Rock and Reservoir Rock for Oil and Gas. **AAPG** (online). Available at http://jeffrey.levineonline.com/wp-

content/uploads/documents/1993.AAPG_Memoir_38.Levine.Coalification.pdf

- Jone, R.W. (1987) Organic Facies. In: Brooks, J and Welte, D. (eds.) Advances in **Petroleum Geochemistry**, Academic Press, London, 2, pp.1 90.
- Killops, S and Killops, V. (2005). Introduction to Organic Geochemistry, Second Edition. Blackwell Publishing, 126.
- Law, C.A. (1999) Evaluating Source Rocks. Volume Treatise of Petroleum Ggeology/Handbook of Petroleum Geology : Exploring for Oil and Gas Traps,
 AAPG Special Volumes. 3, pp. 1 34.
- Lawwongngam, K. and Philp, P.R. (1993). Preliminary investigation of oil and source rock organic geochemisity for selected Tertiary basin of Thailand. Journal of Southeast Asian Earth Science, Vol.8 (1-4), pp.433 – 448
- Lewis, W.D., and McConchie, D. (1937). Practical Sedimentology. New York, America. 197 p. Available at http://trove.nla.gov.au/version/44779937
- Maria, M. Agnieszka, D., James C.Hower, Jennifer M.K.O'Keefe (2011) Chapter 3 –
 Spontaneous Combustion and Coal Petrology. Coal and Peat Fires: A Global
 Perspective V1: Coal-Geology and Combustion. ELSEVIER, pp 47 62
- Mendonca Filho J.G., Menezes T.R., de Oliveira Mendonca J., de Oliveira A.D., da Silva T.F., Rondon N.F., da Silva F.S., (2012). Organic Facies: Palynofacies and Organic Geochemistry Approaches. In: Geochemistry Earth's System Processes, Dr. Dionisios Panagiotaras (Ed.) ISBN: 978-953-51-0586-2
- McKee, R.H. and Goodwin, R.T. (1923) A chemical examination of the organic matter in oil shales. Colorado School of Mines Quart 18(1), pp. 8 20.
- Miles, A.J. (1994). Glossary of terms applicable to the petroleum system. In: Magoon,
 L.B., Dow, W.G., (eds.). The Petroleum System-From Source to Trap: *AAPG Memoir.* 60: 643-644.

- Morley, C.K. Sangkumarn, N., Hoon, T. B., Aliet, A. and Simmons, M. (2001). Late Oligocene-Recent stress evolution in rift basins of northern and central Thailand: implications of escape tectonics. **Tectonophysics. 334**, pp.115 – 150.
- Morley, C.K. and Racey, A. (2011) Tertiary stratigraphy. *In*: Ridd, M.F., Barber, A.J. and Crow, M.J. (eds) **The Geology of Thailand**, Geological Society, London, pp. 223-271.
- O'Leary, H. and Hill, G.S. (1989) Cenozoic basin development in the Sourthern Central Plains, Thailand. Proceedings of the International Conference on Geology and mineral Resources of Thailand, Bangkok, Department of Mineral Resources, Bangkok, 1-8
- Pasley, M. A. (1991) Organic matter variation a depositional sequence; implications for use of source rock data in sequence stratigraphy. Bulletin of the American Association of Petrleum Geologists, 75, 650p.
- Peters, K.E., and Cassa, M.R. (1994). Applied source rock geochemistry. In: Magoon,
 L.B., Dow, W.G., (eds.). The Petroleum System-From Source to Trap.
 AAPG Memoir. 60, pp. 93-120.
- Peters K.E., Walters C.C., Moldowan J.M. (2005). The Biomarker Guide Volume 2:
 Biomarkers and Isotopes in Petroleum Exploration and Earth History.
 Cambridge University Press, Cambridge, pp. 475-1155.
- Peterson, H.I. (2002) A re-consideration of the "oil window' for humic coal and kerogen type III source rocks. **Journal of Geology 25,** 407 432.

- Peterson, H.I. (2006) The petroleum generation potential and effective oil window of humic coals related to coal composition and age. Journal of Coal Geology 67, pp. 221 – 248.
- Petersen, H.I. and Nielsen, L.H. (1995) Controls on peat accumulation and depositional environments of a coal-bearing coastal plain succession of a pullapart basin ; a petrographic, geochemical and sedimentological study, lower Jurassic, Denmark. *International Journal of Coal Geology* 27, pp. 99 – 129.
- Petersen, H.I., Foopatthanakamol, A. and Ratanasthien, B. (2006) Petroleum potential, thermal maturity and the oil window of oil shales and coals in Cenozoic Rift Basin, Central and Northern Thailand. Journal of Petroleum Geology 29(4), pp. 337-360.
- Petersen, H.I., Nytoft, H.P., Ratanasthien, B. and Foopattahanakamola, A. (2006) Oils from Cenozoic rift basins in central and northern Thailand: source and thermal maturity. Journal of Petroleum Geology 30, pp. 59 – 78.
- Piyasin, S. (1972) Geology of the Lampang Quadrangle, Sheet NE 47-7, Scale 1:250,000. Report of Investigation No. 14, 011/30/27, Department of Mineral Resources, Bangkok, Thailand.
- Piyasin, S. (1975) Review of the Lampang Group, *In* Stokes, R.B., Tantisukrit, C., and Campbell, K.V. (eds.). Proceedings of the conference on the geology of Thailand: *1973*. Department of geological sciences Chiang Mai University, 101-108.

- Polachan, S. and Satayarak, N. (1989) Strike-slip tectonic and the development of Tertiary basins in Thailand. Proceedings of the International Symposium on Intermontane Basin: Geology and Resources, Chiang Mai, Thailand, 30 Jan-2 Feb 1989, p. 243 – 253.
- Polachan, S., Srikulwong, S., Yuwanasiri, S., and Tungkaew, T. (1980). Geology of the North-Central Thailand. Onshore Petroleum Exploration Report, no.1. Mineral Fuels Division, Department of Mineral Resources (in Thai). 102 p.
- Polachan, S., Pradidtan, S., Tongtaow, C. Janmaha, S., Intarawijitr, K. and Sangsuwan, C. (1991) Development of Cenozoic basins in Thailand. Marine and Petroleum Geology, 8, pp. 84 – 97
- Praditan, S. (1989) Characteristics and controls of lacustrine deposits of some Tertiary basin in Thailand. In. Thanasuthipitak, T. and Ounchanum, P. (eds)
 Intermontane Basin: Geology and Resources. University of Chiang mai, Chang Mai, pp. 133 145
- Racey, A. (2011) Petroleum Goelogy. In: Ridd M. F, Barber A.J, Crow M.J. (eds)The Geology of Thailand, The Geological Society, London, pp.351 392.
- Ratanasthien, B. (1989) Depositional environment of Mae Lamao basin as indicated by palynology and coal petrography. In: Thanasuthipitak, T. and Ounchanum, P. (eds) International Symposium on Intermontane Bains: Geology and Resources. Chiang Mai Thailand, pp. 205 215
- Ratanasthien, B. (1992) Properties of Tertiary Coal in Northern Thailand. *Chiang Mai* University Library. [Internet]. 2015 [cited 2015 May 26]. Available from: ASEAN Minerals database and Information System.

- Ratanasthien, B., Kojima, T., Tokumitsu, T., Katoh, A. and Uyemura, N. (1992)
 Relationship between elementary analysis, origin and diagenesis of Tertiary
 Thai coals. Proceedings of the National Conference on Geologic Resource
 of Thailand: Potential for Future Development, Bangkok, 273 282.
- Ratanasthien B. (1997; 2015) Algae type of oil source rocks in northern Thailand.
 The internal conference on Stratigraphy and Tectonic Evolution of
 Southese Asia and the South Pacific. Bangkok, Thailand 19–24 August 1997.
- Ratanasthien, B. (1999) Association of oil source algae in some Tertiary basins, northern Thailand. Journal of Asian Earth Science 17, pp.295 299.
- Ratanasthien, B. (1992). Neogene Events Recorded in Coalfields in Northern Thailand. Proceeding of Development Geology of Thailand to the Year
 2000; 13-14 December, 1990; Chulalongkorn University, Bangkok, Thailand, pp.462 – 476.
- Ratanasthien, B., Phromphutha, M., Rayanakorn, M., Srikong, L., Kijsawadpiboon,
 P., Roppiree, P., Yavichal, A. and Aviruthananun, P. (2000). Suitability of
 Thai Coals for Activated Carbon Starting Material. Proceedings of
 Symposium on mineral Energy and Water Resources of Thailand; October
 28-29; DMR, Bangkok, Thailand, p.539 544.
- Ratanasthien, B. (2011) Coal deposits. In: Ridd M. F, Barber A.J, Crow M.J. (eds) **The Geology of Thailand**, The Geological Society, London, pp.393 – 414.
- Roberts, L.N.R., and McCabe, P.J., 1992, Peat accumulation in coastal-plain mires-A model for coals of the Fruitland Formation (Upper Cretaceous) of southern Colorado, U.S.A.: International Journal of Coal Geology, v. 21, pp. 115-138.

- Ronald, W.T. Wikins and George, C.S. (2002) Coal as a source rock for oil: a review. International Journal of Coal Geology, 50, pp. 317 – 361.
- Sebag D., Disnar J.R., Guillet B., Di-Giovanni C., Verrecchia E.P. & Durand A., 2006a. Monitoring organic matter dynamics in soil profiles by "Rock Eval pyrolysis": bulk characterization and quantification of degradation. European Journal of Soil Science 57, pp. 344-355.
- Sebag, D., Di-Giovanni, C., Ogier, S., Mesnage, V., Laggoun-Défarge, F. & Durand,
 A., 2006b. Inventory of sedimentary organic matter in modern wetland
 (Marais Vernier, Normandy, France) as source-indicative tools to study
 Holocene alluvial deposits (Lower Seine Valley, France). International
 Journal of Coal Geology 67, pp. 1-16.
- Selley, R. C. (1985; 1998; 2014) Elements of Petroleum Geology (edition 2) Department of Geology Imperical College London United kingdom
- Sethakul, N. (1984) Pongnok oil field. Symposium on Cenozoic basin of Thailand. Chiang Mai University, Thailand.
- Songtham W. (2003) Stratigraphic Correlation of Tertiary Basins in Northern Thailand Using Algae Pollen and Spore. **PhD thesis**, Chiang Mai University.
- Stach, E., Mackowsky, M.-TH., Teichmuller, M., Taylor, G.H., Chandra, D. and Teichmuller, R. (1975) The maceral of coal. In: Stach, E., Mackowsky, M.-TH., Teichmuller, M., Chandra, D., Taylor, G.H. (eds.) Coal Petrology, Gebruder Borntraeger, Berlin, pp. 54-93.
- Stopes, M. C. and Wheeler, R.V. (1918) The constitution of Coal. HMSO, London (on gehalf of the Department of Science and Industrial Research).

- Suárez-Ruiz, I., Flores, D., Filho, J.G.M., and Hackley, P.C. (2012). Review and update of the applications of organic petrology: Part 1. International Journal of Coal Geology. 99, pp. 54-112.
- Sykes, R. (2001) Depositional and rank controls on the petroleum potential of coaly source rocks. *In*: Hill, K.C. and Bernecker, T. (eds.) Eastern Australasian
 Symposium, a refocused energy perspective for the future. Petrol. Expl. Soc. Austral. Spec. Publ. pp. 591 601.
- Sykes, R. and Snowdon, L.R. (2002) Guidelines for assessing the petroleum potential of coaly source rocks using Rock-Eval pyrolysis. Org. Geochem. 33, pp. 1441 – 1455.
- Sýkorová I., Pickel W., Christanis K., Wolf M., Taylor G.H., Flores D. (2005) Classification of huminiteICCP System 1994. International Journal of Coal Geology 62, pp. 85 – 106.
- Teichmuller M. (1975) Origin of the petrographic constituents of coal. In: Stach E., Mackowsky M.-TH., Teichmuller M., Chandra D., Taylor G.H. (eds) Coal Petrology, Gebruder Borntraeger, Berlin, pp. 176 - 237.
- Teichmuller, M. And Durand, B. (1983) Fluorescence microscopical rank studies on liptinites and vitrinites in peat and coals, and comparison with results of the Rock-Eval pyrolysis. International Journal of Coal Geology 2, pp. 197–230.
- Thomas, B.M. (1982) Land plant source rocks for oil and their significance in Australian basin. Journal of the Australian Petroleum Exploration Association 22, pp.164 178.
- Tissot, B. P. and Welte, D.H. (1978) Petroleum Formation and Occurrence, 2 ed.: Springer-Verlag. Berlin Heidelberg, New York, pp. 430 - 449.

- Tissot, B., and Welte, D.H. (1984). **Petroleum Formation and Occurrence, 2nd ed**. Springer-Verlag, Heidelberg. pp. 669.
- Tissot, B.P., Pelet, R. and Ungerer, P.H. (1987) Thermal history of sedimentary basins, maturation indices, and kinetics of oil and gas generation. AAPG Bull., 71, pp. 1445 – 1466.
- Tsukii Y. (2014) Green algae: *Pediastrumboryanum*. [Internet]. [cited 2014Jan 19]. Available from: http://www2.fcps.edu/islandcreekes/ecology/green_algae.htm
- Tyson, R.V. (1995). Sedimentary Organic Matter: Organic Facies and Palynofacies. Chapman and Hall, London. pp. 615.
- Uttamo, W., Elder, C. and Nichols, G. (2003). Sedimentology of Neogene sequence in the Mae Moh basin, northern Thailand. In: Ratanasheen, B., Riee, S. L and Chantraprasert, S. (eds) Proceedings of the 8th Ingernational Congress of Pacific Neogene Stratigraphy:Pacific Neogene Paleoenvironment and their Evaluation. Chiang Mai, Thailand, pp. 31-48
- Van Krevelen, D.W. (1993) Coal, typology-chemistry-physics-constitution. Elsevier, Amsterdam Oxford, new York.
- Van Krevelen, D.W. (1950). Graphical-statistical method for the study of structure and reaction processes of coal, **Fuel**, **29**, 269-84.
- Wang, H., Shao, L., Hao, L., Zhang, P., Glasspool, I.J., Wheeley, J.R., Wignall, P.B.,
 Yi, T., Zhang, M., Hilton, J. (2011) Sedimentology and sequence stragigraphy
 of the Lopingian (Late Permian) coal measures in sourthwestern China,
 International Journal of Coal Geology 85, 168 183.

BIOGRAPHY

Miss. Piyatida Sangtong was born on February 15, 1987 in Phitsanulok Province, Thailand. She earned her Bachelor's Degree in Science (Geoscience) form Mahidol University in 2008. She then continued her Master's degree in Engineering (Georesources) at Department of Mining and Petroleum Engineering, Chulalongkorn University. Her expertise includes the field of science and engineering related with Geology. During her Master's degree study, she oral presented entitled of *"The Potential Acidity of Coal Mine: A Case Study of Mae Ta Lignite and Ball Clay Mine, Lampang Province, Thailand*" at the International Conference on Mining, Materials, and Petroleum Engineering. After graduation, she has been teacher at Geoscience program under the position of lecture of Mahidol University Kanchanaburi Campus in 2012 She continued with her graduate studies in Geotechnology, Institute of Engineering, Suranaree University of Technology.

> ะ รัว_{อั}กยาลัยเทคโนโลยีสุรบโ